

**TECHNICAL UNIVERSITY OF CRETE
MINERAL RESOURCES DEPARTMENT
PETROLEUM ENGINEERING Msc**

**THE EFFECT OF THE RESERVOIR FLUID PHASE BEHAVIOR
TREATMENT ON THE RESERVOIR SIMULATION
PREDICTIONS OUTPUT**

POLYANTHI-MARIA TRIMI

Supervisor: Professor N.Varotsis

MAY 2017

*To those,
who never give up*

Table of Contents

ABSTRACT.....	7
1. INTRODUCTION	9
2. WHAT A SIMULATOR DOES?.....	12
3.1 GRID DEFINITION	18
3.1.1 Cartesian Grid.....	19
3.1.2 Orthogonal Corner Point	20
3.1.3 Non-Orthogonal Corner Point	21
3.1.4 Radial Grid	22
3.1.5 Quick Pattern Grid.....	22
3.1.6 Grid Orientation Effect	22
3.1.7 Grid Refinement	23
3.1.8 Number of Blocks.....	24
3.1.9 Dynamic Grid (Optional).....	25
3.2 POROSITY SYSTEMS	25
3.2.1 Single Porosity.....	26
3.2.2 Dual Porosity	27
3.2.3 Dual Permeability	27
3.2.4 MINC.....	27
3.2.5 Subdomain.....	28
3.3 SHAPE FACTOR.....	30
3.3.1 Warren And Root	30
3.3.2 Gilman And Kazemi	32
3.4 FAULTS (OPTIONAL).....	33
3.5 ARRAY PROPERTIES-BUILD THE MODEL.....	33
3.6 ROCK COMPRESSIBILITY	40
3.7 COMPACTION-DILATION (OPTIONAL)	40
3.7.1 Compaction.....	41
3.7.2 Dilation	42
3.8 AQUIFERS (OPTIONAL).....	43
3.9 HISTORY MATCHING TOOLS	46
3.9.1 Sectors, Flux Sectors And Lease Planes.....	46

3.9.2 Array Properties- History Matching	46
3.9.3 Rock-Fluid End-Point Properties Modification.....	50
4.1 BLACK OIL FORMULATION	51
4.1.1 Laboratory Data And Field Data	54
4.1.2 Densities	54
4.1.3 Water Properties.....	54
4.2 COMPOSITIONAL MODEL	55
4.2.1 Component Properties	55
4.2.2 Reservoir Temperature.....	58
4.2.3 Equation Of State (EOS)	58
4.2.3.1 SOAVE-REDLICH-KWONG (SRK).....	59
4.2.3.2 PENG-ROBINSON (PR).....	59
4.2.4 Calculation Of Viscosity.....	60
4.2.5 Identification Of The Fluid Phase	62
4.2.6 Aqueous Phase Solubility	63
4.3 RESERVOIR FLUIDS	63
4.3.1 Heavy Oil.....	63
4.3.2 Black Oil.....	63
4.3.3 Volatile Oil.....	64
4.3.4 Dry Gas.....	64
4.3.5 Gas- Condensate	64
4.3.6 Compositional Variances of The Reservoir Fluid.....	64
4.4 IMPROVED OIL RECOVERY (IOR) AND ENHANCED OIL RECOVERY (EOR) METHODS.....	65
4.4.1 Seawater Injection	65
4.4.2 Gas Injection.....	65
4.4.3 Miscible Flooding.....	66
4.4.4 Polymer Flooding	66
4.5 COAL BED METHANE RESERVOIRS	67
5. ROCK-FLUID DATA	69
5.1 WETTABILITY	69
5.2 TWO PHASE DATA.....	70
5.3 THREE-PHASE RELATIVE PERMEABILITY.....	71
5.4 VELOCITY DEPENDENT RELATIVE PERMEABILITY	74

5.5 LEVERETT J-FUNCTION (OPTIONAL)	74
5.6 HYSTERESIS MODELING (OPTIONAL)	75
5.7 NON-DARCY FLOW	75
5.8 ADSORPTION COMPONENTS	77
6.1 INITIALIZATION METHOD	78
6.1.1 Vertical Depth Average	78
6.1.2 Vertical Block Centered	79
6.1.3 User Input	80
6.2 INITIAL FLUID IN PLACE CALCULATION	80
7. WELLS	82
7.1 WELL TYPES	83
7.2 PERFORATIONS	84
7.3 WELL INDEX (WI)	84
7.4 RATE DEPENDENT SKIN FACTOR (OPTIONAL)	85
7.5 GAS INFLOW (OPTIONAL)	85
7.6 WELL AND GROUP CONSTRAINTS	86
7.6.1 Production Wells	86
7.6.1.1 OPERATING CONSTRAINTS AND REMEDIAL ACTIONS	86
7.6.1.2 MONITORING CONSTRAINTS (OPTIONAL)	86
7.6.1.3 PENALTY CONSTRAINTS (OPTIONAL)	87
7.6.2 Injection Wells	88
7.6.3 Group Of Wells (Optional)	88
7.6.3.1 PRODUCTION OPERATING CONSTRAINTS	88
7.6.3.2 PRODUCTION MONITORING CONSTRAINTS (OPTIONAL)	89
7.6.3.3 INJECTION CONSTRAINTS	90
7.7 SEAWATER SCALE BUILD UP (OPTIONAL)	90
7.8 TUBING TABLES (OPTIONAL)	90
7.9 PRESSURE CALCULATIONS	91
7.9.1 Bottom Hole Pressure Calculation	91
7.9.2 Well Bore Pressure Loss Calculation	91
7.9.3 Pressure Drop Between Perforations	91
7.10 GAS LIFT (OPTIONAL)	91
7.11 MANIFOLDS (OPTIONAL)	92
7.12 HYDRAULIC FRACTURING (OPTIONAL)	92

7.13 RECYCLING (OPTIONAL)	93
7.14 ALTERNATING PROCESSES (OPTIONAL).....	94
7.15 RATE DISTRIBUTION (OPTIONAL)	94
7.15.1 Priority Ranking	94
7.15.2 Apportionment.....	95
7.16 HISTORY MATCHING TOOLS	95
7.16.1 Triggers.....	95
7.16.2 Spatial Properties Modification.....	95
7.16.3 Multipliers	96
8. GEOMECHANICS.....	97
8.1 CONSTITUTIVE MODELS.....	97
8.1.1 Material Deformation Behavior.....	97
8.1.2 Shear Failure.....	98
8.1.2.1 MOHR-COULOMB CRITERION.....	98
8.1.2.2 DRUCKER-PRAGER CRITERION	99
8.1.2.3 TRESCA AND VON MISES CRITERIA	99
8.1.3 Compaction failure	99
8.2 DISPLACEMENT CONDITIONS	100
8.3 WELL BOUNDARY UNLOADING.....	100
8.4 CALCULATION OF DEFORMATIONS IN 2D AND 3D	100
9. NUMERICAL CONTROLS.....	102
9.1 NEWTON-RAPHSON METHOD.....	102
9.1.1 Convergence Tolerance.....	103
9.1.2 Relaxation Of The Accumulation Term.....	103
9.2 EXPLICIT, IMPLICIT AND IMPES METHODS.....	104
9.3 ADAPTIVE IMPLICIT METHOD	104
9.4 LINEAR SOLVER	105
9.4.1 Matrix ordering.....	105
9.4.2 Matrix Preconditioning.....	106
9.4.3 Generalized Minimal Residual Method (GMRES)	106
9.5 PARALLEL PROCESSING.....	107
9.6 NUMERICAL DISPERSION CONTROL	107
9.7 GEOMECHANICS	107
10. SIMULATION RESULTS	108

10.1 EXPORTED FILES.....	108
10.2 RUN TIME DIMENSIONING	109
10.3 MAXIMUM NUMBER OF ERRORS REPORT	109
10.4 ACTION ON INTERRUPT DETECTION.....	109
11. MODIFIED BLACK OIL TABLE GENERATION	111
11.1 WHITSON-TORP METHOD	111
11.2 COATS METHOD	111
12. SIMULATION MODEL.....	113
12.1 RESERVOIR.....	113
12.2 GRID DESIGN	114
12.3 RESERVOIR FLUID	114
12.4 ROCK-FLUID DATA	116
12.5 INITIAL CONDITIONS	117
12.6 WELLS DESIGN.....	118
12.6.1 Production Wells.....	119
12.6.2 Injection Wells	120
13. SIMULATION RESULTS	122
13.1 INITIALIZATION RUN RESULTS	122
13.2 SIMULATION RUN RESULTS	123
14. REFERENCES.....	153

ABSTRACT

Two different methods are used for solving the phase behavior problem during reservoir simulation applied to hydrocarbon reservoirs; the black oil Tables and the compositional approaches. The black oil Tables simulators use Tables of volumetric factors (solution gas-oil ratio, oil formation volume factor, gas formation volume factor, oil content) versus pressure and by performing interpolation at each pressure step the produced volumes are calculated. On the other hand, the compositional simulators, perform the phase behavior calculations by using an equation of state so as to calculate the equilibrium phases and their properties at different operating conditions.

The main advantages of the black-oil Tables simulators are that they require low calculation (CPU) time low computer memory. On the other hand, compositional simulators are more accurate and can perform better with volatile oils and gas condensates. Nevertheless, operators still use black-oil simulators to simulate volatile oils and gas condensates, valuing thus more the speed of calculations as the expense of accuracy. The question is how much information is lost with respect to the compositional approach and how much off the black oil tables approach reservoir simulation predictions can be.

For this thesis, the commercial software IMEX and GEM of Computer Modeling Group has been used. These models are presented in detail and the different options that they offer are discussed. The objective of this work was to discuss to present the available models of the black oil tables and compositional simulators as well as their difference in predictions and to assess their differences in predicting the reservoir production performance. A simple reservoir containing volatile oil was modeled and its depletion was simulated using both simulators and their results were compared.

The two simulators exhibited a small divergence between their predictions for the initial volumes in place and the simulation runs. However, the compositional simulator is thought to be more accurate than the black oil simulator in its predictions as it is a compositional simulator. Moreover, it was found that the black oil simulator calculated almost the same amount of initial volumes in place, whereas it over-predicted the oil recovery and the oil cumulative production.

1. INTRODUCTION

This thesis deals with reservoir simulation which is widely used to the petroleum industry. As reservoir simulation is defined, the procedure of building a computer model which is representative of the actual reservoir. This mathematical model subsequently can 'operate' in a way similar to the real reservoir during production (Petrowiki, 2017d). Reservoir simulation is used in order to predict the production of the reservoir, to model the overall reservoir behavior and fluid flow inside it, match the observed production with the model (history matching procedure) in order to increase the accuracy of the reservoir description and to help taking decisions about projects in order to increase the reservoir recovery.

The simulation studies can be divided into three main categories: the black oil, compositional and thermal simulations. The black oil simulators, such as CMG's IMEX perform the calculations by using the black oil Tables formulation. By using this formulation, it is assumed that the reservoir fluid at any pressure consists of two pseudo-components, the stock tank oil and the surface gas and that their composition remains constant throughout the entire production. In the black oil formulation, the calculation of the volumes that are produced is done by performing, at each pressure step, interpolation in the read out Tables of the solution gas oil ratio (R_s), the oil formation volume factor (B_o), the gas formation volume factor (B_g) and the oil content (R_v) with pressure. The main advantages of the black oil formulation method are the low calculation (CPU) time and the low required computer memory. Black oil simulators are mainly used for oils with $R_s < 750$ scf/stb, $B_o < 1.4$ bbl/stb and API gravity < 30 (Petrobras-pemex, n.d.). On the other hand compositional simulators such as CMG's GEM simulator perform the phase behavior calculations by using an equation of state to compute the reservoir oil and gas compositions and volumes at each block and at each time step. Compositional simulations are performed by taking into account the changes in composition of the oil and gas with pressure. This type of simulation requires much more time and memory storage but it provides more accurate results. Compositional simulators are used mainly to model isothermal enhanced oil recovery miscible processes such as hydrocarbon gas injection, carbon dioxide injection, water alternating gas injection, volatile oils and gas-condensates. Thermal simulators are similar to compositional simulators but they also take into account differences in temperature.

Usually for reservoir simulation studies, software companies provide an entire program suite, with each program to be used in collaboration with the others but for a different purpose. The program suite that was used in this thesis is the one provided by CMG. This suite contains the following programs:

- Winprop

Winprop is a program used in order to predict the phase behavior and the fluid properties of a reservoir fluid. The laboratory data are inserted in Winprop and an equation of state is tuned against these data. This tuned equation of state provides the required data by the simulation program in the appropriate form so as the

simulation run to be performed.

- IMEX, GEM and STARS simulators

Since the computer model of the reservoir has been constructed, simulation programs such as IMEX, GEM and STARS are used in order to solve the phase behavior problem. Each of the aforementioned simulators treats the problem in a different way and it is used for different purposes IMEX is a black oil simulator, GEM is a compositional simulator and STARS is a thermal simulator.

IMEX simulator is used in cases of conventional reservoirs, conventional oil in naturally fractured reservoirs, to predict primary recovery, to model improved oil recovery (IOR) such as water flooding and isothermal enhanced oil recovery (EOR) schemes such as polymer flooding (CMG, 2017). GEM simulator can be used for the same applications as IMEX but is primarily used to model conventional and unconventional reservoirs, coal bed methane (CBM) reservoirs, geomechanical deformations, in cases where the composition influences production (eg. the production of two fields have to be mixed in order to achieve a desired viscosity) and for carbon dioxide storage (CMG, 2017;Eng-tips.com, 2008). STARS simulator is used for non isothermal problems and is mainly used for the modeling of thermal tertiary oil recovery processes such as steam injection or in situ combustion processes.

- Results and 3D Results

Results and 3D Results are post processor programs which provide the simulation results in the form of plots and 3D.

- CMOST

CMOST is a post processor program to which the the results of the simulation are introduced that can be used for history matching, sensitivity analysis and optimization program.

- Builder

Builder is a pre-processor program used beforehand in order to construct the reservoir model which will provide results about the reservoir. Builder in order to create a computer model which is representative of the actual reservoir requires information such as the reservoir geometry, the geological features (eg. porosity, permeability), the phase saturations, the relative permeabilities, the initial condition of the reservoir (undersaturated or saturated) and the wells locations. Moreover, the fluid properties and the desired time period of the simulation run have to be inserted so as the simulator that will be used to be able to provide predictions about the reservoir fluid behavior over time.

The objective of this thesis, is to compare the performance of a black oil simulator (IMEX) and a compositional simulator (GEM) for simulating a volatile oil reservoir. For this purpose, a model was created step by step in Builder of which the different options are presented and analyzed in the different chapters of this thesis. Then the created model containing volatile oil was tested in both GEM and IMEX simulators and the predicted initial volumes in place as well as the production predictions provided by the two simulators were compared.

The Builder program is comprised by the following sections:

- Reservoir description

In the reservoir description section the construction of the reservoir model is done. In this section the geometry of the reservoir, the porosity and the permeability types and values, the existence of aquifers and the compressibility of the formation are introduced

- Simulation method

In the simulation method section, the data required for the calculation of the produced volumes are entered according to the method used. In the case that the simulation is done using black oil Tables then volumetric factors are needed whereas in the case that a compositional model is used the fluid composition and the equation of state have to be introduced.

- Rock-fluid data

In the rock-fluid data section, the wettability of the reservoir, the relative permeabilities of the phases, the capillary pressures and the equation by which the non-Darcy flow will be calculated are introduced into the simulator.

- Initialization

In the initialization section, the initial condition of the reservoir is introduced into the simulator and the method that will be used for the calculation of pressures, saturations and the initial volumes of hydrocarbons in place are defined.

- Wells

In the wells section, the position, the type of the wells that exist in the field and the constraints under which these wells operate are introduced into the simulator.

- Geomechanics

In the geomechanics section the failure criterion that will be used in order to take into account the geomechanical deformations occurred to the reservoir by the regional stress regime.

- Numerical controls

In the numerical controls section, the numerical method and its parameters that will be used so as to solve the system of the flow equations are defined.

- Simulation results

In the simulation results section, the information of the simulation that will be printed in the output files are defined.

2. WHAT A SIMULATOR DOES?

A reservoir simulator is a program that having the static model (geometry, porosity etc.) of the reservoir and the data about its initial conditions (pressure, depth of the contacts etc.) gives an estimation of the behavior of the reservoir fluid, the changes in pressure, saturation and the fluid properties during production. This estimation is done by solving the flow, the pressure and the saturation equations as well as the phase behavior problem.

The first step that the simulator does is to find the pressure and saturations values at the current timestep. The equations of the pressure and saturation are non linear equations which can be discretized in space and time and are solved using the Newton-Raphson method.

For simplification reasons the way that the pressure and saturation equations are solved will be presented only for the case of a single phase incompressible fluid.

$$\text{Pressure equation: } \frac{\partial}{\partial x} \left(\lambda_T(S_p) \cdot \frac{\partial P}{\partial x} \right) = 0$$

$$\text{Saturation equation: } \varphi \cdot \frac{\partial S_p}{\partial t} = \frac{\partial}{\partial x} \left(\lambda_T(S_p) \cdot \frac{\partial P}{\partial x} \right)$$

In the above equations the term $\lambda_T(S_p)$ is the mobility of the phase p which is a function of the saturation:

$$\lambda_T(S_p) = \sum \lambda_p(S_p) \quad \text{and can be expressed as follow: } \lambda_p = \frac{k \cdot k_{rp}}{\mu_p}, \quad \text{where } k \text{ is the permeability of the}$$

formation, k_{rp} is the relative permeability of the phase p and μ_p is the viscosity of the phase p.

The discretization in space for each time step n (eg. for the pressure equation) is done as follow:

$$\frac{\partial^2 P}{\partial x^2} = \frac{\left(\frac{dP}{dx} \right)_{fd} - \left(\frac{dP}{dx} \right)_{bd}}{\Delta x} = \frac{\left(\frac{P_{i+1} - P_i}{\Delta x} \right) - \left(\frac{P_i - P_{i-1}}{\Delta x} \right)}{\Delta x} = \frac{P_{i+1} + P_{i-1} - 2 \cdot P_i}{\Delta x^2}, \quad \text{where the subscript } i \text{ denotes the}$$

block number.

The different methods that can be used in order to discretize the pressure and the saturation equations in time are the implicit method and the IMPES (IMPLICIT Pressure- EXPLICIT Saturation) method. In the case that the implicit method is used then the pressure and saturation equations have to be solved simultaneously by using a first assumption for their values and using an iterative procedure so as to provide the solution of the system. On the other hand, when the IMPES method is used the pressure is calculated first by making a first guess for the pressure values and by using an iterative procedure to provide the appropriate pressure value. As soon as the pressure value has been calculated it is substituted to the saturation equation in order the saturation value to be also calculated.

In the case of using implicit method the pressure and saturation equations (eg. for oil) can be expressed as follows:

Pressure equation:

$$\frac{(\lambda_T(S_o^{n+1}))_{i-1/2}}{\Delta x^2} P_{i-1}^{n+1} - \left[\frac{(\lambda_T(S_o^{n+1}))_{i-1/2}}{\Delta x^2} + \frac{(\lambda_T(S_o^{n+1}))_{i+1/2}}{\Delta x^2} \right] P_i^{n+1} + \frac{(\lambda_T(S_o^{n+1}))_{i+1/2}}{\Delta x^2} P_{i+1}^{n+1} = 0$$

In the equation above the subscripts $i+1/2$ and $i-1/2$ denotes the centers of the blocks $i+1$ and $i-1$.

Saturation equation:

$$S_{oi}^{n+1} = S_{oi}^n + \frac{\Delta t}{\phi} \left\{ \left[\frac{(\lambda_o(S_o^{n+1}))_{i+1/2}}{\Delta x^2} (P_{i+1}^{n+1} - P_i^{n+1}) \right] - \left[\frac{(\lambda_o(S_o^{n+1}))_{i-1/2}}{\Delta x^2} (P_i^{n+1} - P_{i-1}^{n+1}) \right] \right\}$$

In the case of using the IMPES method, the pressure equation is the same as for the implicit method whereas the saturation equation can be expressed as follow:

$$S_{oi}^{n+1} = S_{oi}^n + \frac{\Delta t}{\phi} \left[\frac{(\lambda_o(S_o^v))_{i+1/2}}{\Delta x^2} ((P_{i+1}^{n+1})^v - (P_i^{n+1})^v) \right] - \left[\frac{(\lambda_o(S_o^v))_{i-1/2}}{\Delta x^2} ((P_i^{n+1})^v - (P_{i-1}^{n+1})^v) \right]$$

where the pressure values are taken from the last iteration v that was performed by the simulator so as to calculate the pressure.

If we assume for the above equations that a vector x includes the unknowns pressures and saturations terms, a matrix A includes their coefficients and a vector b include the known values of the equations, then, the system takes the form of: $A \cdot x = b$, which can also be expressed as: $F(x) = A \cdot x - b$ and has to be solved as follow: $F(x^{n+1}) = 0$, where $n+1$ is the new timestep. The latter system is solved using the Newton-Raphson iterative method as it is a non linear system of equations. By using the Newton-Raphson method a first guess for the value of $x^{n+1(v)}$ is made and applied to the equation below in order to provide the system solution: $x^{n+1(v+1)} = x^{n+1(v)} + [J(x)^{(v)}]^{-1} \cdot F(x^{(v)})$, where the $J(x)$ is a Jacobian matrix constituted by the derivatives of $F(x)$. The inverse of the Jacobian matrix is found by solving a linear system of equations which is of the form of: $J(x) \cdot J(x)^{-1} = I$, where I is the identity matrix. The solution of the latter system is done by using a linear solver which requires the simplification of the $F(x)$ so as the simulator to be able to inverse easily the matrix J . The simplification of the $F(x)$ is done by re ordering the elements of the matrix so as to minimize its band and by using preconditioners which decompose the original matrix to a product of matrices equal to the original but which is easier to be solved by the simulator.

Since the pressure and saturation values are known then the simulator proceeds to the solution of the phase behavior problem. In the case, of a black oil simulator this is done by interpolating between the values of the provided PVT Table by Winprop. This interpolation is performed so as the simulator to find the volumetric factors and the viscosity value for this specific pressure. On the other hand, a compositional simulator knowing the pressure value uses the already tuned in Winprop equation of state in order to provide the compressibility factor of each phase and then calculates the volume, the density and the viscosity of each phase.

After solving the phase behavior problem then the simulator proceeds to the calculation of flow. Depending on the type of the simulator (black oil or compositional) the flow equations is needed to be solved are slightly different, due to the fact that the phase behavior problem is treated differently, but they are derived in a similar manner. Moreover, it has to be mentioned that two types of black oil tables (BOT) exist: the traditional black oil tables and the modified black oil tables. The traditional BOT tables do not take into consideration any condensation of the oil existing in the gas phase whereas the modified BOT tables do account for this phenomenon using an extra parameter namely the oil content (R_v). The oil content represents the oil which will condense from the gas phase due to pressure drop. As a result, the flow equations of a black oil simulator are different for a black oil and a volatile oil due to the fact that the latter takes into consideration the oil content.

For a black oil simulator the flow equations that are needed to be solved for each phase in three dimensions are presented below:

- For the oil phase

Traditional black oil tables:

$$q_o = \frac{\partial}{\partial t} \left(\frac{\varphi \cdot S_o}{B_o} \right) - \nabla \left(\frac{k \cdot k_{ro}}{\mu_o \cdot B_o} \cdot (\nabla P_o - \gamma_o \cdot \nabla z) \right), \text{ where } q_o \text{ is the flow rate of the oil, } \varphi \text{ is the porosity, } S_o \text{ is}$$

the oil saturation, B_o is the oil formation volume factor, k is the permeability of the formation, k_{ro} is the relative permeability of the oil when other phases are also present, μ_o is the oil viscosity, P_o is the pressure in the oil phase, γ is the gradient of the oil phase and z is the depth.

Modified black oil tables:

$$q_o + R_v \cdot q_g = \frac{\partial}{\partial t} \left(\frac{\varphi \cdot S_o}{B_o} \right) + \frac{\partial}{\partial t} \left(\frac{\varphi \cdot R_v \cdot S_g}{B_g} \right) - \nabla \left(\frac{k \cdot k_{ro}}{\mu_o \cdot B_o} \cdot (\nabla P_o - \gamma_o \cdot \nabla z) \right) - \nabla \left(\frac{R_v \cdot k \cdot k_{ro}}{\mu_o \cdot B_g} \cdot (\nabla P_o - \gamma_o \cdot \nabla z) \right)$$

- for gas:

$$R_s \cdot q_o + q_g = \frac{\partial}{\partial t} \left(\varphi \cdot E_g \cdot S_g + \frac{\varphi \cdot R_s \cdot S_o}{B_o} \right) - \nabla \left(\frac{R_s \cdot k \cdot k_{ro}}{\mu_o \cdot B_o} \cdot (\nabla P_o - \gamma_o \cdot \nabla z) \right) - \nabla \left(\frac{E_g \cdot k \cdot k_{rg}}{\mu_g} \cdot (\nabla P_g - \gamma_g \cdot \nabla z) \right)$$

where R_s is the solution gas-oil ratio, E_g (scf/rcf) is the gas expansion factor which can also be

replaced by the gas formation volume factor B_g (rb/scf) as follow: $B_g = \frac{1}{5.616 \cdot E_g}$

- for water:

$$q_w = \frac{\partial}{\partial t} \left(\frac{\varphi \cdot S_w}{B_w} \right) - \nabla \cdot \left(\frac{k \cdot k_{rw}}{\mu_w B_w} \cdot (\nabla P_w - \gamma_w \cdot \nabla z) \right)$$

Moreover, the well rate of a phase p is calculated by the following equation:

$$q_p = WI \cdot \frac{k_{rp}}{\mu_p} \cdot (P_p - P_{BHP}), \text{ where WI is the well index calculated internally by the simulator.}$$

To all the above equations the following constraints are imposed:

- The summation of the all the phases saturation has to be equal to the unity: $S_o + S_g + S_w = 1$
- The capillary pressure at the contacts has to be equal to the difference of the capillary pressures of phases which that are in contact: $P_{woc} = P_o - P_w$ and $P_{goc} = P_g - P_o$

In the case of a compositional simulator the flow equation that has to be solved is of the form of:

$$\frac{\partial}{\partial t} \left(\varphi \cdot \sum_{\rho=1}^{n_p} x_{c\rho} \cdot \rho_\rho \cdot S_\rho \right) + \nabla \cdot \sum_{\rho=1}^{n_p} x_{c\rho} \cdot \rho_\rho \cdot u_\rho = - \sum_{\rho=1}^{n_p} x_{c\rho} \cdot \rho_\rho \cdot q_\rho, \text{ where } n_p \text{ is the number of the phases (oil,}$$

water and gas) and $x_{c\rho}$ is the molar fraction of the component c (eg. C1, C2 etc.) in the phase p . In this case, the constraints imposed on the flow equations are the same as in the case of the black oil simulator but additional constraints are also imposed. These additional constraints are the following:

- The sum of the molar fractions of the components in each phase have to be equal to the unity:

$$\sum_{\rho=1}^{n_p} x_{c\rho} = 1$$

- The phases have to be in thermodynamic equilibrium, which means that the fugacities (tendency of a component to pass from one phase to the other) of the components between different phases have to be equal: $f_\rho(p_\rho, T, x_{c\rho}) = f_{\rho'}(p_{\rho'}, T, x_{c\rho})$, where f is the fugacity of a component which indicates its tendency to pass from one phase to the other and it is a function of pressure, temperature and composition.

All the above equations are derived using the mass conservation and the Darcy's law for three dimensions. The derivation of the flow equations will be presented for the case of a black oil simulator as for both black oil and compositional simulators the flow equations are derived with the same manner. Moreover for simplification reasons the derivation of these equations will be presented for the simple case of multiphase

flow in one dimension.

The calculation of flow inside the reservoir is done for each block separately based on a mass balance of the inflow and outflow from the block during a time Δt as follows:

- mass accumulation in the block = mass in the block at time $(t+\Delta t)$ – mass in the block at time (t)
- mass of fluid flowing in a block = volumetric flow rate in the block \cdot density of the fluid $\cdot \Delta t$ - volumetric rate of the outflow of the block \cdot density of the fluid $\cdot \Delta t$ – well source/sink term $\cdot \Delta t$

The mass influx of a phase 'p' to a block per unit area is calculated as follow:

$$J = \frac{q_p \cdot \rho_p}{A} = u_p \cdot \rho_p, \text{ where } q_p \text{ is the volumetric flow rate of the phase, } \rho_p \text{ is the density of the phase and } A \text{ is}$$

the area through which the fluid passes. The wells source/sink term is: $q^w = q_p \cdot \rho_p \cdot V$

as a result the mass flowing in the block i is calculated as follow:

$$J = (J_{i-1} - J_{i+1}) \cdot A \cdot \Delta t - q_i^w \cdot \Delta t \Rightarrow J = -(J_{i+1} + J_{i-1}) \cdot A \cdot \Delta t - q_p \cdot \rho_p \cdot V \cdot \Delta t \quad (1), \text{ where } J_{i-1} \text{ is the influx to the}$$

block i from its previous block whereas J_{i+1} is the outflow from the block i to the next block i+1.

The mass of a phase in a block is calculated as follow:

$$m = V \cdot \varphi \cdot S_p \cdot \rho_p, \text{ where } V \text{ is the volume of the block, } \varphi \text{ is the porosity, } S_p \text{ is the saturation of the phase 'p'.$$

The mass accumulation in the block from a time t to the time t+ Δt is calculated as follow:

$$m_{acc} = m_{t+\Delta t} - m_t = (V \cdot \varphi \cdot S_p \cdot \rho_p)_{t+\Delta t} - (V \cdot \varphi \cdot S_p \cdot \rho_p)_t = V \cdot ((\varphi \cdot S_p \cdot \rho_p)_{t+\Delta t} - (\varphi \cdot S_p \cdot \rho_p)_t) \quad (2).$$

By equating the (1) and (2) the following expression is derived:

$$J = m_{acc} \Rightarrow -(J_{i+1} + J_{i-1}) \cdot A \cdot \Delta t - q_p \cdot \rho_p \cdot V \cdot \Delta t = V \cdot ((\varphi \cdot S_p \cdot \rho_p)_{t+\Delta t} - (\varphi \cdot S_p \cdot \rho_p)_t) \Rightarrow$$

$$\Rightarrow -\frac{(J_{i+1} - J_{i-1})}{\Delta x} = \frac{V \cdot ((\varphi \cdot S_p \cdot \rho_p)_{t+\Delta t} - (\varphi \cdot S_p \cdot \rho_p)_t)}{\Delta t} + q_p \cdot \rho_p$$

In order the results to be provided in standard conditions ($\rho_p = \frac{\rho_{p,sc}}{B_p}$) and as Δx and Δt tend to zero the above

equation is transformed as follow:

$$\frac{\partial}{\partial x} J = \frac{\partial}{\partial t} (\varphi \cdot S_p \cdot \rho_p) + q_p \cdot \rho_p \Rightarrow \frac{\partial}{\partial x} \left(\frac{u_p \cdot \rho_{p,sc}}{B_p} \right) = \frac{\partial}{\partial t} \left(\frac{\varphi \cdot S_p \cdot \rho_{p,sc}}{B_p} \right) + \frac{q_p \cdot \rho_{p,sc}}{B_p} \Rightarrow \frac{\partial}{\partial x} \left(\frac{u_p}{B_p} \right) = \frac{\partial}{\partial t} \left(\frac{\varphi \cdot S_p}{B_p} \right) + \frac{q_p}{B_p} \quad (3)$$

The Darcy's velocity for multi phase flow for each phase p is given by: $u_p = -\frac{k_{rp}}{\mu_p} \cdot k \cdot \left(\frac{\partial P}{\partial x} - \gamma_p \cdot \frac{\partial z}{\partial x} \right)$, where

the k_{rp} is the relative permeability of the phase p, μ_p is the viscosity of the phase, k is the permeability of the formation, P_p is the pressure of the phase, γ_p is the specific gravity of the phase and z is the depth. Moreover, the Darcy's velocity for single phase flow is the following: $u_p = -\frac{k}{\mu} \cdot \frac{\partial P_p}{\partial x}$. As a result depending the flow the appropriate form of the Darcy velocity is used.

By substituting the Darcy's velocity for multi phase flow in the equation (3) the following equation is derived for each phase p:

$$\frac{\partial}{\partial t} \left(\frac{\varphi \cdot S_p}{B_p} \right) = \frac{\partial}{\partial x} \left(\frac{-k \cdot k_{rp}}{B_p \cdot \mu_p} \cdot \left(\frac{\partial P_p}{\partial x} - \gamma_p \cdot \frac{\partial z}{\partial x} \right) \right) + \frac{q_i}{B_p} \quad \text{and} \quad \text{by} \quad \text{rearranging} \quad \text{this} \quad \text{equation}$$

$$\frac{q_p}{B_p} = \frac{\partial}{\partial t} \left(\frac{\varphi \cdot S_p}{B_p} \right) - \frac{\partial}{\partial x} \left(\frac{-k \cdot k_{rp}}{B_p \cdot \mu_p} \cdot \left(\frac{\partial P_p}{\partial x} - \gamma_p \cdot \frac{\partial z}{\partial x} \right) \right) \quad (4)$$

For a 3D system the equivalent equation of flow to the equation (4) is of the form of:

$$\frac{q_i}{B_p} = \frac{\partial}{\partial t} \left(\frac{\varphi \cdot S_p}{B_p} \right) - \frac{\partial}{\partial x} \left(\frac{-k \cdot k_{rp}}{B_p \cdot \mu_p} \cdot \left(\frac{\partial P_p}{\partial x} - \frac{g}{B_p} \cdot \frac{\partial z}{\partial x} \right) \right) - \frac{\partial}{\partial y} \left(\frac{-k \cdot k_{rp}}{B_p \cdot \mu_p} \cdot \left(\frac{\partial P_p}{\partial y} - \frac{g}{B_p} \cdot \frac{\partial z}{\partial y} \right) \right) - \frac{\partial}{\partial z} \left(\frac{-k \cdot k_{rp}}{B_p \cdot \mu_p} \cdot \left(\frac{\partial P_p}{\partial z} - \gamma_p \right) \right)$$

3. RESERVOIR DESCRIPTION

This section consists of the following sub sections:

- Grid definition

The grid type and dimensions that will be used by the simulator so as to model the reservoir is defined.

- Porosity systems

The porosity system that will be used by the simulator is defined.

- Shape factor

The shape factor is used if the defined porosity system by the previous sub-section is other than single porosity.

- Faults

The faults that exist in the reservoir are introduced in the simulation model.

- Array properties-build the model

The array properties are used so as to introduce parameters regarding the geology of the reservoir, its depth, the saturation of the phases and other.

- Rock compressibility

This sub-section is used to introduce the rock compressibility in the simulator.

- Compaction/dilation regions

The compaction/dilation regions are used by the simulator to take into consideration compaction or dilation (increase of porosity) phenomena that may occur during the production life of the reservoir.

- Aquifers

This sub-section is used in order to introduce aquifers connected to the reservoir in the simulator.

- History matching tools

Builder provides some tools used for the history matching procedure. These tools help the user during the history matching procedure by providing property information of different reservoir regions as well as the modification of the end-point saturation, relative permeability and capillary pressure of the phases.

3.1 GRID DEFINITION

Grid is used to divide the reservoir volume in discrete blocks, so as to be able to apply the flow equations from one region of the reservoir to another and represent the reservoir structure (K Aziz, 1993; O. Pettersen, 2006). The selection of grid type that will be used for a simulation could have a great impact on the reservoir simulation predictions especially for geological complex reservoirs (K Aziz, 1993). The parameters that should be taken into account are the geology of the reservoir (eg. faults), the desired accuracy of the model, the specifications of the available hardware and the accepted execution time of the simulation runs (K Aziz, 1993; O. Pettersen, 2006).

The available grid system options are:

1. Cartesian
2. Orthogonal corner point
3. Non-orthogonal corner point
4. Radial grid
5. Quick-pattern grid

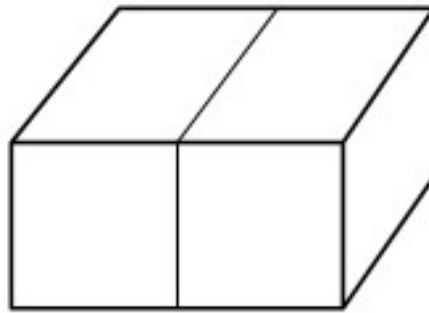
The grid systems are divided into two main categories based on their geometry: the block centered and the corner point grids. The main difference of these two categories is the point where the calculation of the flow term is performed between two adjacent blocks. When using the block centered geometry (eg. Cartesian grid) the calculation is performed between the block centers of the two blocks whereas when the corner point geometry (eg. orthogonal or non orthogonal corner point grid) is used the calculation is done at the center of the interface of these blocks. The simulation results using the two geometries may show a small difference (Fanchi, 2006). In corner point geometry, we should be careful when very irregular blocks (eg. the case of a non orthogonal corner point grid) are formed because this can cause errors to the computation of the flood front as well as problems concerning numerical stability (Fanchi, 2006). Aziz proposed that blocks should be kept as orthogonal as possible in any case (K Aziz, 1993).

The best grid system option with respect to the accuracy of the solution of the flow equation between adjacent blocks is the Cartesian but if we also care also for the accurate representation of the geology and the geometry of the reservoir other grid types should be used such as a corner point grid. By using a corner point grid, a good representation of the reservoir can be achieved by using less blocks (blocks fit better the reservoir geometry and it is not required to use many in order to achieve a better representation of the reservoir geometry) resulting in smaller simulation times (Abdou, Pham, & Al-Aqeell, 1993). As Abdou and Pham mentioned simulation with non orthogonal corner point and the Cartesian grid produced different results with respect to the calculated pressures (Abdou et al., 1993). As they reported, the values of the parameters that are used for history matching are different when using different grid systems (Abdou et al., 1993). Although when the grid blocks are more or less uniform and are close to the rectangular shape, there is no significant difference in numerical results between the Cartesian and the corner point grids (K Aziz, 1993; Computer Modelling Group Ltd, 2010). Finally, corner point grid is the most widely used grid system by the industry as it provides a better representation of the reservoir using less blocks (Chatzichristos, 2016).

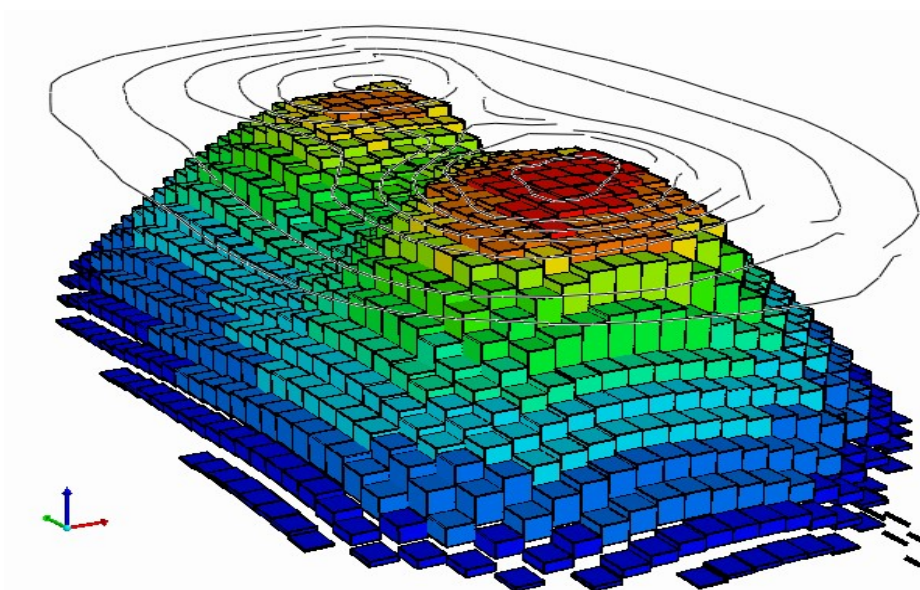
3.1.1 Cartesian Grid

This grid type is the first type of grid that was introduced in reservoir simulation. This grid is composed by rectangular blocks (picture 1) and it is included in the category of block-centered grids. Cartesian grid is not always able to represent the reservoir heterogeneities accurately (picture 2) (K Aziz, 1993; Abdou et al., 1993). Nowadays, is not used all that much by the industry because it can not represent accurately the reservoir geometry and only when a great number of blocks is used, this grid system is able to represent the

reservoir adequately but the simulation time and storage requirements increase dramatically and as a result its use is limited mainly for academic proposes (Chatzichristos, 2016).



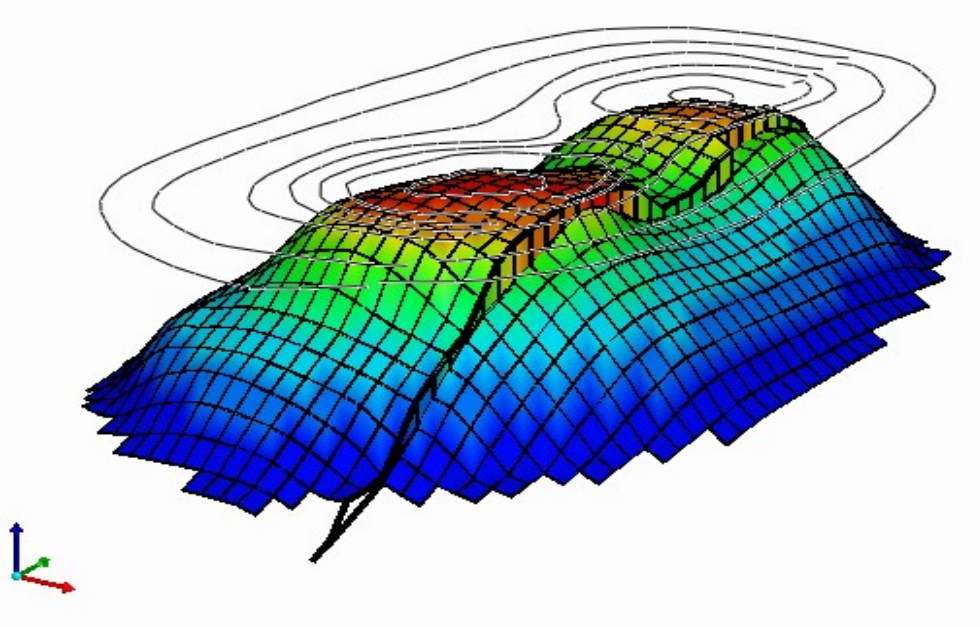
Picture 1: Blocks using the Cartesian geometry (Computer Modelling Group Ltd, 2010)



Picture 2: Graphical representation of a reservoir using Cartesian grid

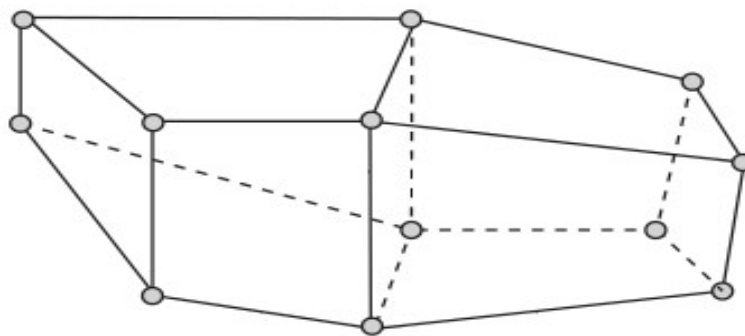
3.1.2 Orthogonal Corner Point

Orthogonal corner point grids (picture 3) are made by introducing to the simulator a mesh of rectangular blocks (picture 4), then this mesh is aligned to the main geological characteristics (eg. fault) and blocks are deformed where necessary so as to fit the reservoir geometric and geological characteristics (K Aziz, 1993). Thus blocks keep a shape as close as possible to orthogonal. Nevertheless, although the representation of a fault is made by aligning the coordinate lines with the fault in order the corners of the blocks to coincide with the fault axis in a reservoir with many faults that type of grid may not be able to represent the reservoir geology accurately.



Picture 3: Graphical representation of a reservoir using orthogonal corner point grid

Corner Point Geometry



Picture 4: Blocks using the corner point geometry (Watt Heriot University, 2005)

3.1.3 Non-Orthogonal Corner Point

By using a non-orthogonal corner point grid, blocks have much more irregular shape (are not rectangular) than orthogonal corner point grid, their faces are not always planar and intrusions of one block to another may occur (Computer Modelling Group Ltd, 2010). Blocks of this type of grid can be extremely distorted and as it was mentioned earlier the calculations can be more inaccurate than using the previous grid types and the required simulation time is greater but this grid type can fit perfectly every heterogeneity of the reservoir (Abdou et al., 1993). As a result, a more accurate calculation of the OIIP (oil initially in place) can be performed as well as a better representation of the flow paths can be achieved. It differs from the previous corner point grid model in the way its mesh is generated. In a non orthogonal corner point grid, the mesh is not predetermined and it is calculated by the simulator from user defined points with respect to the outer

boundary of the reservoir and to the geological features by using the outer and inner control lines respectively. Subsequently, by subdividing the created regions vertically and horizontally, a mesh is created (Computer Modelling Group Ltd, 2006). Moreover, it is the only grid system that allows mapping of sloping faults (the two planes slide on a curved surface) by selecting the sloping fault option. The ability of this grid type to model sloping faults is attributed to the fact that the created blocks can be triangular in shape so as to fit the curvature of a sloping fault (Kocberber, 1993). A sloping fault divides the reservoir in two different zones which are defined by introducing two different contour maps for each zone (one for the top and one for the bottom of each zone) (Computer Modelling Group Ltd, 2006).

3.1.4 Radial Grid

The radial grid is composed by centered rings, starting from the inner to the outer ring in the horizontal plane and can be divided counterclockwise to n_j sections where the coordinate system that is used is the cylindrical one (Computer Modelling Group Ltd, 2010). Radial grid is used only for refining the region around wells and cannot be used for representing the entire reservoir (Chatzichristos, 2016). The flow around wells can be better represented using this grid type since the flow away from the well's drainage areas is linear whereas around the wellbore is radial.

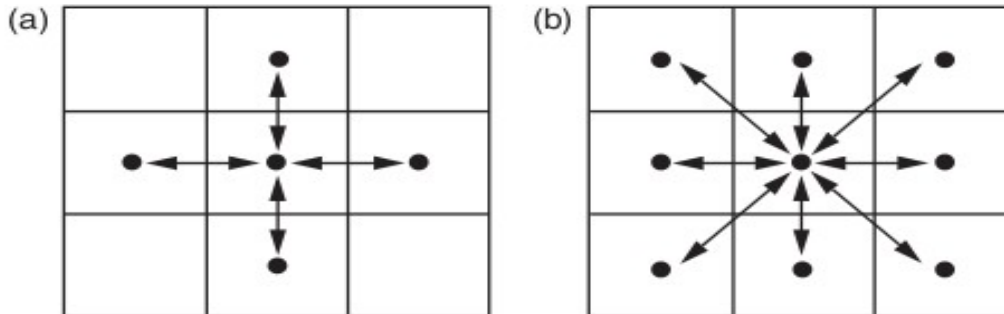
3.1.5 Quick Pattern Grid

It is a Cartesian grid which is used for representing a specific flood pattern such as the five spot flood pattern, nine spot and others (Computer Modelling Group Ltd, 2006). A flood pattern is a scheme where production and injection wells have to be placed with a certain pattern. For example a five point flood pattern is constructed by placing the production well in the center of a square with four injection wells symmetrically placed in the apices thus forming a square. This type of grid is created by introducing the reservoir area, the top and the thickness of the reservoir and the approximate block sizes in the simulator. With these data the simulator calculates the appropriate distance between the production and injection wells and place them accordingly so as to create the desired flood pattern (Computer Modelling Group Ltd, 2006).

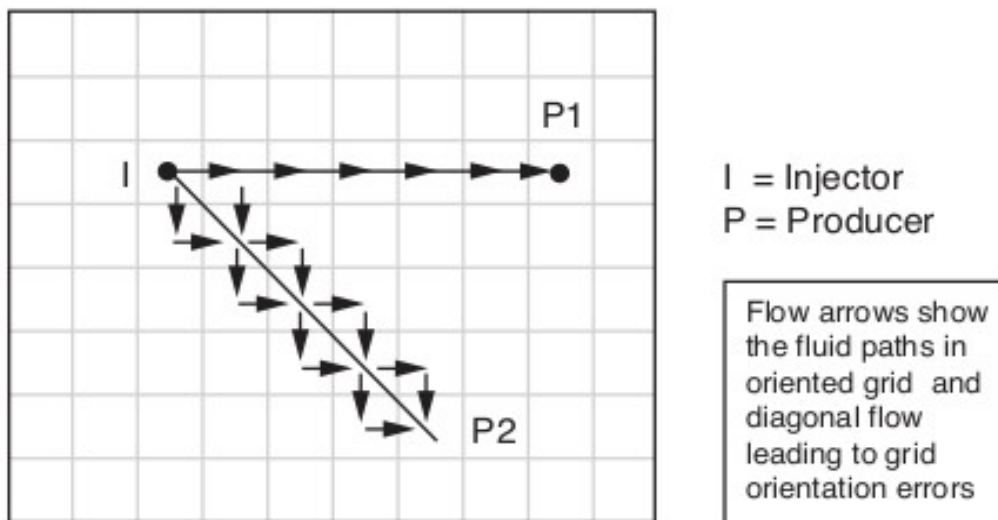
3.1.6 Grid Orientation Effect

In general, the flow equations between two adjacent blocks are not solved to zero due to numerical diffusion and as a result errors occur and propagate inside the reservoir and can be significant in some cases. These errors in a simulation study are expressed as grid orientation effect which is defined as the difference in recovery estimation due to the different flow paths that the simulator will calculate. The grid orientation effect is more pronounced in cases of sharp flooding fronts and in cases of diagonal flow using the five point finite difference grid (Khalid Aziz & Settati, 1979). When the five point difference grid is used, flow through

a block is permitted only by its faces whereas direct flow between diagonal blocks is not allowed and is simulated by zig-zag flow (pictures 5, 6). The grid orientation effect can be reduced either by using the nine point finite difference grid (flow through a block is permitted by its faces and its edges) or by refining the desired the blocks towards the direction of interest.



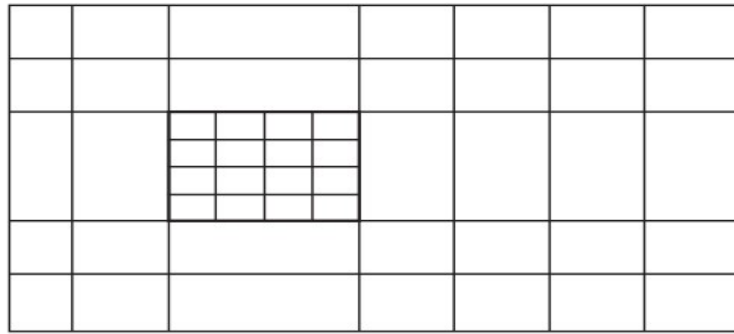
Picture 5: (a)Five point finite difference grid, (b)Nine point finite difference grid



Picture 6: Different flow paths due to the use of the five point finite difference grid

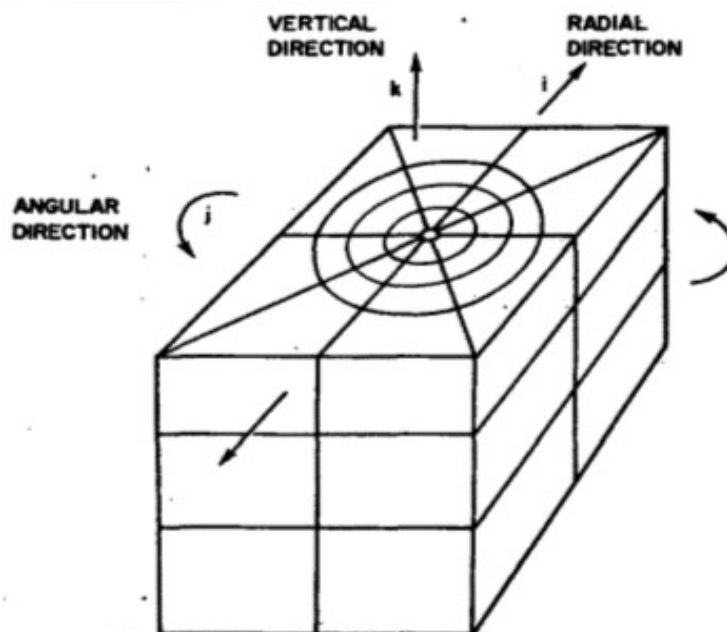
3.1.7 Grid Refinement

In general, grid refinement is used for the regions of a reservoir where rapid changes in saturations or pressures are expected to be encountered (K Aziz, 1993) and usually this is the case for the region around a well or where transition between the phases occurs (Fanchi, 2006). Grid refinement can be made using orthogonal or cylindrical blocks (hybrid grid refinement) (Computer Modelling Group Ltd, 2009a). Orthogonal refinement (picture 7) can be used in cases that a more detailed description of the reservoir and fluid fronts is needed (AAPG, 2016) or in order to reduce the grid orientation effect.



Picture 7: Orthogonal grid refinement

Hybrid grid refinement (picture 8) can represent better the radial flow that occurs around the well and provides a more accurate calculation of the saturation around a well (Pedrosa Jr. & Aziz, 1986).



Picture 8: Hybrid grid refinement around well (Heriot Watt University, 2005)

Refinement can also represent better the coning phenomenon around wells and calculate more accurately WOR and GOR (K Aziz, 1993). The main disadvantage of using hybrid grid is that the base grid should be Cartesian while orthogonal refinement can be used and with the other grid types (Computer Modelling Group Ltd, 2009a). Moreover when the refinement is designed the difference in dimensions between the refined and the base grid blocks has not to be that large so that the grid remains uniform (Soleng & Holden, 1998). In this way, the flow equations can be solved accurately enough without producing erroneous results due to the huge dimension differences between adjacent blocks (K Aziz, 1993).

3.1.8 Number of Blocks

The best method for the selection of the number of blocks is to run a sensitivity study using different block

sizes. By comparing the achieved results with the available data, the optimum block size is defined and it is the one that matches better with the results at the expense of a reasonable computational time (Correia, Ganguli, & Obaidi, 2015). Having defined the dimensions of blocks, the number of blocks is calculated by dividing the reservoir dimensions by the single block dimensions. Some guidelines for the selection of the block sizes are available depending on the layers of the reservoir, the fractures, the changes in pressure and saturation. In the case of a layered reservoir, the block height is defined by the thinnest layer so as to achieve a good representation of the layers (Correia, Ganguli, & Obaidi, 2015). In cases that pressures and saturations are changing rapidly, finer grids have to be used resulting in a larger amount of blocks. If the reservoir is naturally fractured, the block dimensions depend on the fracture spacing (Correia, Ganguli, & Obaidi, 2015). Moreover, the selected number of blocks depends on the variation of properties, in other words on the heterogeneity of the reservoir (Mattax & Dalton, 1990). Finally, Mattax and Dalton reported that the number of the vertical layers has an effect both on the recovery and displacement efficiency of the water/oil displacement process and a number of 12 to 20 blocks in the vertical direction is usually sufficient whereas in a typical reservoir 20 to 80 blocks in the horizontal direction are enough (Mattax & Dalton, 1990).

3.1.9 Dynamic Grid (Optional)

In cases of having moving fronts in the reservoir as it happens in water flooding or other IOR or EOR processes the need of having a better resolution at the front arises. This resolution could be achieved either by increasing the number of blocks or by using a dynamic grid. In general, to increase the number of blocks is not always a viable solution as it leads to a large amount of blocks which may overcome the computer computational capacity. On the other hand, using dynamic gridding does not require to increase the amount of blocks for the whole field as the simulator calculates internally by itself, usually at each timestep, which blocks have to be refined and refines them automatically. Thus, using the dynamic gridding method, great resolution of the area of interest can be achieved providing more accurate results without significantly increasing the simulation time and store requirements.

The dynamic grid calculations can be performed for the entire reservoir, towards specific directions or for some regions of the reservoir. In general, the fronts propagate horizontally and towards a certain direction in the reservoir and as a result the check for dynamic gridding towards the vertical or other directions than the one that the front propagates can be avoided saving in this way computational time. By using dynamic gridding there is the danger that refined regions such as those near wells that have to remain refined throughout the entire simulation time, can be de-refined by the simulator. In order to avoid the de-refinement of these regions the user has to introduce a distance around the wells to which the calculation of the dynamic grid will not be performed. Finally, dynamic gridding can be used only when the single porosity system is selected (Computer Modelling Group Ltd, 2009b).

3.2 POROSITY SYSTEMS

Reservoirs can be seen as unfractured (conventional) reservoirs and naturally fractured (NF) reservoirs.

Naturally fractured reservoirs have primary and secondary porosity whereas conventional reservoirs exhibit only primary porosity. Reservoirs with secondary porosity are mainly limestones or dolomites with fractures (T. P. Ahmed, 2010; Petrowiki, 2016). Fractures occur from tectonic activity (folding/faulting) due to stresses acting on the reservoir (Crain, 2016). As a matter of fact naturally fractured reservoirs exhibit folds and/or faults (Crain, 2016). Fractures follow the stress regime of the region and usually are parallel to the main axis of folds or faults but this is not necessary because in case of faults being present in the reservoir, fractures can also be perpendicular to the main axis of the fault (Crain, 2016). In addition, fractures appear to be generally vertical and horizontal fractures appear to be of limited extent (T. P. Ahmed, 2010; Crain, 2016).

For reservoir simulation depending on the fracture and matrix behavior, the reservoir porosity system can be classified into the following categories:

- Single porosity
- Dual porosity
- Dual permeability
- MINC
- Subdomain

The difference between dual porosity/dual permeability systems has to do with the different interaction between matrix blocks and fracture blocks:

- Single porosity: only matrix to matrix flow is allowed (fractures do not exist)
- Dual porosity: matrix to fracture and fracture to fracture flow is allowed
- Dual permeability: matrix to matrix, fracture to fracture and matrix to fracture flow is allowed
- MINC (Multiple INteraction Continua) and Subdomain: matrix to fracture, fracture to fracture flow and matrix to matrix flow only in the same gridblock is originally allowed (Huang, 2009). Nevertheless, the simulator offers the user the option to allow for matrix to matrix flow between different gridblocks by using 'the subdomain – dual permeability option in the subdomain' option (see § 3.5).

3.2.1 Single Porosity

This type of porosity system is mainly used for unfractured reservoirs (conventional). It can be also used to model fractured reservoirs by using gridblocks to account for fractures but this can increase dramatically the computational time and the storage requirements (Mattax & Dalton, 1990). In this case, the length of the fractures should be smaller or equal than this of the gridblock so that a naturally fractured reservoir can be described as accurately as possible by a single porosity model (Mao Bai, Elsworth, & Roegiers, 1993). Unfortunately this simplification may result to underestimation of the production and breakthrough time in

cases of water flooding (Baker & Kuppe, 2000). These errors arise from the fact that in a dual porosity/permeability model, flow occurs mainly through the high permeability fractures while in a single porosity model flow occurs only through the low permeability matrix (Baker & Kuppe, 2000).

3.2.2 Dual Porosity

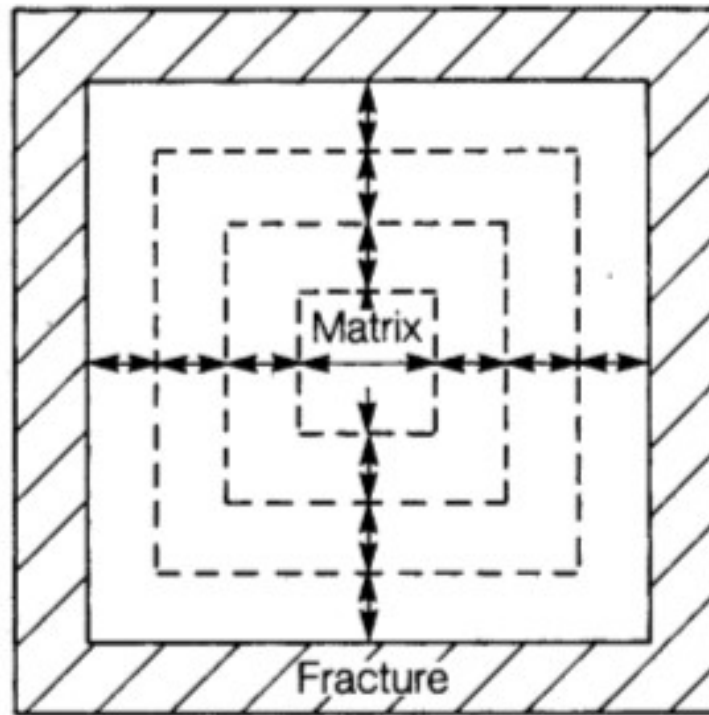
This type of porosity system is used for naturally fractured reservoirs where the matrix has very low porosity and permeability or high porosity but low permeability (in both cases flow cannot occur between matrix blocks) but it provides the necessary space for hydrocarbons storage while fractures have high permeability (but small storage capacity) so that fluids can flow easily through it (Mao Bai et al., 1993; Jack & Sun, 2003). By this type of porosity system, a layered reservoir with high contrast in permeability, which is the usual case of a tight reservoir, could be classified (Mao Bai et al., 1993; Gringarten, 1985; Schlumberger, 2016). As a result, this type of porosity system is used for highly fractured reservoirs where the matrix is completely discontinuous (Computer Modelling Group Ltd, 2009a). This type of behavior usually occurs in reservoirs such as dolomites, tight limestones/sandstones, volcanics, chalks, diatomites, siliceous shale (Jack & Sun, 2003) and vugular carbonates (layered reservoirs with high layered permeability contrasts) (Schlumberger, 2016).

3.2.3 Dual Permeability

This system is used to describe moderate to poorly fractured reservoirs, fractured brecciated reservoirs (Computer Modelling Group Ltd, 2009a), coal bedded methane (Thararoop, Karpyn, & Ertekin, 2012), carbonate reservoirs with super permeability (Al-Shaalan, Fung, & Dogru, 2003) and layered reservoirs where differences in permeability between the layers are not that significant (Gringarten, 1985). This system is the most accurate to model gravity drainage as it takes into account re-infiltration (is a parameter that affects gravity drainage and occurs when oil from the block above passes to the block below it) of oil from an upper matrix block to a lower one as well as the flow between matrix blocks (Collins, 1991). This is the case for reservoirs with gas cap where the vertical flow between matrix blocks has to be considered (Computer Modelling Group Ltd, 2010).

3.2.4 MINC

MINC (multiple interactive continua) was firstly introduced by Pruess and Narishman. It is used for non isothermal problems such as steam injection, EOR and geothermal reservoirs but can also be applied for isothermal problems such as water flooding (Pruess, 1992). In this porosity system each matrix block is divided into n subdivisions of nested rings and only the outer ring is connected to the fracture (picture 9) (Pruess, 1992).



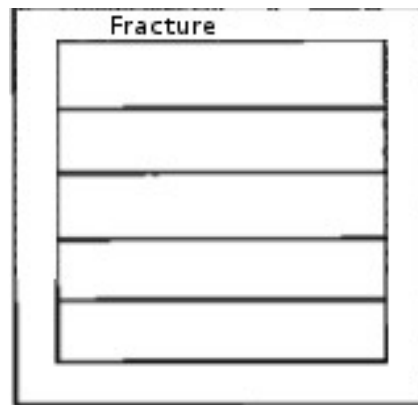
Picture 9: 2D representation of a matrix block using MINC model (Wu & Pruess, 1988)

The advantage of MINC to simulate more accurately these problems than the other systems comes from the subdivision of the matrix blocks which allows to treat fluid flow and heat conduction inside the matrix blocks and between matrix and fractures as transient (the disturbance at the matrix-fracture boundary is not felt immediately at the center of the matrix block) (Amiry, 2014; Wu & Pruess, 1988). The gradient of pressure, for example, in a nested ring depends on its distance from the closest fracture (Amiry, 2014). As Wu and Pruess have shown MINC matches better the production data than the dual porosity method for water flooding in cases of fractured reservoirs with matrix blocks of relatively low permeability. The same happens for water coning problems or when the flow rates are changing and as a result saturations in fractures change rapidly (Wu & Pruess, 1988). Nevertheless, its main disadvantage is that gravity cannot be treated correctly as along the vertical axis it behaves exactly the same as a dual porosity system (Amiry, 2014; Computer Modelling Group Ltd, 2010). Moreover, the MINC method is advantageous compared to the dual porosity one for water/oil imbibition processes especially in cases of low permeability large matrix blocks and heavier oils (Wu & Pruess, 1988). This is happening because a dual porosity model neglects the transient flow period assuming that the flow between matrix and fracture blocks is pseudo steady (Pruess, 1992). Nevertheless, these errors may not be that significant so as to justify the use of the MINC method immediately (Wu & Pruess, 1988). Finally, simulations using the MINC system require slightly more computational time than simulations using dual porosity systems (Wu & Pruess, 1988).

3.2.5 Subdomain

Subdomain porosity system is used in problems where gravity segregation of the fluids is significant

(Computer Modelling Group Ltd, 2010). Phase segregation occurs due to the difference in densities between reservoir fluids. The denser fluid will move to the bottom and the lighter will move towards the top of the reservoir (T. P. Ahmed, 2010) creating a saturation and pressure gradient (Beckner, Chan, McDonald, Wooten, & Jones, 1991). This method subdivides matrix blocks vertically (picture 10) creating a vertical stack of connected matrix blocks to account for these gradients (Beckner et al., 1991).



Picture 10: 2D representation of a matrix block using subdomain model (Collins, 1991)

A matrix block without subdivisions provide only an average value for saturation and pressure whereas a matrix block with subdivisions provides at distribution over the block (J.R. Gilman, 1986). Gravity segregation is more pronounced in reservoirs which are producing with pressure depletion and no actual pressure support (T. P. Ahmed, 2010). Reservoirs with intense gravity segregation usually are producing under combined gas cap drive and gravity segregation mechanism, they exhibit high GOR rates at the shallower wells of the reservoir and the water production if existing is small (T. P. Ahmed, 2010). This porosity system could also represent a layered reservoir with tight layers (Collins, 1991) where flow is mainly horizontal through fractures or a reservoir where large blocks in the simulation model have been used and gravity segregation or temperature distribution are of main interest (J.R. Gilman, 1986). In conclusion this model provides an accurate representation of this phenomena without using huge amount of blocks thus saving storage and computational time (J.R. Gilman, 1986). The subdomain system gives similar results with the dual permeability model (L. Collins, 1991; Computer Modelling Group Ltd, 2010) but for tight reservoirs the use of subdomain model is more effective otherwise a huge amount of gridblocks has to be created so as to achieve adequate resolution (Collins, 1991).

In conclusion, in the industry, single porosity is used most of the time and in cases that faults are present in the reservoir they are included in the model (without considering about fractures present in the vicinity of the faults) whereas the naturally fractured reservoirs are represented with the dual porosity system (Chatzichristos, 2016). The remaining aforementioned porosity systems are used rarely and mainly when the production data can be matched better by using them (Chatzichristos, 2016). This is happening as these porosity systems require much more computational effort and simulation time to give slightly more accurate

results.

3.3 SHAPE FACTOR

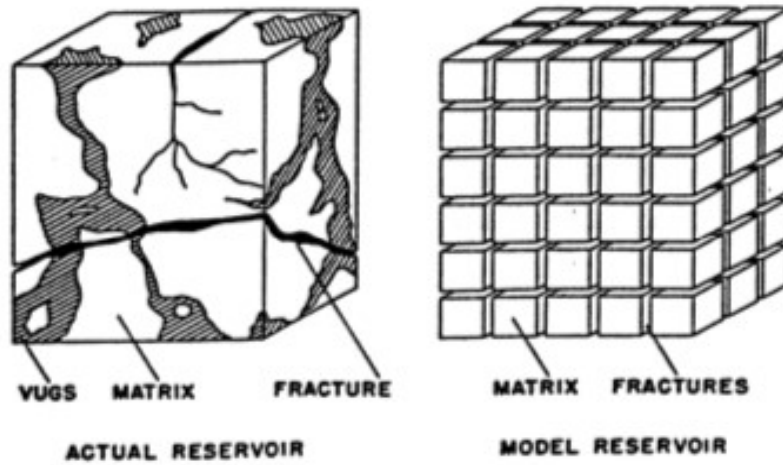
In single porosity models, permeability is enough to account for the flow but this is not the case in dual porosity/permeability models where we have to account also for the matrix to fracture flow (T. P. Ahmed, 2010). The shape factor (σ) is a geometry dependent factor which is similar to transmissibility, which refers to the ease of mass transfer between two blocks, but the former accounts for the ease of mass transfer between the two different media (matrix and fractures) (Ranjbar & Hassanzadeh, 2011; Sonier, 1988). Transmissibility is used for the calculation of the mass exchange between two adjacent blocks whereas, the shape factor is used for the calculation of the mass exchange from matrix to fractures. This factor depends on the shape and the size of matrix blocks, the pressure gradient from fracture to the center of the matrix block and on the fracture spacing (B. Ramirez, H. Kazemi, 2009; James R. Gilman, 2003; Sarma & Aziz, 2006). The mass exchange between matrix and fractures also depends on fluid expansion, viscous displacement, capillary and gravity forces (T. P. Ahmed, 2010). The two proposed equations for the shape factor that are used widely in industry are the following:

- Warren and Root
- Gilman and Kazemi

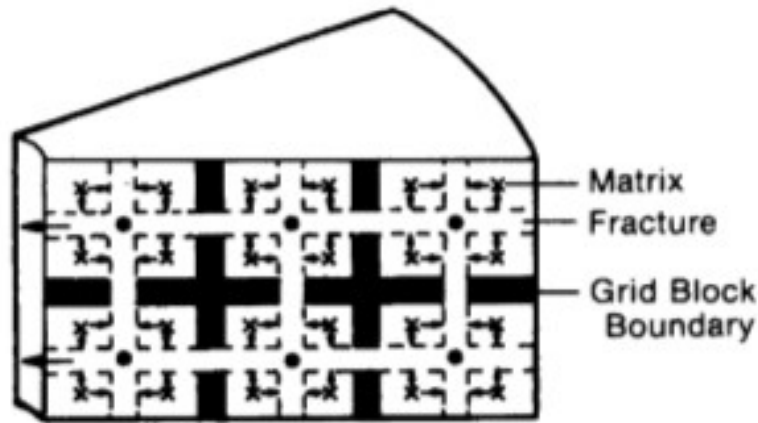
Finally, there is not a single rule for the selection of the shape factor formula and the selection depends on what matches better the production data (Chatzichristos, 2016).

3.3.1 Warren And Root

This shape factor model was firstly proposed in 1969 by Warren & Root and their equation was developed for pseudo steady state flow of a single-phase fluid and as a result is not taking into account gravity and capillary forces (Warren & Root, 1963). Warren-Root shape factor assumes that a certain reservoir matrix can be represented as rectangular blocks also known as 'stack of sugar cubes' representation (picture 11, 12) while fractures are parallel to the coordinate axes and as a result they are also parallel to the permeability axes (Warren & Root, 1963).



Picture 11: Representation of a fractured block by Warren-Root (Warren & Root, 1963)



Picture 12: Graphical representation of the gridblocks when the Warren and Root shape factor is used (Gilman & Kazemi, 1983)

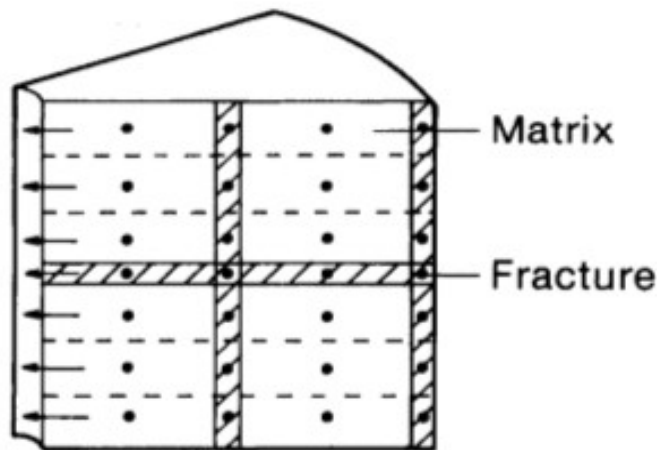
Fractures in contrast with matrix are thought as anisotropic which means that toward different directions they can vary in width and space but along the same direction they have the same width and are equally spaced between matrix blocks (Warren & Root, 1963). The Warren & Root equation for the calculation of the shape factor was mainly developed for well testing and this is its main application (Warren & Root, 1963; Zimmerman, 2005). The equation used by the simulator for the calculation of the shape factor according to Warren & Root is:

$$\sigma = \frac{20}{3} \cdot k \cdot \left(\frac{1}{L_x} + \frac{1}{L_y} + \frac{1}{L_z} \right)^2 \cdot V_m$$

where σ is the shape factor, k is the permeability, L_x , L_y and L_z are the fracture spacing values towards the three directions and V_m is the total matrix volume (Computer Modelling Group Ltd, 2010).

3.3.2 Gilman And Kazemi

Multiphase flow occurs in the majority of the reservoirs and as a result the shape factor of Warren-Root, that was developed for single-phase flow has to be modified. This need comes from the fact that in single phase flow, gravity, viscous and capillary forces are not of great importance thus there is no need to account for them but in cases of multiphase flow this assumption is not valid (Gilman & Kazemi, 1983). In multiphase flow, gravity and capillary forces may have a significant effect (Gilman & Kazemi, 1983). Especially in cases of water flooding and reservoirs that are producing under gas drive mechanism or gas injection, capillary and gravity forces play an important role in recovery (B. Ramirez, H. Kazemi, 2009; Sonier, 1988). Firstly Kazemi et al modified the Warren-Root shape factor so as to include gravity effects and two phase flow of oil and water (Kazemi, Merrill Jr, Porterfield, & Zeman, 1976; Sonier, 1988). Later Gilman and Kazemi altered the Kazemi et al shape factor so as to treat correctly multi phase flow problems such as flow of polymers, tracers and diagonal flow(the simulator assumes that the flow is perpendicular to the faces of a block) (Gilman & Kazemi, 1983; Sonier, 1988). In order to take into account these forces, the matrix blocks as they where designed by the previous shape factor have to be further subdivided as shown in the following picture.



Picture 13: Graphical representation of blocks when the Gilman and Kazemi shape factor is used (Gilman & Kazemi, 1983)

As a result, of the matrix block subdivision, the matrix blocks and the fractures are not lying at the same depth (Gilman & Kazemi, 1983). In that way, we can achieve a better resolution of the saturation profile and calculate the gravity force in each matrix subdivision of the 'parent' matrix block (Gilman & Kazemi, 1983). Moreover, this formulation for the shape factor takes into account the fact that from the matrix boundary to the matrix center the pressure gradient is not constant for a long time period due to the low permeability of the matrix block thus creating a transient flow inside the matrix block (B. Ramirez, H. Kazemi, 2009; Ueda, Murata, Watanabe, & Funatsu, 1989). From the previously mentioned it is obvious that the formula of the shape factor is altered in such a way so as to take into account the gravity and capillary forces as follow:

$$\sigma = 4 \cdot k \cdot \left(\frac{1}{L_x^2} + \frac{1}{L_y^2} + \frac{1}{L_z^2} \right) \cdot V_m$$
 ..Finally, Gilman and Kazemi is the most widely used formula for dual porosity and coal bed methane reservoirs (Mora & Wattenbarger, 2009).

3.4 FAULTS (OPTIONAL)

Faults are often present in reservoirs and have been created by tectonic activity. Faults are generally thought as barriers to fluid flow separating the reservoir into isolated sections but this is not always the case. Some faults can allow flow to occur through them. Faults are represented by the use of permeabilities parallel and perpendicular to the fault axis with the most important one to be the permeability normal to the fault axis (Jourde, Flodin, Aydin, Durlofsky, & Wen, 2002). The most important permeability value is the one perpendicular to the fault because this is the one that determines whether the fault isolates the reservoir regions adjacent to the fault faces or not (Jourde, Flodin, Aydin, Durlofsky, & Wen, 2002). The permeability of a fault is strongly dependent on the stress regime of the region, the temperature, the clay content of the fault and the burial depth of the reservoir while the modeling of the flow across a fault can be seen as a history matching procedure (Fisher & Knipe, 2001; Flodin, Aydin, Durlofsky, & Yeten, 2001).

3.5 ARRAY PROPERTIES-BUILD THE MODEL

This sub section includes parameters required to build the model. The required parameters may vary according to the initialization option (see § 6.1) and the porosity system that is selected. For example, when the user defined input initialization option is used, the reservoir pressure and the saturations of oil and water must also be defined in this sub-section. In the case that a dual porosity/permeability model is used, fracture permeability, porosity and spacing have also to be introduced. A parameter may be introduced for the entire reservoir or separate values can be defined for the different layers. The parameters that have to be included in all cases are:

1. Grid top

By this parameter the depth of the reservoir is defined by inserting a single value or by introducing a map of values. In that tab, if someone tries to input a value for the entire grid, Builder displays a warning message that layer overlapping may occur and suggests that is better to define a value for only one of the reservoir layers unless the reservoir layers are not continuous.

2. Grid bottom

Indicates the depth of the grid bottom. When grid top is defined this property is calculated internally.

3. Grid thickness

A single value of thickness can be defined or a map of thicknesses can be inserted to this keyword.

4. Grid paydepth

If the grid top is defined, the grid paydepth is calculated internally. The grid paydepths are assumed to be at the center of the blocks (Computer Modelling Group Ltd, 2010).

5. Grid centroid X, Y and Z

These values are calculated internally by the simulator once the depth is defined and indicate the coordinates of the block center.

6. Net pay

The net pay is the part of the reservoir that contributes to hydrocarbon production and its value depends on the porosity, the permeability and water saturation (T. P. Ahmed, 2010). It is calculated internally by the simulator once this information has been introduced and is thought to be counted between the centers of the blocks.

7. Net to gross ratio

It is defined as the ratio of the net pay thickness to the gross block thickness and it is calculated internally by the simulator from the net pay thickness (Computer Modelling Group Ltd, 2010).

8. Porosity

To this keyword, a single value of porosity can be defined or a map of porosity values can be inserted.

9. Permeability I, J and K

Indicates the input of permeability values towards each direction.

10. Oil and water saturation

The initial water saturation has always to be introduced whereas the initial oil saturation has to be introduced only in the case that the user defined initialization option is used.

11. Pressure

This option indicates the initial reservoir pressure. This keyword has to be entered only when user input initialization is used while in any other case the pressure is inserted in the respective field in the initial condition section.

In the case that different properties are encountered in different regions of the reservoir and these differences have been introduced into the simulator in the form of different sets of values then these sets of values have to be coupled with the corresponding region. For this purpose, Builder provides the following options:

1. Relative permeability set number (optional)

If multiple relative permeability Tables have been introduced to the simulator, by using this option, each Table is linked to its corresponding region of the reservoir.

2. Rock compaction set number (optional)

As in the previous option, here we may need again to introduce multiple rock compaction values or Tables. This option defines which set of values is going to be used for the selected region.

In case of a naturally fractured reservoir represented by a dual porosity, dual permeability, MINC or subdomain porosity model all the previously mentioned parameters can also be defined for the fractures. Moreover the following extra parameters have to be included:

- Fracture spacing I, J and K

Inputs the fracture dimensions in the 3D space.

- Fracture permeability

Inputs the permeability of the fracture. The fracture permeability is usually much higher than the matrix permeability and because it is difficult to be measured it is calculated as a function of the fracture width from the following formula:

$k_f = 8.44 \cdot 10^9 \cdot W^2$ (Thomas, Dixon, & Pierson, 1983), where when the width is given in centimeters the permeability is in millidarcies or when the width is given in inches the permeability is in darcies.

- Fracture porosity

Fracture porosity is determined with respect to the total volume of the reservoir from the following equation:

$\phi_f = \frac{V_f}{V_t}$, where V_f is the fracture volume and V_t is the total volume (T. P. Ahmed, 2010).

From the above equation it is evident that the fracture porosity is too small compared to the matrix porosity (M Bai, Ma, & Roegiers, 1994). Typical values of fracture porosity range from 0.0001 to 0.001 (Crain, 2016).

- Fracture pressure and saturations of oil and water

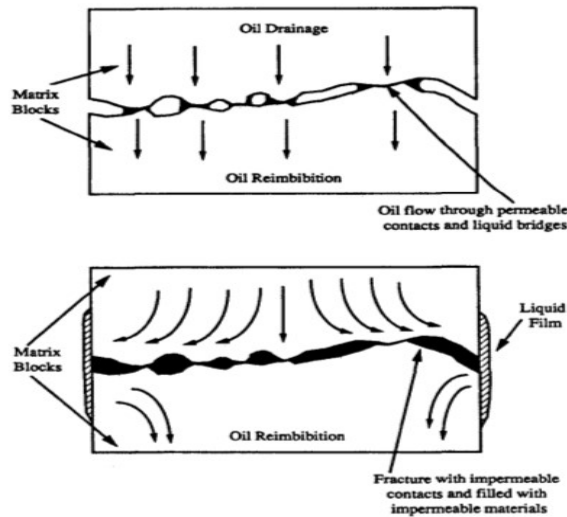
The fracture pressure and saturations were defined previously.

- Subdomain – dual permeability option in the subdomain (optional)

By this option, the Subdomain/MINC models (dual porosity models) are converted into subdomain/MINC models with dual permeability connection (Computer Modelling Group Ltd, 2010). That means that the matrix to matrix flow between different gridblocks does occur. In dual permeability subdomain the last matrix block of the stacked matrix blocks within a gridblock is connected to the first matrix block of the gridblock below it (Computer Modelling Group Ltd, 2010). This option allows gravity drainage to occur directly from subdomain to subdomain (Computer Modelling Group Ltd, 2010).

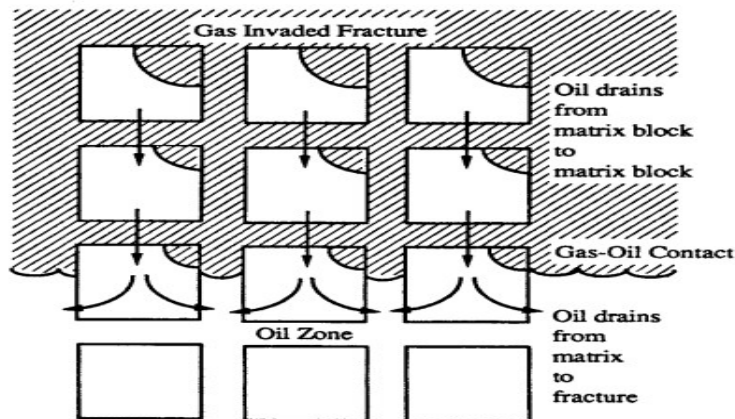
- Subdomain – dual permeability option re-infiltration parameter (optional)

Re-infiltration is a parameter that affects gravity drainage and occurs when oil from the block above passes to the block below it (Uleberg & Kleppe, 2011). This phenomenon is apparent for example in reservoirs that are producing under gas drive mechanism. Re-infiltration can be achieved through a liquid film across the matrix blocks or by liquid bridges (picture 14) (Uleberg & Kleppe, 2011) and can occur only if capillary continuity exists between the matrix blocks in which case, the re-infiltration parameter defines to which extent the matrix blocks are continuous (Fung, 1991).



Picture 14: Oil drainage and re-infiltration (Fung, 1991)

Values of one or zero for the re-infiltration parameter are normally used. A re-infiltration value equal to unity indicates complete matrix continuity while a value of zero indicates that the matrix is interrupted by fractures (Computer Modelling Group Ltd, 2010). If it is necessary to account for limited re-infiltration case values between the 0-1 range may be used. The degree of continuity between the matrix blocks can be assessed from the recovery efficiency of the gas displacement process due to the fact that gas existing in fractures displaces gradually the oil from the upper matrix block to the block below it (picture15) until this oil is produced (eg. production with gas cap drive) (Fung, 1991).



Picture 15: Oil drainage due to gas invading to the matrix blocks (Fung, 1991)

As a result, the higher is the oil recovery the higher is the matrix continuity and higher values of re-infiltration parameter has to be used (Fung, 1991). The capillary discontinuity is inserted by changing the capillary pressure of the bottom block by a scaling factor and it is calculated by the following formula:

$$P_{scale} = 1 - \text{re-infiltration parameter}$$

$$P_{COW} = P_{COW} \cdot P_{scale}$$

$$P_{COG} = P_{COG} \cdot P_{scale}$$

Finally, this option can work only if the subdomain model is converted to a dual permeability model.

In some cases, either for more accurate representation of the reservoir or for numerical stability reasons some blocks need to be treated in a more sophisticated way by the simulator. For this reason, Builder offers the following options:

1. Null blocks (optional)

There are two ways to indicate null blocks: either by setting porosity equal to zero or by using this option. Null blocks are not taken into account for the flow calculations and act as barriers because flow is not permitted to pass through them (Computer Modelling Group Ltd, 2010). Initially, all blocks are considered as active except if a block is flagged as null (Computer Modelling Group Ltd, 2010).

2. Pinch out array (optional)

This option is used to remove layers that are not needed in some regions of the reservoir but are present to other regions in the reservoir (Computer Modelling Group Ltd, 2010). For example, layers that are not present throughout the entire length of the reservoir can be removed by using this option. There are two ways to insert a pinch out array per dataset. The first is by using pinch out tolerance option (the tolerance of how close the blocks need to be so as to be considered that they are connected) and the pinched out blocks are calculated internally by the simulator. The other option is to insert the pinch out blocks by an array (in this way the pinch out tolerance option has to be deactivated) (Computer Modelling Group Ltd, 2009b). In pinch out arrays, blocks without thickness are inserted (Computer Modelling Group Ltd, 2010). Pinch out blocks, in contrast with the null blocks, allow the flow across them but they are not involved in any calculation (Computer Modelling Group Ltd, 2010). Finally, a block that initially was set as pinched out block can be altered and be set as null but the opposite is not allowed.

3. Block volume/ area modifier type (optional)

By this option, we can change the node of a block which is for example initially at its center and assign it to a corner or to a boundary. This is useful for blocks that are located on the reservoir boundary and their nodes originally lie outside the reservoir. By using this option, we can change their locations and put them on the reservoir boundary. The 'volume modifier option' is used, to assign null blocks (Computer Modelling Group Ltd, 2010). This option is used when there is need to model symmetry elements such as a nine point grid pattern (instead of a five point grid pattern) where the node has to be defined on the diagonal of the block indicating that diagonal flow also takes place (Computer Modelling Group Ltd, 2009a).

4. Implicit flag (optional)

It is used to define blocks which are going to be treated implicitly (Computer Modelling Group Ltd, 2010). The IMEX and GEM simulators use the adaptive implicit method by default. In adaptive implicit method, all blocks are treated explicitly (the calculation of a property is done directly) with the exception of a small number of blocks which are treated implicitly (the calculation of a property is done by using the trial-error method). These blocks are normally the well blocks and their neighboring ones around the wells where saturations and pressures change rapidly (Computer Modelling Group Ltd, 2010). In case we need to treat

implicitly more blocks than the aforementioned this option is utilized. This is useful for cases where the vertical equilibrium initialization (the saturations are averaged over the vertical extent of the block) is not used, something that may result in large changes in pressures and saturation. When a gas cap exists, the lower part of the gas cap has to be treated implicitly or at least to set implicit the regions where gas cusping occurs (Computer Modelling Group Ltd, 2010). Gas cusping is when the gas flows from the gas cap through an inclined geological strata towards the well (Petrowiki, 2015a). Finally, this keyword can be used for blocks exhibiting too high permeability and by a slight change in pressure, saturation exhibits extreme changes (Computer Modelling Group Ltd, 2010).

For the array properties sub-section the IMEX simulator also offers the following options:

1. Initial light oil volume fraction

This keyword is required by the simulator when the API-tracking component model which splits the oil to a light and to a heavy pseudo-component is used. By using this keyword, the initial light oil (the light pseudo-component of the API tracking component model) volume existing in the reservoir (measured at surface conditions) is introduced to the simulator. This keyword is used only with the API tracking model (see § 4.3.6) (Computer Modelling Group Ltd, 2010). The API tracking model assumes that the oil is composed by two parts a light and a heavy one (Computer Modelling Group Ltd, 2010). From the definition of the initial light oil volume, the initial heavy oil (the heavy pseudo-component of the API tracking component model) volume can be computed by: $initial\ heavy\ oil\ volume = 1 - initial\ light\ oil\ volume$ (Computer Modelling Group Ltd, 2010).

2. Solvent saturation pressure

This option is used when miscible flooding is used (see § 4.4.3) during which solvent is injected in the reservoir. As solvent saturation pressure is defined the pressure below which solvent is in the gas phase and has escaped from the water (for eg. for CO₂ miscible flooding the CO₂ escapes from the water phase) with which was initially mixed in order to create the displacing front of the miscible flooding. If the solvent saturation pressure is close to zero there is no solvent dissolved in the water phase (Computer Modelling Group Ltd, 2010).

3. Dispersion coefficient I, J and K

Dispersion coefficients denote the tendency of the molecules to be transferred from a high concentration area to a lower concentration area. This keyword is used when polymer injection is simulated and indicates the polymer dispersion coefficients. The oil recovery is affected because dispersion reduces the displacement efficiency of polymers (Sharafi & Jamialahmadi, 2016). Dispersion coefficients are regional and directional dependent and are affected by the transmissibility of the blocks (if transmissibility decreases, the dispersion coefficient decreases too) (Computer Modelling Group Ltd, 2009a). In cases that dispersion occurs, it may be necessary to run the simulation implicitly (Computer Modelling Group Ltd, 2009).

4. Veltab velocity multiplier

The fracture width correction factor is defined by the `veltab` keyword. This correction is mainly used for blocks which represent fractures and are not small enough to accurately model the velocities for a very small fracture width resulting thus to wrong polymer viscosity and concentration values for this block (Computer Modelling Group Ltd, 2010). This option is used only when the polymer model is used in the component section and the polymer-viscosity is calculated using Tables of polymer concentration and viscosity ratio defined for each velocity value (Computer Modelling Group Ltd, 2010).

5. PVT type (optional)

Multiple PVT regions can be introduced to the simulator in sections representing different properties to different regions of the reservoir. This option is used to determine which PVT tables introduced in the components section will be used to each layer.

6. Initial polymer concentration (optional)

By this keyword, the initial polymer concentration is introduced in the simulator. The initial polymer concentration is usually zero as polymers do not initially exist in the reservoir. As a result this keyword can be used when a second cycle of polymer injection in the reservoir takes place.

7. Initial seawater fraction (optional)

This keyword can only be used when seawater injection is to be applied in order to determine the initial seawater that already exists in the reservoir. Usually this value equals zero because only formation water (connate) is present in the reservoir.

For the array properties sub-section, the GEM simulator also offers the following options:

The extra options that GEM offers are the following:

1. Global composition

By this keyword, the composition of the reservoir fluid is introduced in the simulator.

2. Rock density

By this keyword the density of the rock is defined.

3. Longitudinal, transverse dispersivity

This keyword is used for coal bed methane production.

4. Isotropic dispersivity

This keyword is used when the longitudinal and the transverse dispersivity are identical.

5. EOS set (optional)

Multiple EOS sets can be introduced to the simulator representing different properties to different regions of the reservoir. This option is used to determine which EOS set will be used to each layer.

6. Block temperature (optional)

By using this keyword the temperature of specific regions of the reservoir can be altered to a desired value.

3.6 ROCK COMPRESSIBILITY

During the production life of a field, the reservoir pressure drops and as the overburden pressure remains stable compaction is more intense resulting in consolidation of the pores (M. Carlson, 2003). Rock compressibility is defined as the ratio of grains volume change due to one psi pressure change and increases with load (T. P. Ahmed, 2010; Schlumberger, 2016a). Rock compressibility is measured by loading the sample in a way similar to the one by which the stress is applied to the reservoir (Lewis & Gutierrez, 1998). By this keyword, the so measured value of rock compressibility is introduced to the simulator at reference pressure. In reservoir simulation, as rock compressibility we refer to the formation compressibility which might range between 3×10^{-6} to 25×10^{-6} psi^{-1} whereas the maximum value of rock compressibility accepted by the simulator is 6.89×10^{-3} (T. P. Ahmed, 2010; Computer Modelling Group Ltd, 2010). It should be mentioned that when a dual porosity or dual permeability model is used the fracture compressibility has to be inserted too. Rock compressibility is required by the simulator for the calculation of the compaction drive mechanism in the material balance equation. These phenomena occur during the exploitation of a field by changes in reservoir pressure occurring by production or injection of fluids (Fanchi, 2006; Longuemare et al., 2002).

GEM simulator takes into consideration phenomena such as expansion and shrinkage of the rock with temperature and for this reason it also includes the thermal expansion coefficient of formation porosity (represents the expansion of the rock occurred by temperature changes), the reference temperature at which the thermal expansion coefficient is entered and the pressure-temperature cross term coefficient of formation porosity.

3.7 COMPACTION-DILATION (OPTIONAL)

Compaction and dilation phenomena can occur to a reservoir during different periods of its production life or simultaneously in different areas of the reservoir as they are two opposite phenomena. In general, in reservoir simulation, these processes are thought to be related to the fluid pressure assuming that the total stress acting on the reservoir is constant (M. Carlson, 2003). Compaction occurs by the tighter packing of grains due to the stress acting on the reservoir and the fluid production and constitutes a drive mechanism for many reservoirs (Pettersen, 2005). On the other hand, dilation occurs due to injection and indicates the widening of the pores. Increases and reductions of rock compressibility with pressure indicate dilation and compaction phenomena respectively (Beattie, Boberg, & McNab, 1991). The primary force that acts on the reservoir and causes compaction is the overburden pressure but also lateral forces may acting on it (T. P. Ahmed, 2010). As

a result, pressure is not uniformly distributed and each region of the reservoir may be subjected to different amount of stress or stress may act toward different directions, causing thus, reservoir to deform in a non uniform way (T. P. Ahmed, 2010; Lewis & Gutierrez, 1998). Nevertheless, the best method for modeling compaction is to couple the flow simulator with a geomechanical simulator (Fanchi, 2006; Ø. Pettersen, n.d.).

3.7.1 Compaction

Compaction can have a severe economical impact on the project and an accurate knowledge of this phenomenon is of major importance. Firstly having a good knowledge of the compaction effects makes it easier to determine the required injection pressure so as to support the reservoir pressure (Pettersen, n.d.). Moreover, when extended compaction occurs it can cause surface subsidence or destruction of the wells (Longuemare et al., 2002). Depending on the grain packing level of the reservoir, compaction has different effects. Reservoirs may be classified into two categories with respect to the level of the grain packing:

- Weakly or poorly compacted

This reservoir category exhibits a high content of weak sands and compaction constitutes the main drive mechanism having a positive effect on production (Longuemare et al., 2002). Due to grain packing compaction in weak sandstone reservoirs should be thought as an irreversible process (Pettersen, n.d.).

- Highly compacted

These reservoirs are usually fractured or exhibit faults and obviously are also influenced by the regional stress regime (Longuemare et al., 2002). In these cases the effects of compaction are not all that intense and compaction can be thought as a reversible procedure (Longuemare et al., 2002).

The modeling of compaction phenomena can be done either by using a single rock compressibility value at a reference pressure or by using Tables of porosity and permeability values with pressure. The selection of the method that will be used depends on the availability of data although the second method is thought as more accurate and it can model both reversible and irreversible compactations. For modeling a reversible compaction, Builder allows users to enter the following Tables:

1. Main Table

The entered values in these Tables are pressure versus porosity multipliers and permeability multipliers. These multipliers are used so as to modify the porosity and the permeability values in order to model compaction.

2. Hysteresis Table (one or more Tables)

The entries of this Table are the same as of the main Table. This Table refers to re-compaction of the reservoir. For an irreversible compaction only the main Table is allowed to be entered.

From these Tables, porosity and permeability can be calculated as follows: $\varphi = \varphi_{ref} \cdot \left(1 + c_r \cdot (P - P_{ref})\right)$, where φ_{ref} is the porosity value at the reference pressure, c_r is the rock compressibility and P_{ref} the reference

pressure at which the rock compressibility was measured.

3.7.2 Dilation

Dilation occurs due to injection. As fluid is injected into the reservoir, it applies an opposite force to the compressive force that acts on the reservoir and as a result the total acting stress is reduced (Beattie et al., 1991). Due to the fact that the reservoir pressure increases pore spacing also increases and dilation may cause an uplift on surface (Beattie, Boberg, & McNab, 1991). Sometimes, dilation may also occur by hydraulic fracturing when the fluid pressure inside the fracture exceeds the rock failure pressure resulting in widening of other fractures already present in the formation (Rahman, Hossain, & Rahman, 2002). The Tables that are available in Builder in order to model dilation can reproduce a complete unloading-reloading procedure although it is not obligatory all Tables to be inserted (Computer Modelling Group Ltd, 2010). There are three combinations with respect to the Tables that can be entered:

1. Only the elastic Table can be entered
2. The elastic, dilation and unloading Table
3. All the Tables

The offered Tables by the simulator are the following and their entries are the same as those of compaction Tables:

1. Elastic Table

The rock is acting in the elastic zone where the process is thought to be reversible. When a rock acts in its elastic region it means that by removing the acting stress the rock returns to its original shape.

2. Dilation Table

Rock in this region exhibits plastic behavior, the deformations are constant and after the removal of the load rock compressibility increases.

3. Unloading Table

By decreasing the pressure, the rock follows the unloading path. In case that pressure increases again, the same path will be followed until the dilation path is met again (Computer Modelling Group Ltd, 2010).

4. Re-compacting Table

When the pressure acting on the rock decreases to a value lower than the lower pressure in the unloading Table the rock will follow the re-compaction path (Computer Modelling Group Ltd, 2010). When the rock is acting in this region, the rock compressibility decreases with decreasing pressure values.

5. Reloading Table

In the case that after re-compaction the pressure in the rock increases again, the rock compressibility increases with increasing pressure values and the rock acts in the elastic zone until to meet the dilation path where the rock exhibits plastic behavior.

For the GEM simulator, thermal rock properties (thermal option) can be also included as an additional model

is available to be used namely the Palmer and Mansoori one. The thermal option accounts for the heat losses from fluid to rock and includes the rock heat capacity and rock fluid thermal conductivity keywords. As rock heat capacity is defined the amount of energy that it is needed in order to increase the rock temperature by 1 degree and gives a measure of the ability of the rock to store heat whereas by the thermal conductivity keyword the ability of the rock and the fluid to transfer heat is defined.

The Palmer and Mansoori model is mainly used to model the changes in permeability due to changes in rock compressibility and matrix volume in coal bed methane (CBM) reservoirs. In order to use this model, the following should also be used:

- Young's modulus used to calculate pore compressibility (E)
- Poisson ratio used to calculate ratio of bulk to axial modulus (ν)
- Strain at infinite pressure (when the component depended also for each component) (ϵ_L)
- Langmuir pressure (when the component depended also for each component) (p_L)
- Palmer-Mansoori exponent (α).

3.8 AQUIFERS (OPTIONAL)

The majority of the reservoirs are connected with an aquifer that was formed during the migration of hydrocarbons into the reservoir and the displacement of the water that was initially resident there. Usually, the aquifer's properties are estimated from the production data because: (a) it is not economic to drill wells into the aquifer so as to obtain data about their extent and properties and (b) it is impossible to know if other aquifers exist in the nearby region and are inter-connected (T. P. Ahmed, 2010). As a result, the modeling of an aquifer from all aspects is mostly a history matching task (Chatzichristos, 2016). The aquifers are connected directly to the reservoir blocks. Here it has to be mentioned that when a dual porosity/permeability porosity system is used the aquifers are connected with the fractures (Computer Modelling Group Ltd, 2010). There are three types of aquifers with respect to their relative position to the reservoir and their connection points with it:

1. Bottom

The aquifer is connected to the bottom of the reservoir. This type of positioning of the aquifer is frequently encountered in reservoirs with large areal extent with a water-oil contact underlying the reservoir (T. P. Ahmed, 2010). The outflow from a bottom aquifer is mainly vertical (Ahmed, 2010).

2. Edge

The aquifer of this type is connected to some specific regions of the reservoir boundaries entered by the user.

The flow of an edge aquifer is restricted mainly in the horizontal plane with negligible vertical flow (Ahmed, 2010).

3. Regional (Boundary)

The aquifer is connected to the boundaries of the reservoir encircling it. The flow direction of a regional aquifer is restricted mainly to the horizontal (Ahmed, 2010).

Moreover, aquifers can be classified based on their areal extent as of infinite and finite extent. Infinite aquifers assume that the pressure disturbance felt on the reservoir-aquifer interface does not reach the aquifer external boundary during the production history (T. P. Ahmed, 2010). Finite aquifers assume that the pressure disturbance felt on the reservoir-aquifer interface reaches the aquifer external boundary after some time. Usually, the aquifers that have huge areal extent compared to the reservoir are modeled as infinite extent aquifers whereas as finite extent aquifers are classified those that exhibit a small areal extent in comparison with the reservoir (Kinawy, 2016). In general, infinite extent aquifers provide the required pressure support whereas finite aquifers are not able to support appropriately the reservoir pressure (Kinawy, 2016). The classification of an aquifer as finite or infinite is based on the R-ratio which is defined as the ratio of the aquifer radius to the reservoir effective radius (Marques, Petrobras, Trevisan, & Unicamp, 2007; Computer Modelling Group Ltd, 2010). Aquifers with $R < 5$ are thought to be of finite extent whereas aquifers with $R > 5$ are thought to be of infinite extent (Marques, Petrobras, Trevisan, & Unicamp, 2007). Finally, it has to be mentioned that from the above definition an aquifer with $R < 5$ can be modeled as infinite when its permeability is extremely low and the pressure disturbance cannot reach its boundary within a finite time.

In addition to the above categorization aquifers can also be classified with respect to the way that the water influx is calculated by the simulator. In Builder two types are available:

- Numerical aquifers

When a numerical aquifer is used, some blocks are set to be filled with water and to be connected with the reservoir. This modeling type provides the most accurate results but it requires much more computational time because additional blocks have to be inserted in the model accounting for the aquifer (Fanchi, 2006). Moreover numerical aquifers can properly represent flow from the reservoir back to the aquifer occurred by an increase of the reservoir pressure (Computer Modelling Group Ltd, 2010).

- Analytical models

By using an analytical model, the results are provided by using a mathematical model. They provide almost the same results as the numerical models but they need less computational time (Computer Modelling Group Ltd, 2010). Although problems can arise when the leakage from the reservoir back to the aquifer has to be modeled which is a phenomenon that cannot be properly modeled by analytical aquifers. As a result, in this case, it is better to use numerical aquifers when the pressure inside the reservoir is expected to increase

considerably (Computer Modelling Group Ltd, 2010).

Several analytical models have been developed so as to calculate the influx of an aquifer into the reservoir. The most precise solution is thought to be derived from the model that Van Everdingen and Hurst proposed whereas all the other methods are thought as approximations of this approach (T. P. Ahmed, 2010). Unfortunately, this model is not used often due to the fact that its use increases extremely the required computational time (Marques, Petrobras, Trevisan, & Unicamp, 2007). The following four options are available by Builder for the simulator to calculate the aquifer influx into the reservoir:

1. Carter-Tracy(finite and infinite extent)

Builder gives the option of Carter-Tracy's model for finite as well as and for infinite aquifer systems. Carter and Tracy introduced their model in 1960 which can be thought as a simplification of the van Everdingen and Hurst one as it eliminates the use of superposition (Carter & Tracy, 1960; Lee & Wattenbarger, 1996; Marques et al., 2007). The Carter-Tracy method assumes transient flow and constant influx rate from the aquifer to the reservoir (Carter & Tracy, 1960). It solves the problem by using Tables of pressure drop for different influx time periods. Although the Carter-Tracy model is available also for finite aquifers, in a comparative study performed by Marques et al, where the Carter-Tracy and the Fetkovitch model were compared it was concluded that the Carter-Tracy model is not appropriate for small aquifers ($R < 5$) as it was producing six times higher error in the calculation of the water influx than the error produced by using the Fetkovitch model (Marques et al., 2007). This method seems to be preferred for aquifers that are connected to the edges of the reservoir (Lee & Wattenbarger, 1996).

2. Fetkovitch

Fetkovitch in 1971, introduced a model so as to describe the water influx from a finite aquifer assuming pseudo steady state flow from the aquifer to the reservoir (Marques et al., 2007). This assumption does not take into account the transient flow period (Fetkovich, 1971). This method is mainly used for finite extent aquifers as for $R > 5$ the produced errors can be huge (Marques et al., 2007). In general, this model is appropriate for any type of connection between the reservoir and the aquifer (Lee & Wattenbarger, 1996).

In the aquifers sub-section, thickness, porosity, permeability, radius and angle of the aquifer are also required so as to appropriately model an aquifer. The thickness for aquifers connected to the boundary and to a region of the reservoir is defined as the average thickness of the aquifer while for bottom aquifers it is defined as the square root of the contact area between the aquifer and the reservoir (Computer Modelling Group Ltd, 2010). The radius for boundary aquifers is defined as the radius of the circle whose circumference, when multiplied the thickness gives the contact area of the aquifer and the reservoir. For a bottom aquifer, as radius of the aquifer is defined the square root of the area of a side of the reservoir divided by π whereas for a regional aquifer the radius is defined as the square root of the contact area divided by π (Computer Modelling Group

Ltd, 2010). As angle of the aquifer is defined the contact angle of the aquifer-reservoir and it is a fraction of a full circle (Computer Modelling Group Ltd, 2010).

3.9 HISTORY MATCHING TOOLS

3.9.1 Sectors, Flux Sectors And Lease Planes

Sectors, flux sectors and lease planes are used in cases of naturally fractured reservoirs, history matching is a difficult task as the number of the available parameters that can be adjusted is huge (Saidi, 1983). This procedure can be simplified by splitting the reservoir into sectors and study the behavior of each sector separately (Saidi, 1983). By using sectors, the variation of the parameters values at different reservoir parts is more pronounced and as a result a first estimation of the parameters, that have to be used so as to match the production history can be done more efficiently. The input of the blocks can be done by assigning the blocks by their number or by selecting an area on the map. Sectors are user defined groups of blocks that are used to calculate and display statistics for specific regions in the reservoir (Computer Modelling Group Ltd, 2010).

Flux sectors are similar to sectors but they display only the flow that takes place into this sector (Computer Modelling Group Ltd, 2010). The influx to a sector is calculated in the direction of flow from the blocks neighboring to this sector. If two flux sectors share a boundary then the flow from the one flux sector to the other is calculated (Computer Modelling Group Ltd, 2010). In the GEM simulator flux sectors are not available.

Lease planes are used to summarize and report the fluid flow across planes or regions (Computer Modelling Group Ltd, 2010). The definition of blocks that constitute a lease plane is done as in the case of sectors but in this case the direction of the lease plane has to be defined as perpendicular to the flow direction. The simulator allows more than one blocks to be defined only for the two of the three directions whereas towards the third dimension (the flow direction), the simulator allows only one block to be inserted. In the GEM simulator, lease planes are not available.

3.9.2 Array Properties- History Matching

Builder also provides some parameters that are used only for history matching (Technical Support, 2016). These parameters are the following:

1. Net to gross ratio

The net to gross ratio can be also used as a history matching parameter so as to modify the porosity and

permeability in the I and J direction by multiplying these values with the net to gross multipliers (Computer Modelling Group Ltd, 2009a). Finally, this option of changing the net to gross ratio value denotes that less or more pores from those originally calculated by the simulator actually contribute to the hydrocarbon storage and fluid flow.

2. Delta threshold I, J and K direction

By using this keyword, a pressure value is introduced on the boundary of the block below which flow between two adjacent blocks cannot occur (Computer Modelling Group Ltd, 2010). In case that pressure exceeds that value, flow starts and the block remains open to flow (Computer Modelling Group Ltd, 2010).

3. Initial water saturation

Indicates the water saturation that is present in some regions of the formation and it is different from the connate saturation.

4. Trans multiplier I, J and K

Transmissibility accounts for the ease of flow between two adjacent blocks. The transmissibility multipliers are being used for the calculation of flow from the block I to the block I+1.

5. Low side transmissibility multiplier I, J and K

The low side transmissibility multipliers are the opposite from the transmissibility multipliers and can be used in cases where reversals in flow direction may occur. The low side transmissibility multipliers are being used for the calculation of flow from the block I to block I-1 (Computer Modelling Group Ltd, 2009a). Finally, for dual porosity models due to the fact that matrix to matrix flow is not taken into account this keyword cannot be used (Computer Modelling Group Ltd, 2009).

6. Endpoint saturations

Endpoint saturation refers to the saturation at which the relative permeability curves obtain values of zero. These options are used to introduce the endpoint saturation values that may be found in the reservoir. It is a history matching parameter and is used in the regions of the reservoir where the provided data from the laboratory do not fit with the production data.

a) Connate gas, liquid and water saturations

Refers to the lowest saturations of these phases that are found in situ. These saturations have to be compared with the critical saturations so as to determine if the fluid at that saturation is mobile or not.

b) Critical gas and water saturations

Critical saturation refers to the saturation value that when exceeded the fluid becomes mobile. These values can be close enough to the connate saturation values or to exhibit a significant difference in low permeability reservoirs where the critical saturation of water for example may exceed 60% (Ihrdc, n.d.) whereas this saturation is between 5 and 40% (NMT, 2010). Critical gas saturations range from zero to 20% (Petrowiki, 2016a).

c) Irreducible oil saturation for gas - liquid and water - oil Table

Irreducible saturation is the lower oil saturation value that can be achieved when the oil is displaced by gas or water (Schlumberger, 2017b).

d) Residual oil saturation for gas – liquid and water – oil Table

Residual saturations are the ones that remain into the reservoir after the primary and secondary production has ceased (Petrowiki, 2016a).

e) Maximum residual oil saturation for water oil system

This option refers to the maximum residual oil saturation after an imbibition process. This value represents the oil saturation that has remained after an imbibition process that has started from the maximum oil saturation that existed in the reservoir. This is a history matching parameter used when modeling hysteresis (see § 5.6) (Computer Modelling Group Ltd, 2010).

7. Relative permeability of gas (k_{rg}) at connate liquid concentration, relative permeability of oil (k_{rog}) at connate gas, relative permeability of oil (k_{ro}) at connate water saturation and relative permeability of water (k_{row}) at irreducible oil

The relative permeability of gas (k_{rg}) at connate liquid concentration, relative permeability of oil (k_{rog}) at connate gas, relative permeability of oil (k_{ro}) at connate water saturation and relative permeability of water (k_{row}) at irreducible oil keywords are history matching options which allow users to enter different values than those obtained by the laboratory displacement tests in regions of the reservoir that exhibit peculiar behavior (Technical Support, 2016).

8. Water oil (water-gas, oil-gas) surface tension

In the case that the Leverett J-function (see § 5.5) is used the capillary pressure is considered as a function of porosity, permeability and surface tension (T. P. Ahmed, 2010). That array option allows users to define a multiplier for the surface tension in regions of the reservoir where this value is different from the inserted value at the components section which in turns modifies the capillary pressures or the J-function when it is used (Computer Modelling Group Ltd, 2010).

9. Maximum gas-oil and water-oil capillary pressure or maximum gas-oil and water-oil J-function

These keywords can be used to alter the maximum values of the capillary pressure or the J-function in regions of the reservoir which exhibit different capillary pressure values than those obtained by the laboratory data or different J-function values than those calculated by the Leverett function (see § 5.5).

10. Water capillary pressure or J-function shift/offset

This option is used to account for a tilted fluids contact by adjusting the capillary pressure or the J-function of the water obtained by the laboratory tests (Computer Modelling Group Ltd, 2010). Usually a contact map is inserted in Builder and the required capillary pressure or the J-function of the water values are calculated internally. These values create a shift up or down to the capillary pressure curve. The calculation of the final curve is done by adding these offset values to the maximum capillary pressure (Computer Modelling Group Ltd, 2010). Finally, this option is used only with the depth average initialization method (Computer Modelling Group Ltd, 2010).

11. Non equilibrium oil and water saturation

The saturations to the selected regions are set by the user whereas the rest of the reservoir is initialized using gravity equilibrium. This option is useful in cases where some regions of the reservoir exhibit saturations

higher than the expected ones (Heriot Watt University, 2005). During initialization, the saturations for the reservoir are calculated based on the distance of the block from the fluid contacts and the connate saturation. Although in some cases other parameters also influence the saturations such a situation could be encountered at a fracture and its nearby area created by stimulation and filled with water (Computer Modelling Group Ltd, 2010).

12. Forchheimer equation beta correction

By this tab, the modification of the β term in the Forchheimer equation (takes into account non-Darcy flow by adding the $\beta \cdot \rho u^2$ term to the Darcy flow equation) is allowed. This term is the correction term to account for non Darcy flow. By setting a value to this tab the correction factor (β) is altered. This modification is allowed to be applied only to the gas phase when the Frederick-Graves 1 or 2 or the Geertsma equations (see § 5.7) are used whereas when the general equation (see § 5.7) is used for the calculation of the non Darcy flow then the correction applies to all phases (Computer Modelling Group Ltd, 2010). Unity is the default value when non Darcy flow option is allowed in the rock-fluid section if this value is set equal to zero for a region, this region will exhibit Darcy flow (Computer Modelling Group Ltd, 2010).

13. Volume modifiers

The pore volume is calculated internally by the simulator by taking into account the bulk volume of the block. The bulk volume of a block is calculated by the inserted dimensions for the blocks in the grid sub section and the porosity values. This keyword can be used in cases of blocks that are intersected by the reservoir boundary leaving thus a portion of the block volume out of the reservoir (Computer Modelling Group Ltd, 2010). Volume modifier values correspond to the percentage of the block that is inside the reservoir. Another use of that option is when wellbore storage effect comes into effect (Computer Modelling Group Ltd, 2010). Wellbore storage effect occurs after a change of the production rate (Jelmert, 2006). It is thought that after the change has occurred, a part of the production is due to expansion/compression of the fluid that was inside the wellbore or by the movement of a gas oil contact inside the wellbore (Jelmert, 2006). To account for that phenomenon, the simulator allows to modify the well block volume by increasing or decreasing it so as to match the production. In cases that fractures exist in the reservoir, instead of using the well block volume, the fracture volume is used as it is considered as an extension of the wellbore inside the reservoir (Computer Modelling Group Ltd, 2010). Finally, someone could propose to diminish the available pore volume by altering the porosity values but this method is not recommended as it can lead to unusual porosity values (Computer Modelling Group Ltd, 2010).

14. Bubble point pressure

This option is a history matching tool provided by IMEX and it is used so as to modify in certain regions the inserted bubble point pressure. The bubble point pressure value can present regional variations due to composition differences.

15. Dew point pressure

Dew point pressure is needed by the IMEX simulator for the initialization when a gas condensate fluid is simulated. As the previous bubble point array option this option allows user to alter this entry in selected regions of the reservoir where the dew point may differ from the inserted value.

16. Langmuir adsorption constant for each component

This is a history matching tool provided by the GEM simulator used when the component dependent Palmer and Mansoori model is used in the compaction/dilation sub-section in order to fit the production data.

17. Maximal adsorbed mass for each component

By this keyword, the GEM simulator allows the modification of the maximal adsorbed mass for each component (see § 5.8) in order to match the production data.

3.9.3 Rock-Fluid End-Point Properties Modification

This option allows to modify the end-point saturation, relative permeability and capillary pressure of the phases inserted in the rock-fluid data section of the simulator by using this option. This modification can be done in order to match the constructed model to the production data. For this modification, the desired property has to be selected and a new value for this property to be defined. In the GEM simulator this sub-section is not available.

4. SIMULATION METHOD

In the 'component section', information about the reservoir fluid are inserted by uploading a model already created in Winprop. The information about the reservoir fluid is obtained from a laboratory (PVT) analysis and includes the composition, the volumetric behavior and the physical properties of the equilibrium phases. This section is completely different for IMEX and GEM simulators. This happens because the IMEX simulator is a black oil simulator and as a result it requires volumetric data. On the other hand, GEM is a compositional simulator and the required data is a tuned EOS model that has previously been developed using Winprop, the phase behavior simulator of the CMG suite. The simulation method section is constituted by the following sub-sections:

- Black oil formulation

The required data and the way that the black oil formulation calculates the produced volumes are defined.

- Compositional model

The required data and the way that a compositional simulation is performed are defined.

- Reservoir fluids

The different reservoir fluids and the way that they can be modeled in order to perform a black oil simulation are defined.

- Improved oil recovery (IOR) and enhanced oil recovery (EOR) processes

In the improved and enhanced oil recovery processes sub-section the way that these procedures can be modeled is defined.

- Coal bed methane reservoirs

The way that a CBM reservoir is modeled is defined.

4.1 BLACK OIL FORMULATION

Black oil formulation is a simplified approach to the reservoir simulation problem. In black oil formulation the reservoir fluid is thought to be constituted by two pseudo-components; the oil and the gas. The required data for the black oil formulation can either be created using correlations or be obtained by laboratory experiments. The creation of such data using correlations is not all that preferable as laboratory data are always more accurate but it is useful in cases when laboratory data do not exist. The calculation of the produced volumes of oil and gas in this case is done by performing interpolations in the black oil Tables (BOT). The black oil Tables (BOT) are composed by the following:

- Pressure

By this keyword, the pressures at which the data were obtained are inserted in the simulator. The minimum pressure entered in this Table has to be less than any pressure constraint of the production wells whereas the maximum pressure has to be larger than any injection well pressure.

- Solution gas oil ratio (R_s)

The solution gas oil ratio (R_s) is defined as the ratio of the gas volume measured at stock tank conditions

over the produced oil volume measured at stock tank conditions. The solution gas-oil ratio is measured in scf/stb and it is used by the simulator in the material balance calculations.

- Oil formation volume factor (B_o)

As oil formation volume factor (B_o) is defined the volume of oil at reservoir conditions over the volume of the produced oil at stock tank conditions. The oil formation volume factor is measured in rb/stb and it is used by the simulator in the material balance calculation, flow calculations and calculations of oil initially in place (OIIP). Moreover, the simulator offers the option to introduce the oil formation volume factor in a tabulated form for pressures above the bubble point when the oil formation volume factor which except of its pressure dependence can also exhibit a compositional dependence and vary with in a non linear manner which may be the case of cycling processes or light fluids (Computer Modelling Group Ltd, 2010; Coats, 1985). It has to be mentioned that the alternative way of introducing the oil formation volume factor for pressures above the bubble point cannot be used in cases that the oil compressibility has been introduced in the BOT table.

- Gas formation volume factor (B_g) or gas expansion factor (E_g) or gas compressibility factor (z)

The gas formation volume factor (B_g) is defined as the ratio of the gas volume measured at reservoir conditions over the gas volume measured at standard conditions whereas the gas expansion factor is the inverse of the gas formation volume factor. The gas formation volume factor is mainly used for saturated oil reservoirs whereas the gas expansion factor is mainly used in cases of gas reservoirs (Dake, 1978). The gas compressibility factor (z) represents the deviation of the gas from the ideal behavior. It has to be mentioned that this factor at standard conditions where the pressure and temperature is low is considered to be equal to the unity, in other words the gas is assumed to present an ideal gas behavior. Moreover, if the gas compressibility factor is to be inserted in the simulator then also the reservoir temperature has to be inserted

in order to convert internally the gas compressibility factor to gas expansion factor as follow: $E_g = a \cdot \frac{P}{z \cdot T}$, where a is a conversion parameter equal to 198.58 in field units and 2.849 in SI units.

- Oil viscosity (μ_o)

Oil viscosity is defined as the measure of the resistance that oil presents to flow and it is given in centi-poise (cP). The oil viscosity is used by the simulator in the flow calculations, in the mobility ratio calculations and in the well productivity index (TUC, 2016). Moreover, the simulator offers two additional options for the introduction of the oil viscosity for pressures above the bubble point: the one is to introduce the oil viscosity in a tabulated form versus pressure and another one to introduce it as a constant value. In the latter case the calculation of the viscosity is performed as follows: $\mu_o = \mu_{oi} + V_o \cdot (P - P_b)$, where μ_{oi} is the value of oil viscosity at the bubble point and V_o is the pressure dependence of the oil viscosity for pressures above the bubble point.

- Gas viscosity (μ_g)

Gas viscosity is defined exactly in the same way as oil viscosity and is used by the simulator for the same purposes. It has to be mentioned that compared to the oil viscosity, gas viscosity is significantly lower and varies with pressure (T. P. Ahmed, 2010).

- Oil compressibility (c_o)

The oil compressibility shows how much the volume of oil will change by a pressure change. Oil compressibility is used by the simulator for the calculation of the oil formation volume factor (B_o) for

pressures above the bubble point and for the calculation of the total compressibility factor (c_t) which is used in turn for the skin factor calculation. The oil formation volume factor (B_o) above bubble point can be calculated from the following equation: $B_o = B_{oi} \cdot [1 - c_o \cdot (P - P_b)]$, where B_{oi} is the oil formation volume factor at the bubble point. The total compressibility factor (c_t) for three phases being present is defined as: $c_t = c_o \cdot S_o + c_w \cdot S_w + c_g \cdot S_g + c_f$, where c_o , c_w , c_g and c_f are the oil, water, gas and formation compressibility and the S_o , S_w and S_g are the saturations of oil, water and gas (T. P. Ahmed, 2010). Moreover, the simulator offers also the options to introduce the oil compressibility as a constant value (oil is treated as an incompressible fluid) or as a tabulated form of oil compressibility versus pressure for pressures above the bubble point.

- Interfacial tension (σ)

The interfacial tension is the tension that appears at the interface of two immiscible fluids such as oil-water and gas-oil. By introducing the interfacial tension to the simulator the interfacial effects on capillary pressure for every pressure are calculated. For example, taking into consideration the interfacial tension the gas-oil

capillary pressure is altered as follows: $P_{cog} = \frac{\sigma}{\sigma_i} \cdot P_{cogr}$, where σ is the interfacial tension between the liquids, σ_i is the interfacial tension at the reference pressure which is also required by the simulator and P_{cogr} is the capillary pressure at the reference pressure.

- Oil content (R_v)

As oil content (R_v) is defined the ratio of the produced condensate volume at stock tank conditions over the volume that this condensate was occupying as gas in the reservoir and it is measured in stb/scf (Computer Modelling Group Ltd, 2010). The oil content is used so as to improve the predictions of the black oil formulation in cases of volatile and gas-condensate reservoirs.

In cases of volatile oils where oil is produced and from the gas phase during the separation procedure the gas formation volume factor often cannot predict accurately enough the produced volumes of gas and its viscosity. For this reason, the dry gas formation volume factor as well as the dry gas viscosity have been introduced in the BOT formulation.

- Dry gas formation volume factor (B_{gd}) or dry gas expansion factor (E_{gd}) or the dry gas compressibility factor (z_{gd})

The dry gas expansion factor (E_{gd}) or the dry gas formation volume factor (B_{gd}) or the dry gas compressibility factor (z_{gd}) are modifications of the gas expansion factor (E_g), the gas formation volume factor (B_g) and the gas compressibility factor (z_g) to account for the changes in the mixture composition and as a result its volumetric behavior when liquid is produced from the gas phase during the separation procedure. The dry gas formation volume factor (B_{gd}) is calculated as follows:

$$B_{gd} = 0.02827 \cdot \frac{z \cdot T}{P} \cdot \left(\frac{n_{feed}}{n_{sto}} \right),$$

where n_{feed} are the moles of gas at the wellstream and n_{sto} are the moles of

the produced surface gas (Whitson & Torp, 1983). The dry gas expansion factor (E_{gd}) and the dry gas compressibility factor (z_{gd}) can be calculated as previously from the dry gas volume factor. Moreover, the simulator for these factors offers the option to be introduced in a tabulated form for pressures above the bubble point.

- Dry gas viscosity (μ_{gd})

The dry gas viscosity (μ_{gd}) is defined as the gas viscosity (μ_g) when condensate does not exist. This column is available only when a volatile reservoir will be modeled and the volatile oil Table (PVTO) has been selected. Moreover, the simulator for the dry gas viscosity offers the option to be introduced in a tabulated form for pressures above the bubble point.

4.1.1 Laboratory Data And Field Data

Laboratories measure the PVT data in the laboratory that means that the volumes are measured with respect to the oil volume at the bubble point pressure whereas the volumes that the engineers are interested in are measured with respect to the stock tank volume (Dake, 1978). This means that the previously mentioned volume factors have to be converted for field use. Usually, the laboratories provide the PVT data already converted for field use but sometimes these data are not converted and for this case the simulator provides the option to convert these data internally. In order to do this conversion, the user has to introduce the bubble point pressure (the pressure at which the first bubble of gas has been created and with further pressure reduction more gas is liberated from oil), the oil formation volume factor (B_{ob}) and the solution gas oil ratio (R_{sb}) at the bubble point pressure. By using these values the conversion is performed as follows:

$B_o = v_o \cdot B_{ob}$, where v_o is the oil formation volume factor determined by the differential liberation

$R_s = R_{sif} - 5.615 \cdot R_{sb} \cdot B_{ob}$, where R_{sif} is the initial solution gas oil ratio determined by the flash experiment

$$B_g = \frac{1}{5.615 \cdot E_g}$$

4.1.2 Densities

The oil, gas and water densities are required by the simulator so as to be used for the flow equations calculation, for the calculation of the depths of the contacts and for the calculation of the pressure profile in the reservoir. The oil density can be introduced to the simulator as stock tank oil density (ρ_o), as specific gravity (γ_o or Sg_o) or as API gravity (API°) and it is not required in cases of gas reservoirs or when the API-tracking model is used. The gas density can be introduced to the simulator either as gas density (ρ_g) or as gas gravity (γ_g or Sg_g). The water density is thought to be equal to 62.4 lb/ft³ but this may not be valid to all cases as salinity influences its value.

4.1.3 Water Properties

The formation water properties can either be calculated by using correlations or by introducing the reference pressure (P_{rw}) for the water formation volume factor, the water formation volume factor (B_{wi}) and the water compressibility (c_w) by these values the water formation volume factor is calculated by the following formula: $B_w = B_{wi} \cdot (1 - c_w \cdot (P - P_{rw}))$ Water formation volume factor is used by the simulator in the material balance equation so as to calculate water production. Moreover, the water viscosity (μ_{wi} or V_{wi} as it is referred in the Table) at the reference water pressure and its viscosity pressure dependence of water viscosity (V_w) have to be introduced in the simulator so as the water viscosity to be calculated also and for

other pressures than the reference as follow: $\mu_w = \mu_{wi} + V_w \cdot (P - P_{rw})$. The water viscosity is used in the flow calculations.

4.2 COMPOSITIONAL MODEL

In compositional formulation, the fluid is described by its components and the phase behavior problem is solved by the use of a cubic equation of state (EOS) tuned in Winprop and uploaded in the compositional simulator. The equation of state relates the volume, the pressure and the temperature and provides results about the phase behavior of the fluid, the volumes of the phases being present in the reservoir, their compositions and densities.

4.2.1 Component Properties

In order the simulation problem to be solved by using an EOS, the properties of the components have to be introduced in the simulator. The minimum required component properties so as the development of the EOS model are the following:

- Critical pressure (P_c)

The critical pressure is defined as the pressure at the critical point (the point at which the liquid and the vapor phase cannot be discretized) at which all intensive properties (the property is independent of the amount of sample to which it was measured) of the gas and liquid phases are equal (T. P. Ahmed, 2010). Critical pressure is also an intensive property and characterizes the component. This value is used in the calculation of the attraction parameter (a) and the repulsive parameter (b) used in the equation of state.

- Critical temperature (T_c)

Critical temperature is defined similarly to critical pressure and it is also used for the calculation of the attraction parameter (a), the repulsive parameter (b) and the dimensionless component dependent correction term (α) used in the equation of state.

- Critical volume (V_c)

Critical volume is defined as the volume that a component occupies at the critical point conditions. This parameter is used by the simulator so as to calculate the interaction coefficients of the components and the reduced density of the mixture that it is used by turn in the Jossi-Stiel-Thodos correlation for the calculation of the mixture's viscosity.

- Molecular weight (MW)

The molecular weight represents the mass of a molecule and it is used in the viscosity calculation of the oil phase and also in the correlations to calculate other component properties.

- Omega A (Ω_a) and omega B (Ω_b)

The omega A and omega B are the pure component parameters and are used in the calculation of the equation of state (T. P. Ahmed, 2010). The omega A parameter is used for the calculation of the equation of state attraction parameter (a) whereas the omega B parameter is used for the calculation of the equation of state

repulsive parameter (b). The omega A parameter value is equal to 0.45723 for the Peng-Robinson equation of state and to 0.42747 for the Soave-Redlich-Kwong equation of state. The omega B parameter value is equal to 0.0779 for the Peng-Robinson equation of state and to 0.08664 for the Soave-Redlich-Kwong equation of state.

- Acentric factor (ω)

Acentric factor indicates the measure of the deviation of the observed thermodynamic properties of a component from those calculated by the principle of corresponding states due to the fact that its molecules are not spherical (Saville, 2011). For completely spherical molecules, this factor is zero whereas for completely non spherical molecules this factor is unity (Saville, 2011). Finally, this value is used by the simulator in the calculation of the m factor used by the equation of state.

- Hydrocarbon?

By this keyword is denoted whether the specific component is an hydrocarbon or not. This definition of the components as hydrocarbon or non hydrocarbons is used by the simulator in order to define the binary interaction coefficients (coefficients representing the interaction between different components) as these coefficients are different for hydrocarbon components and non-hydrocarbon components.

- Interaction parameters

The interaction parameters or else binary interaction coefficients are used by the simulator in the calculation of the $(a \alpha)_m$ parameter and the repulsive parameter (b_m) of the mixture in the equation of state. The interaction parameters can be used also for history matching purposes (Spencer & Danner, 1972). In general the interaction parameter between hydrocarbon components belonging to the same homologous series and without significant molecular weight difference is thought to be equal to zero whereas the interaction parameter between lighter hydrocarbon components and heavier as well as between hydrocarbons and non-hydrocarbons is greater than zero. As a result, the interaction parameters between hydrocarbons and non-hydrocarbons and lighter and heavier components affect the calculations. The interaction parameters can be introduced by two ways. The first way to define the interaction parameters is to set directly values in the cells of the Table which is available and it is constituted by the components in both rows and columns. The second way of calculating the interaction parameter is to set the exponent (PVC3) so as the Winprop to calculate internally the binary interaction coefficients. By using this keyword, the interaction coefficients of the Table are calculated internally by the simulator. The interaction coefficient is calculated by the simulator using the

following formula: $k_{ij} = 1 - \left| \frac{2 \cdot \sqrt{\sqrt[3]{V_{ci}} \cdot V_{cj}}}{\sqrt[3]{V_{ci}} + \sqrt[3]{V_{cj}}} \right|^{PVC3}$, PVC3 is the entered exponent so as to calculate the

hydrocarbon-hydrocarbon interaction coefficients of the interaction parameter Table and V_c is the critical volume of the components i, j.

Moreover, Winprop offers some additional parameters that can be used to built the EOS model and which are the following:

- Critical compressibility factor (z_c) (optional)

Critical compressibility factor is defined as the compressibility factor of the component at the critical point

and can be derived from the real gas law as follow: $z_c = \frac{P_c \cdot V_c \cdot MW}{R \cdot T_c}$. The critical compressibility factor is required when the critical volume of the component is unknown.

- Specific gravity (SG) and average normal boiling point (T_b) (optional)

The specific gravity and the average normal boiling point (characteristic value of a substance and has the same meaning as the bubble point of a mixture (Cheresources, 2012) are used only for the calculation of the critical properties and the molecular weight when those are not introduced (Computer Modelling Group Ltd, 2010). The specific gravity and the average normal boiling point are not required when the T_c , P_c and MW have been introduced into the simulator.

- Racket compressibility factor (z_{RA}) (optional)

The Racket compressibility factor is a unique constant for each component, its values are different than those of the critical compressibility factor and it is calculated using the acentric factor as follow: $z_{RA} = 0.29056 - 0.08775 \cdot \omega_i$ (Reid, Prausnitz, & Polling., 1987; Donnez, 2007). The Racket compressibility factor is used in the calculation of the volume shift and as a result it affects the liquid density calculation.

- Volume shift (s) (optional)

Volume shift is used in cases where the density predictions of the liquid phase have to be improved and it is recommended to be used in cases that miscible flooding projects are applied to the reservoir (Petrowiki, 2015b). This improvement in predictions is done by changing the values of the molar volumes and as a result and the compressibility values of the components which are predicted by the EOS for both liquid and gas phases. The volume shift can be applied in both equations of state by transforming the calculated

compressibility and the molar volume as follows: $Z = Z_o - \frac{P(V')}{RT}$ and $V' = V_{EOS} - \sum x_i \cdot c_i$, where x_i is the molar fraction of the component i , c_i is the volume shift for each component calculated by the following

formula: $c_i = 0.40768 \cdot (0.29441 - z_{RA}) \cdot \frac{R \cdot T_c}{P_c}$, where the z_{RA} the Racket compressibility (Péneloux,

Rauzy, & Fréze, 1982). In general volume shift parameters are negative for components up to hexane (C6) and positive for heavier components (Computer Modelling Group Ltd, 2009b).

Moreover some of the component properties are not used in the calculation of the EOS but are used in other calculations such as the calculation of the interfacial tension, the heating capacity of the produced gas, the viscosity calculations and the heat losses calculation can be introduced in the simulator and are the following:

- Parachor (P) (optional)

The parachor is used by the simulator so as to calculate the interfacial tension (Computer Modelling Group Ltd, 2010). As Sugden mentioned the interfacial tension and the parachor are related as follow:

$\sigma^{0.25} = \frac{P \cdot (\rho_l - \rho_v)}{MW}$, where σ is the interfacial tension and ρ_l and ρ_v are the densities of the liquid and vapor

phase (Sugden, 1924). If this value is unknown it is calculated internally by the simulator from the molecular weight (Computer Modelling Group Ltd, 2010).

- Heating value (H_r) (optional)

The heating value is defined as the released heat from a complete combustion of a component with oxygen at standard conditions. This value characterizes the component and it is measured in BTU/gmole. By introducing the heating value for each component the separator stream heating value can be calculated using:

$H_r = \sum (x_i \cdot H_{ri})$, where H_r is the heating value of the separator gas stream, x_i is the fraction of each component present in the stream and H_{ri} is each component heating value. This value is required since the gas is not sold based on its volume but on its heating capacity (Donnez, 2007).

- Critical volume (viscosity) (optional)

The critical volume (viscosity) is used by the simulator only for the calculation of the reduced density of the mixture that it is used by turn in the Jossi-Stiel-Thodos correlation for the calculation of the mixture's viscosity.

- Enthalpy coefficient A (H_A), B (H_B), C (H_C), D (H_D), E (H_E) and F (H_F) (optional)

These coefficients are used when the thermal option is used in order to take into account the effect of heat losses from the fluid to the formation.

Finally, it has to be mentioned that since the water is not taken into account in the calculation of the EOS but it is considered only in the calculations of flow, the required parameters are the water density, the water compressibility, the water reference pressure and the water viscosity.

4.2.2 Reservoir Temperature

The reservoir temperature has to be inserted in order to be used in the calculations of the equation of state. The introduction of the reservoir temperature can be done either by using a constant temperature value or by letting the temperature to vary linearly with depth. By using a constant temperature value, every block of the reservoir will have the same temperature whereas by using the second way a temperature profile is created inside the reservoir (Computer Modelling Group Ltd, 2009b). In order to create a temperature profile, the depth and the corresponding temperature value have to be inserted in the available Table.

4.2.3 Equation Of State (EOS)

The most commonly used equations of state in the petroleum industry are those of Soave-Redlich-Kwong (SRK) and Peng-Robinson (PR). The SRK equation of state was introduced in 1972 and it is a modification of the Redlich-Kwong equation which was derived from the Van der Waals equation of state. The PR equation was introduced in 1976 and essentially it is an improvement of the SRK equation of state so as to improve the liquid densities prediction (Peng & Robinson, 1976). The PR is the most commonly used equation and gives slightly better results for gas and condensate reservoirs than the SRK (Adewumi, 2016a).

4.2.3.1 SOAVE-REDLICH-KWONG (SRK)

The SRK equation of state is expressed as $P = \frac{R \cdot T}{V - b} - \frac{\alpha \cdot a}{V \cdot (V + b)}$ or as

$Z^3 - Z^2 + (A - B - B^2) \cdot Z - A \cdot B = 0$, where Z is the compressibility factor of the mixture and A and B are

defined as follows: $A = \frac{(\alpha \cdot a)_m \cdot P}{(R \cdot T)^2}$ and $B = \frac{b_m \cdot P}{R \cdot T}$, where $(\alpha \cdot a)_m$ and b_m are respectively the attractive

and repulsive parameters (accounting for the attraction and repulsive forces between the molecules) of the mixture which are calculated by using the following mixing rules for each phase separately:

$(\alpha \cdot a)_m = \sum \sum (y_i \cdot y_j \cdot \sqrt{(\alpha \cdot a)_i \cdot (\alpha \cdot a)_j} \cdot (1 - k_{ij}))$ and $b_m = \sum y_i \cdot b_i$, where y_i and y_j are the molar fractions of each component, k_{ij} is the binary interaction coefficient, a is the attraction parameter and b the

repulsive for each component which are calculated from: $a = \Omega_a \cdot \frac{R^2 \cdot T_c^2}{P_c}$ and $b = \Omega_b \cdot \frac{R \cdot T_c}{P_c}$, where

$\Omega_a = 0.42747$ and $\Omega_b = 0.08664$. Moreover α is a dimensionless component dependent correction term (introduced by Soave in order to improve the vapor liquid equilibrium predictions) calculated for each component and it is equal to the unity when the temperature is equal to the critical temperature of the

component whereas for other temperatures this number is given by: $\alpha = \left(1 + m \cdot \left(1 - \sqrt{T_r}\right)\right)^2$, where T_r is the

reduced temperature (calculated by: $T_r = \frac{T}{T_c}$, where T is the reservoir temperature and T_c is the critical temperature of the component) and m is calculated from the following formula: $m = 0.48 + 1.574 \cdot \omega - 0.176 \cdot \omega^2$, where ω is the acentric factor (Soave, 1972).

4.2.3.2 PENG-ROBINSON (PR)

The PR equation can be expressed in two ways as follows: $P = \frac{R \cdot T}{V - b} - \frac{\alpha \cdot a}{V \cdot (V + b)^2 - b \cdot (V - b)}$, or

as $Z^3 + (B - 1) \cdot Z^2 + (A - 3 \cdot B^2 - 2 \cdot B) \cdot Z - (A \cdot B - B^2 - B^3) = 0$, while α , A and B are calculated as in the SRK equation but $\Omega_a = 0.45724$ and $\Omega_b = 0.0778$ and m is calculated as follow:

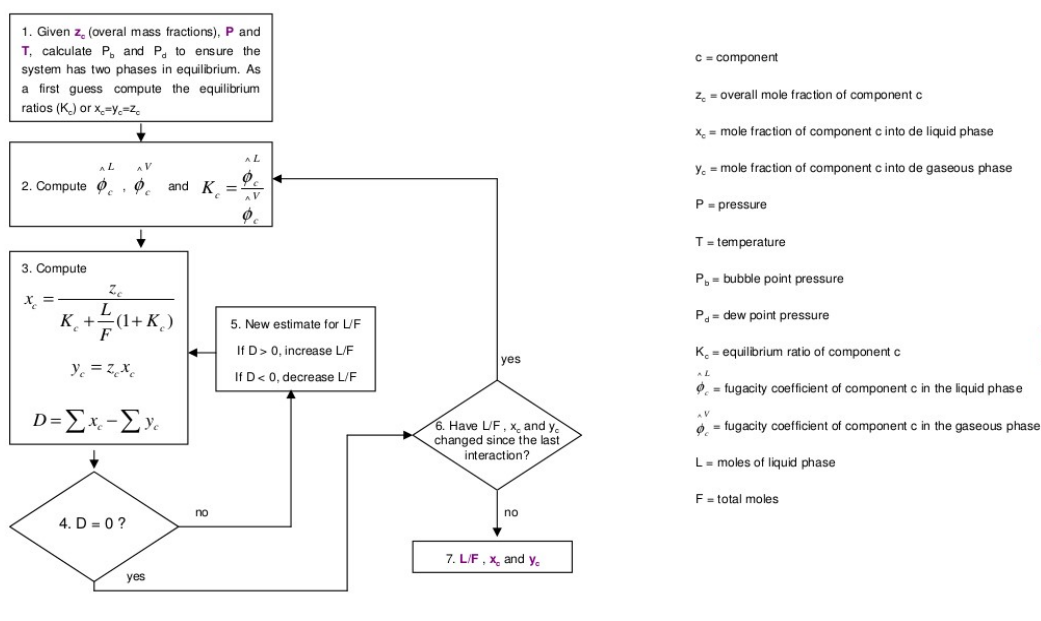
- for lighter components ($\omega < 0.49$) m is given by $m = 0.376 + 1.5423 \cdot \omega - 0.2699 \cdot \omega^2$
- for heavier components ($\omega > 0.49$) m is given by $m = 0.379642 + 1.48503 \cdot \omega - 0.1644 \cdot \omega^2 + 0.016667 \cdot \omega^3$

The solution of the EOS provides one or three real roots. The larger root corresponds to the compressibility factor of the gas phase, the smallest root corresponds to the compressibility factor of the liquid phase whereas the third root has no physical meaning. By using these compressibility factors and by making an assumption about the liquid and gas composition and the mole fractions x and y of the component i in the

liquid and gas phases, the fugacity (tendency of the component to pass from one phase to another) of each component in liquid and gas phase can be calculated using:

$$\ln \phi_i = \ln \frac{f_i}{y_i P} = \frac{1}{RT} \int_V^{\infty} \left(\frac{\partial P}{\partial n_i} - \frac{RT}{V} \right) dV - \ln Z$$

For the phases to be in equilibrium the fugacities of each component in the liquid and gas phase have to be equal. Then the equilibrium ratio can be calculated as follows: $K = \frac{\phi_{i,l}}{\phi_{i,g}}$ and the procedure in the picture 15 is followed in order to compute the composition in the liquid and gas phases.



Picture 15: Flow chart of the compositional formulation (Petrobras-pemex, n.d.)

By knowing the compositions and the compressibility factor, the apparent molecular weight and the density of each phase in the reservoir can be calculated.

4.2.4 Calculation Of Viscosity

In the compositional model, the viscosities of the phases present in the reservoir have to be calculated by using correlations. The viscosities of the phases are used by the simulator for the calculation of the flow equations. For this purpose, the available methods that can be used with the GEM simulator are the following:

- Yoon and Thodos & Herning and Zipperer (HZYT)

By using this option the gas mixture viscosity is calculated by the Herning and Zipperer mixing rules as

follow: $\mu_{(low,mix)} = \frac{\sum \mu_{(low,i)} \cdot \sqrt{MW_i}}{\sum x_i \cdot \sqrt{MW_i}}$, where each component viscosity at low pressures (viscosity at dilute

gas) are calculated using the Yoon and Thodos formula as follow:

$$\mu_{(low,i)} = 4.610 \cdot T_r^{0.618} - 2.04 \cdot e^{-0.449 \cdot T_r} + 1.94 \cdot e^{-4.058 \cdot T_r} + \frac{10^{-5}}{\mu_p}$$

in cp calculated by: $\mu_p = \left(\frac{T_c}{MW^3 \cdot P_c^4} \right)^{1/6}$, where T_c is in K, P_c in atm and MW in g/gmol. Finally, the

mixture viscosity at reservoir conditions is calculated by the Jossi, Stiel and Thodos method:

$$\left(\mu_{mix} - \mu_{(low,mix)} \cdot \mu_{mix} + 10^{-4} \right)^{1/4} = 0.1023 + 0.023364 \cdot \rho_r + 0.058533 \cdot \rho_r^2 - 0.040758 \cdot \rho_r^3 + 0.0093324 \cdot \rho_r^4$$

, where ρ_r is the reduced mixture density which is calculated by: $\rho_r = \frac{V_c}{V_m}$, where V_c is the critical volume

and V_m is the molar volume. In general Jossi, Stiel and Thodos correlation is applicable for 0.1 to 3 range of reduced mixture density values (Dabir S. Viswanath, Tushar K. Ghosh, Dasika. H. L. Prasad, Nidamarty V.K. Dutt, 2007).

- Lee-Eakin (LE)

The Lee-Eakin method is similar to the Yoon and Thodos & Herning and Zipperer method as the viscosity at reservoir conditions is calculated by the Jossi, Stiel and Thodos formula. By using the Lee-Eakin method the

viscosity at low pressures is calculated as follow: $\mu_{(low,mix)} = \frac{10^{-4} \cdot (17.94 + 0.0321 \cdot MW) \cdot T^{3/2}}{1.8 \cdot T + 75.4 + 13.9 \cdot MW}$. Lee Eakin

method is accepted to provide accurate predictions for the gas phase viscosity when the gas phase presents low non-hydrocarbon content (Adewumi, 2016b).

- Use component viscosity values (MIX)

In this case, a mixing rule is applied to the user defined component viscosities so as to calculate the mixture viscosity.

- Pedersen

Pedersen's method is based on the corresponding states theory and provides good predictions for viscosities greater than 2cp (Dabir S. Viswanath, Tushar K. Ghosh, Dasika. H. L. Prasad, Nidamarty V.K. Dutt, 2007).

Pedersen's method uses a reference substance for the calculation of viscosity which normally is methane (Pedersen, Fredenslund, Christensen, & Thomassen, 1984). The calculation of the mixture's viscosity is done

as follows: $\frac{\mu_{mix}(P,T)}{\mu_o(P_o,T_o)} = \left(\frac{T_{c,mix}}{T_{c,o}} \right)^{-1/6} \cdot \left(\frac{P_{c,mix}}{P_{c,o}} \right)^{2/3} \cdot \left(\frac{MW_{mix}}{MW_o} \right)^{1/2} \cdot \frac{a_{mix}}{a_o}$, where the subscript 'mix' refers to the

property of the mixture while the subscript 'o' refers to the property of the reference substance. The

molecular weight and the parameter a are calculated by: $MW = 0.291 \cdot (MW_w - MW_n) + MW_n$, where

MW_w is the weighted average molecular weight, MW_n is the average molecular weight and

$a = 1 + 7.747 \cdot 10^{-5} \cdot \rho_r^{4.265} \cdot MW^{0.8579}$ respectively.

- Modified Pedersen's method

The modified Pedersen's method differs from the Pedersen's method in the way that the reference fluid viscosity is calculated and in the values of the coefficients of the correlation. In this case, the molecular weight and the parameter a are calculated as follows: $MW = 1.304 \cdot 10^{-4} \cdot (MW_w^{2.303} - MW_n^{2.303}) + MW_n$ and $a = 1 + 7.378 \cdot 10^{-3} \cdot \rho_r^{1.847} \cdot MW^{0.5173}$. The modified Pedersen's method provides better predictions than the original method for mixtures constituted mainly by light components such as ethane, propane and carbon dioxide (Dabir S. Viswanath, Tushar K. Ghosh, Dasika. H. L. Prasad, Nidamarty V.K. Dutt, 2007). The increased prediction accuracy is attributed to the higher value of parameter a used for light components resulting in higher liquid viscosities than Pedersen method (Pedersen & Fredenslund, 1986).

4.2.5 Identification Of The Fluid Phase

The phase of the fluid in a block has also to be identified by the simulator so as to use the appropriate relative permeability values and capillary pressures. The identification of the phase is done internally by the simulator. In the case of having a two phase system the simulator always identifies as gas, the phase which presents the lower density whereas the phase with the higher density is always assumed to be the oil phase. On the other hand, in the case of having a single phase system the block fluid density is compared to a reference gas or oil phase density and depending to which density the block fluid's density is closer the fluid is identified as such (Computer Modelling Group Ltd, 2009b). Moreover, the simulator offers the user some additional methods for the identification of the single phase fluid which are the following:

- Oil or gas

When this method is used the single phase fluid is defined directly as oil or gas.

- Pseudo-critical volume method

For super critical conditions (conditions above the critical point) the phase is identified as gas whereas for sub critical conditions (conditions below the critical point) the phase is identified as oil when the $V_m < V_c$.

- Pseudo-critical temperature method

The identification of the single phase is done by comparing the block temperature with the critical

temperature which is calculated as follow: $T_{c,mix} = \frac{\sum z_i \cdot V_{ci} \cdot T_{ci}}{\sum z_i \cdot V_{ci}}$. The identification is done as follow:

- If $T_{block} \geq T_{c,mix}$ then the phase is identified as gas
- If $T_{block} < T_{c,mix}$ then the phase is identified as oil
- User input threshold density

By using the user input method the identification of the phase is done as follow:

- When $\rho_{fluid} < \rho_{ref} - \rho_{th}$ the phase is thought to be gas
- When $\rho_{fluid} > \rho_{ref} + \rho_{th}$ the phase is thought to be oil
- When $\rho_{ref} - \rho_{th} < \rho_{fluid} < \rho_{ref} + \rho_{th}$ then the phase is assumed to be gas if the mole fraction of the gas phase is greater than 0.5.

4.2.6 Aqueous Phase Solubility

The aqueous phase solubility represents how soluble are the components of the fluid in the water phase. In general hydrocarbons are insoluble in water but the lighter hydrocarbons may be slightly soluble in water affecting in that way the amount of the produced gas. The solubility of the hydrocarbons to the water phase can be taken into account when a compositional simulator is used such as GEM. In order to model the solubility of the components the Henry's law is used: $f_i = x_i \cdot H$, where f_i is the fugacity of each component, x_i is the molar fraction of a component and H the Henry's law constant calculated by:

$\ln H = \ln H_i + V_\infty \cdot \frac{(P - P_{is})}{R \cdot T}$, where P_{is} is the reference pressure at which the solubility data are defined and

V_∞ is the partial molar volume of a component in water at infinite dilution (a solution that contains such an amount of solvent to which if more liquid is added the solvent concentration will not change (Kane, 2017). Finally, a Henry's constant value of zero indicates that the component is insoluble to the water phase (Computer Modelling Group Ltd, 2009b).

4.3 RESERVOIR FLUIDS

In this sub-section the general description of the fluid type that exists in the reservoir is entered. As fluid model either the type of oil (heavy oil, black oil, volatile oil etc) or the type of a specific recovery process such as polymer flooding and others is entered. The definition of the reservoir type or the recovery procedure is required as different options are available for each model. Finally, the definition of the reservoir fluid is required only by the IMEX simulator.

4.3.1 Heavy Oil

In a heavy oil reservoir only two phases exist, the oil and the water phase. In this type of reservoirs, the reservoir fluid is constituted mainly from heavy hydrocarbon molecules, it does not contain a significant amount of light hydrocarbons and it exhibits high viscosity values. A heavy oil reservoir can be modeled using the two phase oil-water model provided by the simulator which assumes that gas is not present and variations in solution gas are not taken into account. As a consequence, this model seems to be appropriate for heavy oils to which the amount of solution gas is negligible.

4.3.2 Black Oil

In a black oil reservoir, all three phases (oil, water and gas) can exist simultaneously in the reservoir depending on pressure. If the reservoir pressure is above bubble point then only the oil and the water phases are present in the reservoir whereas if the reservoir pressure is below bubble point then gas also exists. A black oil reservoir can be modeled using the black oil option of the simulator. Although in cases where the reservoir remains undersaturated throughout the entire production history then it can be modeled using the two phase:oil-water model.

4.3.3 Volatile Oil

Volatile oil reservoirs are similar to black oil reservoirs but their fluid contains more dissolved gas and a larger amount of lighter hydrocarbons. Their major difference is that the gases produced by a volatile oil reservoir contain significant amounts of condensable hydrocarbons in the gas phase which can be recovered during separation procedure whereas the gases produced by a black oil reservoir produce a negligible amount of liquid condensate during separation procedure. This type of oil is better to be simulated using a compositional model instead of a black oil.

4.3.4 Dry Gas

Dry gas reservoirs are reservoirs where only gas and water exists. By using the two phase gas-water model the simulator assumes that the phases that can exist in the reservoir are gas and water. As a result, the two phase gas-water model seems appropriate to be used in cases of dry gas reservoirs where the only hydrocarbon phase is the gas phase.

4.3.5 Gas- Condensate

Gas condensate reservoirs are gas reservoirs but some intermediate hydrocarbon components (ethane to hexane) are also present in the gas phase which can condensate from the gas phase by pressure depletion. In gas-condensate reservoirs, by pressure depletion, the condensable hydrocarbons are liquefied (when the pressure drops below the dew point pressure). In undersaturated condensate reservoirs, only gas and water initially exists whereas in saturated condensate reservoirs oil, gas and water are present simultaneously (Ahmed, 2010). The condensate can be either produced directly as liquid from the reservoir (liquefies in the reservoir) or it can be produced as gas from the reservoir and liquefy during the separation procedure (Ahmed, 2010). This type of oil is better to be simulated using a compositional model instead of a black oil.

4.3.6 Compositional Variances of The Reservoir Fluid

In some cases the reservoir fluid may present vertical and horizontal compositional variations. Vertical compositional variations are caused by gravity segregation of the reservoir fluid. When gravity segregation occurs the heavier components of the reservoir fluid are accumulated in the deeper layers of the reservoir thus leaving a lighter fluid at the upper zones of the reservoir. On the other hand, horizontal variations in composition can be caused by permeable faults being present resulting to differences in composition between different parts of the reservoir (Blaskovich, Cain, Sonier, Waldren, & Webb, 1983). The variances in composition affect also the fluid flow inside the reservoir as the heavier hydrocarbons are more difficult to flow compared to the lighter hydrocarbons.

These differences in composition could not initially to be modeled appropriately using a black oil simulator but only using a compositional simulator. Although, due to the high computational cost of a compositional simulation an efficient way known as API-tracking model was found in order to represent accurately the gravity segregation phenomenon in a black oil simulator. In addition, in a comparative study between the API tracking model and the conventional black oil model it was found that the flow rates calculated from the two models were different with the API-tracking model to be more accurate (Beraldo, Blunt, Schiozer, & Qi,

2007). By using the API tracking model, the oil phase is not treated as a homogeneous single phase but it is split into two pseudo-components, one representing the heavier hydrocarbons being present in the oil phase and one representing the lighter hydrocarbons. The properties of each of these different oil pseudo-components are defined by using different PVT Tables for each pseudo-component. Having the properties of the pseudo-components the simulator calculates their flow and at the end of each timestep calculates the overall oil density for each block. As a result, the treatment of two different oil types that may co-exist in a block is possible. Without using the API-tracking method different PVT regions should be assigned in the reservoir but in this case the mixing of the oil would not be possible as the oil in each different region will retain different properties. As a result by using the API-tracking model the oil phase is treated by the black oil simulator not as a single component but as two different components.

The IMEX simulator provides two API tracking models: one for modeling black oil reservoirs and another one for modeling heavy oil and undersaturated reservoirs. The difference between these two models is that the one takes into account gas flow and variations in solution gas whereas the other one does not take into account such phenomena.

4.4 IMPROVED OIL RECOVERY (IOR) AND ENHANCED OIL RECOVERY (EOR) METHODS

The improved and enhanced oil recovery methods are applied after the primary production of the reservoir during which the hydrocarbons production is done by pressure depletion. These methods aim to the recovery of hydrocarbons that have remained into the reservoir by injecting fluids in order to provide the required pressure support so as fluids flow to occur from reservoir to surface. As improved oil recovery methods are usually referred methods such as the water or gas injection. On the other hand, as enhanced oil recovery methods are usually referred methods such as the miscible and polymer flooding.

4.4.1 Seawater Injection

Water injection projects are applied so as to improve oil recovery or to support reservoir pressure. Usually in water flooding projects the injected water is seawater as it is cheaper and in general abundant. When seawater injection is applied to a reservoir, the productivity of the wells is usually lowered due to the formation of scale in the wells caused by the reaction of the injected water with the formation water. The amount of the formed scale is calculated according to the scale buildup/well damage model (the amount of scales as well as the rate of their disposal are entered in the simulator) (Computer Modelling Group Ltd, 2010). The simulation of seawater injection in black oil and heavy oil reservoirs can be modeled by using the two phase oil-water with seawater models can be used. When one of those models is used, the simulator also requires the introduction of the seawater viscosity which can be different from the formation water viscosity value. The seawater viscosity refers to the viscosity value of the seawater at the water reference pressure and it is used by the simulator so as to calculate the viscosity of the formation and seawater mixture.

4.4.2 Gas Injection

Gas injection is an improved oil recovery process which usually uses the separator gas and it is applied

mainly for pressure maintenance of the reservoir by injecting it into the gas cap. Gas injection schemes can be applied in order to increase the recovery of volatile oil and gas condensate reservoirs or in cases of very undersaturated oil reservoirs in order to swell the oil and increase the oil recovery.

4.4.3 Miscible Flooding

Miscible flooding is one of the most widely applied EOR processes and it is used in order to increase recovery of hydrocarbons (Petrowiki, 2015b). Miscible flooding in most cases is applied near the end of the improved recovery (IOR or secondary recovery), where usually water flooding has been applied and residual oil has been left in the reservoir (Petrowiki, 2015b). The aim of miscible flooding is to restore the lost continuity of the residual oil (that has been left after the water flooding) in the reservoir and form a continuous phase (miscible front) by reducing the interfacial tension between the hydrocarbons that have to be displaced (trapped oil) and the displacing phase (solvent) (Tarek Ahmed & Meehan, 2012).

Miscibility of the injected solvent with the residual oil can be achieved either by injecting the solvent at high pressure or by using a solvent of a specific composition so as component exchange between oil and solvent to occur. Both of the aforementioned methods result in the formation of a single phase fluid which can be recovered. As solvents usually liquid petroleum gas (LPG), propane, natural gas enriched with intermediate hydrocarbons (mostly from ethane to hexane), nitrogen and carbon dioxide can be used. The solvent injection can be done with or without injecting chase gas. The injection of chase gas is done in cases where the solvent due to its high cost is injected as slug into the reservoir and chase gas is used so as to displace this slug (Stalkup, 1983). In such cases sometimes also water is injected in a water alternating gas sequence (WAG) in order to enhance the mixing of the chase gas with the solvent (Abdus Satter, Ghulam M. Iqbal, 2007). From the aforementioned solvents, the most widely used is the carbon dioxide due to its availability and its affinity to hydrocarbons. When it is injected in the reservoir and comes in contact with the trapped oil it makes it to expand and reduces its viscosity and as a result makes it to be able to flow again while its continuous injection pushes the oil toward the production wells (Denbury Resources Inc., 2009).

In IMEX simulator, this process is modeled using the pseudo miscible model. The solvent properties are inserted using a solvent PVT Table. In this Table, the solvent volumetric properties, the solvent viscosity and the oil and solvent mixing parameter (defines the mixing of oil with solvent) are inserted. Moreover, the solvent density, the gas and solvent mixing parameter (is used in cases where free gas exists in the reservoir and determines the mixing of the free gas with the solvent), the minimum solvent saturation (is required so as mixing to occur), the gas saturation threshold (is the maximum gas saturation up to which mixing is possible to occur) have to be entered. In cases where the pseudo-miscible model with chase gas is used the initial gas-oil ratio has to be defined. In this case, the solution gas in the oil phase is constituted by the solution gas that was initially dissolved in oil (is assumed to remain always in solution) and from the injected gas (chase gas) that dissolves in the oil. The solution gas that the oil initially contained is represented by the initial gas-oil ratio whereas the injected gas by the solution gas-oil ratio (R_s) column in the BOT Table. The sum of these two values represents the total amount of gas-oil ratio that will be produced. Finally, in GEM simulator miscible flooding is modeled by inserting the solvent composition.

4.4.4 Polymer Flooding

Polymer flooding is an EOR process which is done by injecting polymers dissolved in water into the

reservoir so as to decrease the water velocity. Polymers are long chain molecules with high molecular weight and viscosity, these molecules are used so as to increase the viscosity of the water resulting in a lower mobility ratio (Yasin, 2013). The efficiency of the polymer flooding is mainly attributed to the fact that creates a more uniform front during the flood in order the reservoir to be better swept and avoid by passing of areas that diminish displacement efficiency of the process (Petrowiki, 2017). During a polymer flooding, a portion of the reservoir pore volume remains inaccessible (could be up to 30%) by the polymer because polymer molecules are rather large and cannot pass through the small pore throats (Dawson & Lantz, 1972). Moreover, polymers are adsorbed on the rock and as a result a fraction of them cannot be completely recovered by the chase water thus leaving a residual polymer concentration (residual sorption level) which causes the reduction of the water permeability to be apparent to an extent and after the end of the polymer flooding.

Polymer flooding can be modeled by the IMEX simulator by using one of the two polymer models which treat the polymer as an additional phase. The first polymer model takes into account gas flow or variations in solution gas and seems to be appropriate to be used in cases of black oil reservoirs. The second polymer model does not take into consideration gas flow or variations in solution gas and seems to be appropriate for cases of heavy oil reservoirs or undersaturated black oil reservoirs. For the calculation of the polymer mixture viscosity, the introduction of the polymer's concentration and the polymer's viscosity as well as the mixing rule that will be used have to be introduced into the simulator. The viscosity of this mixture may follow different mixing rules depending on the polymer. As a result, for this reason, the simulator provides four different options for the calculation of the polymer mixture viscosity, namely the linear (the polymer mixture viscosity, is calculated by the reference polymer viscosity and the water viscosity using a linear relationship), non-linear, Table (the polymer mixture viscosity is calculated by interpolating in the Table of relative concentrations versus viscosity ratios) and the velocity Table (different relative concentration versus viscosity ratio Tables for each velocity). Moreover, the inaccessible pore volume has to be entered in the simulator and so as to account for the adsorbed polymer on the rock the maximum amount of the polymer that will be adsorbed by the rock, the residual adsorption level (refers to the polymer concentration that has been left adhered to the rock that cannot be recovered), the residual resistance factor (refers to the reduction of the water mobility which is present and after the end of the polymer flooding due to the adhered polymer on the rock surface) and the absolute permeability (needed for the re-calculation of the water permeability) have to be inserted.

4.5 COAL BED METHANE RESERVOIRS

Coal bed methane (CBM) reservoirs are unconventional natural gas reservoirs where the methane is found in coal deposits (Fekete associates incorporation, 2014). CBM reservoirs are naturally fractured where the methane is stored in the matrix but in a different way than in conventional gas reservoirs. In this case, the gas is adhered on the matrix surface and with a reduction in pressure and concentration the gas molecules are released and produced whereas in conventional reservoirs the gas is compressed and stored in the matrix and due to the gas expansion caused by the pressure drop, gas flows through the fractures and is produced (Fekete associates incorporation, 2014). Coal bed methane reservoirs can only be modeled using the GEM simulator. For modeling a CBM reservoir the parameters that are required to be introduced into the simulator are the following:

- Water density
- Reference pressure for water density

- Coal density
- Coal compressibility
- Langmuir pressure
- Coal diffusion coefficient
- Coal desorption time
- Initial gas composition

5. ROCK-FLUID DATA

This section consists by the following sub-sections:

- Wettability

In the wettability sub-section the wettability of the rock is defined.

- Two phase data

The two-phase relative permeabilities and the capillary pressures are inserted.

- Three phase relative permeability

The model that will be used in order to calculate the three-phase relative permeabilities, if necessary, is defined.

- Velocity depended relative permeability

In the velocity depended relative permeability sub-section the model is defined that will be used in order to take into account the reduction of gas relative permeability in cases of fluid build up near the well.

- Leverett J-function

The Leverett J-function can be used so as the capillary pressures to be adjusted accounting for porosity and permeability changes inside the reservoir.

- Hysteresis modeling

The simulator allows the user to model the hysteresis in the capillary pressures and the relative permeabilities.

- Non-Darcy flow

In the non-Darcy flow sub-section the equation that will be used, when the flow inside the reservoir deviates from Darcy law, in order to calculate the flow rates and the pressure drop is defined.

- Adsorption components

The components that are adsorbed by the rock in case of modeling CBM reservoirs as well as and the amount of adsorption of these components are defined.

5.1 WETTABILITY

As wettability we refer to the preference of the rock to be in contact with a specific fluid instead of another. This is specified by the contact angle between a drop of a fluid and the rock. For rocks with strong wettability preference, this contact angle for the wetting phase tends to 0° while for the non wetting phase this angle is 180° . For example, in the case of a water wet rock if a drop of oil falls on the rock surface then this drop will be displaced by the water which is the wetting phase. As a result the wetting phase occupies the surface of the rock and the smaller pores while the non-wetting phase tends to be in the center of the pores and occupies mainly the larger pores (H.L. Stone, 1970). In general all reservoirs are thought as water wet at least until the migration of hydrocarbons into the reservoir (Abdallah et al., 2007). From that moment and then, oil may alter the wettability of the rock depending the characteristics of the rock and the oil

composition. The reservoir wettability can be:

- water wet
- oil wet
- intermediate wet (reservoirs with no strong preference to be wet neither by water nor by oil)
- mixed wet (some regions of the reservoir are water wet and others are oil wet)

The wettability of a reservoir affects the relative permeabilities of oil and water which are the two phases that can be wetting phases, as the gas is always considered as non-wetting phase (Schlumberger, 2016). In general, it is shown that the relative permeability of the wetting phase is lowered, as the formation exhibits a strong wetting preference (Owens & Archer, 1971). For example, the permeability of water decreases as the formation tends to be more and more water wet. Due to this behavior of the permeabilities, the time of the water breakthrough to the well is significantly different in water and oil wet formations (Schlumberger, 2016). In water wet formations, the water breakthrough occurs later whereas in oil wet formations the water breakthrough occurs earlier. Moreover, in a water wet rock more oil is produced before the water breakthrough whereas in oil wet reservoirs a significant amount of oil is produced and after the water breakthrough (Morrow, 1990). Values for the classification of a rock as oil wet or water wet were provided by Craig and are given in the following Table (Craig, 1971).

	Water wet	Oil wet
S_{wc}	>20-25%	<15% (frequently <10%)
$k_{rw}=k_{ro}$ at S_w (cross over point)	>50%	<50%
k_{ro} at S_{maxw} (or else S_{or})	<30%	>50% (approaches 100%)

Table 1: Table for the classification of wettability (Craig, 1971)

It has to be mentioned, that intermediate wet rocks exhibit both water and oil wet characteristics.

5.2 TWO PHASE DATA

The two phase data include the two phase relative permeabilities and the capillary pressures between oil-water and gas-oil. The two phase relative permeability data can be either calculated using correlations or can be obtained by two phase laboratory displacement tests where the relative permeability of one phase is measured in presence of another phase. The two phase relative permeabilities are required by the simulator so as to account for the effective permeabilities of a two phase system (eg. undersaturated oil or gas reservoir) and in order to calculate the three-phase relative permeabilities in a three phase system (eg. saturated oil reservoir).

The capillary pressure data are measured for drainage (reduction of the wetting phase saturation) and imbibition (increase of the wetting phase saturation) processes. The measurement of the capillary pressures for drainage and imbibition processes is required since during these displacements the capillary pressure presents hysteresis (for the same saturation value drainage and imbibition capillary pressure presents different values). Capillary pressures are used by the simulator for the determination of the height of the transition zone above the phase contact, for the calculation of the pay thickness zone of the reservoir and for

modeling hysteresis.

The two phase data are inserted in Builder using the water-oil and the gas-liquid Table. For a water wet rock in the water-oil Table, the inserted data are the relative permeabilities of water (k_{rw}), the relative permeability to oil (k_{row}), the drainage capillary pressure (P_{cow}) and the imbibition capillary pressure (P_{cowi}) at each water saturation (S_w). It has to be noted that in the water-oil Table the first entry has to be the connate water saturation. In the gas-liquid Table, the inserted data are the relative permeabilities of gas (k_{rg}) and the relative permeabilities of oil (k_{rog}), the drainage capillary pressure (P_{cog}) and the imbibition capillary pressure (P_{cogi}) at each liquid saturation (S_l). In the gas-liquid Table, initially is assumed (eg. for a water wet rock) that the liquid saturation includes oil and connate water. As a result the residual oil saturation (S_{org}) of the gas-oil displacement is calculated internally by subtracting the connate water saturation (S_{wc}) from the residual liquid saturation entered in the Table. Although, for measurements that have not been conducted in presence of connate water saturation the residual oil saturation (S_{org}) is set equal to the value obtained by the Table. Finally, all the aforementioned are applied respectively for oil wet rocks.

5.3 THREE-PHASE RELATIVE PERMEABILITY

Three-phase permeability refers to the relative permeability of a phase when all three phases (oil, water and gas) co-exist in the reservoir. In general, the three-phase relative permeabilities are not easy to be measured because of the simultaneous variation of all phases saturations (Blunt, 2000; Masalmeh & Wei, 2010). Moreover, the available techniques to obtain three phase data are too complex and as a result they have to be calculated by using the two phase data obtained by the laboratory tests or created by correlations (Blunt, 2000). The two phase data required for the calculation of the three-phase relative permeabilities are the water-oil and gas-oil data. Builder for the calculation of the three-phase relative permeabilities offers the following models:

- Stone's first model

Stone's first model was introduced by Stone in 1970 and then was modified by Aziz and Settari. Builder uses the modified form of Stone's first model (Computer Modelling Group Ltd, 2010). Stone's model is a probabilistic model which uses the channel flow theory where the wetting phase is located in the smaller pores, the non-wetting phase is located in the larger pores and the intermediate phase is located between them (H.L. Stone, 1970). As a result, each phase will flow through different paths and the probability of a phase to flow through a specific path has to do with whether that phase is the wetting, the non-wetting or the intermediate wetting phase (Masalmeh & Wei, 2010). Also Stone's assumes that the difficulty of the intermediate phase to flow is due to two independent events; the presence of the wetting and the non-wetting phase, whereas the flow of the wetting and the non-wetting phase depends only on their saturations (Herbert L. Stone, 1973). For example, for a water wet system, the relative permeability of water and the relative permeability of gas are functions solely of the water saturation and the gas saturation whereas the relative permeability of oil is dependent on the saturations of the other two phases (Ahmed, 2010).

Stone's model was initially developed for water wet systems but it can be used also for oil wet systems. Although, the use of the Stone's model for oil wet rocks is better to be avoided as it cannot accurately predict the three-phase relative permeabilities for those cases (Blunt, 2000; Dicarolo, Sahni, Blunt, & Stanford, 2000; Oak, Baker, & Thomas, 1990). The reason due to which this extension is better to be avoided, is that it was found out that for oil wet reservoirs, the non-wetting phase relative permeability does not depend only on its own saturation but also on the saturation of the wetting phase (Blunt, 2000; Dicarolo, Sahni, & Blunt, 2000).

Moreover, Stone's model initially assumes that the gas-oil displacement data were measured at zero water saturation something that in real conditions is not valid and as a result the model produces unrealistic values for the relative permeability of oil (Fayers & Matthews, 1984). In order to avoid this Aziz and Settari modified the Stone's model assuming that the gas-oil two phase data are measured with irreducible water saturation being present (Khalid Aziz & Settati, 1979). The calculation of the oil relative permeability is done by using the following formulas:

$$k_{ro} = \frac{S'_o \cdot k_{row} \cdot k_{rog}}{k_{rocw} \cdot (1 - S'_w) \cdot (1 - S'_g)}, \text{ where } k_{rocw} \text{ is defined as the relative permeability at connate water saturation}$$

and the S'_o , S'_w and S'_g are the normalized forms of saturations calculated from the following equations:

$$S'_o = \frac{S_o - S_{om}}{1 - S_{wc} - S_{om}}$$

$$S'_w = \frac{S_w - S_{wc}}{1 - S_{wc} - S_{om}}$$

$$S'_g = \frac{S_g}{1 - S_{wc} - S_{om}}$$

and S_{om} is the minimum oil saturation and occurs when oil is displaced simultaneously by gas and water and is calculated from the following expression proposed by Fayers and Mathews:

$$S_{om}(S_g) = (1 - a(S_g)) \cdot S_{orw} + a(S_g) \cdot S_{org}, \text{ where } a(S_g) = \frac{S_g}{1 - S_{wcon} - S_{org}}$$

Builder provides the following two options:

- with dependence on S_w and S_g

When this mode is selected and k_{row} and k_{rog} are functions of S_w and S_g respectively.

- with dependence on S_o

When this mode is selected k_{row} and k_{rog} are functions of $1 - S_o$ and $1 - S_{wc} - S_o$ respectively.

- Stone's second model

Due to the difficulty of the determination of the minimum oil saturation, Stone proposed another model in 1973 known as Stone's second model by using all the assumptions of Stone's first model. This model was modified by Aziz and Settari in 1979 for the same reason as the Stone's first model and this is the model used by the simulator. The Stone's second model, as Stone's first model, is not very accurate for oil wet systems but it is a better predictor in high oil saturations whereas in low oil saturations it tends to over-predict the residual oil saturation and as a result to under-predict the three phase oil relative permeability (Saraf, Batycky, Jackson, & Fisher, 1982; Herbert L. Stone, 1973). The calculation of the oil relative permeability is done by using the following formula:

$$k_{ro} = k_{rocw} \cdot \left[\left(\frac{k_{row}}{k_{rocw}} + k_{rw} \right) \cdot \left(\frac{k_{rog}}{k_{rocw}} + k_{rg} \right) - k_{rw} - k_{rg} \right]$$

Finally Builder provides the options of using the Stone's second model with dependence on S_w and S_g or with dependence on S_o which are defined as in the Stone's first model.

- Saturation-weighted interpolation (or segregated model in Builder)

The saturation-weighted interpolation model was introduced by Baker in 1988 (Baker, 1988). The saturation-weighted interpolation model so far is considered as the best predictor of the three-phase permeability for water wet and oil wet rocks (Baker, 1988; Dicarolo et al., 2000; Oak, 1990). The saturation-weighted interpolation model does not assume that the wetting and non-wetting phase relative permeabilities are dependent only on their own saturations but they also depend and on the saturation of the intermediate wetting phase (Baker, 1988). This assumption makes them appropriate to be used for oil wet reservoirs where it was found that the relative permeabilities of the wetting and the non wetting phases do not depend only on their own saturations (Baker, 1988; Dicarolo et al., 2000; Oak, 1990). The prediction of the three-phase relative permeability is done by using the following formulas:

$$k_{ro} = \frac{(S_w - S_{wc}) \cdot k_{row} + (S_g - S_{gr}) \cdot k_{rog}}{(S_w - S_{wc}) + (S_g - S_{gr})}$$

$$k_{rw} = \frac{(S_o - S_{or}) \cdot k_{rwo} + (S_g - S_{gr}) \cdot k_{rwg}}{(S_o - S) + (S_g - S_{gr})}$$

$$k_{rg} = \frac{(S_o - S_{or}) \cdot k_{rgo} + (S_w - S_{wc}) \cdot k_{rgw}}{(S_o - S) + (S_w - S_{wc})}$$

- Linear interpolation model (or linear isoperm model in Builder)

The linear interpolation model was proposed by Baker in the same work in which the saturation-weighted interpolation model was proposed. The linear isoperm model does not assume that the wetting and non-wetting phase relative permeabilities depend only on their own saturations but they also depend and on the saturation of the intermediate phase. The linear isoperm model calculates the three-phase relative permeabilities using linear interpolation between the two-phase relative permeability data. The determination of the three phase relative permeabilities at a point of a given saturation is done by defining a straight line in a ternary diagram passing from this saturation and intersecting the oil-gas and water-gas relative permeability curves at equal relative permeability values. If x_1 and x_2 are two points of the line of equal relative permeabilities and x_3 is the point at which the relative permeability has to be calculated then the distance of the point x_3 from the line defined by x_1 and x_2 is given by the following formula:

$$D^2 = \sum_{j=1}^3 \left[a_j \cdot T + (x_{1j} - x_{3j})^2 \right]$$

$a_j = x_{1j} - x_{2j}$, where x_{1j} and x_{2j} are the saturations of two points on the line of equal relative permeabilities

$$T = \frac{\sum_{j=1}^3 \left[a_j \cdot (x_{3j} - x_{1j})^2 \right]}{\sum a_j}, \text{ where } x_{3j} \text{ is the saturation of the point that the relative permeability has to be}$$

defined.

Moreover, if the point x_1 is located on the line $S_w=S_{wc}$ and the point x_2 is located on the line $S_g=0$ then the gas-oil relative permeability at connate water and the oil-water relative permeability at zero gas saturation can be expressed as functions of x_1 and x_2 respectively.

$$k_{rog}=f_1(x_1)$$

$$k_{row}=f_2(x_2)$$

Finally, to find the desired relative permeability the distance of the point x_3 from the line defined by the x_1 and x_2 and the difference of gas-oil relative permeability at connate water and the water-oil relative permeability at zero gas saturation have to be minimized simultaneously as follow:

$$\min[D^2] \text{ and } \min[f_1(x_1)-f_2(x_2)]$$

Finally, Baker in his work compared Stone's first model, Stone's second model and his two models and found that the prediction efficiency of these models in a descending order is the following: segregated model, linear isoperm model, Stone's second model and Stone's first model.

5.4 VELOCITY DEPENDENT RELATIVE PERMEABILITY

In cases of gas reservoirs which are producing under high gas rates or near critical fluids it was found that in the region near the well, fluid build up occurs. Fluid build up is the phenomenon according to which near the well the liquid saturation increases resulting in a smaller gas relative permeability which is translated as formation damage (see § 7.4). In order to account for this phenomenon, GEM simulator has incorporated the Popes 1 and Popes 2 models which account for a three-phase and a two-phase system respectively.

5.5 LEVERETT J-FUNCTION (OPTIONAL)

Capillary pressure data are given by core tests but those samples are taken from specific parts of the reservoir, thus, are not able to represent accurately the entire reservoir due to differences in porosity and permeability between different regions (Computer Modelling Group Ltd, 2010). Capillary pressure is a function of porosity, surface tension and mean pore radius (Ahmed, 2010). As a result, variations to those values affect the capillary pressure values (eg. lower porosity values result to higher capillary height) which in turn affect the height of the transition zones and the net pay thickness. In order to account for these variations inside the reservoir and obtain a more accurate representation of the reservoir the Leverett J-function is used. The water-oil capillary pressure for each saturation, using Leverett correlation in Builder is given by the following formula:

$$J(S_w) = \frac{\sigma}{P_{cow}} \cdot \sqrt{\frac{\phi}{k}} \cdot CF$$

Where σ is the interfacial tension, k is the block permeability defined as $(\sqrt{k_x \cdot k_y})$ and CF is a conversion factor (for SI system this is equal to 31.8316 and for field units this is equal to 4.61678) (Computer Modelling Group Ltd, 2010).

5.6 HYSTERESIS MODELING (OPTIONAL)

Hysteresis is the phenomenon according to which the obtained capillary pressures and relative permeabilities present different values for the same wetting phase saturation during drainage (reduction in saturation of the wetting phase) and imbibition (increase in saturation of the wetting phase) processes. Hysteresis is caused by the trapping of the non-wetting phase and the different contact angle between the wetting phase and non-wetting phase during drainage and imbibition processes (Bennion, Thomas, & Bietz, 1996). Moreover, hysteresis is more pronounced to the non-wetting phase than to the wetting phase (Jackson, Valvatne, & Blunt, 2003; Bennion, Thomas, & Bietz, 1996).

Capillary pressure hysteresis affects the well coning behavior, especially in reservoirs where coning of water or gas occurs under unstable production rates as after each change of the production rate the saturations of water or gas near the wellbore are different than those in other regions of the reservoir which are in the same distance from the contacts (Cutler & Rees, 1970). On the other hand, hysteresis in relative permeabilities is important to be taken into account in order to obtain a more accurate prediction of the production and the recovery efficiency of IOR methods, especially in cases where alternate injection of wetting and non-wetting phases is applied (F. M. Carlson, 1981).

In the case of a three phase system four different combinations may occur when hysteresis is to be modeled, the DD,DI,ID and II where D refers to drainage and I to imbibition (Land, 1968). For example, in a water wet rock the water-oil relative permeabilities follow the drainage curve during the hydrocarbon migration into the reservoir whereas they follow the imbibition curve in cases of water flooding (Fanchi, 2006). On the other hand, for the same rock the gas-oil relative permeabilities follow the drainage curve when gas cap is moving downwards due to expansion whereas they follow the imbibition curve when the gas cap is moving upwards (due to water flooding) (F. M. Carlson, 1981).

In order hysteresis to be modeled, the required data that have to be introduced in the simulator are the drainage and imbibition capillary pressures of the phases present in the reservoir and the process (drainage or imbibition) that initially is followed. Moreover, the transition between drainage and imbibition capillary pressures and the maximum possible imbibition residual oil or gas saturation (S_{ormax} or S_{grmax}), depending to which phase hysteresis is modeled, have to be introduced.

Based on these data, when the process changes the transition between drainage and imbibition is calculated by the simulator using scanning curves. For example, when the process that it is initially followed is drainage and a reversal occurs, the transition from drainage to imbibition is done by using a scanning curve initiated on the drainage curve at the point where the reversal of saturation occurred and terminated at the imbibition curve which is then followed (M. Carlson, 2003; Plohr, Marchesin, Bedrikovetsky, & Krause, 2000).

5.7 NON-DARCY FLOW

In general the flow inside the reservoir is thought to behave according to Darcy's law but this is not always the case especially for gas reservoirs, and more particularly in, tight reservoirs and at the region near wells where the flow tends to be turbulent (Ahmed, 2010; Fanchi, 2006). According to Darcy's law the flow rate increases proportionally with the pressure drop but when the flow rate is too high or when fluid flows through narrow pore throats an additional pressure drop caused by inertia and turbulence is created (Katz, 1959). To account for this deviation from Darcy's law, Forchheimer proposed an equation with an additional

term to the Darcy's law term so as to account for the additional pressure drop: $\frac{-dp}{dx} = \frac{\mu}{k} \cdot u + \beta \cdot \rho \cdot u^2$. In the previous equation, the second term accounts for the non-Darcy phenomenon and the coefficient β is the non-Darcy flow coefficient which is also called inertial coefficient or turbulence factor. In general this additional term is negligible at low flow rates but in high flow rates this term is far larger than the Darcy term. It has to be noted that non-Darcy flow effects are more intense as the porosity and permeability reduces (Katz, 1959). This was also evaluated by Armenta and Wojtanowicz who concluded that in tight reservoirs which exhibit low porosity and permeability non-Darcy flow could occur even in low flow rates (Armenta & Wojtanowicz, 2003). Moreover, in cases of tight reservoirs, non-Darcy flow occurs in a large region of the reservoir and not only in the region near the well (Saboorian-Jooybari & Pourafshary, 2015). When non-Darcy flow occurs in a reservoir it also affects the skin factor calculation by producing an additional pressure drop (rate dependent skin factor) (Lee & Wattenbarger, 1996). To account for the non-Darcy flow, the inertial coefficient β has to be calculated. For the calculation of the inertial coefficient Builder includes four different equations:

- Frederick and Graves 1

Frederick and Graves introduced their equations in 1994. This equation was derived for single-phase flow but by comparing known data in the literature for multi-phase flow they assumed that this equation can be used also for multiphase flow (Frederick & Graves, 1994).

$$\beta = \frac{7.89 \cdot 10^{10}}{k_e^{1.6} \cdot (\varphi \cdot (1 - S_w))^{-0.404}}, \text{ where } k_e = k \cdot k_{rg}$$

- Frederick and Graves 2

The Frederick and Graves 2 equation was derived exactly as the Frederick and Graves 1 equation. The only difference between these equations is that the porosity on the y axis has also been

taken into account.

$$\beta = \frac{2.11 \cdot 10^{10}}{k_e^{1.55} \cdot (\varphi \cdot (1 - S_w))}$$

- Geertsma

Geertsma derived his equation by using liquid and gas flow through unconsolidated sandstones and gas flow through consolidated sandstones (Lopez-Hernandez et al., 2004). The equation provided by the simulator is the one that accounts for gas single-phase flow in presence of connate liquid saturation (usually water) in the porous media:

$$\beta = \frac{0.005}{k^{0.5} \cdot \varphi^{5.5} \cdot (1 - S_{wi})^{5.5} \cdot k_{rg}^{0.5}}, \text{ where } k_{rel} \text{ is the gas relative permeability and } S_{wi} \text{ the irreducible water}$$

saturation.

Nevertheless, this equation may not be valid for liquid saturations from 40 to 70% because the existing liquid phase has to be immobile and usually liquid saturation values above 40% exceed the critical saturation values (Geertsma, 1974). This equation can be used for unconsolidated/consolidated sandstones, dolomites and limestones (Saboorian-Jooybari & Pourafshary, 2015).

- General

This equation is the only one that accounts for non-Darcy flow to all phases not only to the gas phase as the previous correlations and it is mainly used to model non-Darcy flow in fractures (Computer Modelling Group Ltd, 2010).

$$\beta_p = \frac{1.485 \cdot 10^9}{(k \cdot k_{rp})^{1.021}}, \text{ where } k_{rp} \text{ is the relative permeability of the phase p.}$$

When the general option is used a weighting factor for Forchheimer number has to be also defined which corresponds to the allowed tolerance of Forchheimer number to change over a timestep. Moreover, the maximum Forchheimer number for each phase has to be defined. This maximum Forchheimer number does not allow Forchheimer numbers that overcome this limit to be used in the calculation of non-Darcy flow (Computer Modelling Group Ltd, 2010). The Forchheimer number is used as the Reynolds number and determines the start of turbulent flow in porous media from the following

equation: $Fo = \frac{k \cdot \beta \cdot \rho \cdot u}{\mu}$ (Saboorian-Jooybari & Pourafshary, 2015).

5.8 ADSORPTION COMPONENTS

In cases of modeling coal bed methane reservoirs by the GEM simulator which components can be adsorbed on the rock have to be defined. Normally, only the light components exhibit significant adsorption. Firstly, the maximum adsorption value (ω_{max}) which represents the maximum amount of moles that can be adsorbed per unit mass of rock has to be determined. Secondly, a Table of adsorption values (ω_i) and partial pressures (p_i) for each component has to be defined for the simulator to calculate the amount of the adsorbed mass of each component.

6. INITIALIZATION

The data introduced to the initialization section refer to the initial state of the reservoir (eg. undersaturated or saturated), the calculation method that will be used for the calculation of pressures and saturations and the calculation method for the initial fluid in place. The initialization section consists of the following sub sections:

- Initialization method

In the initialization method sub-section the initialization method that will be used and the initial state of the reservoir are defined.

- Initial fluid in place calculation

In the initial fluid in place calculation sub-section the way that the initial fluid in place will be calculated in GEM simulator is defined.

6.1 INITIALIZATION METHOD

Moreover, in the initialization section the method that will be used for the calculation of the pressure and saturations is defined. The initialization methods that the simulator provides are the vertical depth average, the vertical block centered and the user input methods.

6.1.1 Vertical Depth Average

By using the vertical depth average initialization procedure the pressures are calculated by the hydrostatic pressure relation and the saturations are averaged over the vertical extent of the block using the capillary pressures. The vertical depth average initialization method can be used in reservoirs with large vertical extent where the vertical extent of the phase contacts is small in comparison to the total capillary pressure transition zone and in reservoirs with good vertical permeability (M. Carlson, 2003; Coats, Nielsen, Terhune, & Weber, 1967). Moreover, this method provides the more realistic and accurate results for the calculation of the initial oil in place (IOIP) thus it is better to be used in any case (Chatzichristos, 2016).

When this method is used by the simulator it is required that the user determines if the reservoir is undersaturated, saturated or it is a gas reservoir. It has to be noted that in cases of saturated reservoirs it has also to be defined if the gas cap contains or not residual oil saturation. This definition is required for the calculations to be done accurately. Moreover, the simulator requires the following data to be introduced:

- Bubble or dew point pressure

The bubble or the dew point pressure has to be introduced depending on the reservoir fluid (eg. the bubble point pressure is used for black oil reservoirs and the dew point pressure for gas reservoirs). These saturation pressures can either be introduced as a constant value for the entire reservoir or they be introduced in tabulated form of saturation pressures versus depths which is used when variances in composition with depth are encountered in the reservoir.

- Reference pressure and depth

The reference pressure and depth are introduced in the simulator and are defined as the initial pressure of the

reservoir and depth at which this value was measured. The reference pressure and the depth are used internally by the simulator in order to create the initial pressure profile of the reservoir.

- Phase contact depth

If the depths of the phase contacts are known they have also to be introduced in the simulator. The phase contact depth is used by the simulator for the calculation of hydrocarbons initially in place and for the calculation of saturations. The depth of the oil-water (or gas-oil) contact when the depth average initialization method is used is defined as the depth at which the capillary pressure is equal to the value entered in the 'capillary pressure at phase contacts' field of this tab.

- Capillary pressures at the phase contacts

The capillary pressures at the phase contacts have to be defined for the simulator to calculate the height of the transition zones. For water wet reservoirs the default value is zero whereas for oil wet reservoirs that value is defaulted to the maximum capillary pressure value entered in the simulator.

Moreover, Builder offers the option to define datum depth for pressure. As datum depth usually is defined the depth of the free water level or the middle depth of the reservoir. By using a datum depth for the simulation the pressures in the reservoir are calculated with respect to it and are expressed in terms of fluid potential. The fluid potential shows the tendency of a fluid to flow towards a specific direction due to the pressure difference. Representing the pressures in the reservoir in terms of fluid potential is a more practical way as the user can understand immediately toward which direction the fluid will tend to flow (Dake, 1978). The calculation of the fluid potential is done internally by the simulator using the following formula: $\Phi = P - P_i + \Phi_i$, where Φ and Φ_i are the datum pressures of the block at a given time of the simulation and at the initial conditions (time equal to zero) accordingly and P is the block pressure at the time that the fluid potential is to be calculated and P_i is the initial block pressure. Moreover, when the phase densities change significantly during the simulation and the phase contacts are moving fast, the simulator offers an alternative way to calculate the fluid potential by using the following formula: $\Phi = P + \rho \cdot g \cdot \Delta z$, where ρ is the density specified by the user or calculated by the simulator, g is the gravity acceleration and Δz is the distance between the block and the datum depth level (Computer Modelling Group Ltd, 2010).

6.1.2 Vertical Block Centered

By using the vertical block centered method, the pressure is calculated by the hydrostatic pressure relation and the saturations of each block are set equal to those observed at the center of the block. In case that the user wishes to perform the initialization with this method then the blocks are required to be smaller than the transition zone height so as to achieve a better resolution regarding the phase saturations (M. Carlson, 2003). The vertical block centered method was widely used by early reservoir simulators before the implementation of the depth average initialization option but nowadays is not used anymore (Chatzichristos, 2016).

When the vertical block centered initialization method is used, again the reservoir has to be defined whether it is undersaturated, saturated or gas reservoir as previously. The required data that have to be defined when the vertical block centered method is used, are the saturation pressures, the reference pressure and depth, the depth of the phase contacts and, if required, the datum depth. In the vertical block centered initialization method the depth of the contacts is defined at the free water level depth. For example, the oil-water contact is

defined as the smallest depth at which the water saturation presents its maximum value ($S_w=1$) whereas the depth of the gas-oil contact is defined as the smallest depth at which the gas saturation is zero.

In addition, GEM simulator, so as to take into account compositional grading inside the reservoir when the vertical block centered initialization method is selected, offers the option to introduce the variation of composition as a function of depth. In this case, the critical depth and the fluid composition versus depth have to be provided. The critical depth is used for the identification of the fluid phases. When single phase fluid is encountered above this depth then the fluid is identified as gas whereas if a single phase fluid is encountered below this depth then it is identified as oil.

6.1.3 User Input

By using the user input initialization method, the pressure as well as the saturations of water and oil have to be introduced in the simulator for each block. Moreover, when this method is used with GEM simulator the composition of the fluid has also to be introduced. This initialization option can be used in cases where the pressures inside the reservoir are different in different regions and the depth of the contacts is unknown.

6.2 INITIAL FLUID IN PLACE CALCULATION

When compositional simulation is performed the way that the initial volumes of hydrocarbons in place is calculated has to be defined. The calculation of the initial volume of hydrocarbons in place can be done either by using the initial fluid formation volume factors or by using the surface separator conditions.

For the first option the oil and gas formation volume factors (B_o and B_g) and the gas-oil ratio (R_o) measured at the initial conditions of the reservoir have to be inserted into the simulator. It is recommended to use the surface separator conditions as they can provide more accurate results due to the fact that the simulator takes into consideration the actual separation process that is used. The calculation of the volumes of the phases at each separator is done by using an equation of state. It has to be noted that in the separation process the water phase is not taken into consideration. Moreover, the wells that are attached to each separator train have to be defined in order for the simulator to assign the appropriate rates and composition to each separator. Gem simulator provides two different types of separators the short and the long format.

- Short format

The well stream is entered in the first separator where the separation of gas from oil takes place, the liquid that remains after the separation is directed towards the next separator. This procedure is followed until the liquid reaches the stock tank whereas the liberated gas from each separator composes a single stream. The density of these streams is calculated by using an EOS for each separation stage. The data that has to be introduced when the short format separator is used are the pressures and temperatures at which each separator is working for the EOS calculation to be performed. Finally, the short format separator can be used only when only oil and gas streams are produced.

- Long format

In the long format separator, the calculation of the mass density of each phase in the separator can be done by using an EOS for each phase or by using a table representing the components distribution in the different streams. When the EOS is used, the pressures and temperatures at which the separators are working have to

be defined. By using the EOS, only two streams are allowed as separator outlet streams the gas and the oil streams whose densities are calculated by the EOS.

On the other hand, when a table of components distribution is used, each separator is allowed to have three outlets the oil, gas and natural gas liquid. For a table of component distribution to be used for the calculation of the separator output stream densities, a gas plant table has to be defined first. In the gas plant table, the fractions of each component in the oil, gas and natural gas liquid output streams from the separator have to be introduced. The calculation of the stream densities, when a table of component distribution is used, is done by entering each components density and by using the molecular weight of each component so as to calculate their molar volume. These molar volumes with the molar fractions of the components of the output streams of the separator are used for the calculation of the output streams volumes. Then the simulator, by using the average molecular weight of the components present in the stream and its volume, calculates the density of the output stream.

7. WELLS

In the wells section the location of the wells, their geometry, constraints and their characteristics are introduced in the simulator. This section is constituted by the following sub-sections:

- Well types

In the well types sub-section the wells of the field are introduced to the simulator.

- Perforations

The introduction of the perforations into the simulator is done at this level.

- Well index (WI)

The way that the calculation of the well index will be performed is defined.

- Rate depended skin factor

In the rate depended sub-section, it is defined if the skin factor has to be calculated taking into consideration the turbulent flow in the region near the well.

- Gas inflow

The way that the flow rate will be calculated for gas wells flowing at high rates is defined.

- Well and group constraints

The constraints (eg. rates, pressures etc.) under which the wells or groups of wells operate are defined.

- Seawater scale build up

The amount of scale created in the well are introduced.

- Tubing tables

In the tubing tables sub-section the tubing tables are introduced for the calculation of pressure losses along the tubing and for the artificial lift.

- Pressure calculations

The bottom hole pressure and the calculation of pressure losses along the tubing and between the perforations are defined.

- Gas lift

In the gas lift sub-section the way that the calculation of the gas lift will be done is defined.

- Manifolds

If a manifold is used, then the manifold depth and the streams that are connected to it are defined for the simulator to calculate the pressure drop from the manifold depth and

- Hydraulic fracturing

In the case that hydraulic fractured wells exist in the field, the fracture's characteristics are entered.

- Recycling

In the recycling sub-section the fluid and the rates of re-injection are entered.

- Alternating processes

When alternating processes are used then the cycles, the rates and the duration of each cycle of the alternating process are defined.

- Rate distribution

The way by which the contribution of the each well in a group of wells is given here.

- History matching tools

In the history matching sub-section the simulator allows to apply changes using triggers or multipliers for the wells.

7.1 WELL TYPES

When a well is inserted into the simulator, first of all the type of the well has to be defined. For the IMEX simulator the available well types are the producers, the unweighted and the weighted injectors whereas for the GEM simulator, the available well types are the producers, cyclo-producers and the injectors. The cyclo-producers are production wells from which all or a part of their separator gas is recycled by re injection to the reservoir and are available only for the GEM simulator. The unweighted and the weighted injectors differ in the way that the injection rates are calculated. In the case of the unweight injectors the injection rate is calculated by: $q = WI \cdot (P_{block} - P_{well})$, where WI is the well index (see § 7.3) whereas P_{block} is the block pressure where the well is located and P_{well} is the pressure of the perforations. On the other hand when a mobility weighted injector is going to be used, the mobility of the injection phase is taken into account in the

calculation of the injection rate as it is shown by: $q_p = WI \cdot \frac{k_{rp}}{\mu_p} \cdot (P_{block} - P_{well})$. From these two types of injectors the mobility weighted injectors, are thought to be more accurate due to the fact that they take into account the mobility of the phase (Chatzichristos, 2016).

Once the wells that will be used for the simulation are entered then can be treated either separately or as groups. Groups of wells have to be used when many wells are ending to a single separator, when multilateral wells have been drilled and in cases where many wells exist in a field and for practical reasons is better to handle them as groups. Multiple groups can be defined but a certain 'child to parent' hierarchy is applied. The simulator always assumes a top group which stands for the entire field and to which all the wells and all the existing groups are attached to it. For the same 'parent' group only groups or only wells can be attached to it as 'child'.

Moreover, the status of the well has to be defined between the open, shut in and autodrill. The open and the shut in status indicate that the well is active and inactive respectively. The autodrill status indicates that the well is currently shut in but if it is needed then the well it can be opened during the simulation in order to achieve the target set for the group or the field (Computer Modelling Group Ltd, 2010).

7.2 PERFORATIONS

After the definition of the well type the position of the perforations, the well's trajectory data in cases of deviated wells and the different branches of a multilateral well have to be defined. In order to design the perforations of a well, the coordinates of the perforated blocks have to be defined. This can be done either by clicking directly on the desired blocks on the field's map or by introducing the coordinates of the perforated blocks in the available table.

In the case that the well has multiple perforations, it has to be defined which perforation is connected directly to the surface as well as the sequence of the perforated blocks has to be introduced. When partial perforations (block is not perforated throughout its entire length but only to a part of it) are used, the simulator in order to account for it uses a form factor indicating the percentage of the block length that it is perforated (Computer Modelling Group Ltd, 2010). Finally, the status of the perforations which is similar to the well status has to be defined.

7.3 WELL INDEX (WI)

The well productivity index expresses the ability of the reservoir to deliver fluids to the wellbore. The well productivity index can either be entered into the simulator for each layer directly or to be internally calculated using the geometric information, the dimensions and the permeability of the block in which the well is located. The geometric information refers to the production casing radius, geometric factor, position of the well in the block and skin factor and the direction of the well. The position of the well in the block is defined as a fraction and if this value is equal to unity then it is thought that the well is located at the center of the block whereas if this fraction is equal to 0.5 or 0.25 then the well is located at the edge or at the corner of the block accordingly (Computer Modelling Group Ltd, 2010).

The well index is calculated by the simulator using:

$$WI = \frac{2 \cdot \pi \cdot wfrac \cdot k \cdot L_p \cdot ff}{\ln\left(\frac{r_e}{r_w}\right) + S},$$

where *wfrac* defines the

well's position in the block, L_p is the perforations length, *ff* is a factor accounting for partial completions, r_w is the production tubing radius, *S* is the skin factor and r_e is the equivalent radius of the region where is thought that radial flow occurs.

The simulator for the calculation of the equivalent radius offers different models for isotropic and anisotropic permeabilities accounting either only for the well's block permeability or for the entire layer's permeability. In the case that an anisotropic model is used then the effective well radius is calculated by Peaceman's well model. The equivalent radius in the case of a well parallel to one of the I, J or K directions and isotropic

permeability is given by the following formula: $r_e = geofac \cdot \sqrt{\frac{V}{\pi \cdot h \cdot wfrac}}$, where *geofac* is the geometric factor, *V* is the bulk volume of the perforated grid block and *h* is the block thickness. On the other hand, in the case of a well parallel to the K direction (for I and J directions the equation has to be adjusted accordingly) and anisotropic permeability the equivalent radius is given by the following formula:

$$r_e = 0.28 \cdot \frac{\sqrt{\Delta x^2 \cdot \sqrt{\frac{k_y}{k_x}} + \Delta y^2 \cdot \sqrt{\frac{k_x}{k_y}}}}{\left(\frac{k_y}{k_x}\right)^{1/4} + \left(\frac{k_x}{k_y}\right)^{1/4}}, \text{ where } k_x \text{ and } k_y \text{ are the permeabilities towards the x and y direction}$$

(Peaceman, 1983).

When the XYZ directions are used the well is thought to be deviated and parallel to the XYZ coordinates system which forms an angle θ with the IJK coordinate system. In this case the effective radius as well as and the permeability has to be recomputed with respect to the XYZ coordinates system. Since the effective radius has been calculated for the IJK directions then the effective radius is:

$$r_e = \frac{r_e(I) \cdot \cos^2(\theta_I) \cdot \sin^2(\theta_J) \cdot \sin^2(\theta_K) + r_e(J) \cdot \cos^2(\theta_J) \cdot \sin^2(\theta_K) \cdot \sin^2(\theta_I) + r_e(K) \cdot \cos^2(\theta_K) \cdot \sin^2(\theta_I) \cdot \sin^2(\theta_J)}{\cos^2(\theta_I) \cdot \sin^2(\theta_J) \cdot \sin^2(\theta_K) + \cos^2(\theta_J) \cdot \sin^2(\theta_K) \cdot \sin^2(\theta_I) + \cos^2(\theta_K) \cdot \sin^2(\theta_I) \cdot \sin^2(\theta_J)}$$

, whereas the calculation for the permeability is done by the same way but the re(I), re(J) and re(K) are replaced by k(I), k(J) and k(K) where $k(I) = \sqrt{k_y \cdot k_z}$, $k(J) = \sqrt{k_x \cdot k_z}$ and $k(K) = \sqrt{k_y \cdot k_x}$.

7.4 RATE DEPENDENT SKIN FACTOR (OPTIONAL)

In cases of gas wells which flowing under high rates, turbulent flow appears in the region near the well which causes an additional pressure drop. This pressure drop created by the high flow rate is translated as rate dependent skin factor in addition to the skin factor created by the formation damage. The new skin factor is calculated as follow: $S' = S + D \cdot q$, where S' is the modified skin factor, S is the skin factor due to formation damage and the D and q product is the skin factor due to turbulent gas flow (Ramey, 1964). The D factor is calculated internally by the simulator using the following

formula: $D = \frac{2.715 \cdot 10^{-15} \cdot \beta \cdot k_{rg} \cdot MW \cdot P_{sc}}{h \cdot r_w \cdot T_{sc} \cdot \mu_{gwf}}$, where h is the net formation thickness, μ_{gwf} is the viscosity of

this phase evaluated at the perforations level (Wattenbarger & H.J., 1968). The β factor in the previous equation is calculated either by the non-Darcy flow equation selected in the rock fluid section or when the non-Darcy flow option is not activated the β factor is calculated by the following equation:

$$\beta = 1.88 \cdot 10^{10} \cdot k_{rg}^{-1.47} \cdot \phi^{-0.53} \quad (\text{Computer Modelling Group Ltd, 2010; Lee \& Wattenbarger, 1996}).$$

7.5 GAS INFLOW (OPTIONAL)

In cases of gas wells that are flowing at high rates the flow rates, can be calculated either by using a quadratic or a pseudo pressure gas inflow. By using the quadratic pressure gas inflow relation it is assumed that the density of the gas near the well bore is proportional to the pressure drop and it is calculated by:

$$q = \frac{WI \cdot (\text{Phasemobility}) \cdot (P_{block}^2 - P_{well}^2)}{2 \cdot P_{block}} \quad (\text{Computer Modelling Group Ltd, 2010}).$$

On the other hand, by using the pseudo-pressure gas inflow relation it is assumed that near the well the density and the viscosity of the gas are changing with pressure and the calculation is done as following:

$$q = WI \cdot k_{rg} \cdot \rho_g \cdot \left(\frac{E_g}{\mu} \right)_{ave} \cdot (P_{block} - P_{well}), \text{ where } \left(\frac{E_g}{\mu} \right)_{ave} = \frac{\left(\frac{E_g}{\mu} \right)_{well} + \left(\frac{E_g}{\mu} \right)_{block}}{2} \text{ (Computer Modelling$$

Group Ltd, 2010).

7.6 WELL AND GROUP CONSTRAINTS

In order the already defined wells to operate, some constraints have to be imposed on them. These constraints are different for producers and injectors and for individual wells and well groups. These constraints can be categorized in operating, monitoring and penalty constraints. As operating constraints are defined the constraints based on which a production well or the production wells of a group are producing. The monitoring constraints are constraints that the well is not operated based on them but they are checked periodically. The penalty constraints are applied only on producers and are used so as to avoid overproduction. In general, the production of gas and water is restricted by government regulations which are applied for environmental reasons and when the production does not behave to the restriction, fines are imposed on companies. When a constraint is violated, remedial actions have to be taken in order the constraint to stop being violated. These remedial actions are needed as these constraints have not to be violated otherwise problems related to the production and the equipment may arise and cost increases.

7.6.1 Production Wells

7.6.1.1 OPERATING CONSTRAINTS AND REMEDIAL ACTIONS

The sequence of definition of the operating constraints is important as the first defined constraint is the primary constraint. The primary constraint is the constraint based on which the well produces whereas the rest of the operating constraints are checked periodically. This primary constraint may be altered if another operating constraint is violated and the defined remedial action allows this switching. Normally only the bottom hole pressure and the oil rate are defined as operating constraints as these two values are the most important but other values are also available by the simulator.

The available parameters that can be set as operating constraints can be surface and reservoir rates of each phase, the bottom hole and the wellhead pressure and the pressure draw down of the layers (as layer is defined the layer that the perforations exist) of the well.

In cases where these constraints are violated then the available remedial actions that can be taken is to stop the simulation, to allow the simulation to continue by setting the violated constraint as primary constraint, to continue and repeat the time step after the switch of the constraint, to shut in the well and to shut in the well and repeat the time step after the shut in.

7.6.1.2 MONITORING CONSTRAINTS (OPTIONAL)

The available monitoring constraints for production wells are the surface rates of the phases, the bottom hole and well head pressures, the gas-oil, water-gas, solvent-oil, gas and solvent over oil, the water-cut, the wellbore hydraulic stability and the back flow monitoring. The wellbore hydraulic stability constraint allows

the well to operate only above a certain rate in order the bottom hole pressure to be in the stable region of the wellhead pressure curve and can be used only in cases where and the wellhead pressure is also calculated (Computer Modelling Group Ltd, 2010). The back flow monitoring constraint allows to check if the wellbore pressure is higher than the layers pressure and the fluid flows back to the reservoir. Moreover, in the GEM simulator, the components mole percentages are also available.

The available remedial actions for the monitoring constraints are the same as the remedial actions for the operating constraints but some additional actions are also available. The additional actions are the auto-well, the shut layer, the auto-layer, the recompleat up, the recompleat down and the workover. The auto-well action is similar to the shut in action but the constraint is checked at each time step and the well is reopened if the constraint stops being violated. The shut layer action plugs the most offending layer (the layer that presents the highest value of the violated constraint) whereas the auto-layer action plugs the most offending layer but it checks periodically the constraint and if the constraint stops to be violated then it re-opens the layer. The recompleat up or down actions plug the most offending layer as well as the layers above or bellow it.

Moreover, in some cases where the well cannot produce at lower rates than the desired a workover procedure is applied. A workover procedure can be constituted by different works such as the injection of acids in the well in order to clean the scale of the wellbore or to reduce the formation damage in the region near the well and works such as the tubing replacement. All these works have as a result an increase in the productivity index of the well which is defined as the ratio of the production rate over the pressure draw-down needed to achieve this rate (Petrowiki, 2017b). As a result, when the workover action is used, in order to avoid the violation of the constraint the well productivity indices are increased for all layers of the well by multiplying the productivity index of the well before the workovers by a user specified factor. This multiplication is done once per timestep and can be done as many times as the user defines whereas in the case that the maximum number of multiplications is done and the constraint keeps been violated then the simulation either stops or the simulator shuts in the well depending the user selection.

7.6.1.3 PENALTY CONSTRAINTS (OPTIONAL)

The available penalty constraints are the gas oil ratio (GOR), the water-oil ratio (WOR) and the water-gas ratio (WGR). The penalty constraints values are not stable but they depend on the production history. The restriction limit defined by the government's regulations is entered as a fixed (base) value to the simulator and the penalty constraint value that it is imposed on the well at each production period is calculated internally. For the penalty constraints calculation the simulator offers the following options:

- Phase 2

The phase 2 is a calculation mode by which the rate target that it is assigned refers to the second phase for example to the gas phase for the gas-oil ratio (GOR) and to the water phase for the water-oil ratio (WOR) and water-gas ratio (WGR) constraints. For example, when the GOR option has been selected the calculation is done as follow: $Q_{gasnew} = Q_{oilmax} \cdot GOR_{base}$, where the Q_{gasnew} is the new allowed maximum gas rate that will be applied on the next time step, Q_{oilmax} is the maximum oil rate of the well and the GOR_{base} is the user specified penalty constraint rate (Computer Modelling Group Ltd, 2010).

- No damp

By using the damp calculation mode the reference phase target rate (oil for GOR and WOR and gas for WGR

constraints) is calculated by: $Q_{new} = Q_{max} \cdot PF$, where PF is the penalty factor. The penalty factor (PF) is the ratio of the base value to the produced value of the selected ratio calculated at the previous time step. For example, for the gas-oil ratio the penalty factor is calculated by: $PF_{GOR} = \frac{GOR_{Base}}{GOR_{Produced}}$.

- Damp

By using the damp calculation mode, the calculation of the constraint value is performed using the geometric mean of the maximum oil rate ($Q_{oil\ max}$) of the well and the actual produced oil rate ($Q_{oil\ old}$) of the stream by the following formula: $Q_{oilnew} = \sqrt{(Q_{oilmax} \cdot PF \cdot Q_{oilold})}$.

Finally, the penalty constraints remedial actions are the same as the operating constraints remedial actions.

7.6.2 Injection Wells

For injection wells only operating and monitoring constraint parameters are available. The operating constraints as well as the remedial actions for injection wells are the same as those for production wells. The available monitoring constraints parameters are the same as the monitoring constraint parameters for production wells whereas the available remedial actions are to stop the simulation, to shut in the well, to shut in the well and repeat the time step calculations after the shut in, the auto layer and the auto well actions.

7.6.3 Group Of Wells (Optional)

7.6.3.1 PRODUCTION OPERATING CONSTRAINTS

The operating constraints of a group of wells can be defined as

- Target type

The target type constraint of a group defines the value of the production rate that has to be accomplished by the wells that constitute the group.

- Maximum or minimum type

The maximum or minimum constraint type define the maximum or minimum values that a parameter can take throughout the simulation. The available parameters that can be defined with the target and the maximum and minimum constraint types are the surface rates of the phases, the bottom hole fluid rates, the manifold pressure and the compressor surface pressure.

- Voidage replacement type

The voidage replacement constraint type indicates the percentage of pores that have to be refilled by the injection fluid. By using the voidage replacement constraint type the simulator adjusts the fluid production in such a way so as to be proportional to the fluid injection (Computer Modelling Group Ltd, 2010). In this way, the pores that are empty due to fluid production are refilled with the injection fluid.

- Recycle type

In some cases, the production wells of the group produce at such great rates that the injected fluid is

produced and then it is reinjected in the reservoir. This amount of reinjected phase is defined by the recycle constraint type.

- Pressure maintenance type

When it is desired to maintain the reservoir pressure the pressure maintenance constraint type can be used along with the desired pressure value.

The remedial action that can be taken when a target constraint type is violated is to shut in the most offending layer whereas the available remedial actions that can be taken when a maximum or minimum constraint type is violated are:

- Stop the simulation
- Continue the simulation run by switching the target of the group to the violated constraint
- Shut the most offending well (the well with the highest rate) or wells (a well's priority sequence is created by the simulator and the wells are shut in with respect to it)
- Shut in the most offending layer (the layer that presents the highest rate)
- Shut in all the well's layers downwards or upwards from the most offending layer
- Shut in all the wells of the group

7.6.3.2 PRODUCTION MONITORING CONSTRAINTS (OPTIONAL)

The available parameters to be set as monitor constraints are:

- Gas-oil and water-gas ratios
- Water cut
- Maximum and the minimum surface gas and water rates
- Minimum bottom hole fluid rate

When the minimum surface gas and water rates and the minimum bottom hole fluid rate constraints are violated, the available remedial actions are to stop the simulation and to shut all the wells of the group. When the gas-oil and water-gas ratios constraints, the water cut constraint and the maximum surface gas and water rates constraints are violated, the remedial actions that can be taken are the following:

- Stop the simulation
- Shut the most offending well
- Shut the most offending wells
- Shut the most offending layer
- Shut the most offending layer-down
- Shut the most offending layer-up
- Shut all the wells of the group

7.6.3.3 INJECTION CONSTRAINTS

The constraints types for the injectors of a group are the same with the operating constraints types for the producers of a group with exception of the minimum constraint type that is not available for injectors.

7.7 SEAWATER SCALE BUILD UP (OPTIONAL)

As seawater passes through the tubing causes damage due to scale precipitation (created by the seawater salinity) in the tubing thus diminishing the tubing diameter and resulting in lower production or injection. As a result the monitoring of the scale formation and the damage that it causes is necessary in order to obtain a more realistic prediction of the production and to program the necessary maintenance works. The modeling of the scale deposition in the tubing of the wells is done by introducing the scale deposit and the scale damage Tables. In the scale deposition Table, the amount of scale deposition per unit of seawater flow rate through the well is introduced whereas in the scale damage Table, the damage factor multiplier used in order to represent the reduction in the productivity or injectivity of the well for different scale deposit amounts is entered. Finally, these Tables are available only in the IMEX simulator and have to be introduced when a seawater model is used.

7.8 TUBING TABLES (OPTIONAL)

In the tubing tables sub-section, data with respect to the flow inside the well are entered. These data are used by the simulator for the more accurate calculation of the production and injection rates and are required for the calculation of the well head pressure and for the calculation of the artificial lift. The tubing tables can be entered either by the user in the tubing tables interface or by uploading a CMG, PROSPER or ECLIPSE file that holds these information.

The required data for the construction of a tubing table are the reference depth, the phase for which the flow rates refer and the well head and bottom hole pressures for each flow rate. The reference depth field accounts for the depth at which the pressures and flow rates of the table have been measured. This value is used by the simulator so as to convert the tubing table data to the well's actual depth or to the depth where the manifold is located when groups of wells is used.

For production wells the flow rate of the well, the gas fraction (eg. gas-oil ratio), the water fraction (eg. water-oil ratio) and the well head pressure have to be introduced in the table of the flow rates. Moreover when an artificial lift project is to be applied to the well the gas lift injection rate or the injection gas-liquid ratio or the total gas-liquid ratio or the oil surface density or the gas surface density or the artificial lift quantity have to be introduced in the table. For injection wells only the flow rate of the injected phase (water, gas or solvent) and the well head pressure have to be introduced in the table.

7.9 PRESSURE CALCULATIONS

7.9.1 Bottom Hole Pressure Calculation

The bottom hole pressure can be calculated either by setting a pressure drop gradient between the perforations or by introducing a reference depth for the calculation of the bottom hole pressure. In general, the latter way is used in cases where the bottom hole pressure is to be calculated at a point different than the point from which the perforations start (nearest to the well head). The bottom hole pressure is calculated internally by the simulator using the following formula when a pressure gradient is entered: $\Delta P = \nabla P \cdot (D_{BHP} - D_{perf})$, whereas when a reference depth is entered the gradient term is replaced by the gravity acceleration times the mobility weighted fluid density (Computer Modelling Group Ltd, 2010).

7.9.2 Well Bore Pressure Loss Calculation

As the fluid travels to the surface pressure losses are generated along the wellbore. The well bore model is optional but it is required for the calculation of the well head pressure. The pressure loss calculations can be done either by using the tubing tables or by using a single phase gas flow correlation in cases of gas wells. In the latter case the depth of the perforations, the length, the relative roughness, the well head and the bottom hole temperature, the well radius and the molecular fractions of the gas components have to be defined.

7.9.3 Pressure Drop Between Perforations

The pressure drop between perforations influences the well's ability to produce as it makes the lift of the fluid from the perforations level to the surface more difficult. In extreme cases the fluid may not be able to flow inside the well and this is more likely to happen to horizontal wells. The pressure drop between the completions occurs due to gravity and it is calculated internally by the simulator. Nevertheless, the simulator also offers the option to assume that no pressure drop exists between the completions in order to model cases of wells that pumps are used to transfer the fluid up to surface. Moreover, for horizontal or multilateral wells where the pressure losses are more significant, the simulator can calculate these losses by using correlations.

7.10 GAS LIFT (OPTIONAL)

The gas lift is an artificial lift method that is used when the well cannot produce naturally as the liquid column is too heavy to be lifted up to the surface. By this method, gas is injected to the liquid column at specified depths from the gas lift valves. This is done so that the hydrostatic column weight is reduced. Moreover, the fluid already existed into the tubing is getting lighter (because it is mixed with the gas used for the gas lift) and as a result it is easier to be lifted.

The gas lift calculation can either be done by inserting a value for the desired gas liquid production rate (GLR option) or by calculating the gas lift in order to achieve the maximum oil production rate (GLOPT option). It has to be noted that in the latter case the user entered values of the minimum well head pressure, the minimum bottom hole pressure, the maximum water cut and the minimum oil production rate have to be introduced and when these values are violated gas lift is applied.

The gas lift controls are constraints imposed on the well which are checked periodically and when these constraints are violated then gas lift is applied to the well (Computer Modelling Group Ltd, 2010). These constraints are the minimum well head pressure, minimum bottom hole pressure, maximum water cut and the minimum oil production rate. Finally, the simulator requires the introduction of the tubing tables that will be used for the calculation of the gas lift.

7.11 MANIFOLDS (OPTIONAL)

When multi-lateral wells are drilled so as to make use of many different areas of the reservoir, these wells for economical reasons are drilled down to a point as a single well and then are distributed in the different areas of the reservoir. At the point where all these wells deviate from the single well a manifold is placed. A manifold is a piece of equipment so as to control the fluid flow and to distribute the streams of all these wells up to the surface (Oilgasglossary.com, 2014).

When a manifold is used for a group of wells it is necessary these wells to have equal manifold pressures. Based on this when a pressure or a rate constraint is applied on a manifold group then these constraints have to be translated to equal well head pressures for all the wells of the group. Moreover, when a manifold is used: also the

- Tubing tables
- Depth at which the manifold is placed so as to calculate the pressure drop from the manifold up to the wellhead
- Streams that are connected at the manifold have also to be entered

In addition, when an artificial lift project is to be applied from the manifold depth and upwards the manifold artificial lift quantity has to be entered into the simulator for the calculations of the artificial lift to be performed by using the tubing tables.

7.12 HYDRAULIC FRACTURING (OPTIONAL)

Hydraulic fracturing, is a well stimulation method which is applied in cases where the formation damage is such that the production of this well is not profitable or in cases that the permeability of the reservoir is too low. This method is applied by pumping fluid at a high rate so as the well's pressure overcomes the pressure that the formation can withstand. Immediately after this pressure limit is exceeded, fractures are created to the formation in the vicinity of the well and as soon as these fractures are wide enough proppant is injected to the well so as to keep them open. In an ideal case, the fracture is opened vertically to the well's axis and propagates in two symmetrical wings forming a 180° angle (Petrowiki, 2017). This procedure can be done to all the perforated layers of a well or to some of them. If a layer has been defined as hydraulically fractured then the fracture half length (L_{frhalf}), the fracture width (W_{fr}), the fracture permeability (k_{fr}), the non Darcy beta A and B (β_a and β_b) and the non Darcy fracture conductivity correction factor (CCF) have to be introduced. The non Darcy beta A and B (β_a and β_b) vary with the different proppant sizes as it is presented in the following table:

Proppant sand mesh size	Non Darcy beta A (β_a)	Non Darcy beta B (β_b)
8-12	$538.108 \cdot 10^9$	-1.24
10-20	$850.525 \cdot 10^9$	-1.34
20-40	$3411.752 \cdot 10^9$	-1.54
40-60	$2143.503 \cdot 10^9$	-1.6

Table 2: Non Darcy beta A and B (β_a and β_b) parameters for different proppant sand mesh sizes

The dimensionless fracture conductivity which is calculated by the: $F_{CD} = \frac{k_{fr} \cdot W_{fr}}{k \cdot L_{frhalf}}$ for Darcy flow it represents how easily the fluid can flow through the fracture (Fekete associates incorporation, 2012). When non Darcy flow occurs then the fracture conductivity calculated by the previous equation has to be reduced by: $\frac{1}{1 + Fo_{fr}}$, where the Forchheimer number for the flow in the fracture which is in turn calculated by: $Fo_{fr} = \frac{CCF \cdot \beta_a \cdot (k_{rp} \cdot k_{fr})^{\beta_b} \cdot \rho \cdot k_{rp} k_{fr}}{\mu \cdot h_{fluid} \cdot h_{layer}}$, where the h_{fluid} and h_{layer} are the heights of the fluid and the layer accordingly and k_{rp} is the relative permeability of the phase p.

7.13 RECYCLING (OPTIONAL)

The injection phase recycling is a widely used method as it is more economical in cases where the injected phases are too expensive or when the availability of these phases is limited. A full recycle of a phase consists from its injection into the reservoir, its production, its recovery in the surface facilities and its re-injection into the reservoir. The injection fluids can be recovered from a group and can be injected to the same or to another group. The group from which the recycled phases are recovered has to be defined along with either the re-injection target or the maximum rate.

In cases that the recovered fluid is not enough then in order the injection target to be achieved, a supplementary stream (make-up stream) taken from other groups is used to the injection. In case that a make-up stream is contributing to the injection the make-up target or the maximum rate have to be defined.

In cases that gas is recycled some additional parameters are also available such as the maximum fuel (natural gas) consumption rate (to cover the surface facilities energy needs), the fuel consumption fraction, the maximum sales rate and sales rate fraction in cases where part of the recovered fluid is utilized in the surface facilities as fuel or it is solved instead of being re-injected into the reservoir. Moreover, in the GEM simulator, the make up stream composition and the fuel, sales and recycled gas component reduction factor have to be entered. The fuel, sales and recycled gas component reduction factor defines the component reduction factors that will be applied in order to find the new composition of gas which is available for re-injection, as alternations to the composition may appear due to its usage as fuel to the surface facilities or gas sales.

7.14 ALTERNATING PROCESSES (OPTIONAL)

An alternating process is a process according to which different phases are injected into the reservoir with a specific sequence and in general is used to improve the reservoir recovery. The most common alternating processes are the water alternating gas injection (WAG) and the cyclic steam injection.

Firstly, the streams that participate in the cycling process and the number of sub-cycles that constitute a complete cycle have to be defined. For each separate cycle, the maximum surface or bottom hole rates of the streams that participate in the cycling process have to be introduced. It has to be noted that for injection wells, the values of the stream maximum rate can be either introduced by user or is calculated internally by the simulator using the injection stream voidage replacement fractions. Finally, the duration of each sub-cycle can be determined by using the maximum cumulative production or injection, maximum or minimum bottom hole pressure, minimum injection rate or oil rate or depletion index (only for producers), total number of sub-cycles to complete and the maximum sub-cycle duration.

7.15 RATE DISTRIBUTION (OPTIONAL)

7.15.1 Priority Ranking

The wells belonging to a group have to be prioritized for their contribution to the group's stream to be calculated. The calculation of the priority sequence of the wells is done internally by the simulator. One option is to calculate the priorities based on the rates appeared under the most restrictive constraint whereas the second option is to calculate the priorities based on the instantaneous rates appeared at a specific bottom hole pressure defined by the user to the corresponding field.

Subsequently the weighting coefficients A and B for all the streams have to be entered, where A_0 and B_0 are constants and the rest of the coefficients are the weighting coefficients of each phase. The priority of a well

for each stream is calculated by the following formula: $Priority_{iw} = \frac{A_0 + \sum_{i=1}^n A_i \cdot Q_i}{B_0 + \sum_{i=1}^n B_i \cdot Q_i}$, where Q is the rate

calculated either under the most restrictive constraints or by using the instantaneous potential at a specific bottom hole pressure.

The lower and upper limits of the the pool target-capacity ratio have to be entered in the simulator. The pool target-capacity ratio is the ratio of the defined target and the capacity of the reservoir to achieve it. The assigned values for this ratio represent the lower and the upper fractions of each well's maximum operating rate. The selection of which value (lower or upper) of this parameter is going to be used for the calculation of the rate at which a well will operate is done based on the well's priority position. The discrimination for the priority to highest and lower is done based on a 'swing' well. A 'swing' well is defined as the well which when it is added to the highest priority wells, the group target is exceeded. Once the priorities of the wells have be defined then the wells with the higher priorities will operate using the upper limit of the pool target-capacity ratio for the calculation of their rates whereas the wells with the lower priorities will use the lower limit.

7.15.2 Apportionment

When groups of wells are used each well contributes its share to the target to be achieved. The distribution of the production and the injection rates among the wells of the group can be either determined by the user or is calculated internally by the simulator. When the apportionment is to be calculated internally this is done either by using the instantaneous potential or the priority ranking. By using the instantaneous potential method, the simulator calculates internally the contribution percentage of each well. By using the priority ranking method, the determination of the apportionment of the wells is done based on their priority. Finally, since the contribution of the streams is defined, the originally defined rates of the wells that belong to the group are overwritten by the products of the percentage of contribution and the maximum rate of the well.

7.16 HISTORY MATCHING TOOLS

7.16.1 Triggers

Triggers are used during the history matching procedure and can be applied to a well, a group of wells, a layer, a sector, or the entire field and depending on this selection, the available parameters to be set as test conditions are changing. In order the trigger test condition to be defined, a value for this parameter has to be entered as well as the test condition that will be applied on it (greater or lower). The trigger conditions are tested at the end of a time step and if they are satisfied then the actions that should be taken are applied at the beginning of the next time step. As trigger action any keyword of the wells section can be used. Moreover, in the trigger definition, the maximum number of times that the trigger can be tested to ascertain if the trigger condition is satisfied, the time delay either from the trigger definition time or from the start of the simulation before the trigger condition to be tested, the maximum number of times that the specified actions can be taken and to increase the trigger value each time the trigger condition is satisfied.

The test conditions for triggers that can be applied to a well are the production or injection surface rates, the cumulative production and injection of the phases, the bottom hole and the well head pressures, the gas-oil ratio, the gas-liquid ratio, water-gas ratio, water cut, the back flow and the the molar percentage of each component in the production or injection stream (for GEM simulator only). In the case that a trigger is applied to a group of wells or to the field the test conditions are the same with those for individual wells, but also the voidage replacement and the recycled gas minimum injection rate are also available . If the trigger is applied to a layer, the available conditions are the production or injection rates, the gas-oil ratio, the water cut, the water-gas ratio, the gas-liquid ratio, the bottom hole pressure and the layer pressure drawdown. If the trigger is applied to a sector, the available conditions are the average pore volume pressure and saturation and the stock tank volumes in place of the phases appeared in the reservoir.

7.16.2 Spatial Properties Modification

The spatial properties modification is a history matching tool which allows the modification of properties in different regions of the reservoir (Technical Support, 2016). The property that is to be modified, the date from which this property is modified and for which blocks this modification will be applied have to be introduced in the simulator. The property modification can be done either for each block or for one direction of the I,J or K. The properties which are available for modification are the following:

- The gas relative permeability at the connate liquid saturation and the water relative permeability at irreducible oil saturation
- The oil relative permeability at the connate water and gas saturation
- The gas oil capillary pressure at connate liquid saturation
- The connate gas, liquid and water saturation
- The critical gas and water saturations
- The irreducible oil saturation in the gas-liquid and in the water-oil table
- The residual oil saturation in the gas-liquid and in the water-oil table
- The maximum residual oil saturation
- The non Darcy correction term calculated by the equations available in the non Darcy flow option in the rock-fluid data section
- The permeabilities, the transmissibilities and the low side transmissibilities of the blocks in the I,J and K directions
- To change the calculation method of the blocks from implicit to explicit

7.16.3 Multipliers

In cases that it is needed to alter the production or injection constraints values during the history matching procedure the multipliers option can be used. When a multiplier is used in order to alter the constraints the new constraint value is calculated internally by the simulator by multiplying the constraint value with the multiplier.

8. GEOMECHANICS

By using a geomechanical model coupled with the flow model, a more accurate representation of the production history of the reservoir is provided. This happens because flow is influenced by the regional stress regime, as the applied loads on the reservoir cause deformation, compaction, changes in porosity and permeability. Moreover, the applied loads on the reservoir in extreme cases can cause casing damage and well bore stability issues. As a result, such analysis is important because flow may significantly change especially in cases of overpressured reservoirs (Fekete associates incorporation, 2017). The calculation of the deformations is done at each time step where the calculated pressures and temperatures of the reservoir are used for the simulator to calculate the new stresses, strains and displacements which are in turn used to update the porosities that will be used in the next time step by the flow simulator (Tran, Settari, & Nghiem, 2004). The geomechanical modeling is available only for the GEM simulator and only when the reservoir model is constructed using Cartesian grid. The geomechanical section is constituted by the following sub-sections:

- Constitutive models

In the constitutive sub-section the behavior of the material along with the failure criterion that will be used for the calculation of the stresses and deformations of the reservoir rock are introduced.

- Displacement conditions

In the displacement conditions, the allowed displacement that may occur in a reservoir region is introduced into the simulator.

- Well boundary unloading

In the well boundary unloading sub-section, the amount of the stress unloading that occurs on the well boundary is introduced.

- Calculation of deformations in 2D and 3D

In the calculation of deformations in the 2D and 3D sub-section the directions toward which and the points where the calculation of the deformations will be performed are defined.

8.1 CONSTITUTIVE MODELS

For the calculation of stresses and deformations of the reservoir to be done a constitutive model with a failure criterion has to be used. The constitutive model accounts for the changes of the stresses acting on the reservoir, the changes in porosity values and the deformations which depend on the behavior that the rock material exhibit with loading. On the other hand, the failure criterion accounts for the required load (yield stress) for failure to occur and its extent. The calculation of the geomechanical deformations can be done either for all blocks or for the user desired blocks.

8.1.1 Material Deformation Behavior

A material such as the rock can present different types of behavior during the loading and unloading procedures. The rocks present elastic behavior prior to their failure and after that point the rock present

plastic behavior and the deformations are permanent. When a rock presents elastic behavior then the deformations of the rock caused by its loading are reversible. Depending on the way that the strain varies with the applied stress the rock may exhibit linear or non linear elastic behavior.

When a rock exhibits linear elastic behavior then the strain varies linearly with the applied stress. On the other hand, a rock can present a non linear elastic behavior in cases where the stiffness (resistance of the material to deform) of the material is not constant. The stiffness of a material is not constant when the strain do not vary linearly with stress or in cases where the deformations are that great so they change the entire geometry of the formation under study (Hawk Ridge Systems, 2014). The two types of non linear behavior that can be found are the hypoelastic and the hyperelastic.

An hypoelastic material behaves elastically only when small changes in stress result in small changes in strain whereas for big changes in stress the material does not behave elastically and the material presents hysteresis as the unloading procedure follows a different path than the loading procedure (Wittel, 2016). On the other hand, when a material presents hyperelastic behavior an hyperbolic relationship between the stress and the strain is used which describes that large deformations occurring by small stress changes (Autodesk, 2017). Finally, the hyperelastic model is mainly used for soils and can represent accurately cases where cycling loading occurs (Autodesk, 2017).

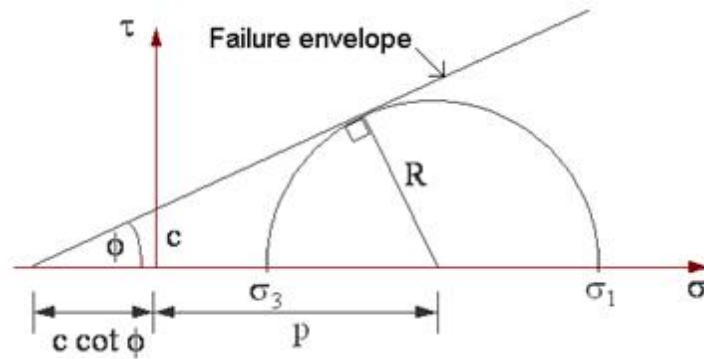
8.1.2 Shear Failure

Shear failure occurs when the shear along a plane overcomes a limiting value and rock fails due to shear stresses creating cracks along this plane and the rock losses its capacity to carry load. The limiting value at which shear failure occurs is called yield stress and it is defined by the shear failure criteria.

8.1.2.1 MOHR-COULOMB CRITERION

The Mohr-Coulomb criterion is the most commonly used criterion to represent shear failure of rocks. The Mohr-Coulomb criterion assumes that the shear stress that causes the failure is a function of the normal stresses acting on the rock. In order to determine when failure occurs diagrams of shear stress versus normal stress are used. In these diagrams, the space is divided by a straight line to a safe region where the rock presents elastic behavior and to a region where failure occurs. In such a diagram firstly the shear stress that is applied on the rock has to be represented. This is done by using the Mohr circle defined by the maximum and the minimum normal stresses (σ_1 and σ_3). Moreover, in the same diagram a line defining the maximum shear stress that the rock can withstand is plotted and if the Mohr circle exceeds this line then shear failure occurs. This line is a function of the tangent of the internal friction angle (ϕ) of the rock, the normal stress that it is applied on the rock and the cohesion of the rock (c) and it is calculated as follows: $\tau = \tan\phi \cdot \sigma_n + c$. The internal friction angle represents the angle that if exceeded then failure of the rock occurs whereas the cohesion of the rock represents the amount of force that has to be exceeded for failure to occur and it is

calculated as follows: $c = \frac{(\sigma_1 - \sigma_3)}{2}$.



Picture 16: Mohr-Coulomb failure criterion

8.1.2.2 DRUCKER-PRAGER CRITERION

The Drucker-Prager after the Mohr-Coulomb criterion is the second most commonly used criterion to represent the failure of soils and rocks. The Drucker-Prager criterion is thought to give more realistic results than Mohr-Coulomb criterion as the latter underestimates the yield strength of the material (Jiang & Xie, 2011). The Drucker-Prager criterion is calculated by the following expression: $(\sigma_1 - \sigma_2)^2 + (\sigma_1 - \sigma_3)^2 + (\sigma_2 - \sigma_3)^2 = C_1 \cdot (\sigma_1 + \sigma_2 + \sigma_3 + C_2)^2$, where C_1 and C_2 are parameters related to the material and σ_2 is the intermediate stress acting on the rock.

8.1.2.3 TRESCA AND VON MISES CRITERIA

The Tresca and the von Mises criteria were developed for ductile materials and as a result they are used mainly for metals but in some cases soils and unconsolidated sand can exhibit such behavior (Fossen, 2010). Both Tresca and von Mises criteria assumes that the shear failure is independent from the stress applied on the rock.

Tresca criterion can be thought as a special case of the Mohr-Coulomb criterion when the internal angle is equal to zero and as a result the line that defines when the shear failure occurs is a function only of the principal stresses and it is calculated as follows: $\tau = \frac{(\sigma_1 - \sigma_3)}{2}$. On the other hand, the von Mises criterion takes into consideration also the intermediate stress (σ_2) and it is calculated by the following equation: $c = \sqrt{(\sigma_1 - \sigma_2)^2 + (\sigma_1 - \sigma_3)^2 + (\sigma_2 - \sigma_3)^2}$ (Fjaer, 2008). Finally, the Tresca and the von Mises criteria as GEM manual refers are implemented into the simulator only for testing purposes.

8.1.3 Compaction failure

In cases where the rock exhibits high porosity values the rock can fail due to compaction of the pores occurred by the hydrostatic compression (Grueschow & Rudnicki, 2005). During compaction, the grains are rearranged in space in order to fill better the empty space and may be crushed. Contrary to shear failure where the rock losses its ability to carry load, in this type of failure, the rock retains its ability to carry load and it may increase it as its structure is getting denser (Fjaer, 2008). This failure type can be represented by

using a hardening yield elliptic surface (cap) along with the Drucker-Prager shear failure criterion.

8.2 DISPLACEMENT CONDITIONS

In general, the reservoirs are deformed due to the overburden pressure acting on them whereas it is not usual to be deformed by the stresses acting on its sides and bottom. For this reason the simulator assumes by default that the reservoir is bounded at its sides and bottom. Although, this assumption may be invalid in cases where the regional stress regime is such that the stresses acting on the sides or the bottom of the reservoir cause deformation.

For the simulator to account for deformations at the sides and the bottom of the reservoir the model offers the user the option to introduce which blocks are deformed and the direction and the amount of the displacement. Moreover, when deformation does not occur in a region of the reservoir this region can be set as a fixed boundary. The same can be applied also when vertical deformation does not occur by setting the cap rock as fixed and constraint by this way any movement of the formation towards the vertical direction.

8.3 WELL BOUNDARY UNLOADING

When a well is drilled, a distortion of stresses around the well occurs. This disturbance of stresses around the well results to higher stresses to be applied on the boundary of the well. On the other hand, the fluid which circulates in the well produces an opposite force to that of the stresses acting on the well boundary. As a result, the actual stress applied on the well boundary is diminished and the amount of the unloading that occurs depends on the well's pressure. The unloading value on the well boundary along with the well's radius have to be introduced into the simulator in order the stresses in the well region to be calculated accurately.

8.4 CALCULATION OF DEFORMATIONS IN 2D AND 3D

When the option of 3D is enabled then the deformation calculations are performed in all three dimensions. By using the 3D option the geomechanical phenomena that take place during production can be represented accurately but the simulation time is significantly increased. On the other hand, when the 2D option is selected, the calculations are performed to parallel planes that are perpendicular to the I (or J) axis which means that the stresses acting parallel to I (or J) axis are equal to zero. The selection of the direction of the normal plane (perpendicular to the I or J axis) depends on the direction towards which the strains are so small that can be ignored without generating big errors (Computer Modelling Group Ltd, 2009b). In general, the direction of the smallest strains coincides with the direction along which the reservoir presents the greater horizontal extent. By using the 2D option, an adequate representation of the deformations can be done without requiring a great amount of computer resources.

Moreover, the nodes for which the simulator will calculate the deformations have to be introduced. In general, the more are the nodes where the simulator calculates the deformations the more accurately the deformations are represented. The nodes for which the simulator is able to calculate the deformations for a block are the following:

- The four corners of a block surface
- The four corners of a block surface as well as the nodes lying in the middle of the edges of this block

surface

- The four corners of a block surface, the nodes lying in the middle of the edges of this block surface and the node at the center of the block surface

9. NUMERICAL CONTROLS

For the reservoir simulation to be performed, the flow equations have to be solved. These equations are partial non linear (parameters in the equation depend on the unknown value) differential equations and are solved numerically by the simulator as these equations cannot be solved directly. The numerical method that the simulator uses to approximate the exact solution is the Newton-Raphson method.

The first step for the solution of the flow equations is to discretize them in time (eg. implicit) and space (to each block) by using a finite difference method. Since their discretization has been done then the system of equations that is required to be solved by the simulator is of the form: $A \cdot x = b$ where A is a matrix in which the coefficients (eg. density, permeability) are stored, x is the vector of the unknowns (pressure and saturation) and b is a vector updated at each time step and includes the total compressibility.

The numerical control section is constituted by the following sub-sections:

- Newton-Raphson method

The required tolerance values for the convergence of the Newtonian iterations are defined.

- Explicit, implicit and IMPES methods

The solution method is selected.

- Adaptive implicit method

In the adaptive implicit method sub-section, the criterion based on which IMPES blocks will switch to implicit and vice versa is defined.

- Linear solver

The procedure that it is followed for the linear system of equations to be solved is defined.

- Parallel processing

In the parallel processing sub-section, the parameters that have to be defined for the system of equations to be solved in parallel is selected.

- Numerical dispersion control

The way by which the numerical dispersion will be minimized is defined.

- Geomechanics

The required numerical controls for the deformation modeling are defined.

9.1 NEWTON-RAPHSON METHOD

The Newton-Raphson method applied at each timestep needs to start the calculation by making an initial guess which has to be close to the actual solution and uses the tangent line to the function to be minimized in order to find, hopefully, a point that is closer to the actual solution (interception point of the tangent line with the x axis) than the initial guess and if the iterations continue then the Newton-Raphson method should be getting closer and closer to the actual solution. If this solution deviates from the actual solution within an accepted tolerance (convergence tolerance) then the simulator assumes that the algorithm has been converged and the provided solution is accepted. On the other hand, if the provided solution is not in the accepted

tolerance range then the simulator continues iterating until the provided solution is accepted or until the maximum allowed number of iterations is reached. In the case that the Newton-Raphson method iterates until the maximum allowed number of iterations and is not able to provide an accepted solution then the timestep has to be cut in smaller timesteps and the simulator has to repeat the calculation procedure.

The Newton-Raphson algorithm which provides the solution of the system of the non linear flow equations for each iteration is given by the following formula:

$x^{(v+1)} = x^{(v)} - \left[J(x^{(v)}) \right]^{-1} \cdot F(x^{(v)})$, where $x^{(v)}$ and $x^{(v+1)}$ are the unknowns (pressures and saturation) solved for the v and $v+1$ iterations of the Newton-Raphson method performed at each time step, J is the Jacobian matrix constituted by the derivatives of the $F(x)$ and the F matrix is defined as follow: $F(x) = A \cdot x - b$, where the matrix A includes the coefficients of the pressures and saturations and vector b includes the known values of the equations.

9.1.1 Convergence Tolerance

For the simulator to proceed to the next time step of the simulation, the Newtonian iteration performed for the previous time step should have converged. The convergence of the Newtonian iterations is required so as the simulator to be able to provide the pressure and saturation values that will be used for the solution at the next time step. Although, the convergence of the iterations is constraint by some specific limits so as the calculations to be performed as accurately as possible and provide more realistic results. These limits are the normal variation and the maximum allowed variation of properties (eg. pressure, saturation, saturation pressure, composition) per timestep.

Moreover, the material balance of the flow equations is not solved to zero due to numerical dispersion and as a result, an error occurs and propagates from time step to time step (Computer Modelling Group Ltd, 2010). The magnitude of this error is called residual value (R) and it is calculated by the following equation: $R = (SourceTerm) - (SinkTerm) - (AccumulationTerm)$, as sink and source terms are referred the outflow and inflow to a block accordingly whereas as accumulation term is referred the mass that remains in the block. The simulator in order to limit the error propagation, which has occurred by the use of big timesteps, sets limiting constraints for the maximum allowed changes in pressure and saturations during the time step or the maximum allowed residual values by the solution of the material balance of the flow equations.

9.1.2 Relaxation Of The Accumulation Term

For large simulation problems with many blocks direct methods are difficult to be applied for the calculation of the accumulation term and as a result an iterative method namely relaxation should be used (Peaceman, 1977). The relaxation option is applied to the accumulation term of the mass balance. Relaxation is nothing more than the convergence tolerance for this term. The simulator for the relaxation of the accumulation term offers the following two options:

- Over relaxation

This keyword enables over relaxation in accumulation term and may be helpful in cases of gas appearance

and disappearance problems.

- Under relaxation

The under relaxation of the accumulation term prevents the disappearance of gas from a block for three Newtonian iterations that means that if the simulator predicts the disappearance of gas for more than three iterations only then the gas will disappear. This may lead to faster convergence in cases that the gas is being liberated in the reservoir but it can cause difficulties in cases where free gas is present and the reservoir pressure is rising (Computer Modelling Group Ltd, 2010).

9.2 EXPLICIT, IMPLICIT AND IMPES METHODS

Explicit and implicit methods are different ways used for discretizing the partial differential equations in time. The calculation of the value of a property (pressure, saturation) for a specific block, using the explicit method depends on the value of the property of this block and its neighboring blocks calculated at the previous time step. On the other hand the calculation of a property value for a specific block, using the implicit method depends on the property value of this block calculated at the previous time step and the values of this property of the neighboring blocks at the new time step. Moreover, except the implicit and explicit methods for the calculation of the pressures and saturation, a widely used method in reservoir simulation is the IMPES (implicit in pressure-explicit in saturation) method. By using the IMPES method, the pressures are calculated by using the saturations of the old time step and then these pressure values are used for the explicit calculation of the saturations (Fanchi, 2006).

Due to the fact that the implicit methods calculate the properties at the current time step they are more stable (do not maximize the errors occurred during the simulation from time step to time step) than the explicit methods (Research Gate, 2017). As a result, implicit methods can use greater time steps than explicit methods, although, implicit methods require much more computer resources and time than the explicit methods. On the other hand, the IMPES method requires smaller memory and time than the implicit method but smaller time steps have to be used (Computer Modelling Group Ltd, 2010).

9.3 ADAPTIVE IMPLICIT METHOD

The two methods that are commonly used in reservoir simulation are the fully implicit and the IMPES methods. In a field the majority of the blocks can be solved using the IMPES method whereas only a small number of blocks is required to be solved using the implicit method.

The blocks that need to be treated implicitly are blocks in which sharp changes in pressures and saturation values occur. This situation is apparent at the well's blocks, the blocks near the wells and in cases of fronts that propagate in the reservoir. As a result, during a simulation run some blocks which were initially set to be solved using the IMPES method may have to be solved using the implicit method for some period of time and vice versa. The method that allows this switching between the two solution methods during the simulation is the adaptive implicit method (AIM). By using the adaptive implicit method, the simulator uses some criteria so as to check if blocks have to switch from IMPES method to implicit (forward switching) or from implicit to IMPES (backward switching) (Wig, Codln, Nghlem, & Group, 1989). The available criteria of the simulator based on which it will be determined if a block will switch from IMPES to implicit and vice versa are the following:

- Stability switching criterion

By the stability switching criterion the IMPES blocks are checked if they have to be changed to implicit mode by using the stability criterion. The stability criterion defines if the used selected method provides the required stability. The stability check can be done either for the IMPES neighbors of implicit blocks or for all the blocks of the field which is more reliable but increases considerably the CPU time in large simulation problems with many blocks.

- Threshold switch criterion

When the threshold switch criterion is used the switch is based on pressure and saturation or polymer concentration. When this method is used, a fraction for pressure and saturation or polymer concentration has to be introduced. This fraction is by turn multiplied with the value entered in normal variation per time step and their product determines the value of the threshold criterion. The switching of blocks to implicit mode is done when the calculated value by the simulator changes over the threshold criterion value.

- Stability switching criterion and threshold switch criterion

In case the stability switching criterion and the threshold switch criterion the simulator is used the simulator checks the IMPES blocks which are in contact with implicit blocks for stability switching and at the same time it checks all the blocks of the field for threshold switching. When this option is selected then also the threshold pressure and threshold saturation or polymer concentration fractions also have to be defined.

- Stability switching criterion using backward switching

By using this option the switch of a block from implicit to IMPES is based on the stability criterion. When this option is selected then the frequency of checking for backward switching has also to be introduced into the simulator. This check is done periodically and if a block is found that can provide the required stability by using the IMPES method then the block switches from implicit to IMPES.

9.4 LINEAR SOLVER

The linear solver is used during each Newtonian step to inverse the Jacobian matrix constituted by the derivatives of the function $F(x) = A \cdot x - b$. For the Jacobian matrix to be invertible the simulator has to transform the system of the flow equations $F(x)$ to a system that it is easier to be solved. This is done by re-ordering the matrix F and using preconditioners so as to decompose it to a product of matrices which is equal to the original matrix but is easier to be solved.

9.4.1 Matrix ordering

For the simulation to be performed, a system constituted by all the equations for all the field blocks has to be solved simultaneously. This system of equations is stored in a matrix and each cell of the matrix represents a block of the field. In that matrix many elements are equal to zero (sparse matrix) indicating that there is no connection between these blocks or in other words that they are not neighboring blocks. These zero elements can be eliminated from the matrix in order to minimize the store requirements (Golub & Van Loan, 1996). This elimination of the zero elements can be done by re-ordering the cells of the matrix trying to concentrate the non zero elements close to each other. This re-ordering of the matrix is done by using specific techniques also known as ordering algorithms.

The ordering techniques provided by the simulator are:

- Red black ordering
- Natural ordering
- Reverse Cuthill-McKee ordering

9.4.2 Matrix Preconditioning

Matrix preconditioning, is called the procedure during which the previously re-ordered matrix is decomposed to a product of matrices which is equal to the original matrix. This preconditioning of the matrix is done to generate a system that provides the same solution as the original system but it can be solved much more easily by the iterative solver.

A method based on which the simulator decomposes the matrix is the QR decomposition method. This decomposition can be done by using an orthogonal matrix (Q) and an upper triangular matrix (R) whose product is equal to the initial matrix A ($A = Q \cdot R$). As a result, after this decomposition, the original system of equations $A \cdot x = b$ that has to be solved is transformed as following: $Q \cdot R \cdot x = b \Rightarrow Q \cdot Q^T \cdot R \cdot x = Q^T \cdot b \Rightarrow R \cdot x = Q^T \cdot b$ which can be solved easier as the R is a triangular matrix.

Moreover, GEM simulator also offers an alternative way to decompose the matrix A by using incomplete LU factorization. In this case, matrix A is decomposed to a lower and an upper triangular matrices by using incomplete Gaussian elimination. Gaussian elimination is an algorithm by which the system of equations is reduced by performing row and column operations in the matrix so as to create as many zero entries as possible and for computational reasons, the elimination stops before the matrix becomes totally reduced (Golub & Van Loan, 1996). By using the complete LU factorization, the original system of equations is transformed as follows: $L \cdot U \cdot x = b$. By setting the product U and x equal to y, the problem can be solved in two steps, firstly by calculating $L \cdot y = b$ and then by calculating $U \cdot x = y$. Nevertheless, this cannot be done in the case that incomplete elimination is done, as the L and U product of the triangular matrices are not exactly equal to the matrix A ($A \approx L \cdot U$) and as a result the system $A \cdot x = b$ cannot be solved exactly but approximately. Therefore, the product of the lower and upper triangular matrices is set equal to a matrix M ($M = L \cdot U$).

9.4.3 Generalized Minimal Residual Method (GMRES)

As soon as the decomposition has taken place, the system is solved by using the generalized minimal residual method (GMRES). The generalized minimal residual method is an iterative solver which makes a first estimate for the solution of the system (a first estimate for the unknown vector x) and by using iterations it is improving this estimation thus approximating the exact solution of the system. For the simulator to assume that the system is solved, the provided solution is required to minimize the residual values (r) of the system which are defined as follow: $r = b - A \cdot x$ (Chen, 2015).

9.5 PARALLEL PROCESSING

In cases of large simulation problems, in order to avoid extremely high computational times, clusters of computers are used so as to solve in parallel the simulation problem. When the simulation is to be performed in parallel then the field has to be divided in different domains (classes) that do not communicate directly so that the simulator can solve them simultaneously. Moreover, the number of the computer processors (threads) that will be used has to be defined.

9.6 NUMERICAL DISPERSION CONTROL

Numerical dispersion depends on the discretization in time and space of the partial differential equations and it is caused by the fact that numerical methods do not provide an exact solution but they provide an approximation to this solution (Fanchi, 2006). In general, the coarser is the grid (big discretization in space) the bigger is the timestep (eg. using the implicit method) and the more pronounced is the numerical dispersion as the occurred errors from the solution of the equations are greater. These errors propagate during the simulation time inside the reservoir and look like physical dispersion. As a result, the simulator cannot provide an accurate description of a front movement (Fanchi, 2006). For the GEM simulator to minimize the numerical dispersion, it offers the option to use a flux limiter which imposes a limit to the spatial derivatives in order to be maintained in a realistic range of values.

The two flux limiters that the simulator offers are the Fromm limiter and the minimally extended scheme (MES) limiter. The Fromm limiter dispersion control is preferred to be used in cases where the grid is in general uniform with almost equal blocks to any direction whereas the minimally extended scheme limiter is preferred in cases of non uniform grids (Sammon, Masanori, & Jialing, 2001). Finally, both methods increase the accuracy of the recovery predictions and the movement of the fluid fronts.

9.7 GEOMECHANICS

For the solution of the geomechanic deformations, the simulator creates a matrix with the force balance equations and solves it in the same manner as the flow equations. In the case that deformations are modeled, a pressure tolerance multiplier has to be introduced so as to be multiplied with the pressure convergence tolerance of the Newtonian iterations. This multiplier has to be applied as deformations may cause large pressure changes and cause convergence problems. Moreover, an allowed tolerance with respect to the displacement of the block nodes due to deformation has to be determined. Finally, if the calculated node displacement is less than the tolerance value then the equations is thought to have converged.

10. SIMULATION RESULTS

During the simulation, the results of the simulation run are stored in files. In the simulation results section, the parameters that will be written in the output files are defined. Moreover, in this section, the simulator calculates the required memory that will be needed so as the simulation to be performed and allocates it in order to save time. This section is constituted by the following sub-sections:

- Exported files

The output files of the simulation and the data that contain are defined.

- Run time dimensioning

In the run time dimensioning sub-section, the simulator calculates approximately the memory that will be needed for the simulation run.

- Maximum number of errors report

The maximum allowed number of syntax errors before aborting the simulation is defined.

- Action on interrupt detection

The actions that the simulator has to take as soon as the user decides to stop the simulation are defined.

10.1 EXPORTED FILES

The file in which all the introduced data are written for the simulation to be performed is a text file (.dat). This text file is introduced into the simulator to run the simulation and the results of the run are printed into the output files. The output files that the simulator creates are the following:

- Main results file (.mrf)

The main results file is a binary file that cannot be read by the users and contains all the information about the simulation run.

- Results file (.irf)

The results file is used in the CMG' s graphs program so as to create diagrams or to the CMG' s 3D results in order to display the simulation results to a 3D model. In this file, information about the wells (eg. production/injection rates, cumulative production/injection), the reservoir (values inserted in the array properties), the grid (the calculated values of the array properties) and the total influx of a flux sector can be printed.

- Text output file (.out)

The text output file is mainly used in cases that debugging is required. This file includes information about the input data, the production and injection of the wells and the influx of a sector can be printed.

- Diary file (.log)

In the diary file, information such as the production and injection rates of the wells and the reservoir pressure are printed for each timestep.

- Rewindable results file (.rrf)

The rewindable results file is the file of the restart record. Sometimes in order to save time it is preferable to keep a record from a previous run of the simulation up to a date. This is especially useful when a simulation run needs to be stopped, make the necessary changes and continue the simulation. By using a restart file, time is saved as it is not required to perform a simulation from the beginning which is a procedure that can keep hours.

- Geomechanics file (.geo)

The geomechanics file is printed only in the case that geomechanics deformations are going to be taken into account during the simulation. In this file, the principal stresses and the displacements are printed.

The date from which the file writing will start as well as the frequency by which information will be written in these files has to be defined. The file writing can be done either at each date defined in the wells section or by a user specified frequency in timesteps.

10.2 RUN TIME DIMENSIONING

By using this keyword, a first estimation of the storage requirements for the simulation run is done. In this sub-section, the maximum allowed amount of the used parameters (eg. active and null blocks, aquifers, percent of fully implicit blocks etc.) is set and the simulator allocates the required memory before the start of the simulation. CMG suggests that if the user wishes to make a change in this sub section should firstly consult the technical support.

10.3 MAXIMUM NUMBER OF ERRORS REPORT

When the simulator reads the script then it may encounter syntax errors or values that exceed limits. If these errors are encountered in the initial conditions or in the wells and recurrent data section of the data set then the simulation stops immediately whereas if the errors are encountered to any other section then only when these errors exceed a maximum value the simulation is aborted (Computer Modelling Group Ltd, 2010).

10.4 ACTION ON INTERRUPT DETECTION

By this keyword, the actions that should be done when the user interrupts the simulation by pressing 'ctl+c' or by typing 'kill -2' are determined. The action that the simulator can take in such case can be one of the following:

- Write, restart and stop

By using the 'write, restart and stop' option, the simulator is allowed to complete the current time step, print the data to the files and write a restart file (Computer Modelling Group Ltd, 2010).

- Write, restart and continue

By using the 'write, restart and continue' option the simulator writes immediately the data to the files, creates a restart record and then continues the simulation (Computer Modelling Group Ltd, 2010).

- Close file and stop immediately

By using the 'close file and stop immediately' option, the simulation is terminated immediately, the current time step is not completed and the data are written to the files and exported so as to prevent file corruption (Computer Modelling Group Ltd, 2010).

- Stop immediately

By using the 'stop immediately' option, the simulation stops without writing anything in the files. This action is useful only in cases where all the other actions are too time consuming (Computer Modelling Group Ltd, 2010).

11. MODIFIED BLACK OIL TABLE GENERATION

As it was mentioned in the simulation method chapter, the black oil table method is mainly used for the simulation of fluids with low volatile content such as black oils and heavy oils. Due to its simple approach to the phase behavior problem, the black oil approximation was extended for fluids of high content in light hydrocarbons such as volatile oils and gas-condensates with the provision that surface oil may occur also from reservoir gas. This extension of the black oil approach was done by introducing the oil content (R_v) and it is also known as modified black oil table (MBO) formulation. For the creation of the modified black oil tables two methods are used namely the Whitson-Torp and the Coats method. The difference between these two methods is found to the different way that the oil content is calculated. In order a modified black oil table to be created both methods require the use of a depletion experiment such as a constant volume depletion (CVD) and the use of an EOS which will be tuned against these data. This tuned EOS will be by turn used for the calculation of the multistage flashes.

11.1 WHITSON-TORP METHOD

The Whitson-Torp method calculates the formation volume factors, the solution gas-oil ratio and the oil content by flashing separately through the surface separation train the equilibrium oil and gas of each pressure step of the depletion experiment (Whitson & Torp, 1983).

By flashing the phases separately, the volumes of the stock tank oil and gas produced by the reservoir liquid for each pressure step as well as from which phase have been produced (eg. volume of oil produced by the gas phase) are known. As a result, the formation volume factors, the solution gas-oil ratio and the oil content can be calculated creating in this way the BOT table for each pressure step of the depletion experiments. Due to the fact that Whitson-Torp assumed that the stock tank oil and gas densities remain constant throughout the depletion, the reservoir densities that they provide are not totally reliable.

11.2 COATS METHOD

By using Coats method, the creation of the BOT table is done by taking only the volume of gas from each pressure step (for pressures below the saturation pressure) of the depletion experiment and flashing it through the separation train calculating by this way only the oil content (Keith H Coats, 1985). Moreover, mass conservation of oil and gas between each separation stage has to be satisfied. The mass conservation between two separation stages (the higher pressure stage is denoted by the subscript 1 whereas the lower pressure stage is denoted by the subscript 2) is expressed as follow:

$$\text{For gas: } V_2 \cdot (B_g \cdot S_g + B_o \cdot R_s \cdot S_o)_2 = V_1 \cdot (B_g \cdot S_g + B_o \cdot R_s \cdot S_o)_1$$

$$\text{For oil: } V_2 \cdot (B_g \cdot R_v \cdot S_g + B_o \cdot S_o)_2 = V_1 \cdot (B_g \cdot R_v \cdot S_g + B_o \cdot S_o)_1$$

The density of oil at each pressure step is given by the following equation:

$$\rho_{o_2} = B_{o_2} \cdot (\rho_{o_{sc}} + c_1 \cdot R_{s_2}) \Rightarrow B_{o_2} \cdot R_{s_2} = \frac{-\rho_{o_{sc}} \cdot B_{o_2} + \rho_{o_2}}{c_1}, \quad \text{where}$$

$$c_1 = \frac{\rho_{g,sc}}{5.6146} = \frac{P_{sc} \cdot MW_g}{R \cdot T_{sc} \cdot Z \cdot 5.6146} = \frac{14.7 \cdot MW_g}{10.73 \cdot 520 \cdot 1 \cdot 5.6146} = 0.000469 \cdot MW_g$$

By substituting the density equation to the mass conservation equations the latter are transformed as follow:

$$B_{g,2} \cdot S_{g,2} - \frac{B_{o,2} \cdot R_{s,2} \cdot \rho_{o,sc}}{c_1} = \frac{V_1}{V_2} \cdot (B_g \cdot S_g + B_o \cdot R_s \cdot S_o)_1 - \frac{S_{o,2} \cdot \rho_{o,2}}{c_1}$$

$$B_{g,2} \cdot R_{v,2} \cdot S_{g,2} + B_{o,2} \cdot S_{o,2} = \frac{V_1}{V_2} \cdot (B_g \cdot R_v \cdot S_g + B_o \cdot S_o)_1$$

In the above equations the already calculated oil content value is substituted and the system of mass conservation and oil density equations can be solved for the $B_{g,2}$ the $B_{o,2}$ and the $R_{s,2}$ values to be calculated (Keith H Coats, 1985).

As it was mentioned previously by using the Coats method the formation volume factors, the solution gas-oil ratio and the oil content are calculated for pressures below the saturation pressure. As a result, the formation volume factors, the solution gas-oil ratio and the oil content for pressures above the saturation pressure have to be calculated by extrapolating the obtained values which can lead to negative compressibility values (Izgec, 2003). Finally, Coats method provides more reliable gas and oil densities than the Whitson-Torp method as the density values are not assumed to remain constant but to satisfy the previously mentioned mass balance (Keith H Coats, 1985).

12. SIMULATION MODEL

The reservoir used for the simulation runs was the one that CMG provides in its suite, whereas the oil that was tested was a volatile oil provided also by CMG. The procedure that was followed for constructing the model and the data used are presented in the simulation model chapter. The constructed model was run with the IMEX and GEM simulators and the results of the simulation runs were compared and presented in Chapter 13.

12.1 RESERVOIR

For the reservoir construction an isobath map, a porosity map and a thickness map were used. The reservoir is lying at the depth of 9801 ft and presents mainly horizontal extent towards the J direction (Picture 17) and exhibits temperature equal to 215 F. The dimensions of the reservoir are the following:

Direction	I	J	K
Length (ft)	7920	13530	566

Table 3: Reservoir dimensions

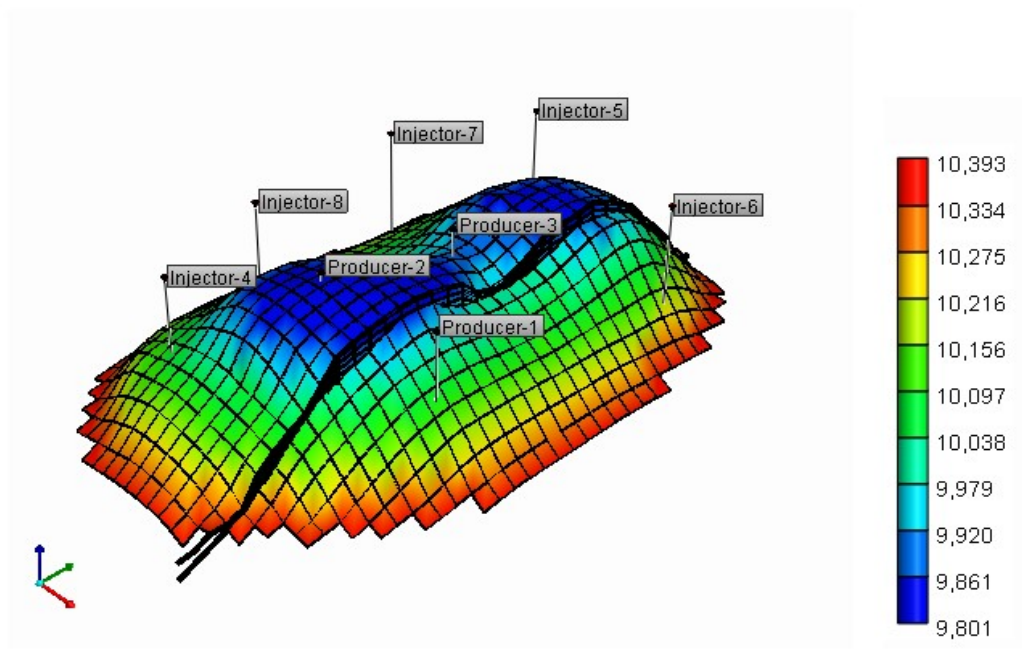
It is a water wet sandstone reservoir, single porosity system, constituted by two anticlines and by four geological layers. The permeability values used for each layer are presented in the Table 4:

Direction	I and J (md)	K(md)
Layer 1	50	5
Layer 2	250	25
Layer 3	500	50
Layer 4	100	10

Table 4: Permeabilities of the reservoir layers

In addition, a semi permeable fault (0.5 transmissibility) is present to all four layers, it is parallel to the J direction and crosses over the entire reservoir. The migration of the reservoir fluid across the fault was calculated by using a lease plane parallel to the fault and this could be done only for IMEX simulator as GEM does not allow the use of lease planes. Finally, the rock compressibility was set equal to 4×10^{-6} 1/psia at the pressure of 5000 psia.

Grid Top (ft) 2017-05-10



Picture 17:3D view of the reservoir

12.2 GRID DESIGN

For the construction of the model, the orthogonal corner point grid was used so as to match better the geometry of the reservoir. The dimensions and the number of blocks that were used for its construction are available in Table 5:

Direction	Number of blocks	Block dimensions
I	25	360
J	35	410
K	10	-

Table 5: Number of blocks and dimensions

It has to be mentioned that the block length towards the K direction was calculated internally by Builder, by dividing the reservoir depth over the desired number of blocks along the K direction. The number of blocks that were used to represent the first and the second geological layer were three for each layer whereas the number of blocks used to represent the third and the fourth geological layers were two.

12.3 RESERVOIR FLUID

The files with the fluid properties that were used for the simulation were generated and uploaded by

Winprop. The reservoir fluid that was used, for the purposes of the simulation was a volatile oil with bubble point pressure equal to 4833 psia and of the composition shown in Table 6. It has to be mentioned that, the four hypo components are characterized by their critical properties (see Table 7). The oil density of the reservoir fluid was equal to 50.504 lb/ft³ at stock tank conditions, whereas the gas density was equal to 0.05 lb/ft³ at stock tank conditions.

Components	Composition (mole%)
N2 to C1	67.07
CO2 to C2	8.55
C3	5.15
IC4 to NC4	3.31
IC5 to FC6	3.89
HYP01	3.643
HYP02	4.964
HYP03	2.764
HYP04	0.658

Table 6: Composition of the reservoir fluid

Component	HC	Pc (atm)	Tc(K)	Vc(l/mol)	Acentric Factor	Molecular Weight	Specific Gravity
N2 toC1	1	45.359509	190.35832	0.098965436	0.0081145072	16.085833	0.30118085
CO2toC2	1	48.741633	305.36933	0.14617028	0.10201053	30.510211	0.36540074
C3	1	41.9	369.8	0.203	0.152	44.097	0.507
IC4toNC4	1	37.020623	419.73204	0.25750472	0.18765861	58.124	0.57723498
IC5toFC6	1	32.945375	485.65591	0.32334176	0.25626324	78.737285	0.65877043
HYP01	1	30.38506	534.65258	0.41654663	0.30220736	102.22057	0.73269891
HYP02	1	21.446372	626.81401	0.64726352	0.48461482	157.56134	0.77690984
HYP03	1	13.612846	747.01706	1.0907892	0.7824305	266.08216	0.83403706
HYP04	1	10.54969	851.95932	1.6784973	1.1684923	455	0.89688196

Table 7: Components properties

p	Rs	Rv	Bo	Eg	μo	μg
14.7	0	0	1.0574	4.3303	1.49524	0.012834
500	152.02	1.00E-005	1.1702	154.04	0.62679	0.013208
1000	317.53	1.80E-005	1.2678	322.51	0.44615	0.014052
1500	498.58	2.26E-005	1.37	498.19	0.33446	0.015434
2000	701.51	2.81E-005	1.4818	673.58	0.25855	0.017397
2500	933.25	3.71E-005	1.6075	840.8	0.20473	0.020077
3000	1203.96	5.00E-005	1.7532	991.8	0.16517	0.023565
3500	1531.19	6.79E-005	1.9289	1119.1	0.13494	0.027979
4000	1951.85	9.38E-005	2.1564	1214.6	0.11059	0.033705
4300	2288.97	0.00011622	2.342	1251.5	0.09742	0.038275
4600	2775.44	0.00014967	2.6175	1265	0.08389	0.044792
4833.44	3580.92	0.00020309	3.1	1235.9	0.06919	0.054949

Table 8: Black oil Table used for the simulation with IMEX

Due to the fact that, the fluid was a volatile oil, modified black oil Tables (Table 8) were used for IMEX simulator, which were developed using the Whitson-Torp method as it is thought to be more accurate than Coats method.

Moreover, it has to be mentioned that the GEM simulator presented problems to the single phase fluid identification, as the single phase fluid was identified as gas instead of oil. This happened because the fluid had lower density than the reference density that the simulator used for the identification. This problem was overcome, by using the internal pseudo-critical temperature identification method.

12.4 ROCK-FLUID DATA

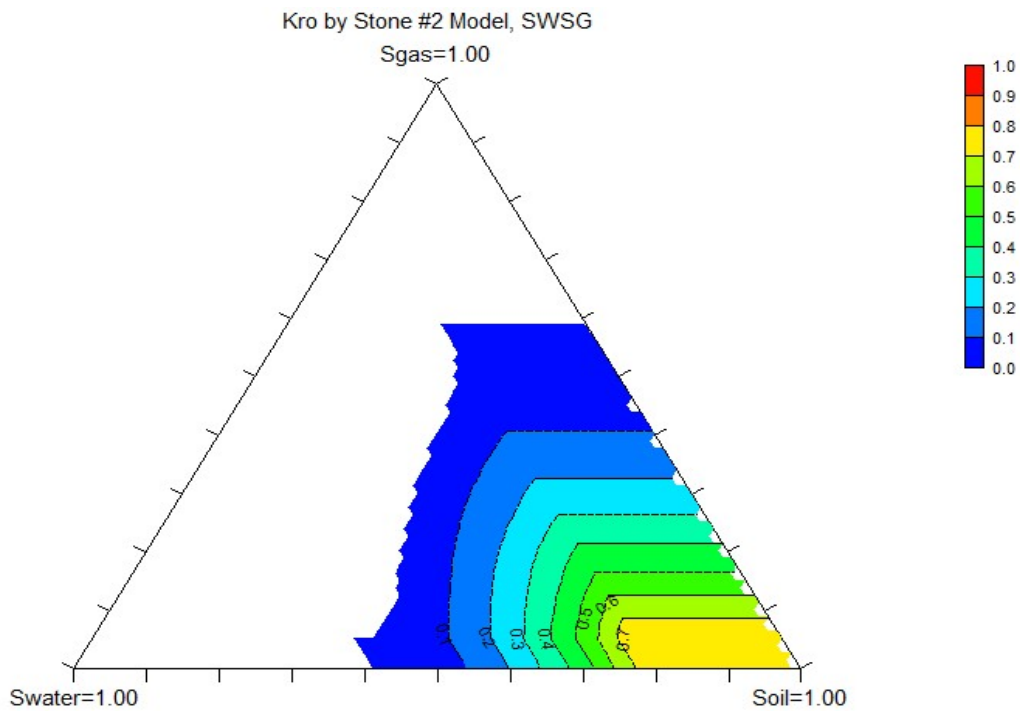
Two phase relative permeability data (water-oil and liquid-gas) were inserted into the simulators (Tables 9 and 10). Then by using the Stone's second model (see § 5.3), which is appropriate for water-wet reservoirs, the three phase relative permeabilities were calculated internally (picture 18).

Sw	krw	krow
0.2	0	0.8
0.225	0.00117187	0.703125
0.25	0.0046875	0.6125
0.275	0.0105469	0.528125
0.3	0.01875	0.45
0.325	0.0292969	0.378125
0.35	0.0421875	0.3125
0.375	0.0574219	0.253125
0.4	0.075	0.2
0.425	0.0949219	0.153125
0.45	0.117187	0.1125
0.475	0.141797	0.078125
0.5	0.16875	0.05
0.525	0.198047	0.028125
0.55	0.229688	0.0125
0.575	0.263672	0.003125
0.6	0.3	0

Table 9: Water-oil relative permeabilities

SI	kr _g	k _{rog}
0.4	0.3	0
0.434375	0.263672	0.003125
0.46875	0.229688	0.0125
0.503125	0.198047	0.028125
0.5375	0.16875	0.05
0.571875	0.141797	0.078125
0.60625	0.117188	0.1125
0.640625	0.0949219	0.153125
0.675	0.075	0.2
0.709375	0.0574219	0.253125
0.74375	0.0421875	0.3125
0.778125	0.0292969	0.378125
0.8125	0.01875	0.45
0.846875	0.0105469	0.528125
0.88125	0.0046875	0.6125
0.915625	0.00117188	0.703125
0.95	0	0.8

Table 10: Oil-gas relative permeabilities



Picture 18: Three-phase relative permeability of oil, as it was calculated using Stone's second model

12.5 INITIAL CONDITIONS

For the initialization of the reservoir, the vertical depth average method was used. When this method is used, the initial saturations of the phases are taken by the relative permeability Tables as the first saturation entry in these Tables refers to the connate saturation of the reservoir. The reservoir was assumed that it did not exhibit

gravitational segregation and as a result, a constant bubble point pressure value for the entire reservoir was used. The reservoir was undersaturated and the initial reservoir pressure was 5000 psia at the depth of 10000 ft. Moreover, the water-oil contact was initially lying at the depth of 10300 ft. It has to be mentioned that, both simulators assumed that the rock underlying the reservoir (base rock) was impermeable.

In the GEM simulator, for the calculation of the initial volumes in place the separator was used so the initial hydrocarbon volumes were calculated more accurately. Two separator stages were used, the one was working at 300 psia and 75F and the other at 14.7 psia and 60F.

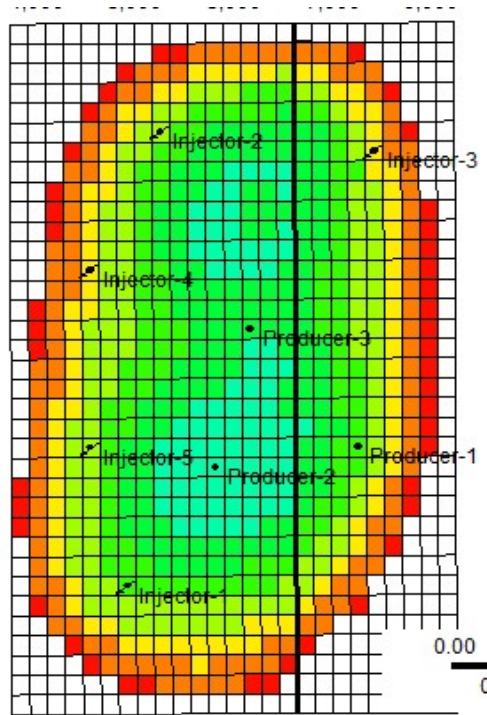
12.6 WELLS DESIGN

For the exploitation of the reservoir, eight vertical wells were used out of which the three were producers and the five injectors. The reservoir was let to produce due to pressure depletion only for the first year. The water injection initiated with the start of the simulation (year=0) and continued for 26 years with variable rates, so as to provide the required pressure support as the reservoir pressure was too close to the bubble point pressure of the reservoir fluid.

The location of the wells, their rates of production and the time that these wells were operating was decided after trials, so as to find the optimum values for these parameters. The aim of the designed well scheme was to:

- Maximize the hydrocarbon recovery
- Minimize the injection needs
- Take advantage of flow paths in the reservoir

Before proceeding in a more detailed analysis of the well's scheme, it has to be mentioned that, all the wells had been located at their block centers, the production tubing casing was 0.25 in and the blocks were perforated throughout their entire length.



Picture 20: Well's location

12.6.1 Production Wells

The production wells, was decided to be located in the higher porosity regions of the reservoir. This was done so as the reservoir fluid to flow easily towards the producers. The perforations of the production wells were located from layer 4 to layer 6 of the reservoir, as the oil saturation in these blocks was remaining high for a longer time period.

Moreover, the lower perforations (block 6) of the production well's was decided to close, when the water saturation of this zone became too high in the region nearby the well. This was done, so as to force the well to produce from the zone of higher oil saturation minimizing thus the produced water and optimizing the oil production. The location of the producers, the time period that the perforations remained open and the skin factor of each well can be seen in Table 11:

Well	Perforated Blocks	Time	Skin Factor	Depth
Producer 1	(20, 22, 4:6)	2017/5/10 to 2039/1/10	2	10080-10170 ft
Producer 1	(20, 26, 4:5)	2039/1/10 to 2050/1/10	2	10080-10161 ft
Producer 2	(12, 23, 4:6)	2017/5/10 to 2041/9/10	2	9912-10028 ft

Producer 2	(12, 23, 4:5)	2041/9 /10 to 2050/1/10	2	9912-9995 ft
Producer 3	(14, 16, 4:6)	2017/5/10 to 2038/12/10	3	9952-10044 ft
Producer 3	(14, 16, 4:5)	2038/12/10 to 2050/1/10	3	9952-10021 ft

Table 11: Perforated blocks of the production wells, time period that these perforations are open and skin factor

The constraints that were imposed on the production wells were the daily oil rate, the bottom hole pressure and the water cut (Table 12). The oil rate constraint was imposed, so as to force the production wells to produce at a constant rate. The bottom hole pressure constraint was used, so as to prevent an unlimited pressure drop in the reservoir which can lead to non physically sound reservoir pressure values (eg. 14.7 psia). The water-cut constraint was imposed on the production wells, in order not to allow the wells to operate and produce a high amount of water along with oil.

The primary operating constraint was the oil rate and the secondary operating constraint was the bottom hole pressure. The action that was imposed on both operating constraints was the continue action. As a result, when a well could not produce anymore with the desired constant oil rate, the primary operating constraint was switching to the bottom hole pressure. After this, the well was producing at as many barrels as the bottom hole pressure was allowing.

Well	Production rate (stb/day)	Bottom hole pressure (psia)	Water-cut (%)
Producer 1	1100	4500	10
Producer 2	900	4500	10
Producer 3	700	4500	10

Table 12: Constraints imposed on the production wells

Finally, in GEM simulator the production wells were linked to the separator train so as the produced volumes of the reservoir fluid to be calculated more accurately.

12.6.2 Injection Wells

The injection wells location, the time that each injector shuts in and the water injection rates (Tables 13), were decided after several trials so as to achieve the desired pressure support and the maximum oil recovery factor. More specifically, the injectors was decided to be located close to the reservoir boundaries, so as to push the oil towards the center of the reservoir where the producers were located. The perforations of the injection wells was decided to be located at the three lower layers of the reservoir model (layer 7 to 10).

Moreover, the skin factor that the injection wells exhibit is shown in Table 12. The reduction of the injection rates at 2042 was decided so as to minimize the injection needs and simultaneously trying not to affect significantly hydrocarbons recovery.

Well	Perforated Blocks	Injection rate (bbl/day)	Skin Factor	Time	Depth
Injector 1	(7, 29, 7:10)	1600	3	2017/5/10 to 2040/9/10	10130-10200 ft
Injector 1	(7, 29, 7:10)	600	3	2040/9/10 to 2042/10/10	
Injector 2	(9, 6, 7:10)	1800	2	2017/5/10 to 2039/12/10	10125-10255 ft
Injector 2	(9, 6, 7:10)	1300	2	2039/12/10 to 2042/10/10	
Injector 3	(21, 7, 7:10)	1600	2	2017/5/10 to 2042/10/10	10199-10228 ft
Injector 4	(5, 13, 7:10)	1300	3	2017/5/10 to 2039/12/10	10211- 10278 ft
Injector 4	(5, 13, 7:10)	500	3	2039/12/10 to 2042/10/10	
Injector 5	(5, 22, 7:10)	1300	2	2017/5/10 to 2037/9/10	10144-10219 ft
Injector 5	(5, 22, 7:10)	500	2	2037/9/10 to 2042/10/10	

Table 13: Location of the perforations, injection rates, skin factor and dates of operation of the injection wells

Finally, the simulation run was performed for 34 years (2017/54/10 to 2049/12/10) of production with a monthly timestep and the implicit method was used for the solution of the system of equations. The use of the implicit method was necessary, as convergence problems were encountered with both simulators. The simulation runs were performed by a dual core processor (AMD E1-6010) and 4 GB RAM. The operating system was Windows 7 and the CMG suite version that was used was the 2012.10 one.

13. SIMULATION RESULTS

The model that was developed as above was run with both IMEX and GEM simulators. An initialization run (the simulator runs only one timestep) and a simulation run (the simulation is performed for the entire time period that the reservoir was set to production) were performed with both simulators. The initialization run provides information about the initial state of the reservoir, such as the initial volumes of hydrocarbons and water in place, the initial saturations of the phases and the initial average pressure of the reservoir as it was calculated by the simulator. The simulation run provides the recovery factors of the phases, the residual saturations of the phases, the cumulative produced volumes of the reservoir fluid and the abandonment pressure of the reservoir. The results of the initialization and the simulation runs from both simulators were compared and found to be different.

13.1 INITIALIZATION RUN RESULTS

The information about the initial state of the reservoir and the differences between IMEX and GEM simulators can be seen in the Table 14.

		GEM	IMEX	Difference GEM-IMEX	Percentage difference GEM-IMEX
Pore Volumes					
Total Pore Volume	M rft3	1.62E+006	1597678.5	18591.5	1.15
HC. Pore Volume Originally in Place	M rft3	1.28E+006	1269834.45	14775.55	1.15
Stock Tank Oil	M STB	74511	74001	510	0.69
Gas at Surface	MM SCF	2.66E+005	264879	796	0.30
Water at Surface	M STB	59956	56624	3332	5.55
Average Saturation					
Oil	%	79.48	79.48	0	0.00
Gas	%	0	0.00E+000	0.00E+000	0.00
Water	%	20.52	20.52	0	0.00
Average Pressures					
Total PV Average	psia	5009.7	5009.5	0.2	0.00
HC PV Average	psia	5009.3	5009.2	0.1	0.00

Table 14: Initial conditions calculated by IMEX and GEM simulators

The GEM simulator, calculated that more barrels of oil, gas and water existed initially in place, than the IMEX simulator. The slight difference between the two simulators with respect to the average pore and hydrocarbon pressures calculated seems to be normal, as GEM calculated more barrels of water and as a result the pressure gradients were different.

Moreover, in the left hand side of the fault, larger amount of hydrocarbons is stored, than the right hand side of the fault, as this part represents the larger part of the reservoir and it has also greater porosity (Appendix

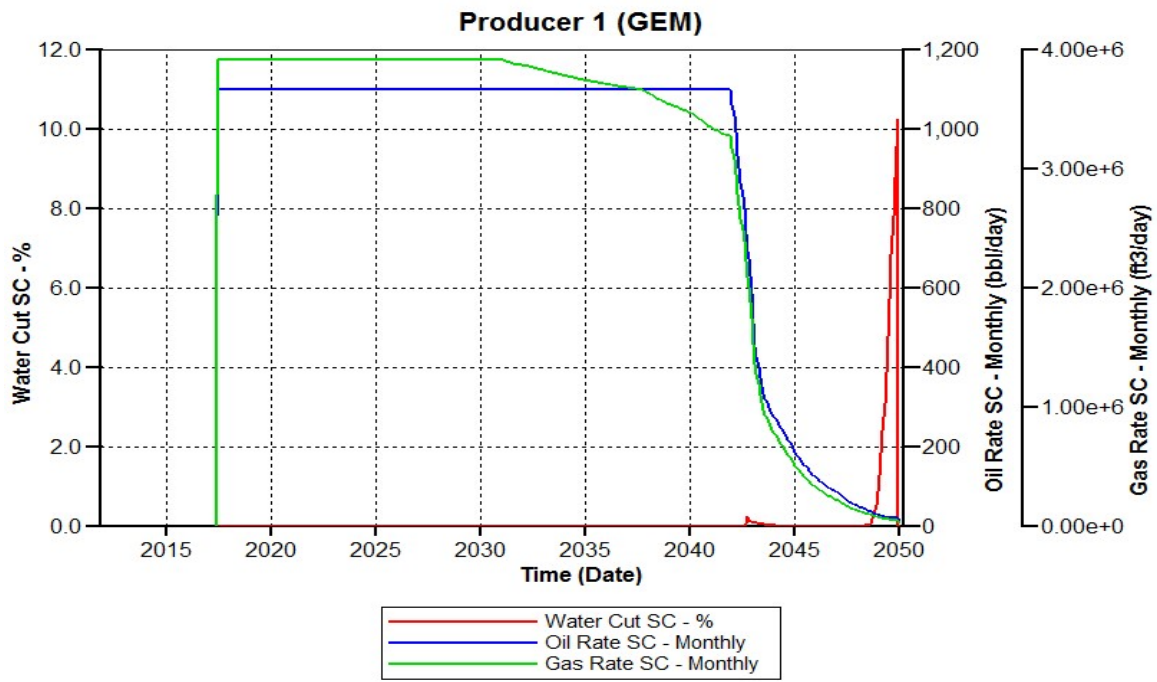
C). Small differences were also exhibited between the two simulators in the calculation of the initial volumes in place for the two parts of the reservoir which are separated by the fault, however due to the fact that these differences were negligible as it can be seen from the Tables in Appendix C, only the values of the initial fluids in place that GEM simulator calculated will be presented here. The reservoir part on the left hand side of the fault, according to the GEM simulator had originally 63074 Mstb of oil, 224896 MMscf of gas and 50254 Mstb of water. On the other hand, the right hand side of the fault according to GEM simulator had originally 11437 Mstb of oil, 40779 MMscf of gas and 9701 Mstb of water.

Finally, the differences exhibited between the two simulators have to do with the fact that the phase behavior problem is solved differently.

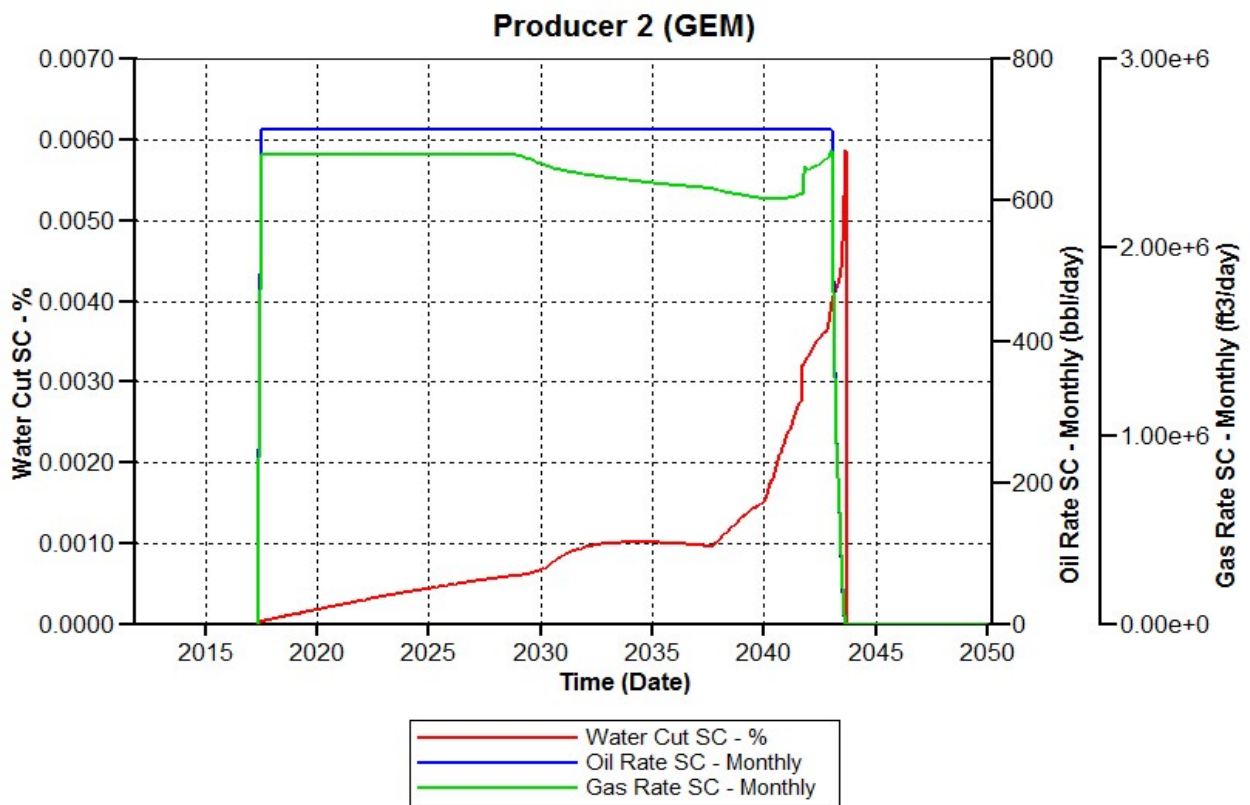
13.2 SIMULATION RUN RESULTS

The simulation runs were performed under the same conditions and for the same years of production for both simulators, whereas the cumulative water injection in both cases was equal to 63979 Mstb. The main drive mechanism was the water drive occurred by the water injection, whereas the gas drive and the compaction drive mechanisms, also influenced the production of the reservoir. The compaction drive mechanism, was found to be slightly more intense when the reservoir was simulated with GEM simulator than with IMEX. This difference, was probably caused by their difference in the pressure reduction rate as the pore volume is a function of pressure. Moreover, due to the fact that the pressure declined in a different way between the two simulators has as a result the different reduction in pore volume.

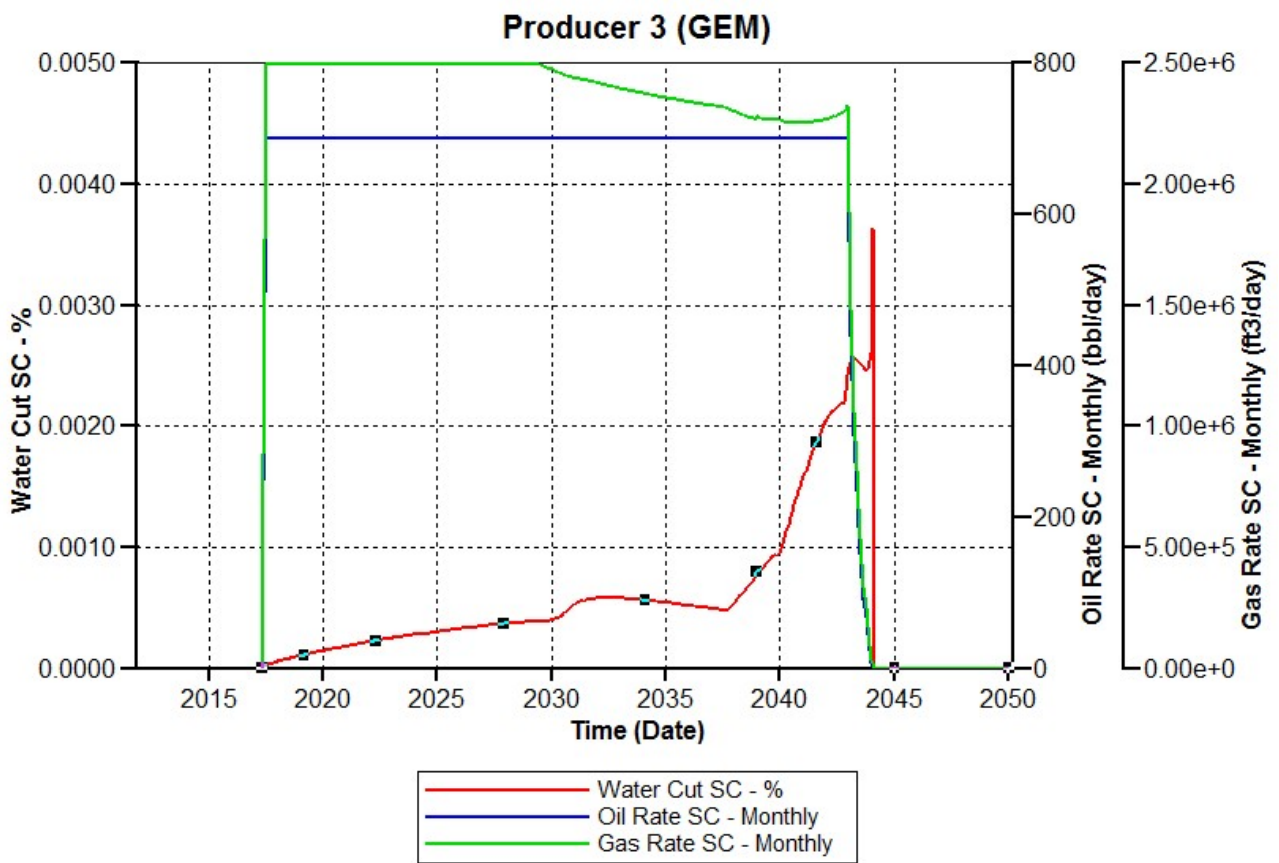
First of all, it has to be noted that, water flooding achieved a good sweep efficiency, as no fingering was observed to occur to any of the 10 layers of the reservoir (some representative pictures can be found in Appendix B). Secondly, differences were exhibited in production predictions between the GEM and IMEX simulators but they were small (Table 16 and pictures 21 to 31), with GEM simulator to predict that less oil, gas and water will be overall produced. These differences, were also depicted to the slightly oil recovery factors that the two simulators predicted. However, GEM simulator predicted that the residual saturations of oil and water will be less than those predicted by IMEX due to the fact that GEM predicts that more gas will be liberated and remain inside the reservoir.



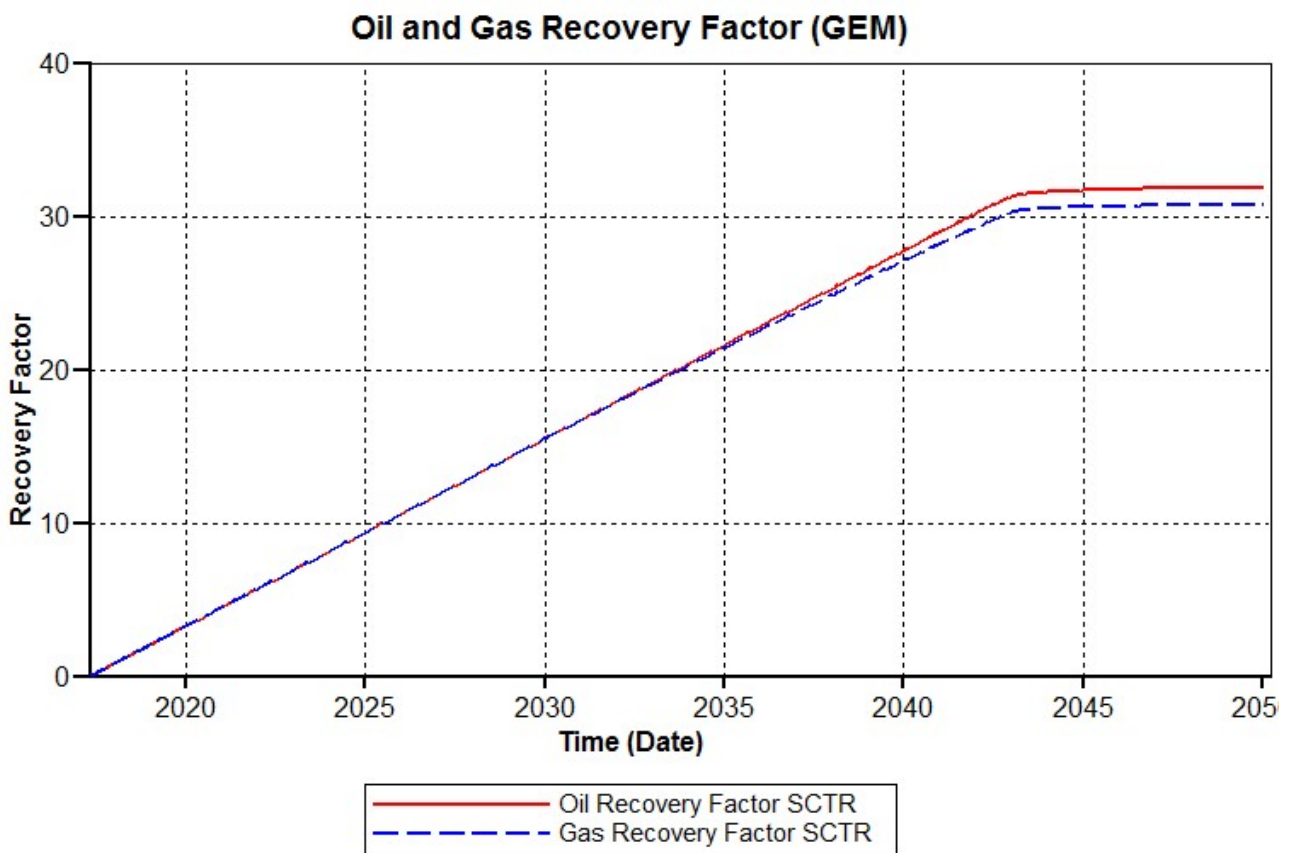
Picture 21: Producer 1 (GEM simulator)



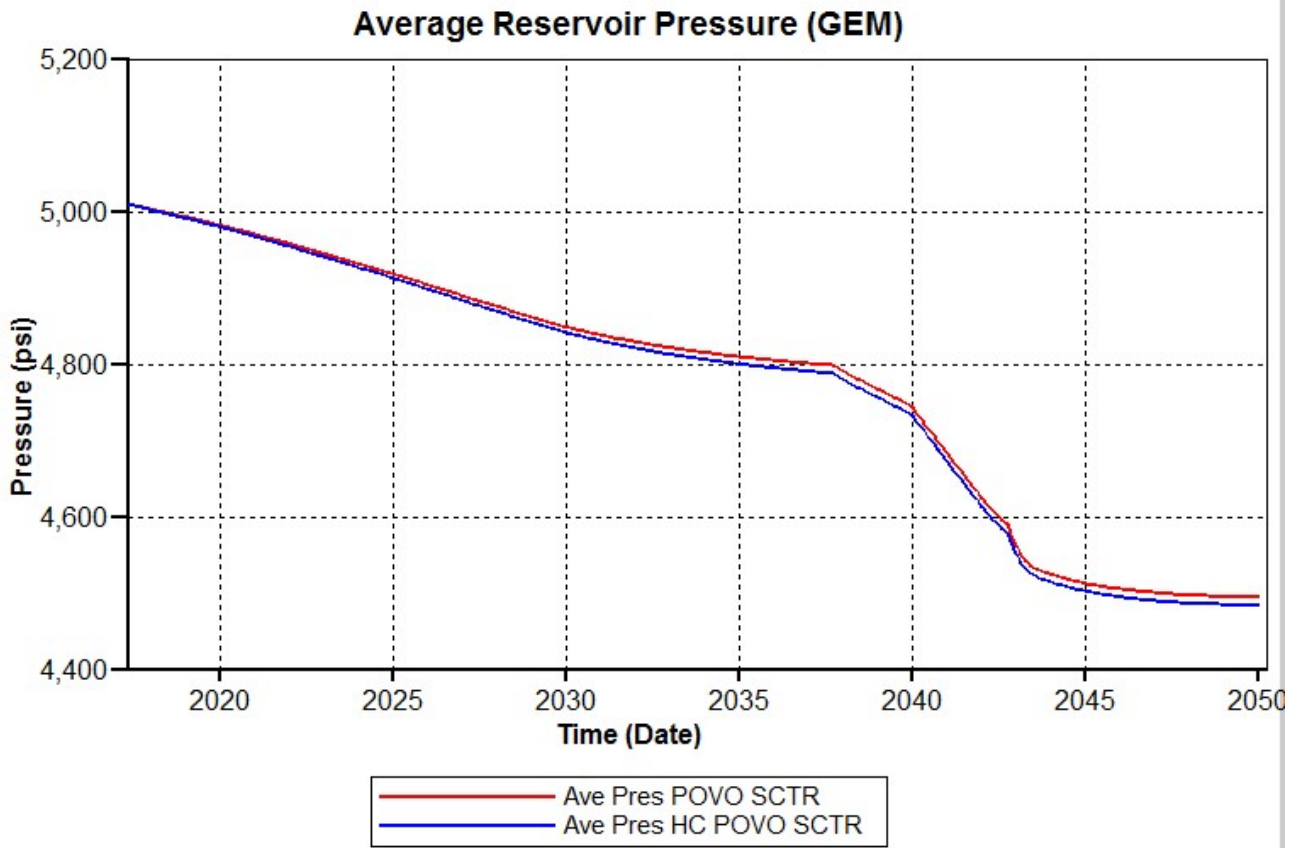
Picture 22: Producer 2 (GEM simulator)



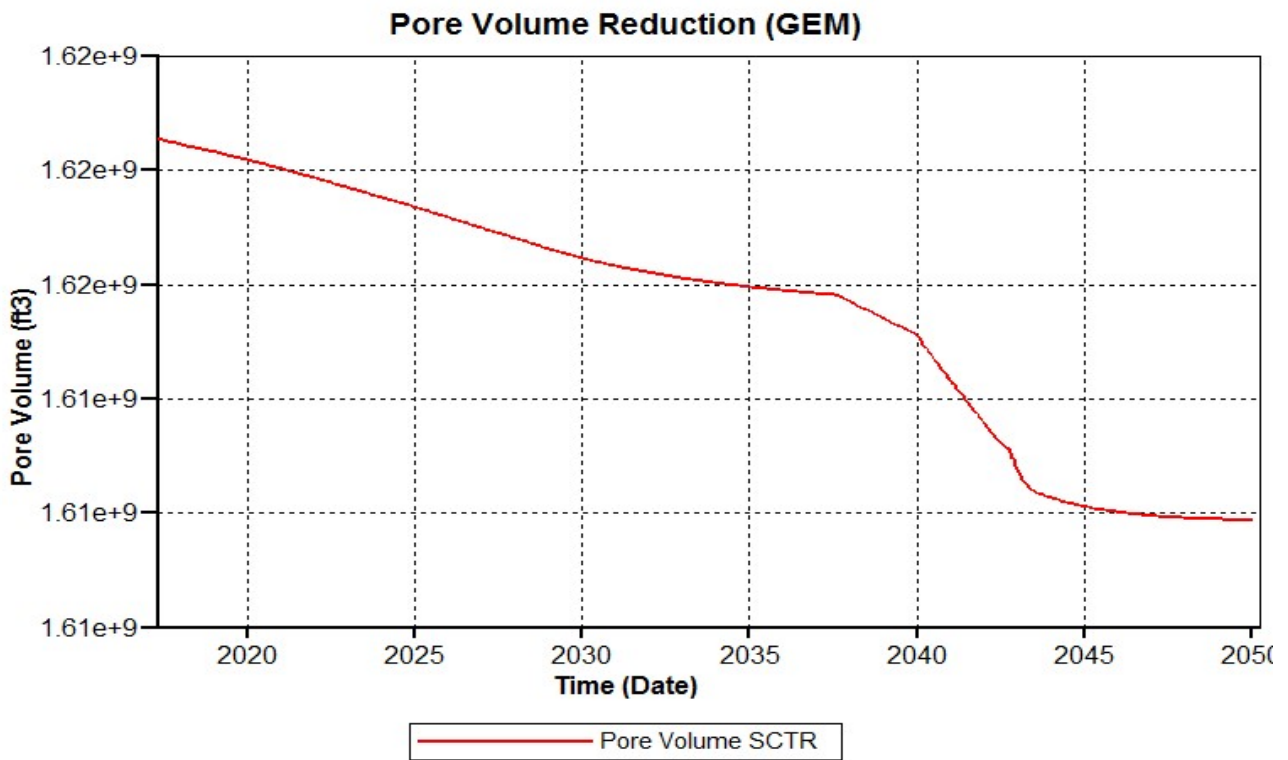
Picture 3: Producer 3 (GEM simulator)



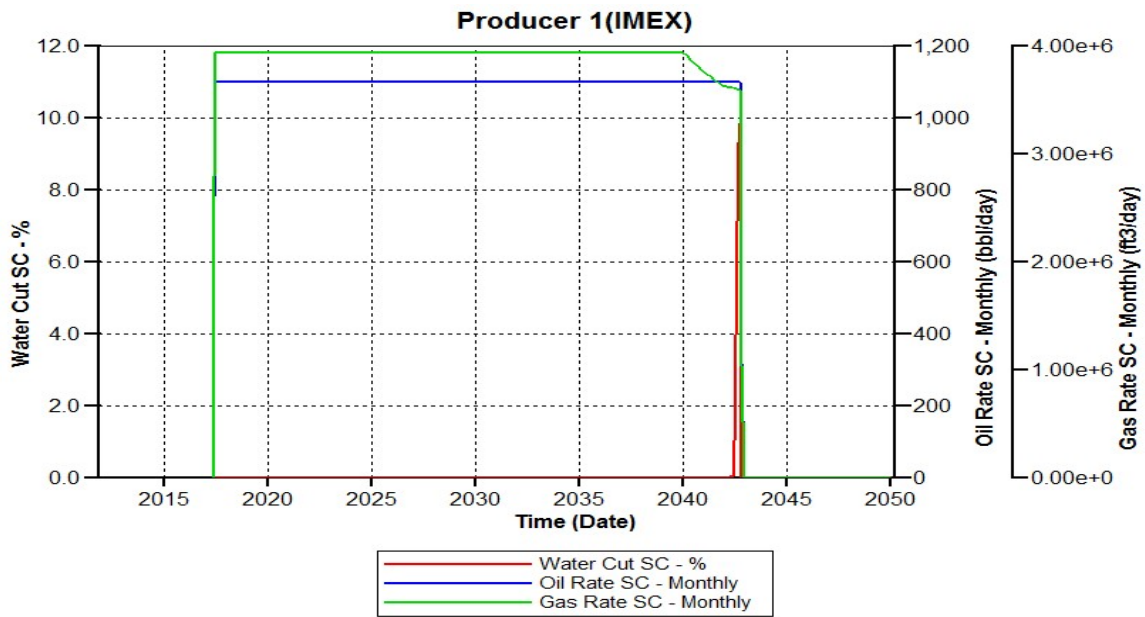
Picture 24: Recovery factor(GEM simulator)



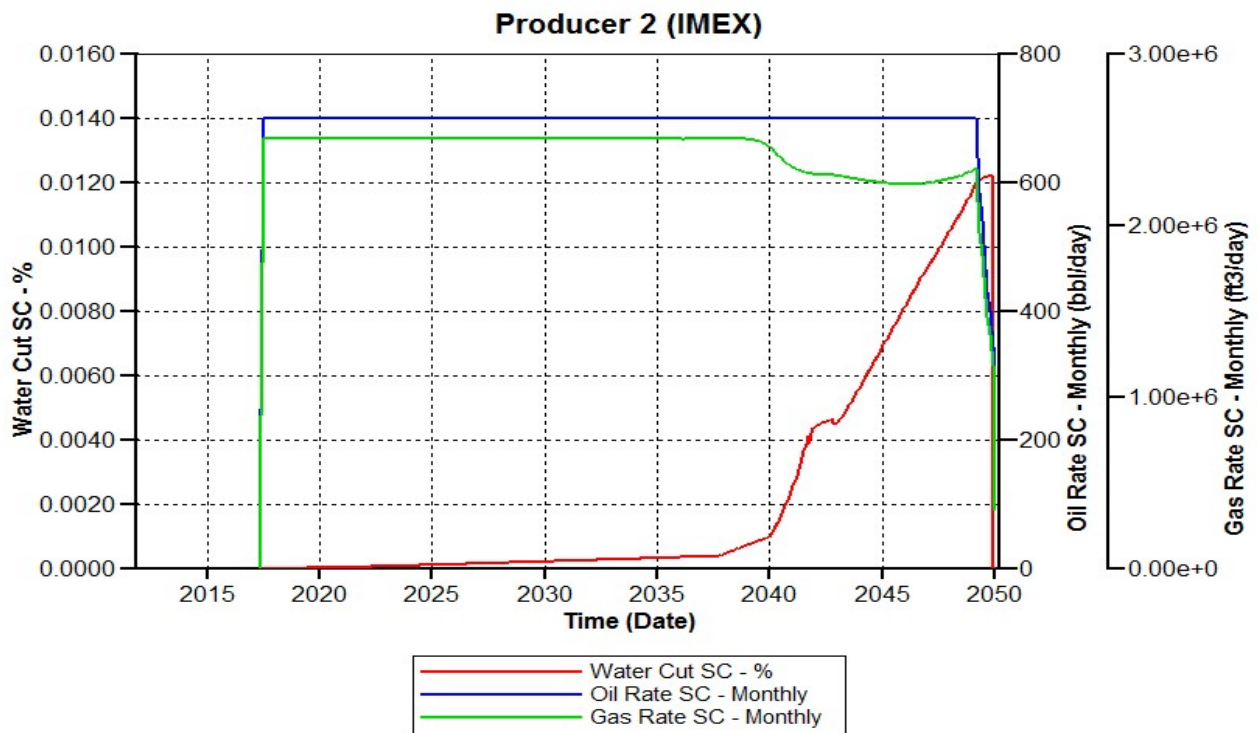
Picture 25: Average reservoir pressure (GEM simulator)



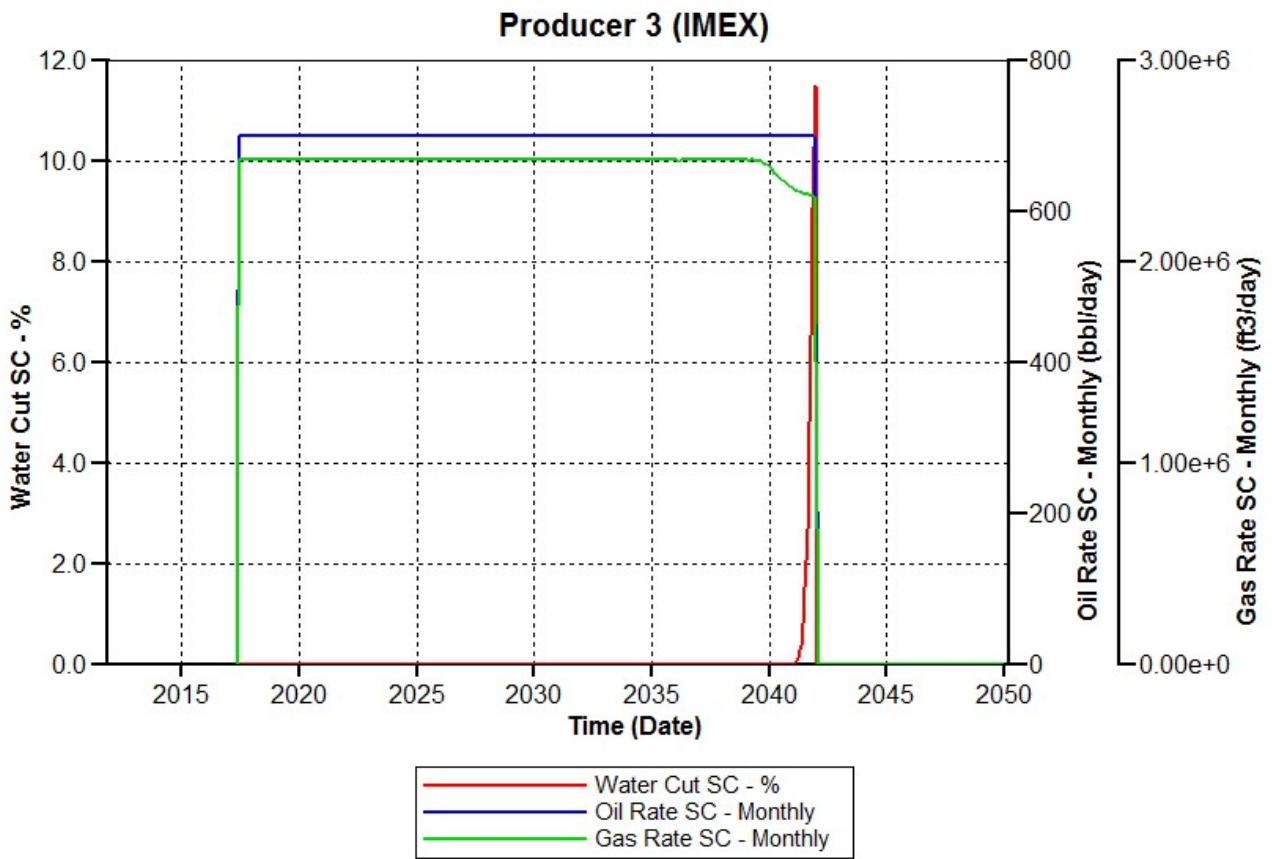
Picture 26: Pore volume reduction (GEM simulator)



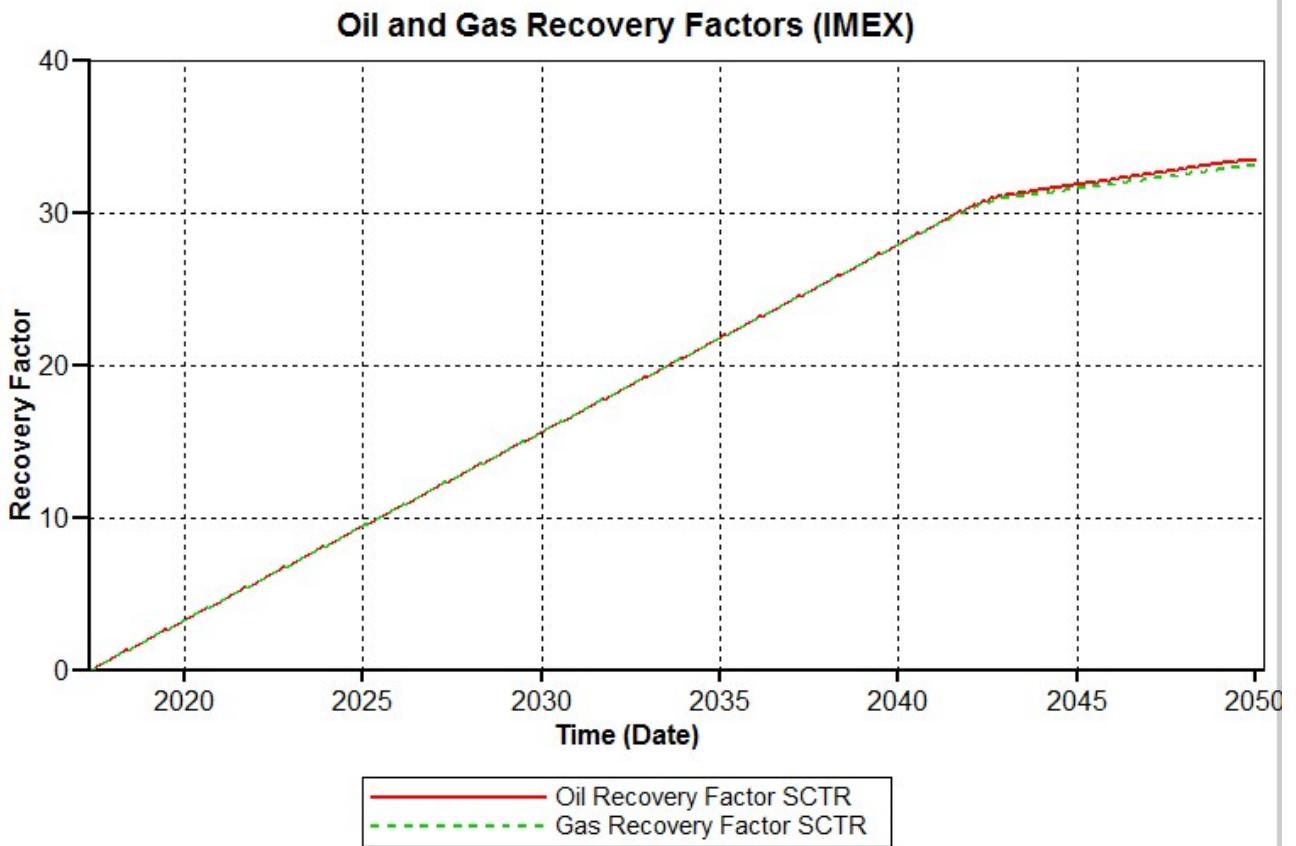
Picture 26: Producer 1 (IMEX simulator)



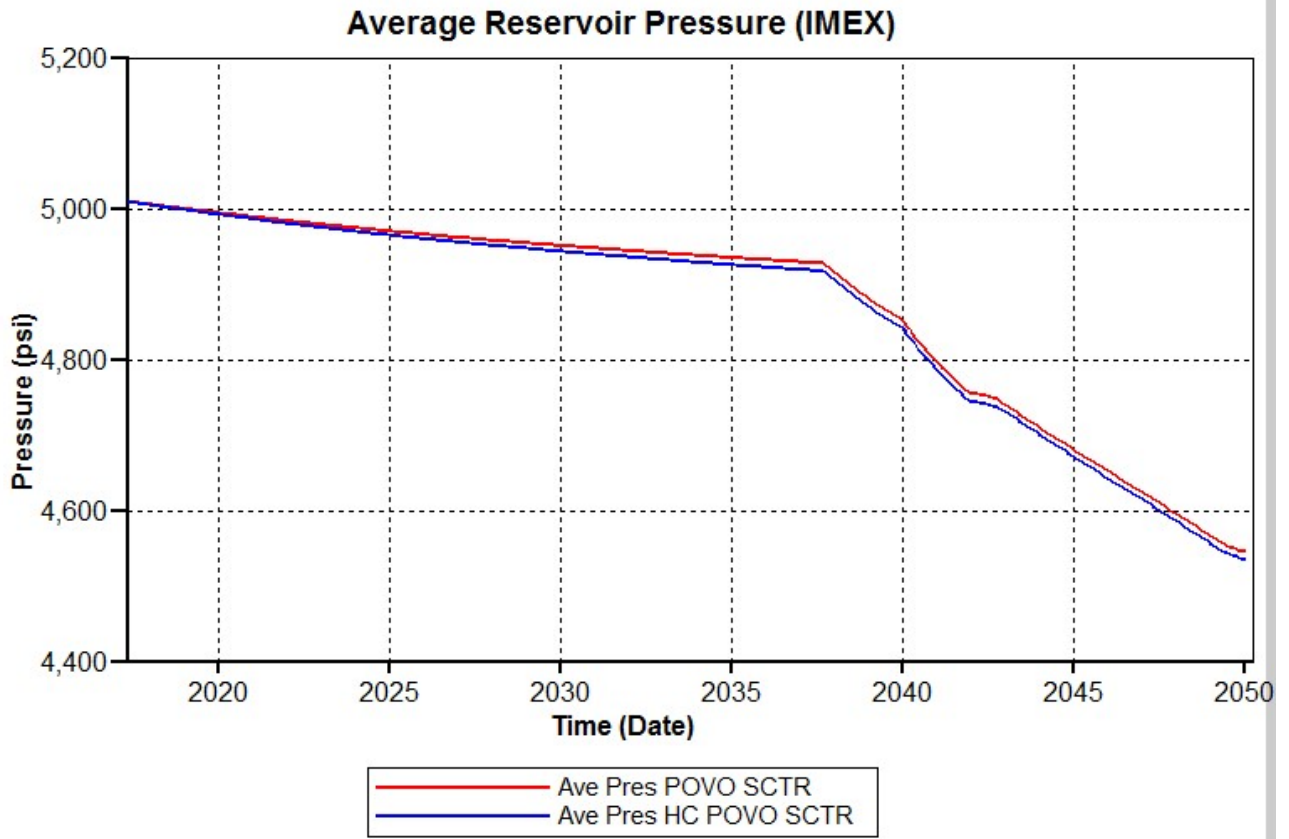
Picture 27: Producer 2 (IMEX simulator)



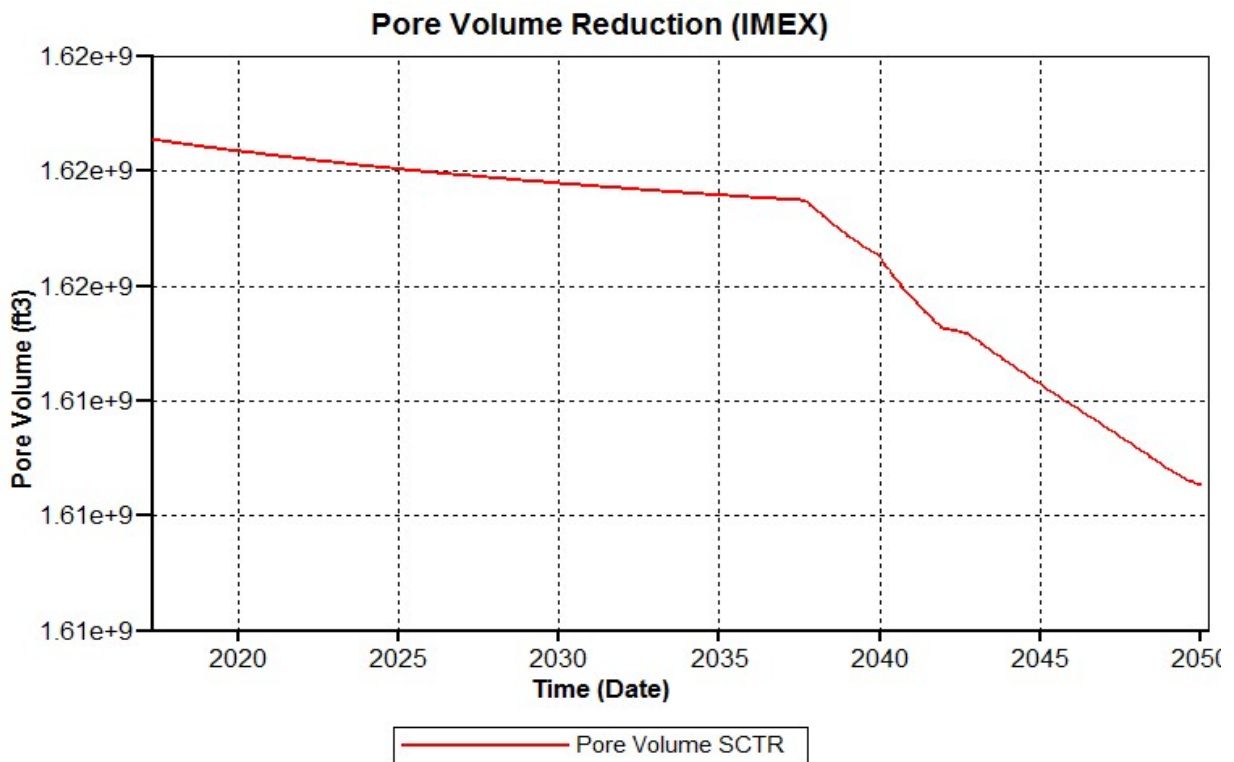
Picture 28: Producer 3 (IMEX simulator)



Picture 29: Recovery factor (IMEX simulator)



Picture 30: Average reservoir pressure (IMEX simulator)



Picture 31: Pore volume reduction (IMEX simulator)

		GEM	IMEX	Difference GEM-IMEX	Percentage difference GEM-IMEX
Pore Volumes					
Total Pore Volume	M rft3	1.61E+006	1594714.8	18225.2	1.13
HC. Pore Volume	M rft3	9.26E+005	874763.25	51475.75	5.56
Currently in Place					
Stock Tank Oil	M STB	50753	49210	1543	3.04
Gas at Surface	MM SCF	1.84E+005	177320	6993	3.79
Water at Surface	M STB	1.24E+005	120581	3374	1.83
Average Saturations					
Oil	%	34.39	34.682	-0.292	-0.84
Gas	%	23.036	20.172	2.864	12.43
Water	%	42.574	45.146	-2.572	-5.70
Average Pressures					
Total PV Average	psia	4494.2	4545.7	-51.5	-1.13
HC PV Average	psia	4483.7	4535.6	-51.9	-1.14
Percentage Recovery					
Stock Tank Oil	%	31.88	33.466	-1.586	-4.97
Gas at Surface	%	30.755	33.063	-2.308	-6.98
Water	%	-106.7	-112.95	-6.25	-19.60
Cumulative Production					
Oil	M STB	23755	24765	-1010	-4.25
Gas	MM SCF	81709	87578	-5869	-6.70
Water	M STB	0.80919	20.087	-19.27781	-95.97

Table 15: The results provided by GEM and IMEX simulators after the complete simulation run and their difference

Both simulators predicted that the recovery factors of the phases will be greater for the left hand side of the fault than for the right hand side (Appendix A). Moreover, both simulators predicted that in the right hand side of the fault greater residual saturations of oil and water will occur than at the right hand side as well as in the block layers where the perforations of the producers exist (Appendix A). However, the opposite applied with respect to the gas residual saturation which was greater for the left hand side which is the swallower part of the reservoir. Additionally, fluid flow occurred across the fault but it could be printed in the output file only for IMEX simulator as GEM simulator does not allow the use of lease planes. In general, it was observed in both simulators, the fact that the fault was permeable had a positive impact on the hydrocarbons recovery. The cumulative migration of the reservoir fluid from the left part of the reservoir to the right part and the opposite is shown in the following Table:

	Oil (Mstb)	Gas (Mscf)	Water (Mstb)
Left to right	4005.7649	14070525	2354.1944
Right to left	2527.1876	9378457.7	1699.0903

Table 16: Cumulative fluid flow across the fault (IMEX simulator)

With respect to the pressure depletion, the rates with time of the pressure drop were slightly different (Tables 17 and 18 and pictures 25 and 30). Their difference in pressure depletion can be explained by the different treatment of the phase behavior problem but mainly by the small pressure reduction rate. The difference in pressure reduction rate also influenced the overall production of the reservoir. The main difference that had a great effect on the time at which the reservoir pressure dropped below the bubble point pressure, was the small reduction rate of pressure. With respect to GEM simulator the reservoir pressure was less than the bubble point at 2030/10/10 and it was equal to 4832 psia. On the other hand, with respect to IMEX simulator, the reservoir pressure was found to be less than the bubble point at 2040/2/10 and it was equal to 4832psia.

Dates	Pressure HC (GEM)	Pressure HC (IMEX)	Difference in HC pressure (GEM-IMEX)	Percentage difference in HC pressure (GEM-IMEX)
2017/5/10	5009.3	5009.2	0.1	0.00
2020/1/10	4979.71	4992.17	-12.46	-0.25
2025/1/10	4912.54	4964.65	-52.11	-1.05
2030/1/10	4841.86	4942.96	-101.1	-2.05
2035/1/10	4799.25	4925.74	-126.49	-2.57
2040/1/10	4726.78	4840.71	-113.93	-2.35
2045/1/10	4501.84	4670.85	-169.01	-3.62
2050/1/10	4483.7	4535.6	-51.9	-1.14

Table 17: Difference in hydrocarbon pressures between GEM and IMEX simulators

Dates	Pressure pore volume (GEM)	Pressure pore volume (IMEX)	Difference in pore volume pressure (GEM-IMEX)	Percentage difference in pore volume pressure (GEM-IMEX)
2017/5/10	5009.7	5009.5	0.2	0.00
2020/1/10	4982.71	4995.23	-12.52	-0.25
2025/1/10	4918.95	4969.62	-50.67	-1.02
2030/1/10	4850.26	4950.87	-100.61	-2.03
2035/1/10	4809.73	4935.21	-125.48	-2.54
2040/1/10	4746.91	4855.37	-108.46	-2.23
2045/1/10	4512.91	4680.15	-167.24	-3.57
2050/1/10	4494.2	4545.7	-51.5	-1.13

Table 18: Difference in pore volume pressures between GEM and IMEX simulators

The time and the reason for which the production wells switch their primary operating constraint to the bottom hole pressure one (the time that the production at the plateau ended) was different for the two simulators (Table 19). With respect to GEM simulator all the production wells finished their plateau production due to switching of their primary operating constraint to the bottom hole pressure constraint. On the other hand, for IMEX simulator producers 1 and 3 finished their plateau due to high water cuts whereas producer 2 finished its plateau due to switching of the primary operating constraint to the bottom hole pressure constraint. In general, IMEX simulator predicted that the producer 2 could produce with constant rate for five years more than GEM simulator. This time lag, between the two simulators, for switching the primary operating constraint, was the result of the exhibited difference in pressure reduction between the two simulators.

	GEM	IMEX
Producer 1	2041/12/10	2042/10/10
Producer 2	2043/1/10	2048/7/10
Producer 3	2042/12/10	2041/12/10

Table 19: Time when the plateau production finished

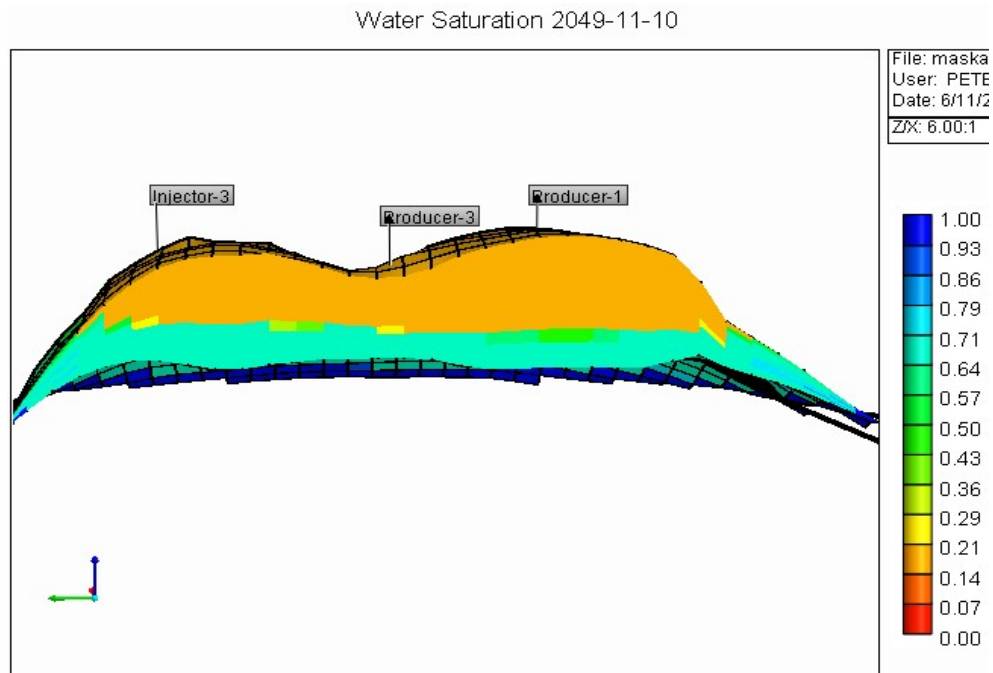
With respect to, the production of the injected water, some of the wells exceeded the limit imposed for the water cut (10%). When the reservoir was simulated with IMEX, two of the production wells were shut in due

to high water cut (Table 20), whereas in GEM simulator, only one well was shut in due to water cut although this well produced with low rates and was to shut in any case.

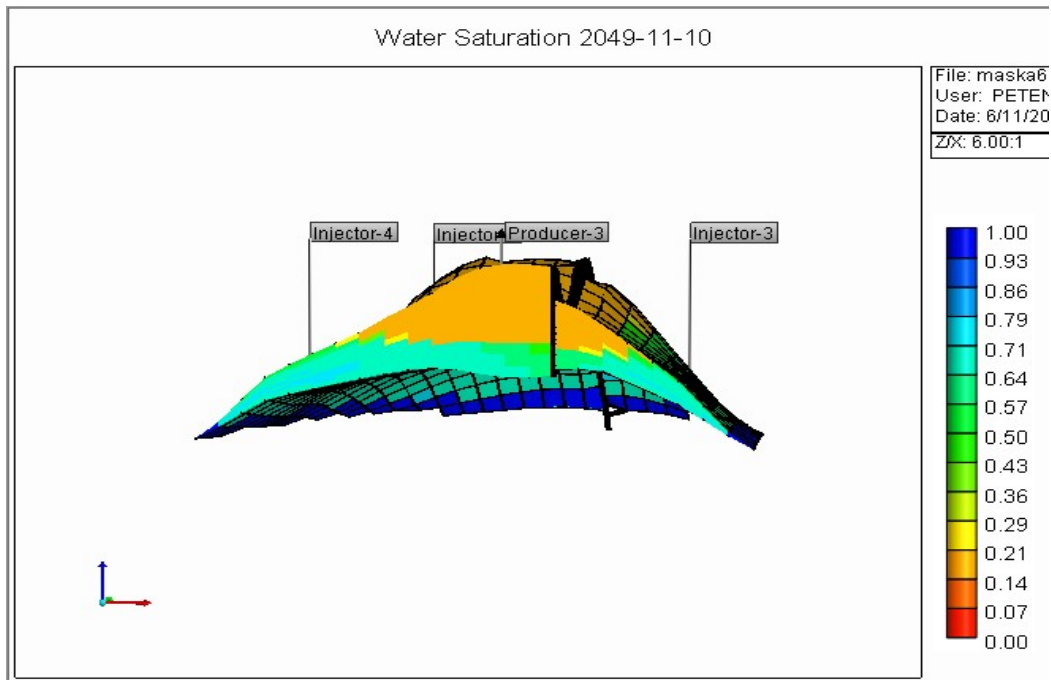
	GEM	IMEX
Producer 1	10.24 %	10.36 %
Producer 2	0.0058 %	0.012 %
Producer 3	0.0036 %	11.51 %

Table 20: Highest water-cut values of the producers calculated from GEM and IMEX simulators

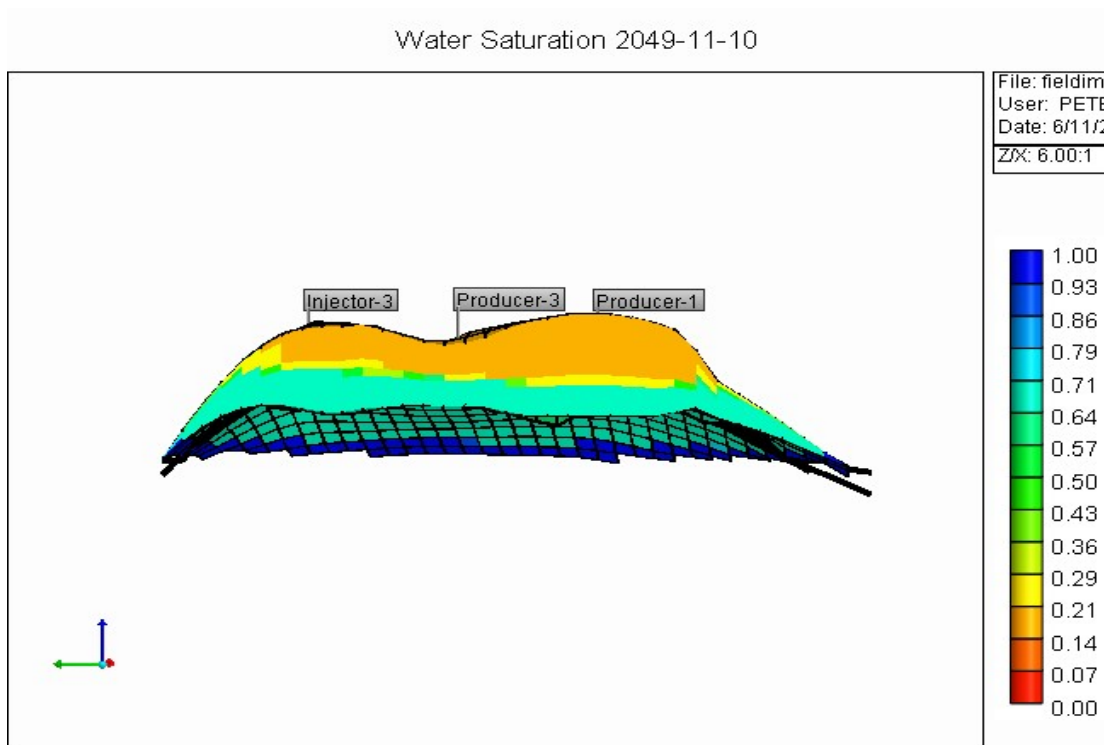
Concerning the water-oil contact (pictures 32 to 35) which was initially set at the depth of 10300ft, both IMEX and GEM simulators provided similar results. The shallower depth of the water-oil contact, at the end of the simulation run using IMEX simulator, was calculated to be at the depth of 10000ft and was close to the producer 3, whereas the deepest point of the water-oil contact lied at the depth of 10212ft and was close to injector 4. On the other hand, the shallower depth of the water-oil contact that GEM simulator calculated was at 10049ft and was close to producer 3, whereas the deeper point of the water-oil contact was lying at the depth of 10212ft and was close to injector 4. As it was mentioned earlier, the rock underlying the reservoir was assumed by the simulator to be impermeable, as a result, the water was coming into the reservoir only from the sides of the anticlines and was moving towards the center of the reservoir. Due to this movement of the water-oil contact the production wells were not influenced all that fast by the contact.



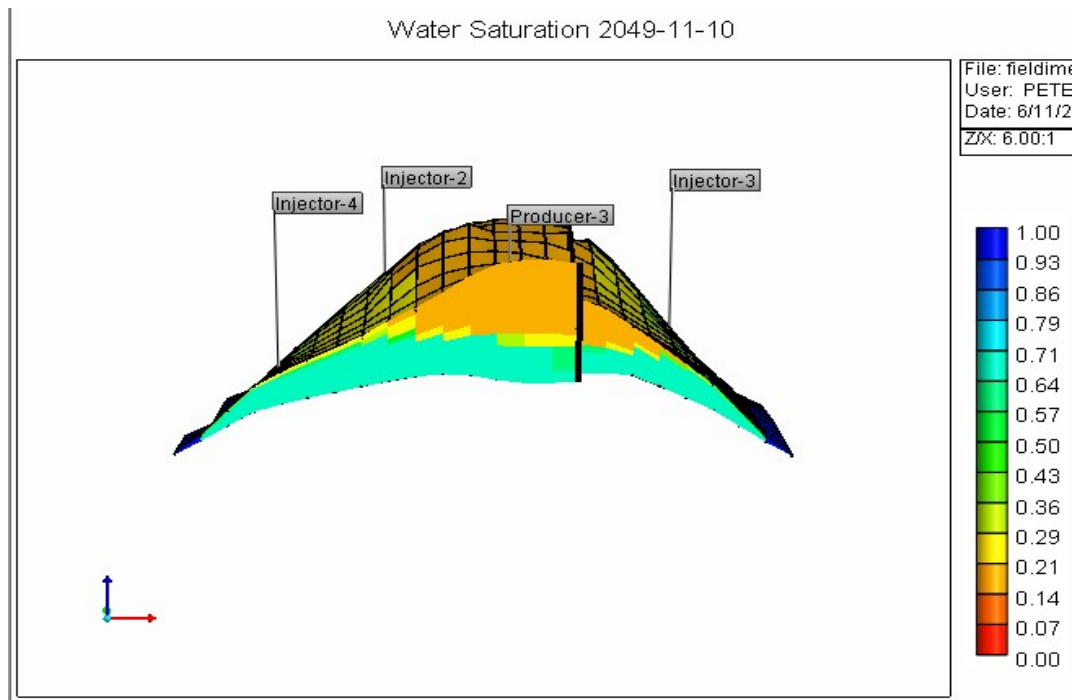
Picture 32: Water-oil contact (cut parallel to J axis) (GEM simulator)



Picture 33: Water-oil contact (cut parallel to I axis) (GEM simulator)

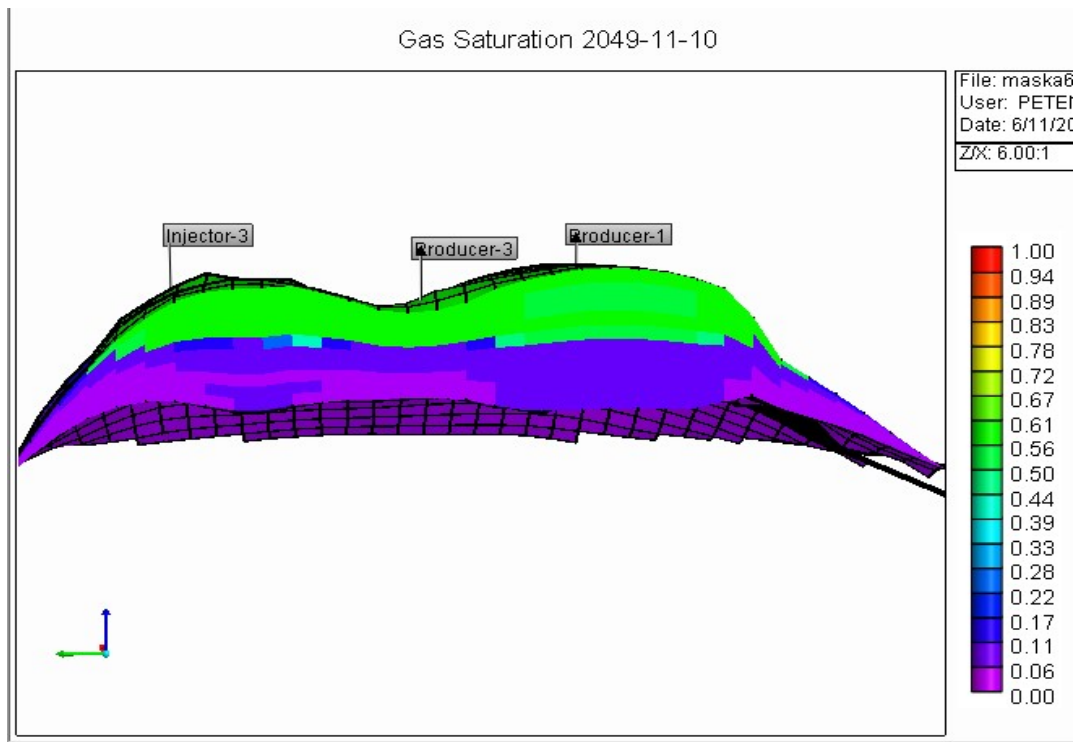


Picture 34: Water-oil contact (cut parallel to J axis) (IMEX simulator)

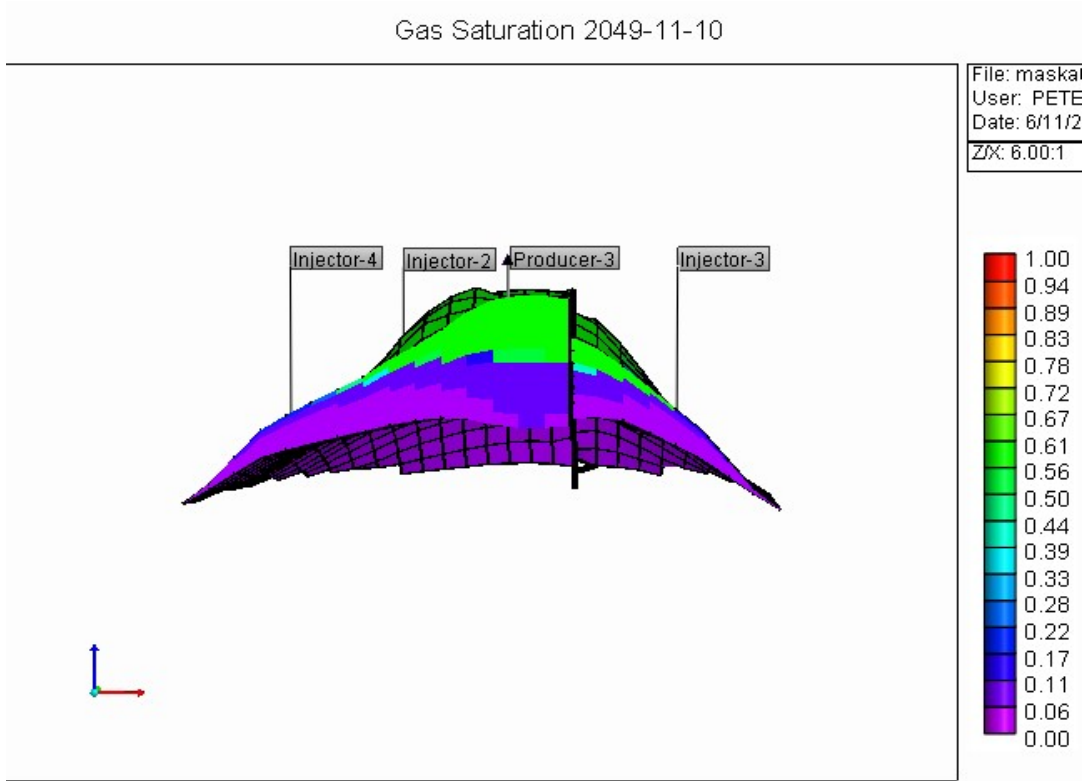


Picture 35: Water-oil contact (cut parallel to I axis) (IMEX simulator)

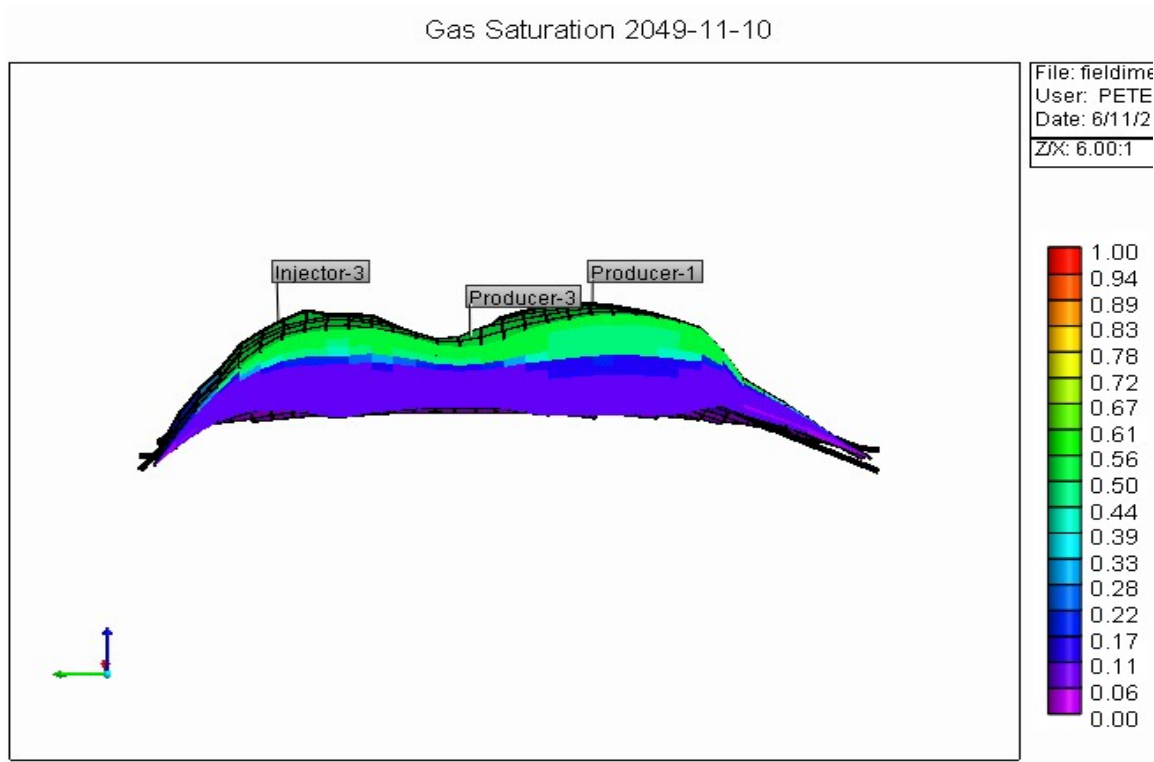
Concerning the gas-oil contact (pictures 36 to 39) GEM simulator calculated that the shallower depth of the gas-oil contact at the end of the production period was at 9970 ft and close to producer 2, whereas the highest depth that the gas-oil contact existed was at 10212 ft and close to injector 4. Similarly, IMEX simulator calculated that the shallower depth of the gas-oil contact was at 9898 ft and close to producer 2, whereas the highest depth that the gas-oil contact existed was at the 10300 ft and close to injector 4. The fact that both simulators calculated that the highest depth of the gas-oil contact was at 10212 ft and at 10300 ft respectively is explained by the numerical dispersion in combination with the low vertical permeability of the first geological layer and was more intense for IMEX simulator.



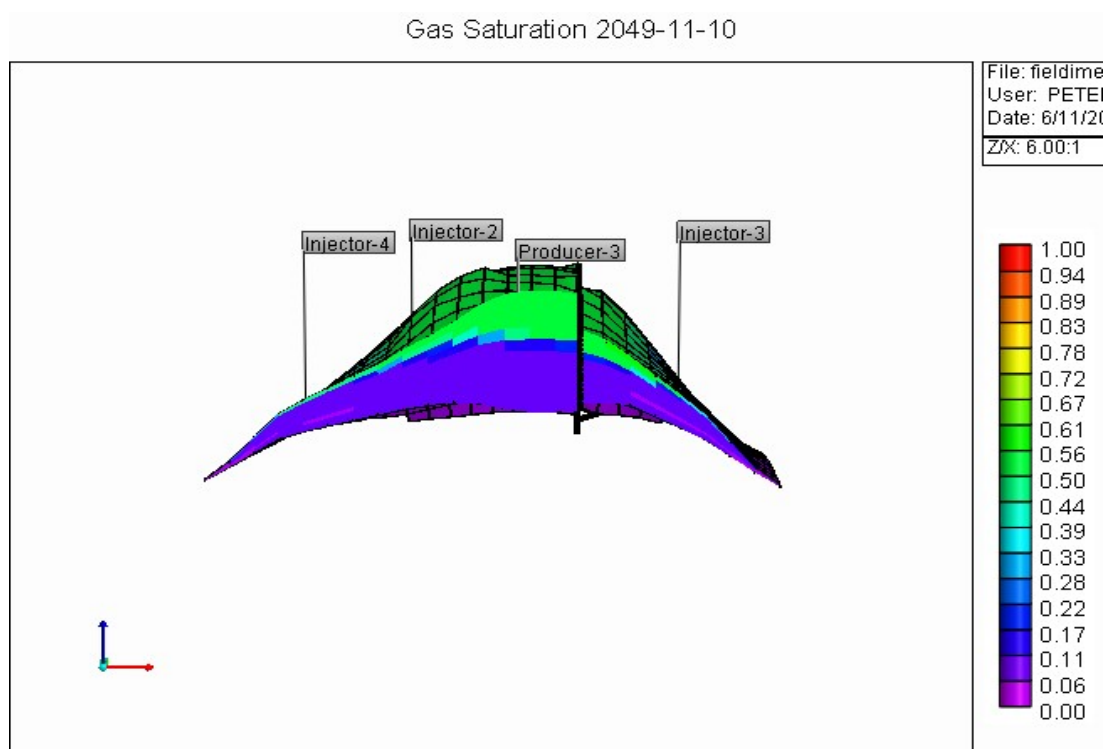
Picture 36: Gas-oil contact (cut parallel to J axis) (GEM simulator)



Picture 37: Gas-oil contact (cut parallel to I axis) (GEM simulator)



Picture 38: Gas-oil contact (cut parallel to J axis) (IMEX simulator)



Picture 39: Gas-oil contact (cut parallel to I axis) (IMEX simulator)

Finally, both simulators, did not encounter convergence problems throughout the simulation study. As it can be seen from Table 21, IMEX simulator ran faster than GEM, something that was expected since it is a black oil simulator.

	GEM	IMEX	Difference GEM- IMEX	CPU Percentage difference GEM- IMEX (%)
CPU time (sec)	1704.578	806.47	898.108	52.68
Elapsed time (sec)	1791.297	842.16	949.137	52.98

Table 21: CPU and elapsed time that GEM and IMEX simulators needed to perform the simulation study

Summarizing all the above we end up to the following conclusions:

- GEM simulator is thought to be more accurate whereas IMEX over predicted production of the oil and gas phases
- GEM simulator needed almost double the time to perform the simulation than IMEX
- IMEX simulator predictions deviated from GEM's with the volatile oil even though modified black oil Tables were used
- GEM simulator calculated that a larger initial pore volume by 5.55% is occupied by the hydrocarbons than IMEX simulator did
- The different decline of the pressure and the small pressure reduction rates influenced the time that the reservoir pressure fall below the bubble point pressure as GEM simulator predicted that the reservoir pressure will fall below bubble point a decade earlier than IMEX
- The difference between the two simulators in the pressure reduction rates along with the small pressure reduction influenced the production performance of the reservoir as the reservoir produced for a longer time period below the bubble point pressure
- GEM simulator predicted slightly less oil (4.25%) and gas (6.7%) recovery in comparison to the IMEX simulator
- The two simulators exhibited a great difference in the prediction of the water production (95.97%), with GEM simulator to predict that less water will be produced as GEM predicted lower reservoir pressures than IMEX and as a result the two of the three production wells switched their primary operating constraint to bottom hole pressure and shut in due to the low production rate and not to water cut as IMEX predicted
- The percentage recovery of oil for the same years of production using the GEM simulator was slightly less (4.97%)
- IMEX simulator predicted that producer 2 could produce for almost five years more with its plateau production than GEM did, as in GEM simulator this well switched to the bottom hole pressure constraint due to the fact that the reservoir pressure was that low that this constraint was violated
- In both simulators, the part of the reservoir to the left hand side of the fault exhibited higher residual volumes, lower recovery factors and higher gas residual saturation compared to the reservoir part to right hand side of the fault

- Numerical dispersion in combination with the low vertical permeability of the first geological layer resulted to a gas cap that extended deeply in the reservoir
- Problems were encountered for the identification of the single phase fluid as its density was closer to the gas density

Finally, taking into consideration the above conclusions, IMEX simulator is proposed for the simulation runs as its deviation from GEM was small and the simulation time was short. However, the operator has to keep in mind that IMEX tends to slightly over predict the production of oil and gas and be more sensitive to numerical dispersion.

APPENDIX A

Appendix C, is constituted by Tables presenting the differences in reserves, residual volumes and saturations and recovery factors between the left and the right hand side part of the fault, parts of the reservoir.

		GEM		IMEX		Difference LHS GEM-IMEX	Percentage difference LHS GEM-IMEX	Difference RHS GEM-IMEX	Percentage difference RHS GEM-IMEX
		Left Hand Side of the fault	Right Hand Side of the fault	Left Hand Side of the fault	Right Hand Side of the fault				
Originally in Place									
Stock Tank Oil	M STB	63074	11437	62648	11353	426	0.6753971526	84	0.734458337
Gas at Surface	MM SCF	2.25E+005	40779	224241	40638	655	0.2912457314	141	0.3457662032
Water at Surface	M STB	50254	9701.9	47453	9171	2801	5.5736856768	530.9	5.4721240169

A1: Initial volumes in place as they were calculated by GEM and IMEX simulators for the left and the right hand side of

		GEM		IMEX		Difference LHS GEM-IMEX	Percentage difference LHS GEM-IMEX	Difference RHS GEM-IMEX	Percentage difference RHS GEM-IMEX
		Left Hand Side of the fault	Right Hand Side of the fault	Left Hand Side of the fault	Right Hand Side of the fault				
Currently in Place									
Stock Tank Oil	M STB	43349	7404	42234	6975.7	1115	2.572146993	428.3	5.784710967
Gas at Surface	MM SCF	1.59E+005	24858	152791	24529	6664	4.179235521	329	1.3235175799
Water at Surface	M STB	1.02E+005	22245	99474	21107	2235	2.1974456538	1138	5.1157563497
Recovery Factor									
Oil	%	20.95	92.159	23.229	89.951	-2.279	-9.8110120969	2.208	2.3958593301
Gas	%	20.293	88.458	22.851	179.99	-2.558	-11.194258457	-91.532	-50.8539363298
Water	%	-99.6	-143.5	-105.46	-151.72	5.86	-5.5566091409	8.22	-5.417875033
Average Saturation									
Oil	%	30.106	31.049	34.142	31.795	-4.036	-11.8212172691	-0.746	-2.3462808618
Gas	%	27.668	18.52	20.847	16.507	6.821	24.6530287697	2.013	10.8693304536
Water	%	42.226	50.431	45.011	51.699	-2.785	-6.1873764191	-1.268	-2.4526586588

the reservoir

A2: Residual volumes and saturations and recovery factors as they were calculated by GEM and IMEX simulators for the left and the right hand side of the reservoir

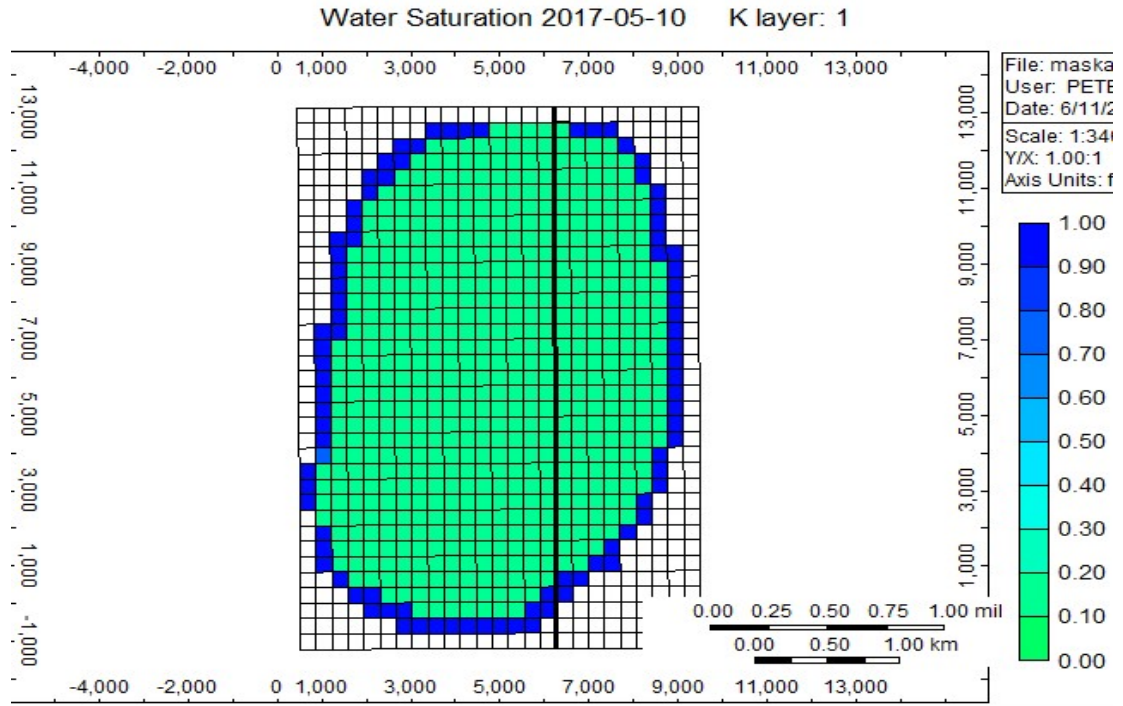
Average Saturation % (GEM)	LAYER 1	LAYER 2	LAYER 3	LAYER 4	LAYER 5	LAYER 6	LAYER 7	LAYER 8	LAYER 9	LAYER 10
Oil	23.358	25.248	27.095	29.991	44.46	57.07	48.468	32.651	28.703	26.851
Gas	57.48	46.075	42.715	38.712	22.655	6.89471	6.0211	5.54236	5.57952	5.42857
Water	25.894	28.677	30.19	31.297	32.885	36.035	45.511	61.807	65.718	67.721
Average Saturation % (IMEX)										
Oil	26.387	28.388	31.303	41.438	52.169	46.94	37.47	28.722	27.343	26.666
Gas	50.262	42.331	37.321	25.462	11.162	8.7747	7.3561	6.1992	6.5228	6.337
Water	23.351	29.281	31.376	33.101	36.67	44.285	55.174	65.079	66.134	66.997
Percentage difference GEM-IMEX										
Oil	-3.029	-3.14	-4.208	-11.447	-7.709	10.13	10.998	3.929	1.36	0.185
Gas	7.218	3.744	5.394	13.25	11.493	-1.87999	-1.335	-0.65684	-0.94328	-0.90843
Water	2.543	-0.604	-1.186	-1.804	-3.785	-8.25	-9.663	-3.272	-0.416	0.724

A3: Residual saturations of each block layer

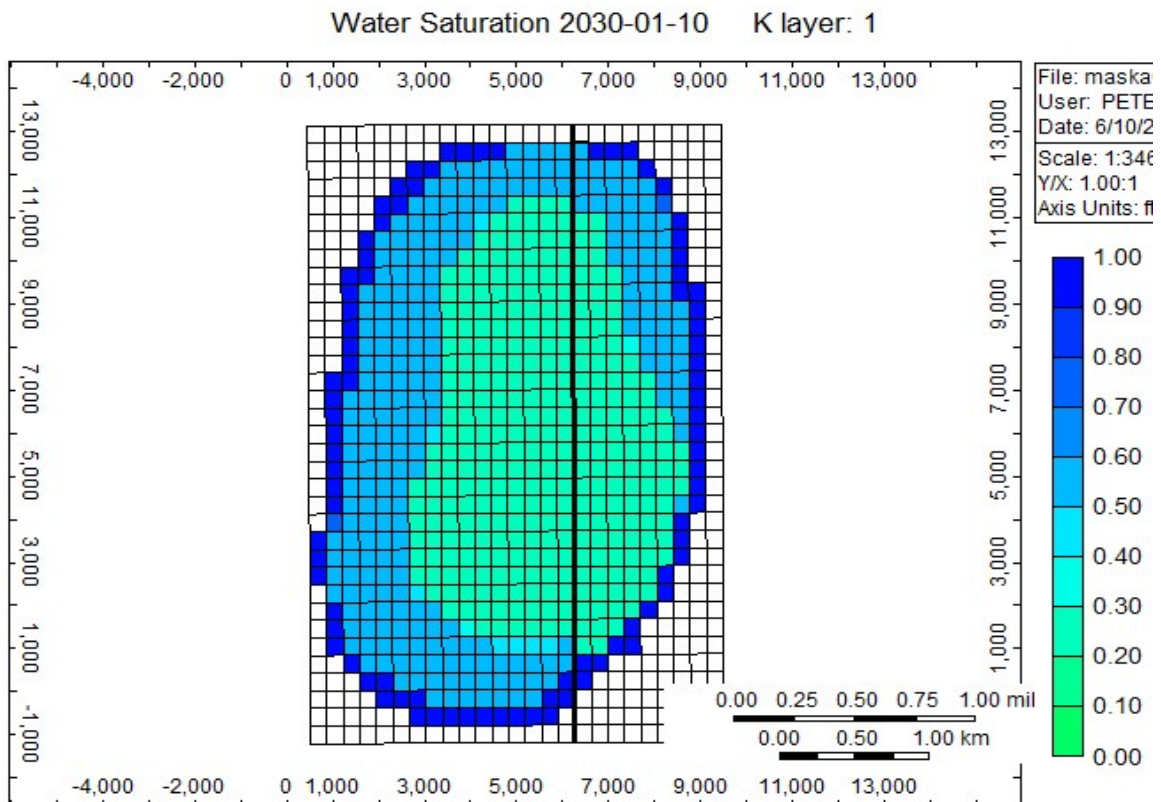
APPENDIX B

The Appendix B is consisted by captures of three representative block layers in order to present the sweep efficiency of the water flooding as it was predicted by GEM simulator.

Block layer 1

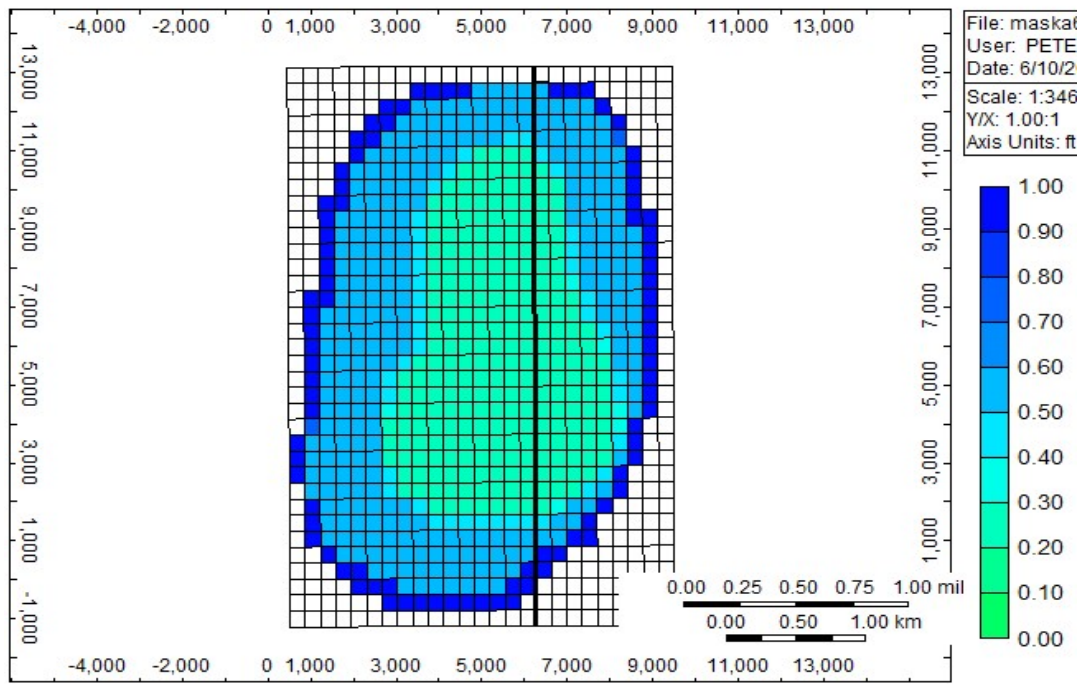


B1: Water saturation of the block layer 1 at 2017



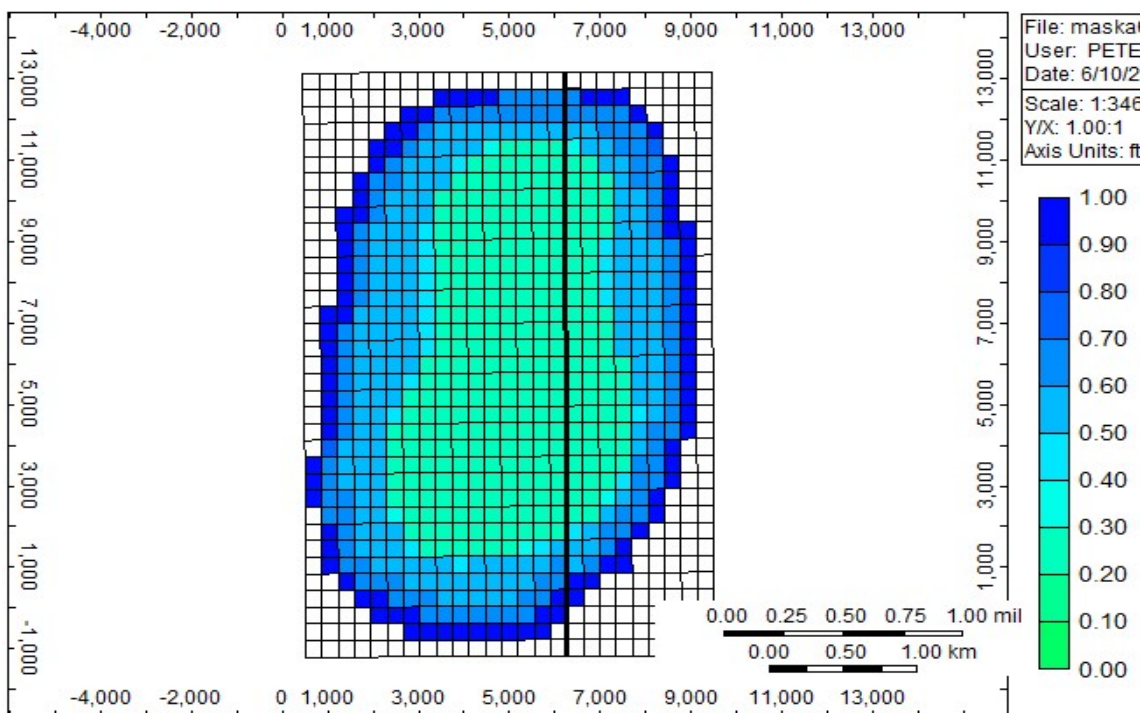
B2: Water saturation of the block layer 1 at 2030

Water Saturation 2040-01-10 K layer: 1



B3: Water saturation of the block layer 1 at 2040

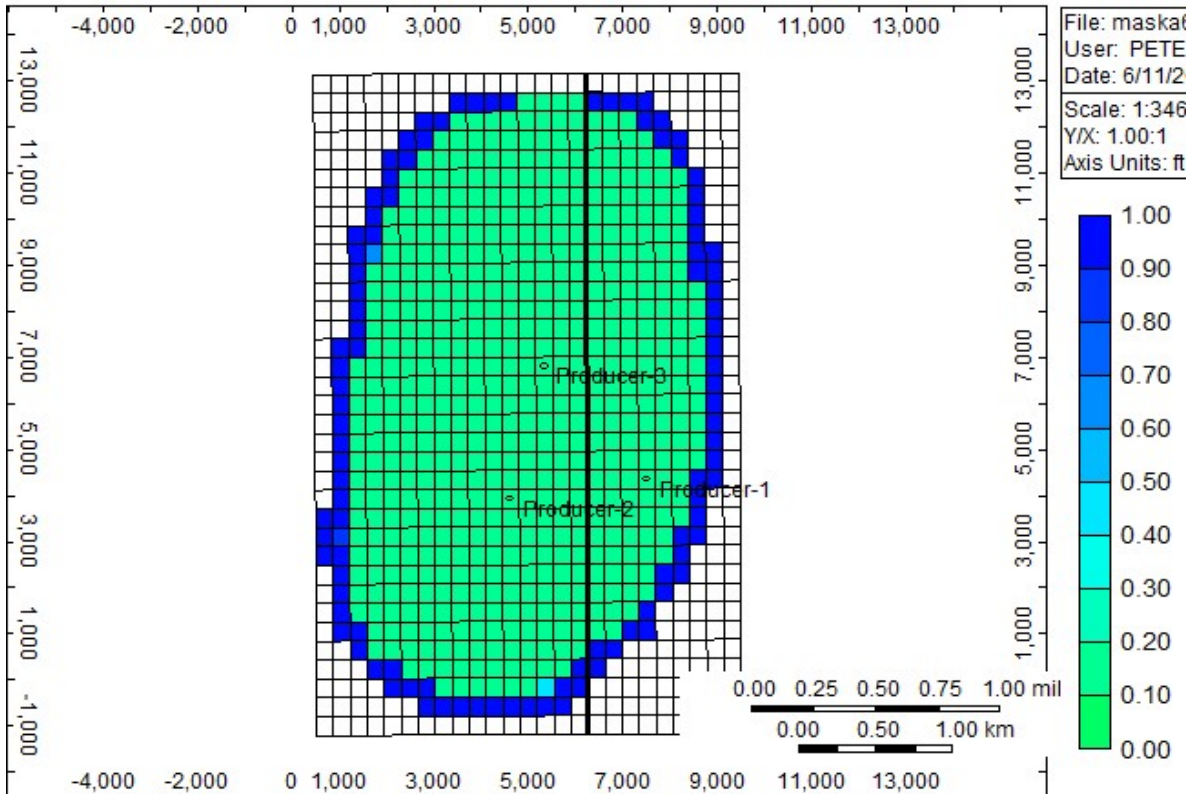
Water Saturation 2049-12-10 K layer: 1



B4: Water saturation of the block layer 1 at 2049

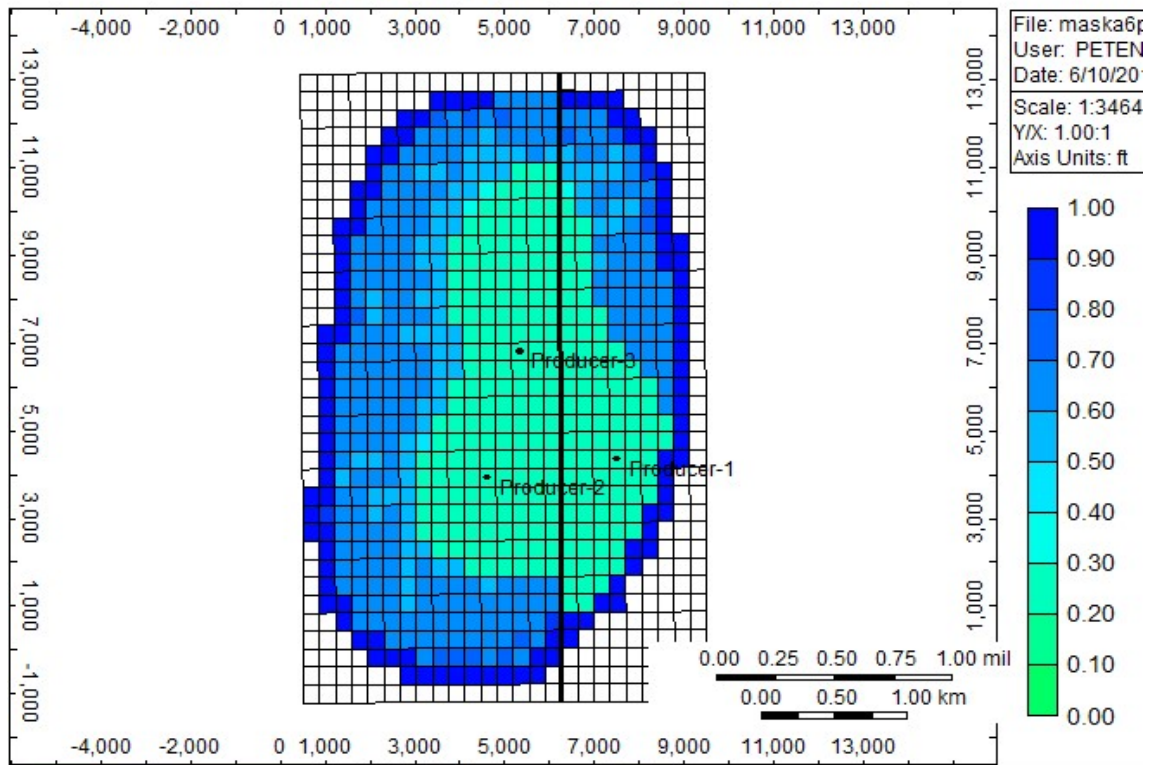
Block layer 5

Water Saturation 2017-05-10 K layer: 5

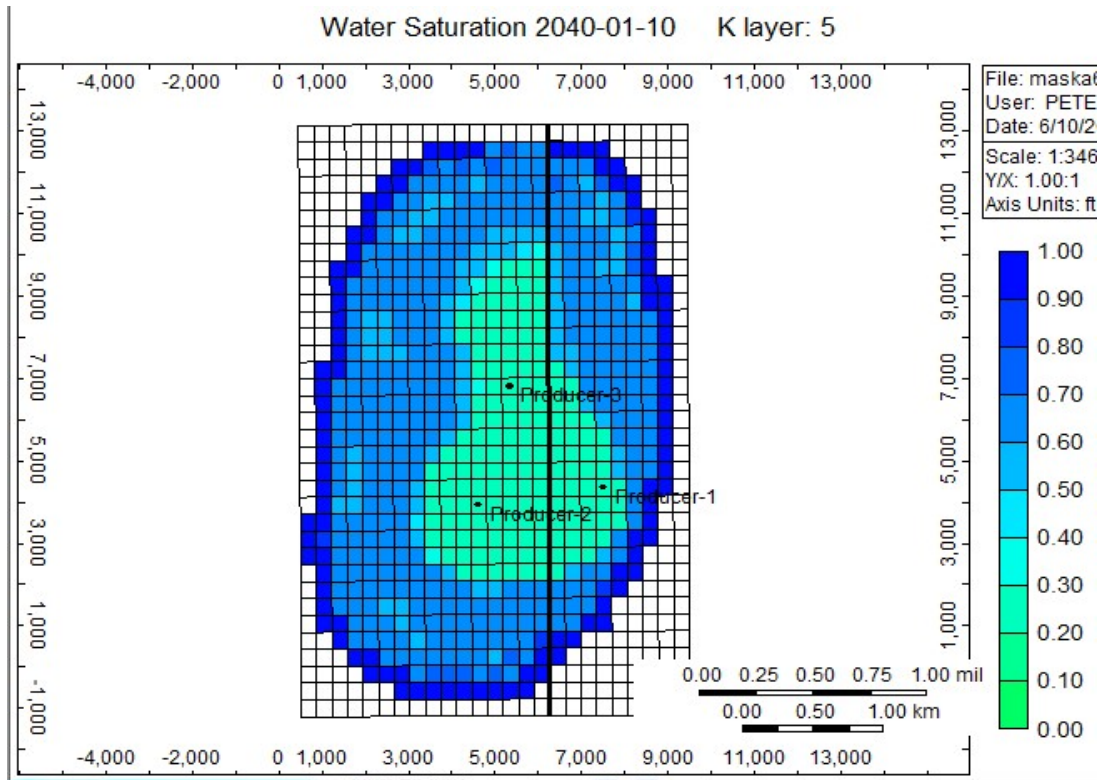


B5: Water saturation of the block layer 5 at 2017

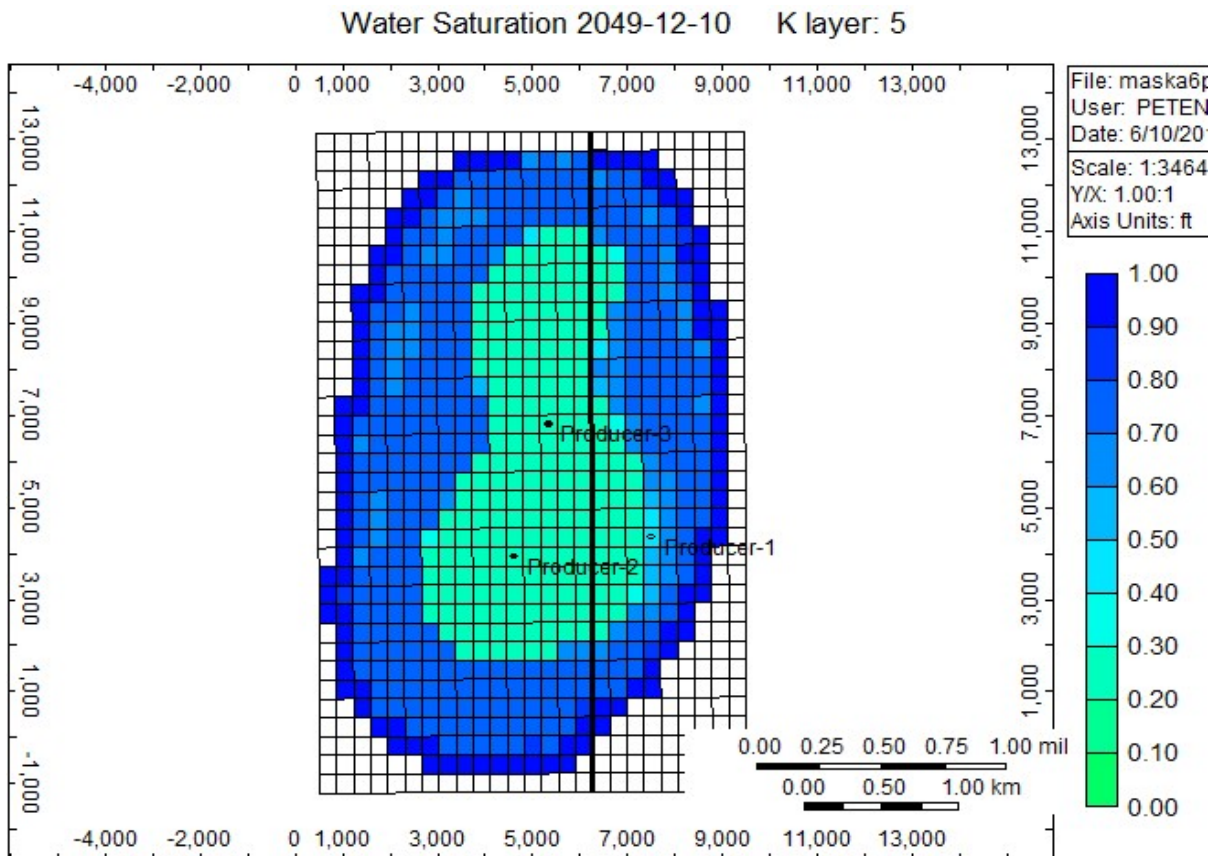
Water Saturation 2030-01-10 K layer: 5



B6: Water saturation of the block layer 5 at 2030



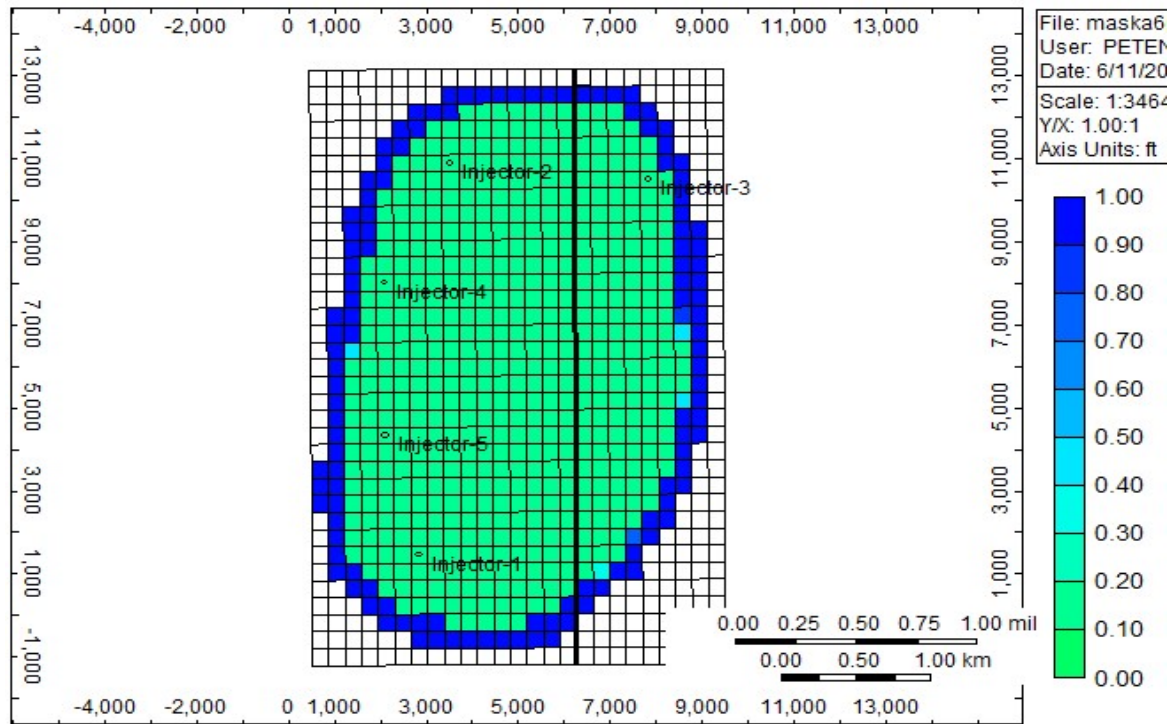
B7: Water saturation of the block layer 5 at 2040



B8: Water saturation of the block layer 5 at 2049

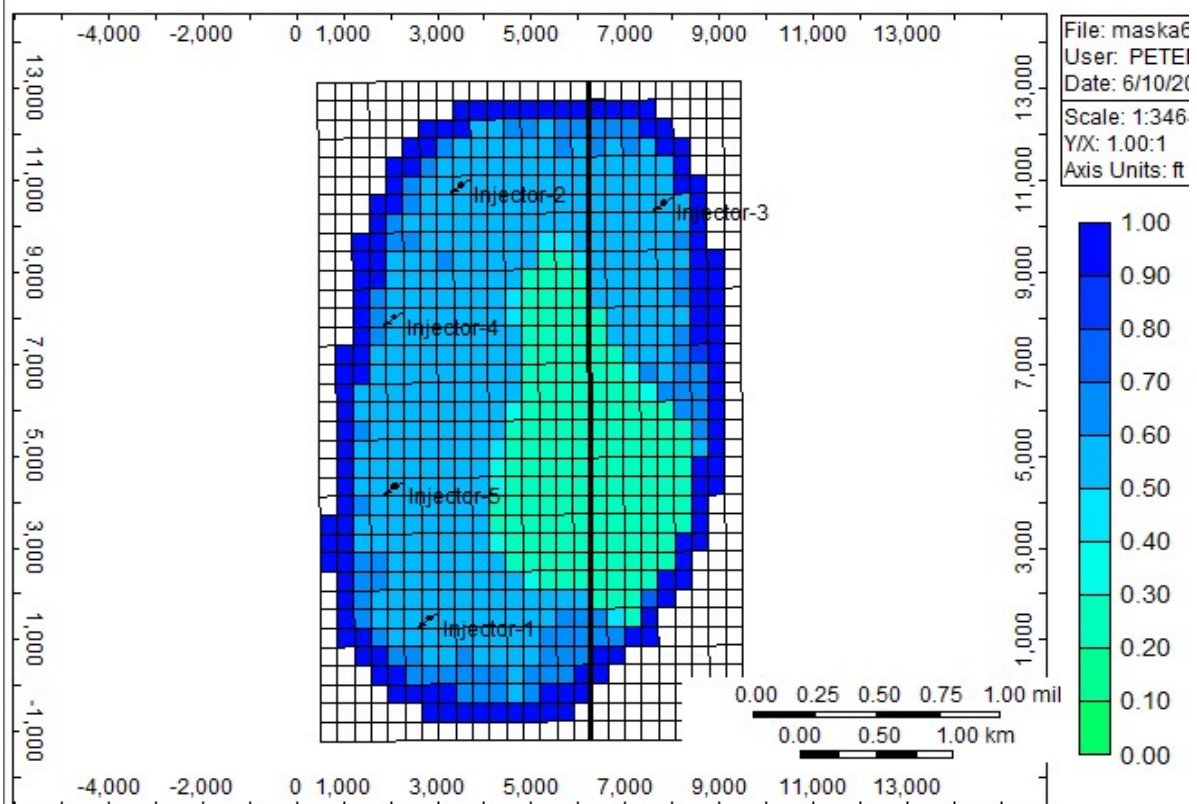
Block layer 10

Water Saturation 2017-05-10 K layer: 10



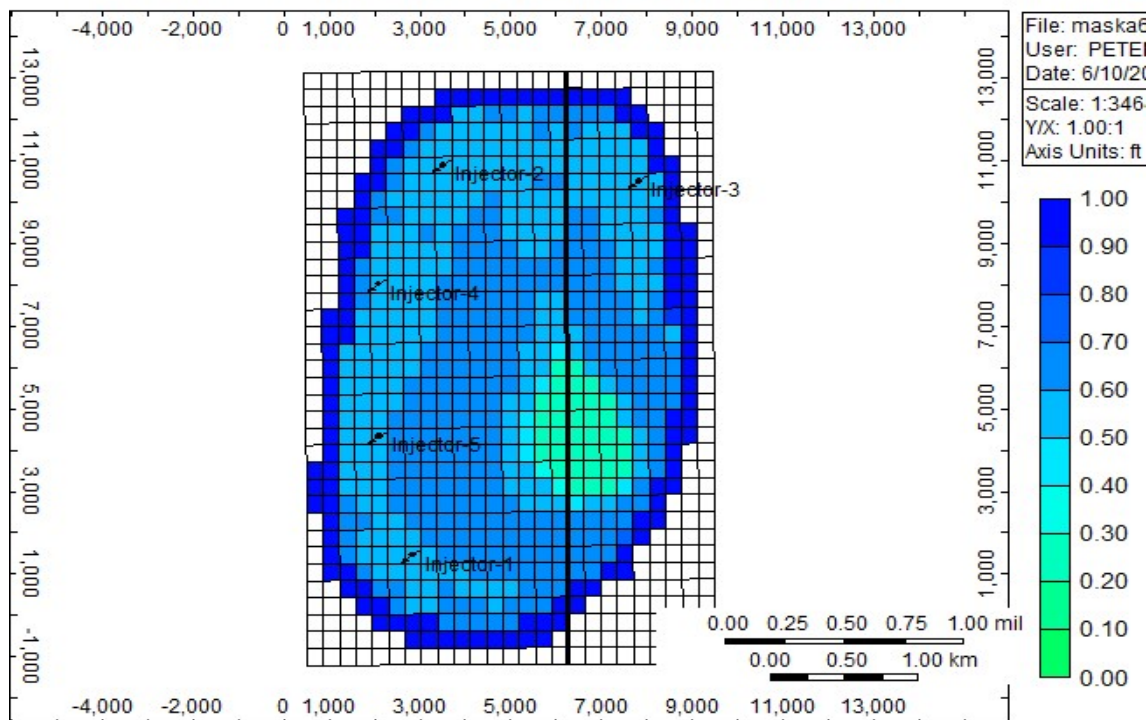
B9: Water saturation of the block layer 10 at 2017

Water Saturation 2030-01-10 K layer: 10



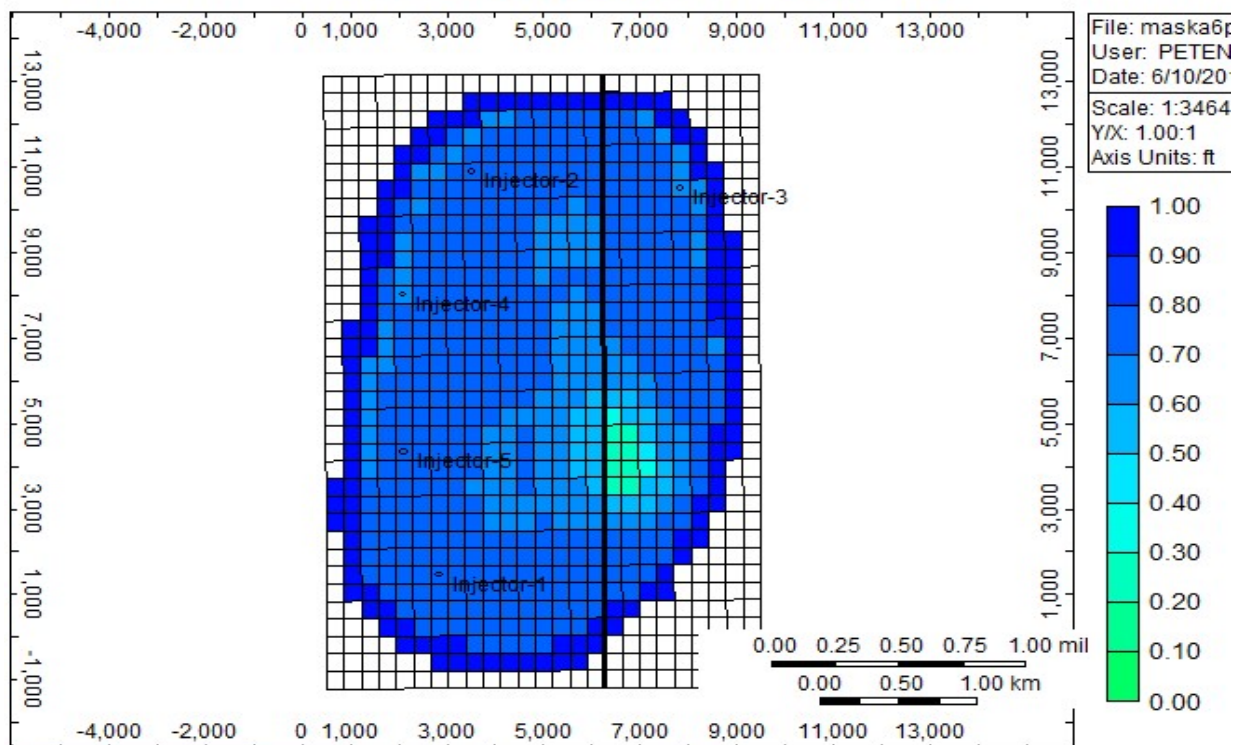
B10: Water saturation of the block layer 10 at 2030

Water Saturation 2040-01-10 K layer: 10



B11: Water saturation of the block layer 10 at 2040

Water Saturation 2049-11-10 K layer: 10

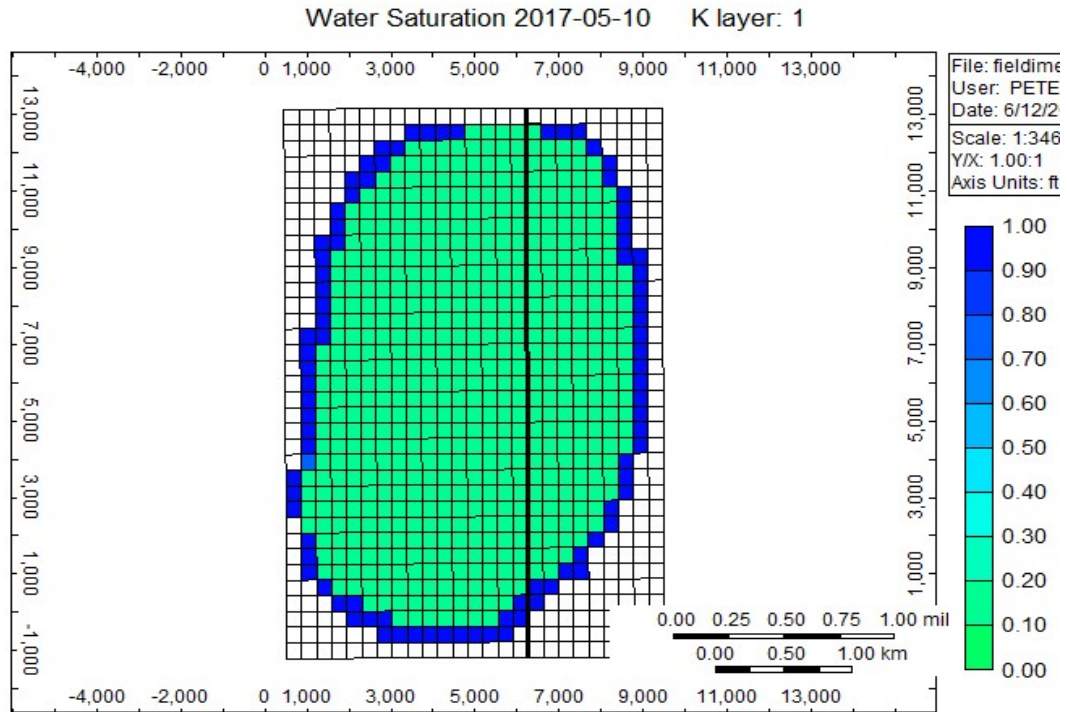


B12: Water saturation of the block layer 10 at 2049

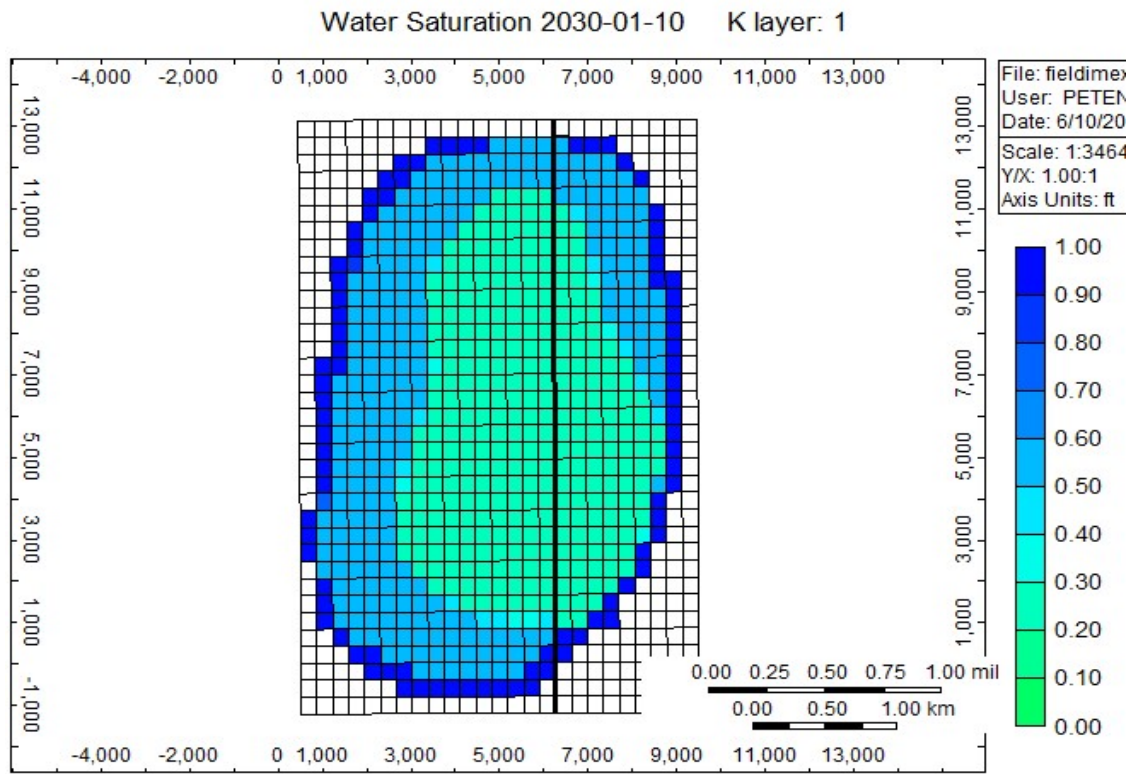
APPENDIX C

The Appendix C consists by captures of three representative block layers in order to present the sweep efficiency of the water flooding as it was predicted by IMEX simulator.

Block layer 1

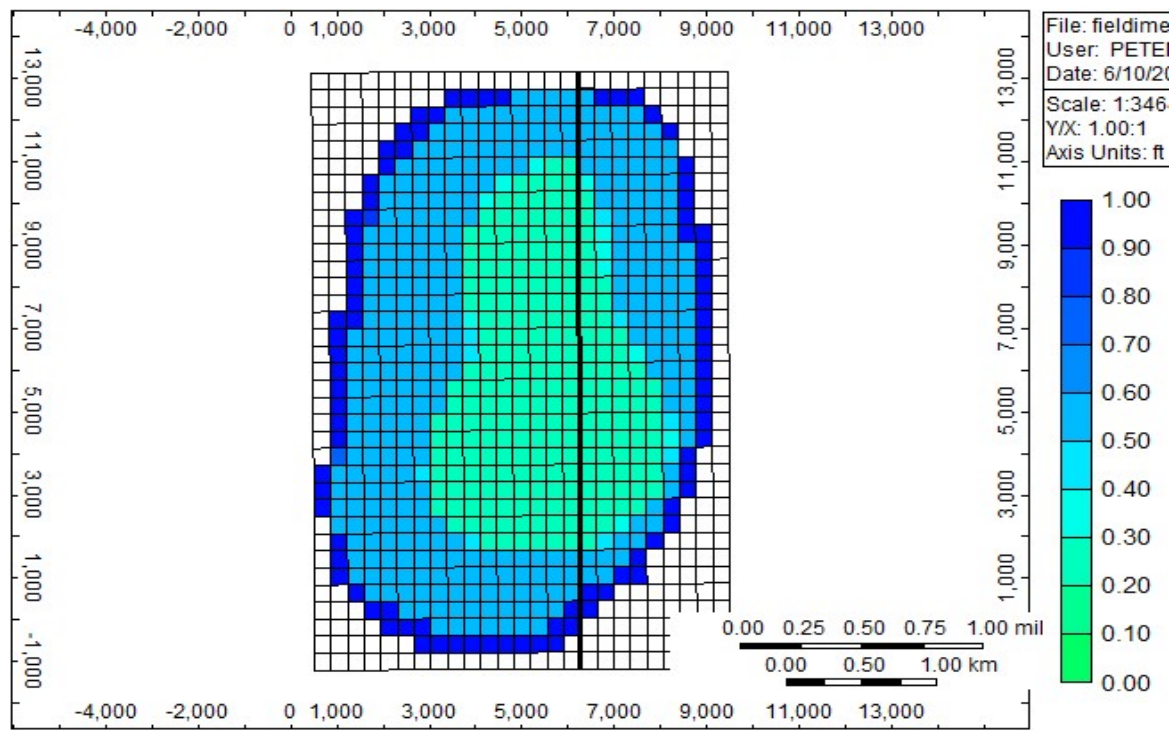


C1: Water saturation of the block layer 1 at 2017



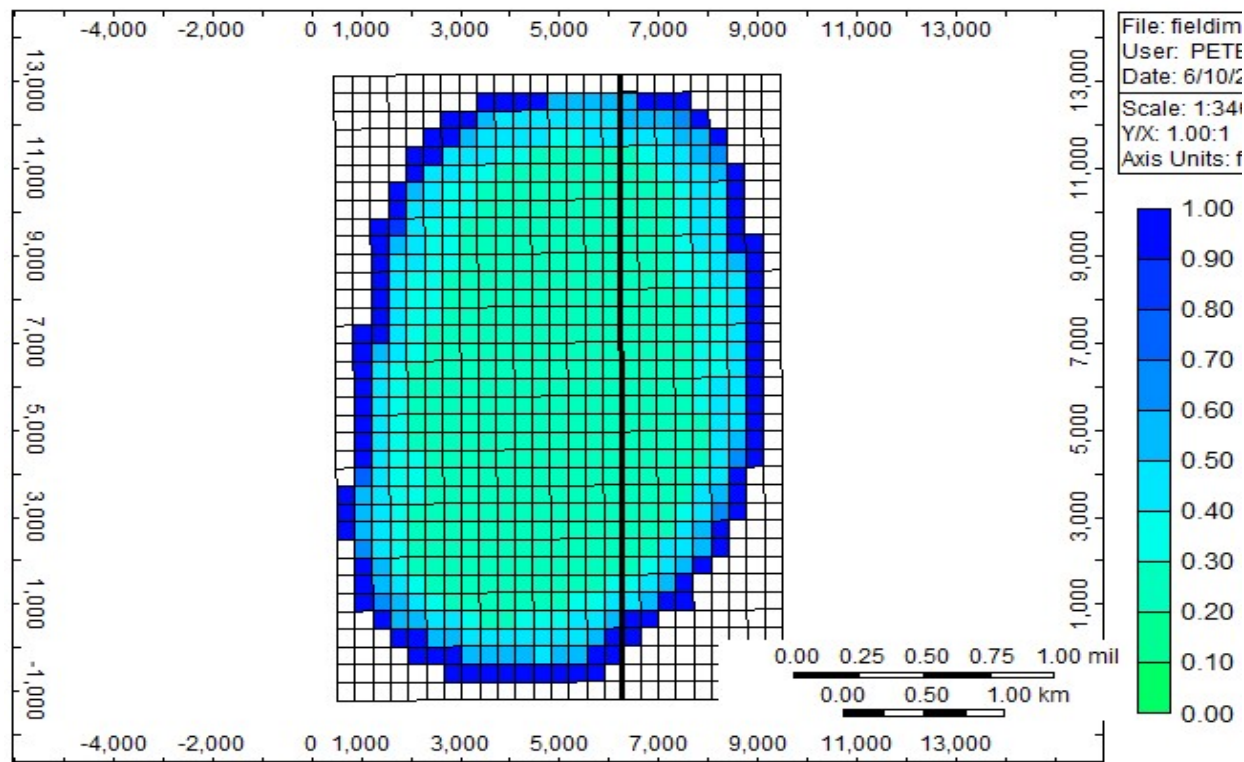
C2: Water saturation of the block layer 1 at 2030

Water Saturation 2040-01-10 K layer: 1



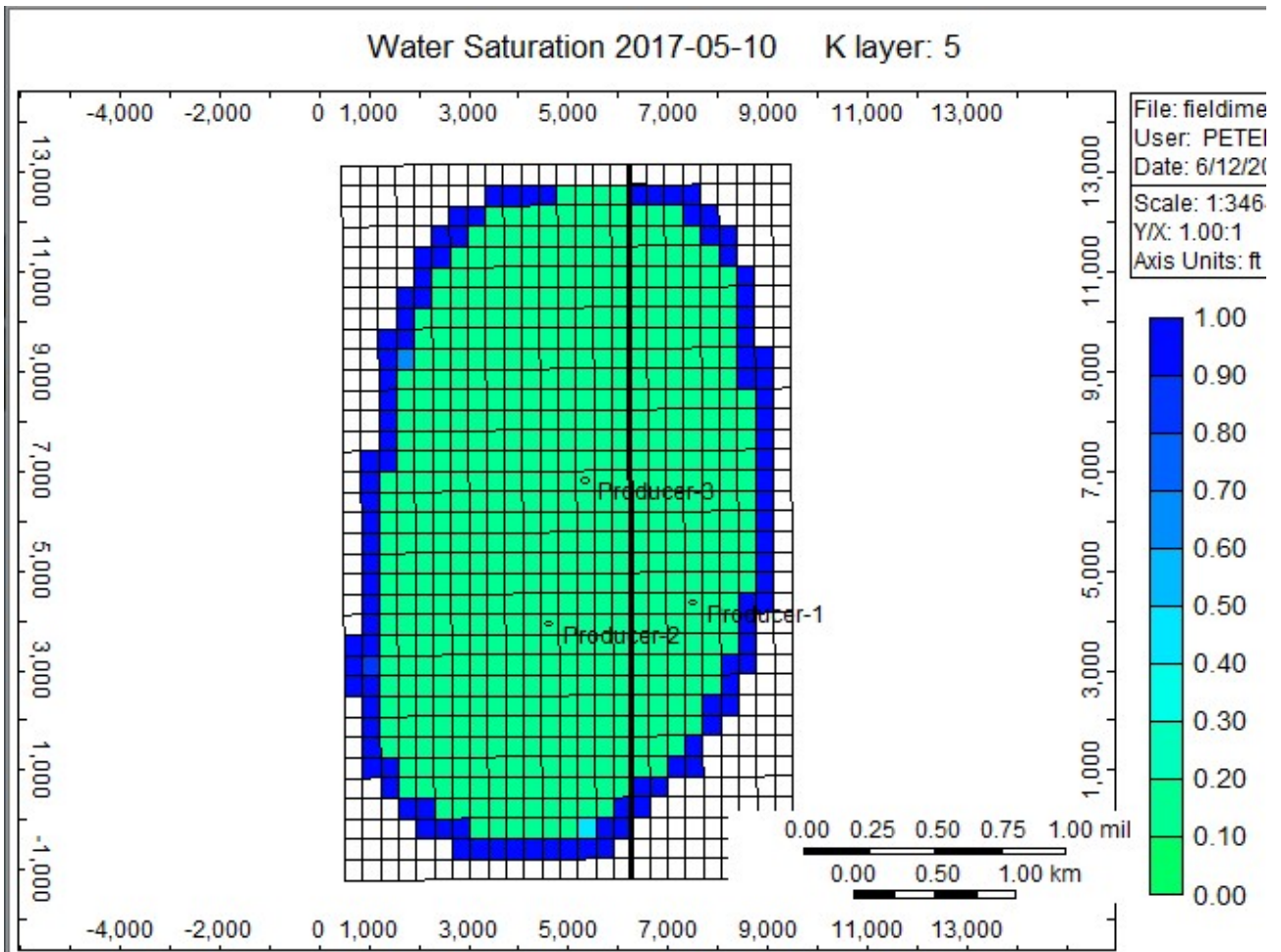
C3: Water saturation of the block layer 1 at 2040

Water Saturation 2049-12-10 K layer: 1

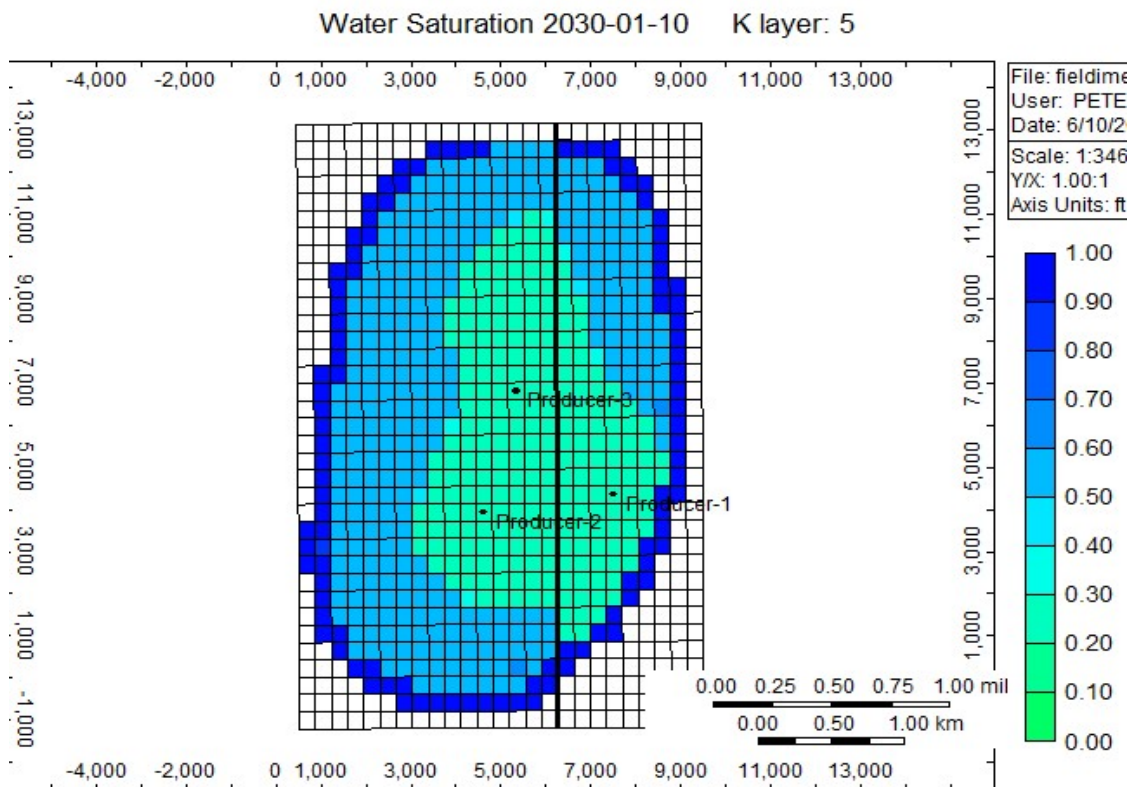


C4: Water saturation of the block layer 1 at 2049

Block layer 5

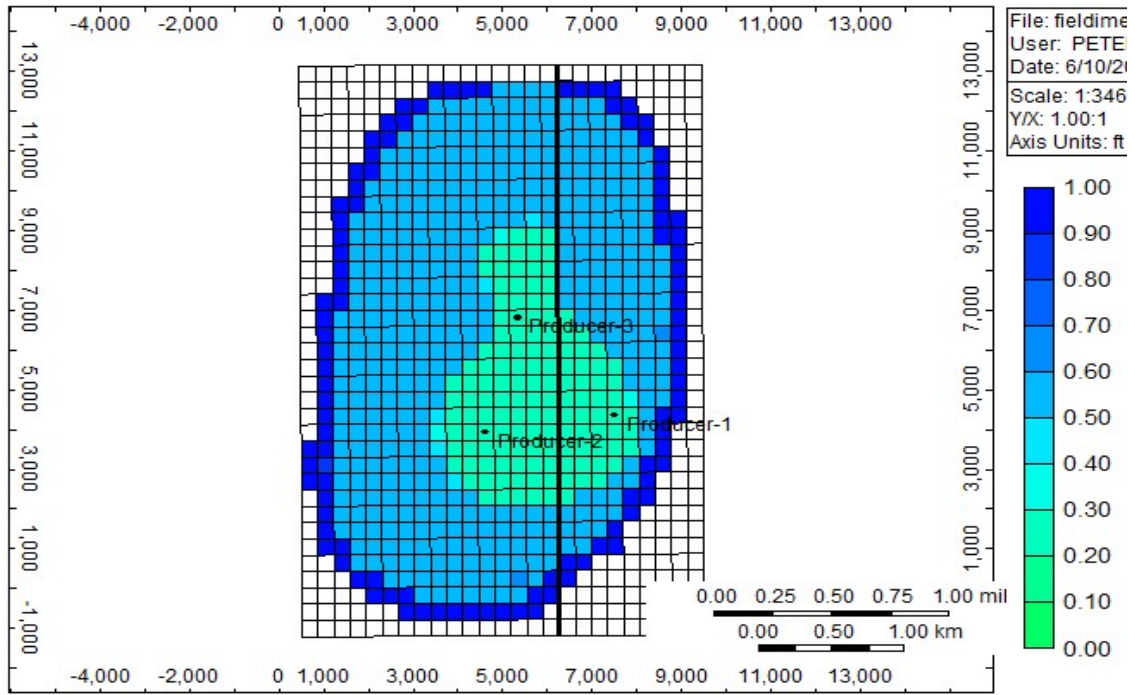


C5: Water saturation of the block layer 5 at 2017



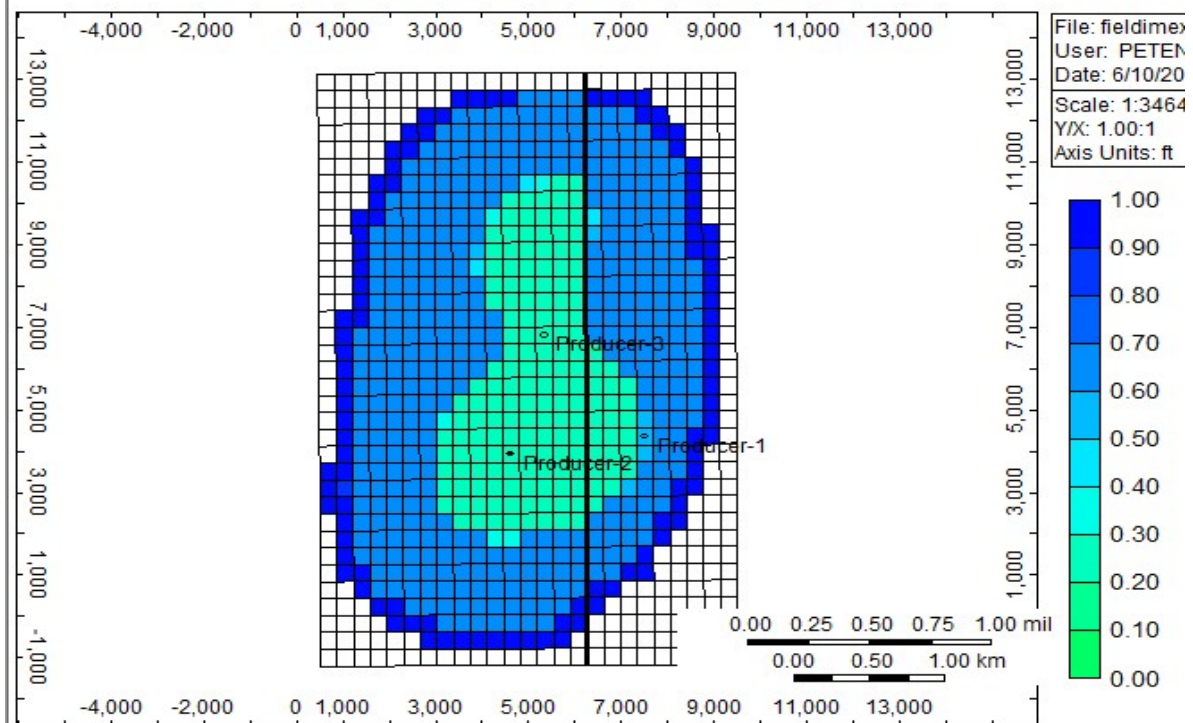
C6: Water saturation of the block layer 5 at 2030

Water Saturation 2040-01-10 K layer: 5



C7: Water saturation of the block layer 5 at 2040

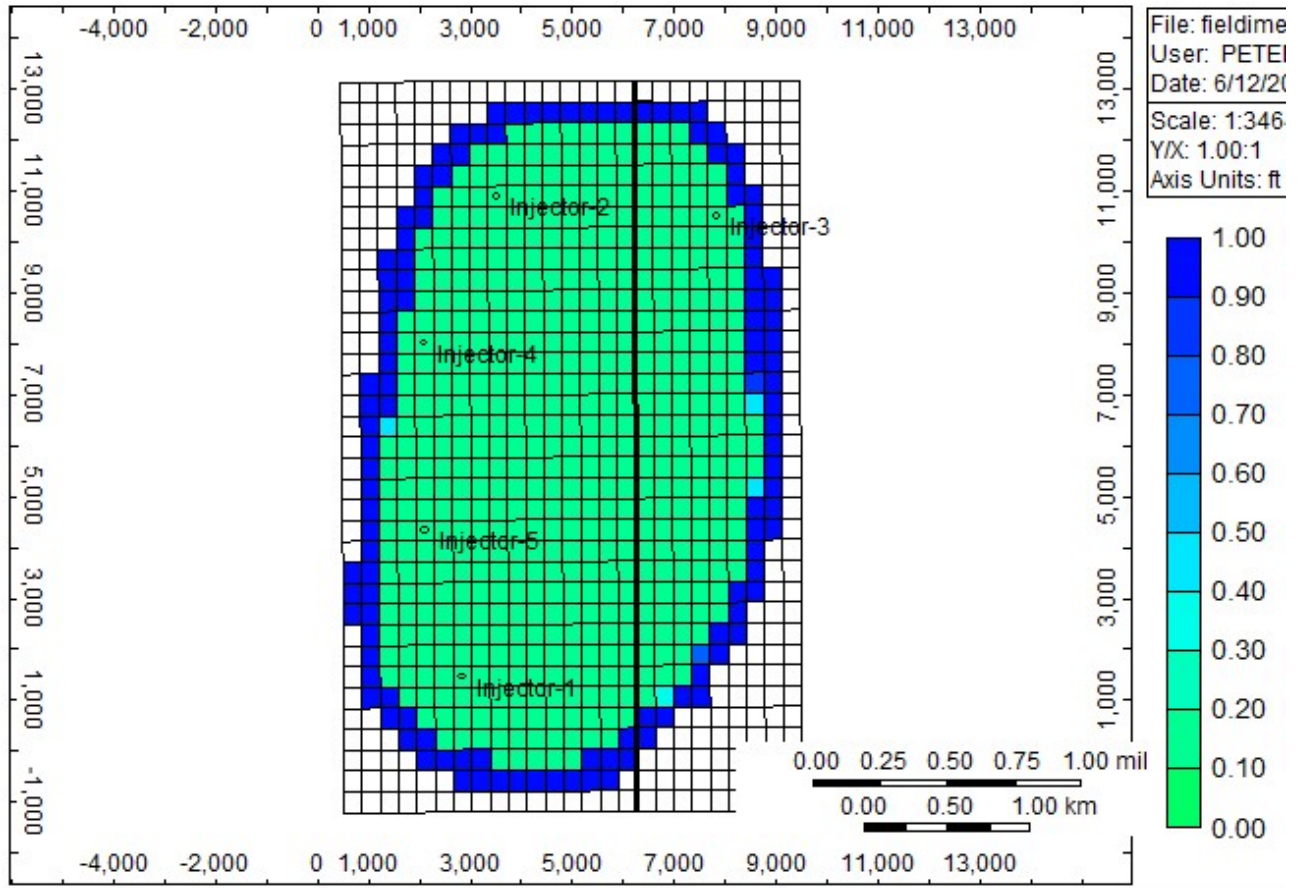
Water Saturation 2049-12-10 K layer: 5



C8: Water saturation of the block layer 5 at 2049

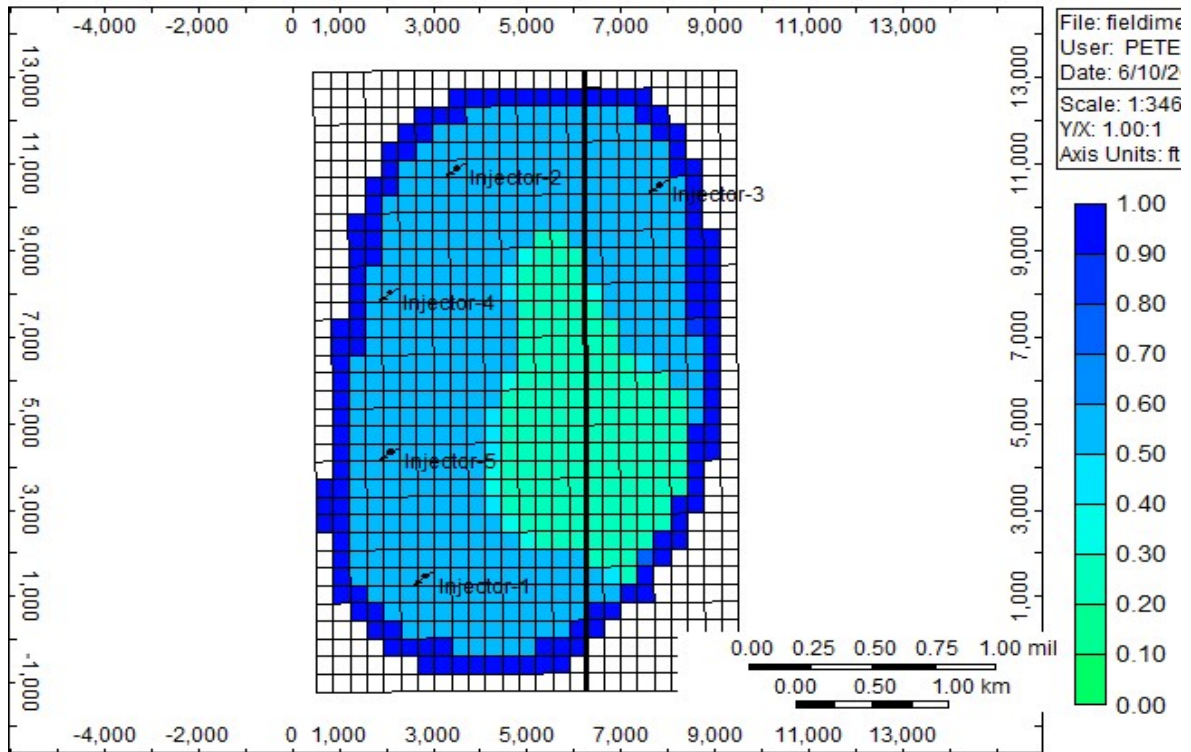
Block layer 10

Water Saturation 2017-05-10 K layer: 10



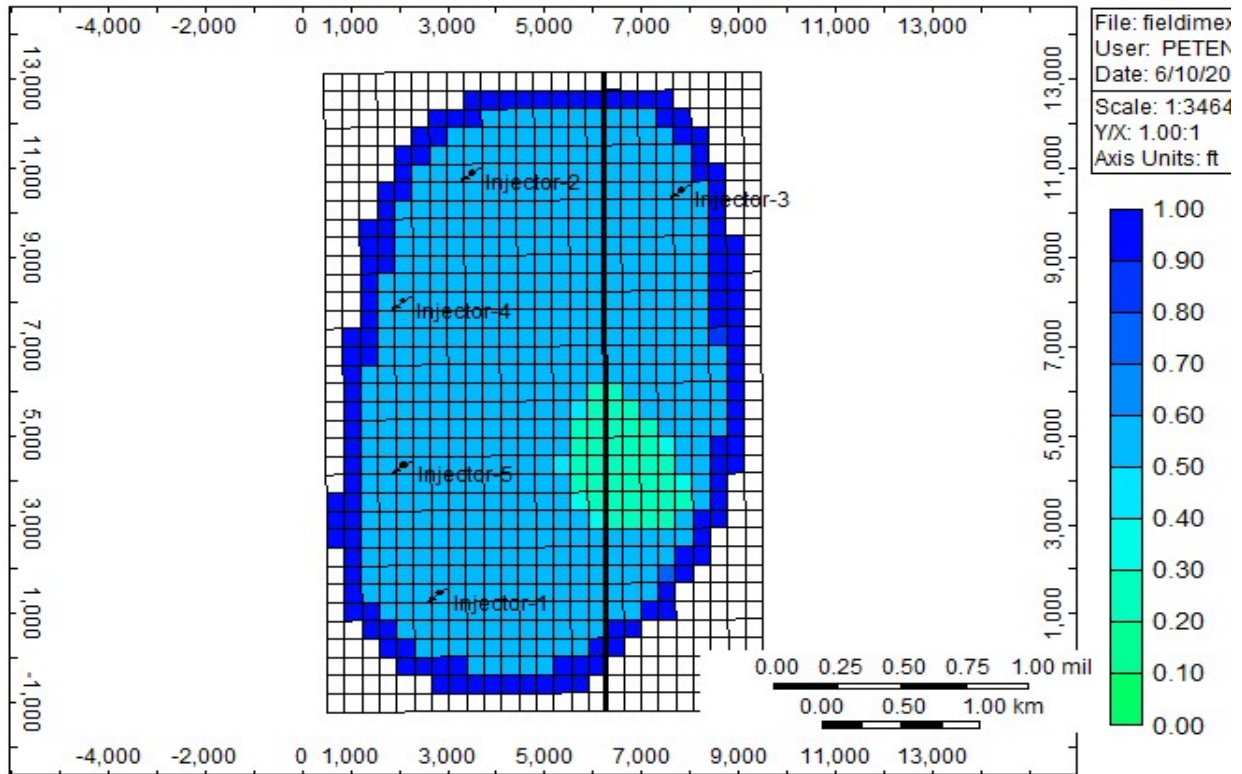
C9: Water saturation of the block layer 10 at 2017

Water Saturation 2030-01-10 K layer: 10



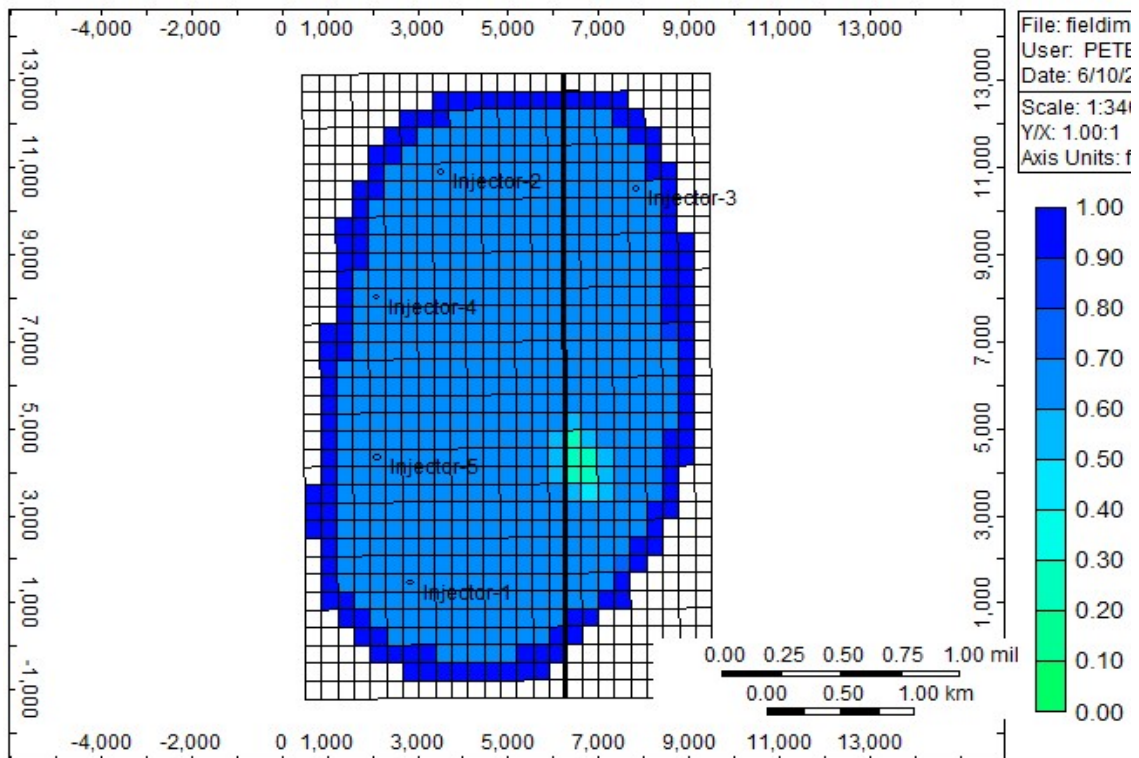
C10: Water saturation of the block layer 10 at 2030

Water Saturation 2040-01-10 K layer: 10



C11: Water saturation of the block layer 10 at 2040

Water Saturation 2049-12-10 K layer: 10



C12: Water saturation of the block layer 10 at 2049

14. REFERENCES

- AAPG, W. (2016). reservoir simulation study. Retrieved from http://wiki.aapg.org/Reservoir_simulation_study
- Abdallah, W., Buckley, J. S., Carnegie, A., Edwards, J., Herold, B., Fordham, E., ... Ziauddin, M. (2007). Fundamentals of Wettability. *Oilfield Review*, 44–61. Retrieved from https://www.slb.com/~media/Files/resources/oilfield_review/ors07/sum07/p44_61.pdf
- Abdou, M. K., Pham, H. D., & Al-Aqeel, A. S. (1993). Impact of Grid Selection on Reservoir Simulation. *Journal of Petroleum Technology*, 45(7), 664–669. <https://doi.org/10.2118/21391-PA>
- Abdus Satter, Ghulam M. Iqbal, J. L. B. (2007). *Practical Enhanced Reservoir Engineering: Assisted with Simulation Software*.
- Adewumi. (2016a). Peng-Robinson EOS (1976). Retrieved from https://www.e-education.psu.edu/png520/m11_p2.html
- Adewumi. (2016b). Viscosity. Retrieved from https://www.e-education.psu.edu/png520/m19_p4.html
- Ahmed, T. P. (2010). *Reservoir Engineering Handbook, Fourth Edition*.
- Al-Shaalan, T., Fung, L., & Dogru, A. (2003). A Scalable Massively Parallel Dual-Porosity Dual-Permeability Simulator for Fractured Reservoirs with Super-K Permeability. *Proceedings of SPE Annual Technical Conference and Exhibition*. <https://doi.org/10.2523/84371-MS>
- Amiry, M. T. (2014). Modeling Flow Behavior in Naturally Fractured Reservoirs, (February). Retrieved from https://online.unileoben.ac.at/mu_online/voe_main2.showMask?pOrg=1&pPersonNr=0&pCurrPk=33580&pVtKbz=HFB&pStatus=A&pSiteNr=1004600
- Armenta, M., & Wojtanowicz, A. K. (2003). Rediscovering Non-Darcy Flow Effect In Gas Reservoir. *SPE Annual Technical Conference and Exhibition*, 1–8. <https://doi.org/10.2118/84071-MS>
- Autodesk. (2017). Duncan-Chang Theoretical Description. Retrieved from http://download.autodesk.com/us/algos/userguides/mergedProjects/setting_up_the_analysis/Nonlinear/Materials/Duncan-Chang_Theoretical_Description.htm
- Aziz, K. (1993). Reservoir Simulation Grids - Opportunities and Problems (Jpt, Vol 45, Pg 658, 1993). *Journal of Petroleum Technology*, 45(July), 856. <https://doi.org/10.2118/25233-PA>
- Aziz, K., & Settati, A. (1979). *Petroleum Reservoir Simulation*. Elsevier Applied Science Publishers.
- B. Ramirez, H. Kazemi, M. A. (2009). A Critical Review for Proper Use of Water/Oil/Gas Transfer Functions in Dual - Porosity Naturally Fractured Reservoirs: Part I. *SPE Reservoir Evaluation & Engineering*, 12(2), 200–210.
- Bai, M., Elsworth, D., & Roegiers, J.-C. (1993). Multiporosity/multipermeability approach to the simulation of naturally fractured reservoirs. *Water Resources Research*. <https://doi.org/10.1029/92wr02746>
- Bai, M., Ma, Q., & Roegiers, J. C. (1994). Dual-Porosity Behavior of Naturally Fractured Reservoirs. *International Journal for Numerical and Analytical Methods in Geomechanics*, 18(6), 359–376. <https://doi.org/Doi.10.1002/Nag.1610180602>
- Baker, L. E. (1988). Three-Phase Relative Permeability Correlations. *SPE Enhanced Oil Recovery*

Symposium. <https://doi.org/10.2118/17369-ms>

- Baker, & Kuppe. (2000). Reservoir characterization for naturally fractured reservoirs. *Society of Petroleum Engineers, SPE 63286*(October), 1–11. <https://doi.org/10.2118/63286-MS>
- Batenburg, D. Van, & Bosch, M. (2011). Application of Dynamic Gridding Techniques to IOR / EOR-Processes. *SPE Reservoir ...*, 1–16. Retrieved from <http://www.onepetro.org/mslib/servlet/onepetroreview?id=SPE-141711-MS>
- Beattie, C. I., Boberg, T. C., & McNab, G. S. (1991). Reservoir Simulation of Cyclic Steam Stimulation in the Cold Lake Oil Sands. *SPE Reservoir Engineering*, 6(2), 200–206. <https://doi.org/10.2118/18752-PA>
- Beckner, B. L., Chan, H. M., McDonald, a. E., Wooten, S. O., & Jones, T. a. (1991). Simulating Naturally Fractured Reservoirs Using a Subdomain Method. *Proceedings of SPE Symposium on Reservoir Simulation*. <https://doi.org/10.2118/21241-MS>
- Bennion, D. B., Thomas, F. B., & Bietz, R. F. (1996). Hysteretic Relative Permeability Effects and Reservoir Conformance - An Overview.
- Beraldo, V., Blunt, M., Schiozer, D., & Qi, R. (2007). Streamline Simulation With an API Tracking Option. *Proceedings of EUROPEC/EAGE Conference and Exhibition*. <https://doi.org/10.2523/107496-MS>
- Blaskovich, F. T., Cain, G. M., Sonier, F., Waldren, D., & Webb, S. J. (1983). A Multicomponent Isothermal System for Efficient Reservoir Simulation. *Society of Petroleum Engineers*. <https://doi.org/http://dx.doi.org/10.2118/11480-MS>
- Blunt, M. J. (2000). An Empirical Model for Three-Phase Relative Permeability. *SPE Journal*, 5(4), 435–445. <https://doi.org/10.2118/67950-pa>
- Carlson, F. M. (1981). Simulation of Relative Permeability Hysteresis to the Nonwetting Phase. *SPE Annual Technical Conference and Exhibition*. <https://doi.org/10.2118/10157-ms>
- Carlson, M. (2003). Practical Reservoir Simulation.
- Carter, R. D., & Tracy, G. W. (1960). Carter-Tracy Paper, 219, 415–417.
- Chatzichristos. (2016). *Personal Communication*.
- Chen, Z. (2015). *Computational methods for mutiphase flows in porous media*. PhD Proposal (Vol. 1). <https://doi.org/10.1017/CBO9781107415324.004>
- Cheresources. (2012). *Relationship Between Boiling Point And Bubble Point*. Retrieved from <http://www.cheresources.com/invision/topic/16686-relationship-between-boiling-point-and-bubble-point/>
- Coats, K. H. (1985). Simulation of Gas Condensate Reservoir Performance. *Journal of Petroleum Technology*, 37(10), 1870–1886. <https://doi.org/10.2118/10512-PA>
- Coats, K. H., Nielsen, R. L., Terhune, M. H., & Weber, A. G. (1967). Simulation of Three-Dimensional, Two-Phase Flow In Oil and Gas Reservoirs. *Society of Petroleum Engineers Journal*, 7(4), 377–388. <https://doi.org/10.2118/1961-PA>
- Collins, L. S. K. F. D. A. (1991). AN EVALUATION OF THE IMPROVED DUAL POROSITY MODEL FOR THE SIMULATION OF GRAVITY EFFECTS IN NATURALLY FRACTURED RESERVOIRS
An evaluation of the improved dual porosity model for the simulation of gravity effects in naturally

fractured reservoirs. *Canadian Petroleum*.

- Computer Modelling Group Ltd. (2009a). Advanced Process and Thermal Reservoir Simulator.
- Computer Modelling Group Ltd. (2009b). GEM User's Guide - Advanced Compositional and GHG Reservoir Simulator, 1142.
- Computer Modelling Group Ltd. (2010). Advanced Oil/Gas Reservoir Simulator, 1146.
- Computer Modelling Group Ltd. (2017). IMEX. Retrieved from <http://www.cmgl.ca/imex>
- Correia, P., Ganguli, S. S., & Obaidi, K. Al. (2015). *How to determine optimum gridblock size in a reservoir model that does not result in large reduction in accuracy without running multiple cases?* Retrieved from https://www.researchgate.net/post/How_to_determine_optimum_gridblock_size_in_a_reservoir_model_that_does_not_result_in_large_reduction_in_accuracy_without_running_multiple_cases2
- Craig. (1971). *Reservoir engineering aspects of water flooding*.
- Crain. (2016). FRACTURED RESERVOIR BASICS. Retrieved from <https://www.spec2000.net/22-fraclocl.htm>
- Cuthill, E., & McKee, J. (1969). Reducing the Bandwidth of Sparse Symmetric Matrices. *Proceedings of the 1969 24th National Conference of the ACM*, 157–172. <https://doi.org/10.1145/800195.805928>
- Cutler, J. M., & Rees, W. A. (1970). A Study of Water Coning in the Oil Creek Reservoir, North Antioch Field, Oklahoma.
- Dabir S. Viswanath, Tushar K. Ghosh, Dasika. H. L. Prasad, Nidamarty V.K. Dutt, K. Y. R. (2007). *Viscosity of liquids. Climate Change 2013 - The Physical Science Basis*. <https://doi.org/10.1017/CBO9781107415324.004>
- Dake. (1978). *Fundamentals of Reservoir Engineering*.
- Dawson, R., & Lantz, R. (1972). Inaccessible Pore Volume in Polymer Flooding. *SPE Journal*, 12, 448–452. <https://doi.org/10.2118/3522-PA>
- Denbury Resources Inc. (2009). *Denbury Resources CO2 Enhanced Oil Recovery Process*. Retrieved from <https://www.youtube.com/watch?v=NMBhX1IxajU>
- Dicarlo, D. a, Sahni, A., Blunt, M. J., & Stanford, U. (2000). Three-Phase Relative Permeability and Mixed-Wet Sandpacks. *SPE Journal*, 5(1), 27–30. <https://doi.org/10.2118/60767-PA>
- Donnez. (2007). *Essentials of reservoir engineering*.
- Eng-tips.com. (2008). Black oil model vs. Compositional model? Retrieved from <http://www.eng-tips.com/viewthread.cfm?qid=218881>
- Fanchi. (2006). *Principles of Applied Reservoir Simulation* (Vol. 1). <https://doi.org/10.1017/CBO9781107415324.004>
- Fayers, F. J., & Matthews, J. D. (1984). Evaluation of Normalized Stone's Methods for Estimating Three-Phase Relative Permeabilities. *SPE Journal*, 24, 224–232. <https://doi.org/10.2118/11277-PA>
- Fekete associates incorporation. (2012). Fracture Flow Capacity (kfwf). Retrieved from http://www.fekete.com/SAN/TheoryAndEquations/WellTestTheoryEquations/Fracture_Flow_Capacity.

htm

- Fekete associates incorporation. (2014). Coalbed Methane Properties. Retrieved from http://www.fekete.com/SAN/WebHelp/FeketeHarmony/Harmony_WebHelp/Content/HTML_Files/Reference_Material/General_Concepts/CBM_Properties.htm
- Fekete associates incorporation. (2017). Geomechanical Reservoir Models. Retrieved from http://www.fekete.com/SAN/WebHelp/FeketeHarmony/Harmony_WebHelp/Content/HTML_Files/Reference_Material/General_Concepts/Geomechanical_Reservoir_Models.htm
- Fetkovich, M. J. (1971). Fetkovich Paper. *Journal of Petroleum Technology*, 23(7), 814–828. <https://doi.org/10.2118/2603-PA>
- Fisher, Q. J., & Knipe, R. J. (2001). The permeability of faults within siliciclastic petroleum reservoirs of the North Sea and Norwegian Continental Shelf. *Marine and Petroleum Geology*, 18(10), 1063–1081. [https://doi.org/10.1016/S0264-8172\(01\)00042-3](https://doi.org/10.1016/S0264-8172(01)00042-3)
- Fjaer. (2008). *Petroleum Related Rock Mechanics*.
- Flodin, E. A., Aydin, A., Durlafsky, L. J., & Yeten, B. (2001). Representation of Fault Zone Permeability in Reservoir Flow Models. *SPE Annual Technical Conference and Exhibition*, 1–10. <https://doi.org/10.2118/71617-MS>
- Fossen, H. (2010). Structural Geology. Retrieved from [https://books.google.gr/books?id=01PI5jhjiiQC&pg=PA112&lpg=PA112&dq=ductile+geology+definition&source=bl&ots=DvRaIG6u-X&sig=-OW_1od3l gxhs1oTpApEo3saJpw&hl=en&sa=X&ei=eGYFUdmSHseO0AWD5oDACg&redir_esc=y#v=onepage&q=ductile geology definition&f=false](https://books.google.gr/books?id=01PI5jhjiiQC&pg=PA112&lpg=PA112&dq=ductile+geology+definition&source=bl&ots=DvRaIG6u-X&sig=-OW_1od3l gxhs1oTpApEo3saJpw&hl=en&sa=X&ei=eGYFUdmSHseO0AWD5oDACg&redir_esc=y#v=onepage&q=ductile%20geology%20definition&f=false)
- Frederick, D. C., & Graves, R. M. (1994). New Correlations To Predict Non Darcy Flow Coefficients at Immobile and Mobile Water Saturation SPE 28451, 915–921.
- Fung, L. S. K. (1991). Simulation of Block-to-Block Processes in Naturally Fractured Reservoirs. *SPE Reservoir Engineering*, 6(4), 477–484. <https://doi.org/10.2118/20019-PA>
- Geertsma, J. (1974). Estimating the Coefficient of Inertial Resistance in Fluid Flow Through Porous Media. *Society of Petroleum Engineers Journal*, 14(5), 1–6. <https://doi.org/10.2118/4706-PA>
- Gilman, J. R. (1986). An Efficient Finite-Difference Method for Simulating Phase Segregation in the Matrix Blocks in Double-Porosity Reservoirs. *SPE Reservoir Engineering*, 1(4), 403–413. <https://doi.org/10.2118/12271-PA>
- Gilman, J. R. (2003). Practical Aspects of Simulating NFRs. *Geriatric et Psychologie Neuropsychiatrie Du Vieillessement*, 9(3), 255–258. <https://doi.org/10.1684/pnv.2011.0293>
- Gilman, J. R., & Kazemi, H. (1983). Improvements in Simulation of Naturally Fractured Reservoirs. *Society of Petroleum Engineers Journal*, 23(4), 695–707. <https://doi.org/10.2118/10511-PA>
- Golub, & Van Loan. (1996). Matrix computations.
- Gringarten. (1985). *Interpretation of transient well test data*. (Dawe & Wilson, Eds.). Elsevier Applied Science Publishers.
- Grueschow, E., & Rudnicki, J. W. (2005). Elliptic yield cap constitutive modeling for high porosity

- sandstone. *International Journal of Solids and Structures*, 42(16–17), 4574–4587. <https://doi.org/10.1016/j.ijsolstr.2005.02.001>
- Hawk Ridge Systems. (2014). *SOLIDWORKS Simulation Theory - Linear vs. Nonlinear*. Retrieved from <https://www.youtube.com/watch?v=L55orKqnhNg>
- Heriot Watt University. (2005). *Reservoir Simulation*.
- Huang, C.-K. (2009). *Development of a general thermal oil reservoir simulator under a modularized framework*. University of Utah.
- Ihrdc. (n.d.). Irreducible water. Retrieved from https://www.ihrdc.com/els/ipims-demo/t26/offline_IPIMS_s23560/resources/data/G4108.htm
- Izgec, B. (2003). *Performance Analysis Of Compositional And Modified Black-Oil Models For Rich Gas-Condensate Reservoirs With Vertical And Horizontal Wells*.
- Jack, A., & Sun, S. (2003). Controls on Recovery Factor in Fractured Reservoirs: Lessons Learned from 100 Fractured Fields. *Proceedings of SPE Annual Technical Conference and Exhibition*, 1–18. <https://doi.org/10.2523/84590-MS>
- Jackson, M. D., Valvatne, P. H., & Blunt, M. J. (2003). Prediction of wettability variation and its impact on flow using pore- to reservoir-scale simulations. *Journal of Petroleum Science and Engineering*, 39(3–4), 231–246. [https://doi.org/10.1016/S0920-4105\(03\)00065-2](https://doi.org/10.1016/S0920-4105(03)00065-2)
- Jelmert, T. A. (2006). Wellbore storage, 1–9.
- Jiang, H., & Xie, Y. (2011). A note on the Mohr-Coulomb and Drucker-Prager strength criteria. *Mechanics Research Communications*, 38(4), 309–314. <https://doi.org/10.1016/j.mechrescom.2011.04.001>
- Jourde, H., Flodin, E. A., Aydin, A., Durlofsky, L. J., & Wen, X. H. (2002). Computing permeability of fault zones in eolian sandstone from outcrop measurements. *AAPG Bulletin*, 86(7), 1187–1200. <https://doi.org/10.1306/61EEDC4C-173E-11D7-8645000102C1865D>
- Kane. (2017). Definition of Infinite Dilution. Retrieved from http://www.ehow.com/about_5459313_definition-infinite-dilution.html
- Katz, D. L. (1959). *Handbook of Natural Gas Engineering*.
- Kazemi, H., Merrill Jr, L. S., Porterfield, K. L., & Zeman, P. R. (1976). Numerical Simulation of Water-Oil Flow in Naturally Fractured Reservoirs. *Society of Petroleum Engineers Journal*, 16(6), 317–326. <https://doi.org/10.2118/5719-PA>
- Kinawy, M. M. (2016). aquifer. BP.
- Land, C. S. (1968). Calculation of Imbibition Relative Permeability for Two- and Three-Phase Flow From Rock Properties. *Society of Petroleum Engineers Journal*, 8(2), 149–156. <https://doi.org/10.2118/1942-PA>
- Lee, J. (Texas A. U. ., & Wattenbarger, R. A. (Texas A. U. . (1996). *Gas Reservoir Engineering - SPE Textbook Series Vol. 5*.
- Lewis, R. W., & Gutierrez, M. (1998). The Role of Geomechanics in reservoir simulation. *Society of Petroleum Engineers*, 10. <https://doi.org/10.2118/47392-MS>
- Longuemare, P., Mainguy, M., Lemonnier, P., Onaisi, A., Gérard, C., & Koutsabeloulis, N. (2002).

- Geomechanics in reservoir simulation: Overview of coupling methods and field case study. *Oil and Gas Science and Technology*, 57(5), 471–483. <https://doi.org/10.2516/ogst:2002031>
- Lopez-Hernandez, H. D., Valko, P. P., & Pham, T. T. (2004). Optimum Fracture Treatment Design Minimizes the Impact of Non-Darcy Flow Effects. Retrieved from http://www.pe.tamu.edu/valko/public_html/CV/ValkoPDF/2004Lopezpaper00090195.pdf
- Macleod. (1922). On a relation between surface tension and density.
- Marques, J. B., Petrobras, S. A., Trevisan, O., & Unicamp. (2007). Classic Models of Calculation of Influx: A Comparative Study.
- Masalmeh, S. K., & Wei, L. (2010). Impact of Relative Permeability Hysteresis, IFT dependent and Three Phase Models on the Performance of Gas Based EOR Processes, (Stone 1973). <https://doi.org/10.2118/138203-MS>
- MathWorks. (2017a). Generalized minimum residual method (with restarts). Retrieved from <https://www.mathworks.com/help/matlab/ref/gmres.html>
- MathWorks. (2017b). Natural order row sort. Retrieved from <http://www.mathworks.com/matlabcentral/fileexchange/47433-natural-order-row-sort>
- Mattax, & Dalton. (1990). *Reservoir Simulation*. SPE.
- Mora, C. A., & Wattenbarger, R. A. (2009). Analysis and verification of dual porosity and CBM shape factors. *Journal of Canadian Petroleum Technology*, 48(2), 17–21. <https://doi.org/10.2118/09-02-17>
- Morrow, N. R. (1990). Wettability and Its Effect on Oil Recovery. *Journal of Petroleum Technology*, 42(12), 1476–1484. <https://doi.org/10.2118/21621-PA>
- NMT, N. M. I. of M. and T. (2010). *Fluid Flow in Porous Media. Fluid Flow in Porous Media* (Vol. V).
- Oak, M. J. (1990). Three-Phase Relative Permeability of Water-Wet Berea. *SPE/DOE Enhanced Oil Recovery Symposium*. <https://doi.org/10.2118/20183-MS>
- Oak, M. J., Baker, L. E., & Thomas, D. C. (1990). Three-Phase Relative Permeability of Berea Sandstone. *Journal of Petroleum Technology*, 42(8), 1054–1061. <https://doi.org/10.2118/17370-pa>
- Oilglossary.com. (2014). manifold. Retrieved from <http://oilglossary.com/manifold.html>
- Owens, W. W., & Archer, D. L. (1971). The Effect of Rock Wettability on Oil- Water Relative Permeability Relationships. *Journal of Petroleum Technology*, (July), 873–878. <https://doi.org/10.2118/3034-PA>
- Peaceman. (1977). *fundamentals of numerical reservoir simulation*.
- Pedersen, K. S., Fredenslund, A., Christensen, P. L., & Thomassen, P. (1984). Viscosity of crude oils. *Chemical Engineering Science*, 39(6), 1011–1016. [https://doi.org/10.1016/0009-2509\(84\)87009-8](https://doi.org/10.1016/0009-2509(84)87009-8)
- Pedersen, & Fredenslund. (1986). *An improved corresponding states model for prediction of oil and gas viscosities and thermal conductivities*.
- Pedrosa Jr., O. A., & Aziz, K. (1986). Use of a Hybrid Grid in Reservoir Simulation. *SPE Reservoir Engineering*, 1(6), 611–621. <https://doi.org/10.2118/13507-pa>
- Péneloux, A., Rauzy, E., & Fréze, R. (1982). A consistent correction for Redlich-Kwong-Soave volumes. *Fluid Phase Equilibria*, 8(1), 7–23. [https://doi.org/10.1016/0378-3812\(82\)80002-2](https://doi.org/10.1016/0378-3812(82)80002-2)

- Peng, D.-Y., & Robinson, D. B. (1976). A New Two-Constant Equation of State. *Industrial & Engineering Chemistry Fundamentals*, 15(1), 59–64. <https://doi.org/10.1021/i160057a011>
- Petrobras-pemex. (n.d.). Black oil vs . compositional simulation in gas injection processes.
- Petrowiki. (2015a). Conformance problems. Retrieved from http://petrowiki.org/Conformance_problems
- Petrowiki. (2015b). Isothermal compressibility of oil. Retrieved from http://petrowiki.org/Isothermal_compressibility_of_oil#Isothermal_compressibility_of_oil
- Petrowiki. (2015c). Miscible flooding. Retrieved from http://petrowiki.org/Miscible_flooding
- Petrowiki. (2016a). Critical gas saturation. Retrieved from http://petrowiki.org/Relative_permeability#Critical_gas_saturation
- Petrowiki. (2016b). Recognizing naturally fractured reservoirs. Retrieved from http://petrowiki.org/Recognizing_naturally_fractured_reservoirs
- Petrowiki. (2017a). Gas lift. Retrieved from http://petrowiki.org/Gas_lift
- Petrowiki. (2017b). Hydraulic fracturing. Retrieved from http://petrowiki.org/Hydraulic_fracturing
- Petrowiki. (2017c). Reservoir pressure data interpretation. Retrieved from http://petrowiki.org/Reservoir_pressure_data_interpretation
- Petrowiki. (2017d). Reservoir simulation. Retrieved from http://petrowiki.org/Reservoir_simulation
- Petrowiki. (2017e). Reservoir simulation linear equation solver. Retrieved from http://petrowiki.org/Reservoir_simulation_linear_equation_solver
- Petterson, O. (2006). Basics of Reservoir Simulation. *Lecture Notes*.
- Petterson, Ø. (n.d.). Some Aspects of Modelling Rock Fabric and Impact on Fluid Flow in Sandstone Reservoirs – Faults and Compaction, (1), 1–10.
- Petterson, Ø. (2005). Sandstone Compaction Modelling and Reservoir Simulation.
- Plohr, Marchesin, Bedrikovetsky, & Krause. (2000). Modeling hysteresis in porous media flow via relaxation.
- Pruess, K. (1992). Brief guide to the MINC-Method for modeling flow and transport in fractured media. *Lbl-32195*, 1–15. Retrieved from <papers2://publication/uuid/FF62F235-30A8-4132-8359-1A37221015D6>
- Rahman, M. K., Hossain, M. M., & Rahman, S. S. (2002). A shear-dilation-based model for evaluation of hydraulically stimulated naturally fractured reservoirs. *International Journal for Numerical and Analytical Methods in Geomechanics*, 26(5), 469–497. <https://doi.org/10.1002/nag.208>
- Ramey, H. J. (1964). Non-Darcy Flow and Wellbore Storage Effects in Pressure Build-Up and Drawdown of Gas Wells. *Journal of Petroleum Technology*, (I), 223–233. <https://doi.org/10.2118/1058-PA>
- Ranjbar, E., & Hassanzadeh, H. (2011). Matrix-fracture transfer shape factor for modeling flow of a compressible fluid in dual-porosity media. *Advances in Water Resources*, 34(5), 627–639. <https://doi.org/10.1016/j.advwatres.2011.02.012>
- Reid, R. C., Prausnitz, J. M., & Polling., B. E. (1987). *The Properties of Gases and Liquids*No Title. McGraw-Hill Book Company.

- Research Gate. (2017). What is the difference between consistency, stability and convergence for the numerical treatment of any PDE? Retrieved from https://www.researchgate.net/post/What_is_the_difference_between_consistency_stability_and_convergence_for_the_numerical_treatment_of_any_PDE
- Saboorian-Jooybari, H., & Pourafshary, P. (2015). Significance of non-Darcy flow effect in fractured tight reservoirs. *Journal of Natural Gas Science and Engineering*, 24, 132–143. <https://doi.org/10.1016/j.jngse.2015.03.003>
- Saidi, a. M. (1983). Simulation of Naturally Fractured Reservoirs. *Proceedings of SPE Reservoir Simulation Symposium*, v, 361–371. <https://doi.org/10.2523/12270-MS>
- Sammon, P., Masanori, K., & Jialing, L. (2001). Applying High-Resolution Numerical Schemes in Reservoirs Described by Complex Corner-Point Grids. *Proceedings of SPE Reservoir Simulation Symposium*, 1–13. <https://doi.org/10.2118/66344-MS>
- Saraf, D. N., Batycky, J. P., Jackson, C. H., & Fisher, D. B. (1982). An Experimental Investigation of Three-Phase Flow of Water-Oil- Gas Mixtures Through Water-Wet Sandstones. *SPE California Regional Meeting*. <https://doi.org/10.2118/10761-ms>
- Sarma, P., & Aziz, K. (2006). New Transfer Functions for Simulation of Naturally Fractured Reservoirs with Dual-Porosity Models. *SPE Journal*, 11(3), 328–340. <https://doi.org/10.2118/90231-PA>
- Saville. (2011). Acentric factor. Retrieved from <http://www.thermopedia.com/content/287/>
- Schlumberger. (2016a). compressibility. Retrieved from <http://www.glossary.oilfield.slb.com/Terms/c/compressibility.aspx>
- Schlumberger. (2016b). dual porosity. Retrieved from http://www.glossary.oilfield.slb.com/Terms/d/dual_porosity_reservoir.aspx
- Schlumberger. (2016c). gridding. Retrieved from <http://www.glossary.oilfield.slb.com/Terms/g/gridding.aspx>
- Schlumberger. (2017). irreducible water. Retrieved from http://www.glossary.oilfield.slb.com/Terms/i/irreducible_water.aspx
- Settari, a. T., & Aziz, K. (1972). Use of Irregular Grid in Reservoir Simulation. *SPE Journal*, 12(2), 103–114. <https://doi.org/10.2118/4720-PA>
- Sharafi, M. S., & Jamialahmadi, M. (2016). Mathematical model for prediction of oil recovery of core-flood tests in process of viscoelastic polymer flooding. *Petroleum Science and Technology*, 34(11–12), 1098–1105. <https://doi.org/10.1080/10916466.2016.1172090>
- Soave, G. (1972). Equilibrium constants from a modified Redlich-Kwong equation of state. *Chemical Engineering Science*, 27(6), 1197–1203. [https://doi.org/10.1016/0009-2509\(72\)80096-4](https://doi.org/10.1016/0009-2509(72)80096-4)
- Soleng, H., & Holden, L. (1998). Gridding for petroleum reservoir simulation. *Of the 6th International Conference on ...*. Retrieved from <http://publications.nr.no/publications.nr.no/grid98.pdf>
- Sonier, F. (1988). Numerical Simulation of Naturally Fractured Reservoirs, (November).
- Spencer, C. F., & Danner, R. P. (1972). Improved equation for prediction of saturated liquid density. *Journal of Chemical and Engineering Data*, 17(2), 236–241. <https://doi.org/10.1021/je60053a012>
- Stalkup, F. I. (1983). Status of Miscible Displacement. *Journal of Petroleum Technology*, 35(4), 815–826.

<https://doi.org/10.2118/9992-PA>

- Stone, H. L. (1970). Probability Model for Estimating Three-Phase Relative Permeability. *J. Pet Tech*, 22, 214–218. SPE-2116-PA. <https://doi.org/10.2118/2116-PA>
- Stone, H. L. (1973). Estimation of Three-Phase Relative Permeability and Residual Oil Data. *Journal of Canadian Petroleum Technology*, 12(4), 53–61. <https://doi.org/10.2118/73-04-06>
- Sugden. (1924). A Relation between surface tension, density, and chemical composition.
- Tarek Ahmed, & Meehan, N. (2012). *Advanced Reservoir Management and Engineering*.
- Technical Support, C. (2016). *personal conversation*.
- Thararoop, P., Karpyn, Z. T., & Ertekin, T. (2012). Development of a multi-mechanistic, dual-porosity, dual-permeability, numerical flow model for coalbed methane reservoirs. *Journal of Natural Gas Science and Engineering*, 8, 121–131. <https://doi.org/10.1016/j.jngse.2012.01.004>
- Thomas, L. K., Dixon, T. N., & Pierson, R. G. (1983). Fractured Reservoir Simulation. *SPE Journal*, 23(1), 42–54. <https://doi.org/10.2118/9305-PA>
- Tran, D., Settari, A., & Nghiem, L. (2004). New Iterative Coupling Between a Reservoir Simulator and a Geomechanics Module. *SPE Journal*, 9(3), 20–23. <https://doi.org/10.2118/88989-PA>
- TUC. (2016). Reservoir Simulation.
- Ueda, Y., Murata, S., Watanabe, Y., & Funatsu, K. (1989). SPE 19469 Investigation of the Shape Factor Used in the Dual-Porosity Reservoir Simulator, 35–44.
- Uleberg, K., & Kleppe, J. (2011). Dual Porosity, Dual Permeability Formulation for Fractured Reservoir Simulation. *Reservoir Recovery Techniques*, 11–12.
- University of Utah. (2017). Introduction to Fill-In. Retrieved from <http://www.math.utah.edu/~pa/fill/intro/>
- Warren, J. E., & Root, P. J. (1963). The Behavior of Naturally Fractured Reservoirs. *Society of Petroleum Engineers*. <https://doi.org/10.2118/426-PA>
- Wattenbarger, R., & H.J., R. (1968). Gas Well Testing With Turbulence, Damage and Wellbore Storage. *Journal of Petroleum Technology*, 20(8), 877–887. <https://doi.org/10.2118/1835-PA>
- Whitson, C. H., & Torp, S. B. (1983). Evaluating Constant-Volume Depletion Data. *Journal of Petroleum Technology*, ?(?), 610–620. <https://doi.org/10.2118/10067-pa>
- Wig, L. S., Codln, D. A., Nghlem, L. X., & Group, C. M. (1989). An Adaptive-Implicit Switching Criterion Based on Numerical Stability Analysis, (February).
- Wittel. (2016). Mechanics of building materials: non linear elastic behavior.
- Wu, Y.-S., & Pruess, K. (1988). A Multiple-Porosity Method for Simulation of Naturally Fractured Petroleum Reservoirs. SPE-15129-PA. *SPE Reservoir Engineering*, 3(1), 327–336. <https://doi.org/10.2118/15129-PA>
- Yasin, A. U. (2013). Enhance Oil Recovery : Chemical Flooding. Retrieved from <https://www.youtube.com/watch?v=K8cKQKiKm7s>
- Young. (2014). Iterative Solution of Large Linear Systems.

Zimmerman, R. W. (2005). Shape Factors for Dual-Porosity Fractured Reservoir Models Royal Institute of Technology, (September), 1–22.